Physical Processing

Course notes TU Delft, TA3390 part A

Revised and extended November 2011

Lectured by Dr. ir. R Chaigneau.

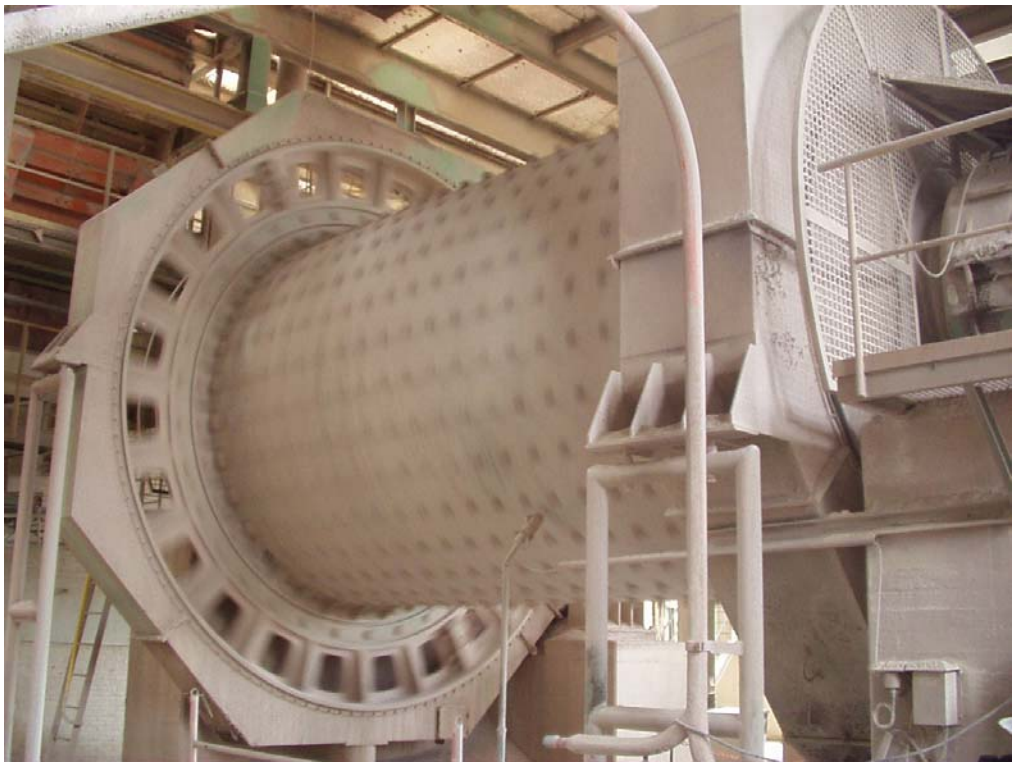

Ball mill for limestone, Ankerpoort N.V., Maastricht, The Netherlands

Table of contents:

1. SCREENING

1.1. Introduction

Screening is defined as the separation of a particle population in two or more size fractions using a semi-permeable surface: the screen deck. It distinguishes itself from stream classification (Chapter 2) by the fact that the size separation is not based on differential particle motion in a medium such as air or water. For wet processing screening is dominant for cut diameters > 1 mm, while below 1 mm classification is dominant. For dry processing this limit is usually higher, up to 5...10 mm.

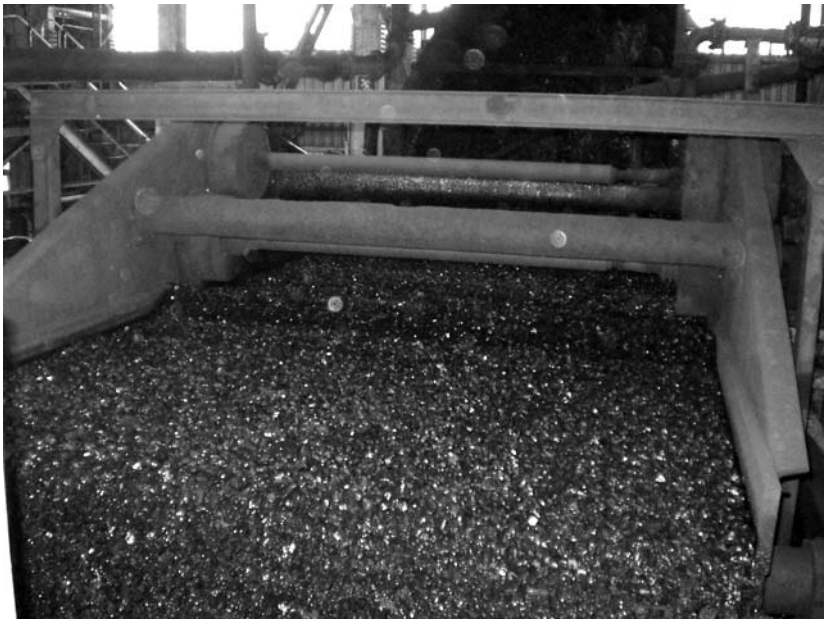

Fig. 1.1.1 - Screening at Anglo Coal's Kleinkopje coal preparation plant, South-Africa [TU Delft].

The usual objective of screening is to split the particle population into two or more fractions of different size, but can be carried out for other reasons as well, such as dewatering or loosening a bed of compacted particles. In general screening can be applied for one or more of the following reasons:

- Splitting in several size classes, each intended for a process optimised for that particular size class
- Classifying into sizes as required by the market (examples: heating coal, gravel, sands)
- Undersize removal before crushing
- Recovery of HMS medium solids (drain and rinse screening)
- Desliming (generally below 0.5 mm)
- Dewatering

A screen produces a coarse fraction (oversize) and an undersize fraction with fines. The material can be split in any desired amount of size fractions by installing screens of decreasing mesh size sequentially. Fig. 1.1.2, left, gives a schematic representation of the screening process. The results of screening are not perfect. The oversize still contains fines and the undersize still some coarse material, since mesh openings may vary or may be damaged. A typical screening result is given by Fig. 1.1.2, right, indicating the size distributions of feed, oversize and undersize material. x_{cr} is the critical particle size: the **cut diameter** or **cut size**. It is defined as the size of the material that is equally distributed in over- and undersize. Note that in industrial screening x_{cr} is typically ≈20% smaller as the aperture size.

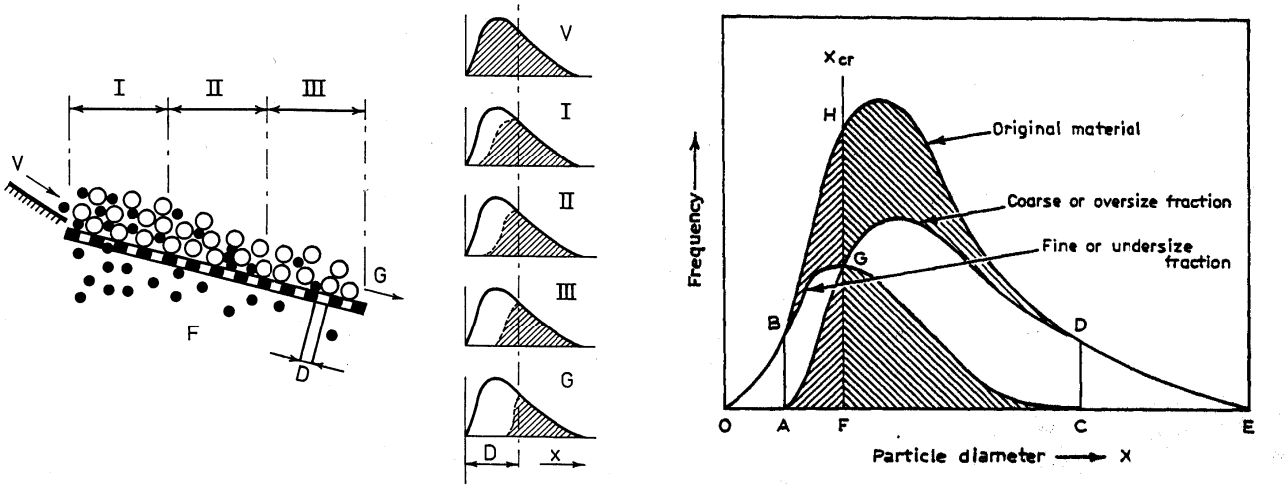

Fig. 1.1.2 - Left: screening process: size distribution of feed (V), intermediate products (I, II and III) and coarse fraction (G). Right: Screening results [Schubert, Vol. I (l)].

Models that quantitatively predict optimised screening conditions do not exist. The reason is the large number of variables that affect screening efficiency. They are broadly categorised as follows:

Effect of **material properties**:

- particle shape
- bulk density
- moisture content
- electrostatic charge
- percentage of problematic size fraction (the percentage of material having $0.7<x<1.5$) with x = mesh size. This material may cause blinding of mesh openings. Smaller material easily passes, while the coarser material is easily retained and transported over the deck.

Effect of the **screening method**:

- amplitude of vibration
- frequency of vibration
- screen angle with the horizontal
- screen length and width
- direction of vibration
- feeding method
- capacity.

Effect of the **screen deck**:

- mesh size
- mesh shape
- uniformity of the deck
- percentage open area of the deck
- construction material (steel, rubber or plastics).

Moisture and electrostatic charge bind particles together (agglomeration) and are often the cause of poor screening results. Despite the complexity of the screening process, some useful methods are available that assist in understanding and optimising screening operations. They are briefly described in this chapter.

1.2. Passage probabilities

Passage probability of a sphere of diameter x through a screen of mesh width D and mesh wire thickness d when approaching it perpendicular, equals (Fig. 1.2.1, left):

$$P = \frac{(D-x)^2}{(D+d)^2} \qquad (1.2.1)$$

or

$$P = \frac{(D-x)^2}{D^2} \cdot \frac{D^2}{(D+d)^2} \qquad (1.2.2)$$

The first term describes the relation between particle diameter and mesh width; the second gives the relation between open and total screen surface. When neglecting mesh wire thickness we obtain:

$$P \geq \frac{(D-x)^2}{D^2} \quad \text{when d<<D} \qquad (1.2.3)$$

Eq. 1.2.3 gives a minimum for P, since a particle may pass indirectly via the mesh wire (Fig. 1.2.1, right).

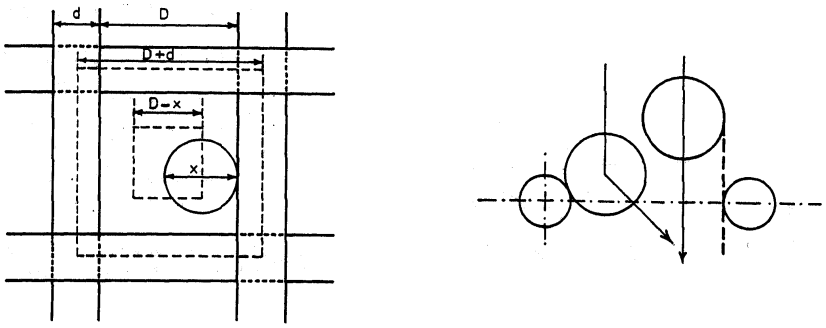

Fig. 1.2.1 - Passage of a sphere through a square mesh (left). Indirect passage of a particle via mesh wire (right).

The probability that a particle is still on top of the screen after one attempt amounts:

$$1 - P = \left[1-\left(\frac{D-x}{D}\right)^2\right] \qquad (1.2.4)$$

The probability, r_i, that after i attempts it is still on the screen amounts:

$$r_i = \left[1-\left(\frac{D-x}{D}\right)^2\right]^i \qquad (1.2.5)$$

Hence r_i is the fraction that remains on the screen after i attempts. Eq. 1.2.5 is shown graphically in Fig. 1.2.2. r_i increases rapidly when $x/D \rightarrow 1$.

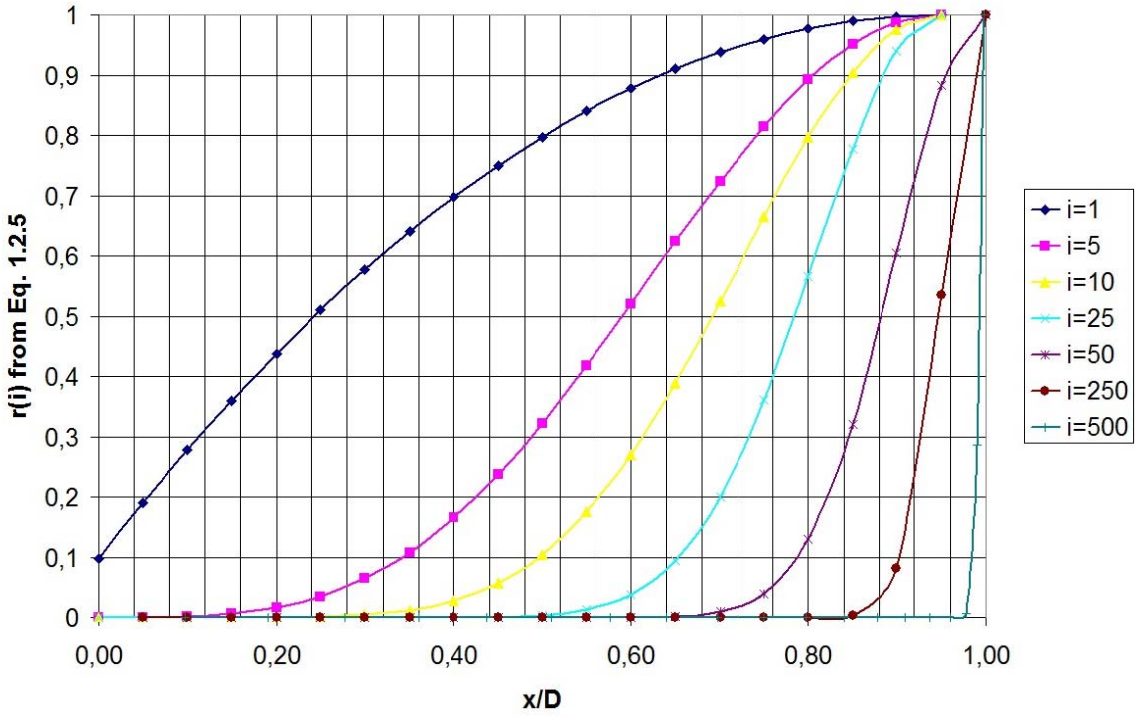

Fig. 1.2.2 - Fractional retention of particles as a function of trails at passage.

Eq. 1.2.5 is simplified by taking the logarithmic values of both sides:

$$\ln\left(r_i\right) = i \cdot \ln\left[1 - \left(\frac{D\text{-}x}{D}\right)^2\right] \qquad (1.2.6)$$

Because (D-x)/D must be smaller than 1 the right term can be developed in a Taylor series and approximately yields:

$$\ln(r_i) \approx i\left(\frac{D-x}{D}\right)^2 \qquad (1.2.7)$$

When we take for x the size of the particles of which 50% remain on top, then it follows with $x = x_{0.5}$ and $r_i = 0.5$:

$$\ln\left(0.5\right) = -i \cdot \left(1 - \frac{d_{0.5}}{D}\right)^2 \qquad (1.2.8)$$

$$d_{0.5} = D - \left(\frac{0.832 \cdot D}{\sqrt{i}}\right) \qquad (1.2.9)$$

With I the number of passage attempts per unit length and assuming a constant I throughout the screen length L, then i=IL and Eq. 1.2.9 becomes:

$$d_{0.5} = D - \frac{1}{\sqrt{L}} \cdot \left(\frac{0.832 \cdot D}{\sqrt{I}}\right) \qquad (1.2.10)$$

Consequently, when under- and oversize are sampled at various distances from the feed and we plot $d_{0.5}$ against $1/\sqrt{L}$, a straight line is obtained and I and D can be determined. I is interpreted as screen index (passage trials per meter) and D as a measure for the effective screen opening. When I and D of an application are known, i is consequently known and using Eq. 1.2.5 size distribution of under- and oversize can be calculated based on a size distribution of another composition.

Exercise 1.2.A

→ *For this exercise you need a computer on which Microsoft Excel is installed.*

*Re-create figure 1.2.2 by making a table containing r_i values for the range of passage trials from 1 to 500 and for x/D values with an increment of 0.05. Hint: x^y in excel is calculated as exp(y*ln(x)).*

1.3. Screening kinetics

Whitby (1958) did carefully designed experiments determining the amount of undersize as function of time. The experiments were carried out batch-wise. The results are generalised in Fig. 1.3.1:

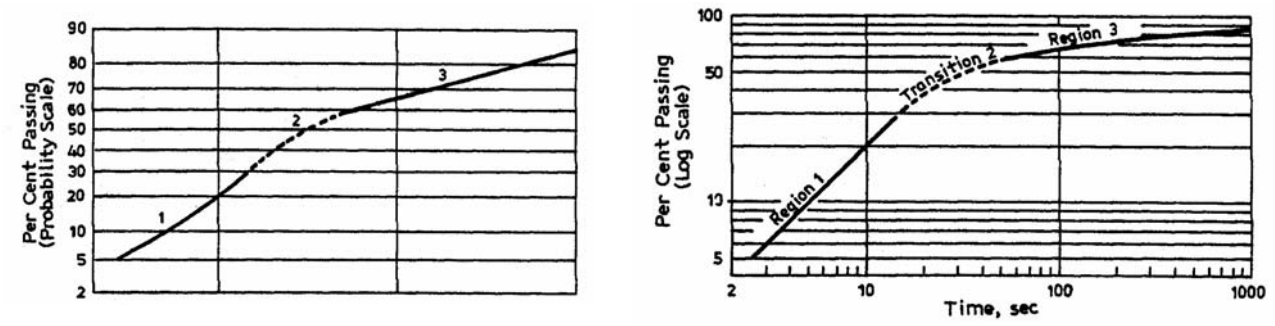

Fig. 1.3.1 - Screening regions according to Whitby.

Three different regions are distinguished:

Region 1, with a linear relationship between log(undersize) against time
Region 2: transition
Region 3: linear relationship between undersize on a log-probability scale against time (also equilibrium zone)

The screening rate decreases with time and is much smaller in Region 3 compared to Region 1.

In region 1 mainly the <0.7x material passes, while in region 3 the material approximately equal to the mesh opening x passes. Screening rate (the decrease in material to be screened per unit of time and per unit of area) is represented by a linear relationship:

$$\frac{dC(W,t)}{dt} = K \cdot \frac{W}{A} \quad \rightarrow \quad C(W,t) = C(W.t_0) - KWt/A \qquad (1.3.1)$$

C(W, t) is the cumulative weight having passed the screen at time t, W the weight of the material on the screen, K a constant, and A the screen surface.

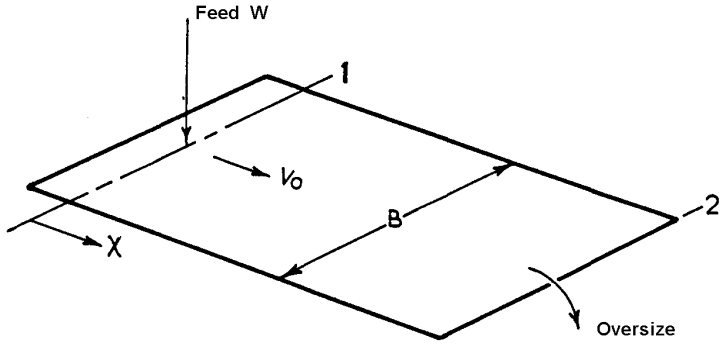

Fig. 1.3.2 - Continuous screening.

In Region 3 kinetics is controlled by a probability mechanism. Each particle has a low probability of passing the mesh openings. The total amount passing is the sum of the random passages. Under these conditions log(t) is distributed with a Gaussian (Whitby, 1958). Eq. 1.3.1 can easily be modified in order to meet the conditions for continuous screening. For an ideal screen with linear material transport of constant speed v_o (Fig. 1.3.2):

$$\frac{dC(W,x)}{B dx} = K \cdot \frac{W}{A} \qquad (1.3.2)$$

$dC(W, x)$ is the amount of material passing the screen at location x per unit of time. Eq. 1.3.2 applies until the value of x represents the start of transition region 2. The following applies for region 2 and 3:

$$\frac{dC(W,t)}{dt} = f(t) \cdot \frac{W}{A} \qquad (1.3.3)$$

Instead of constant K for region 1 we have $f(t)$. This has important consequences, since Eq. 1.3.2 states that the screening capacity depends on the surface A, while Eq. 1.3.3 states that for regions 2 and 3 the capacity depends on screening time instead of area. Whitby (1958) gives a more detailed proof and elaboration of Eq. 1.3.3.

When screening needs to be carried out into regions 2 and 3, the operation may be split, in order to keep a low transport velocity across the second screen. The transition from region 1 to 3 can be determined with a screening experiment. Besides this method, the following approximation is often used to express screening kinetics:

$$C(W,t) = 100 \cdot \left[1 - \exp(-kt)^n\right]\% \qquad (1.3.4)$$

n and k are empirical constants.

Exercise 1.3.A

→ You need: about 1 kg of dry (beach) sand, a laboratory screen set, screen machine with timer, balance (<0.1 g accuracy), computer with Excel.

- *Select a screen that would screen off between 50% and 80% of the sand and give its aperture: ___ µm*
- *Determine the area of the screen: ____ cm^2.*
- *Carefully load the screen with the sand until it has a height of about 10 mm on the screen.*
- *Place the screen in the machine with closed bottom pan and lid.*
- *Record the undersize as function of time for at least 20 minutes by removing the undersize at specific time intervals. In the beginning you may take short intervals (e.g. 5 or 10 seconds), later you can take longer intervals (up to 60 seconds).*
- *Plot the data in an XY Excel graph onY_log / X_linear scale, and on Y_log / X_log scale. Only show* ***measured*** *data points (so no"interpreted" lines from Excel that you did not measure between the data points). Give complete and appropriate titles and labels.*
- *Clean up everything and leave the equipment as you found it.*

Exercise 1.3.B

→ You need the data from 1.3.A and a computer with Excel

- *Split the data set into a part that can be described as "linear","transition" and "probability" screening.*
- *Take the "linear" data set and determine K from Eq. 1.3.1 using least squares*
- *Take the "probability" data set and determine k and n of Eq. 1.3.4 using least squares.*
- *Plot Eq. 1.3.1. and Eq. 1.3.4 in the data set using the values for K, k and n that you found.*

1.4. Screening parameters

The following parameters must be adjusted to optimise screen motion to a specific feed:

a	Amplitude of the screen deck	[cm]
n	Frequency	[min^{-1}]
ω	Angular velocity	[s^{-1}]
α	Throw angle (Fig. 1.4.1)	[°]
β	Inclination of screen deck (Fig. 1.4.1)	[°]

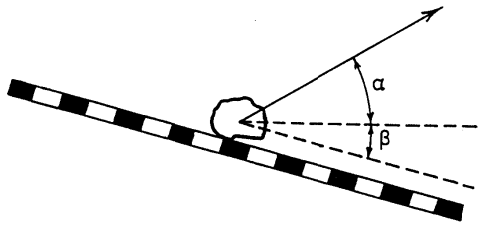

Fig. 1.4.1 - Throw angle α and inclination β.

A machine parameter K and screen parameter K_v are often used to compare different screening devices. K expresses the ratio between generated centrifugal acceleration and gravity:

$$K = \frac{a\omega^2}{g} \approx \frac{an^2}{90000} \qquad (1.4.1)$$

K_v expresses the ratio between the components of the maximum centrifugal acceleration perpendicular to the screen surface and gravity (Fig. 1.4.2):

$$K_v = \frac{(b_s)\max}{g \cdot \cos(\beta)} \qquad (1.4.2)$$

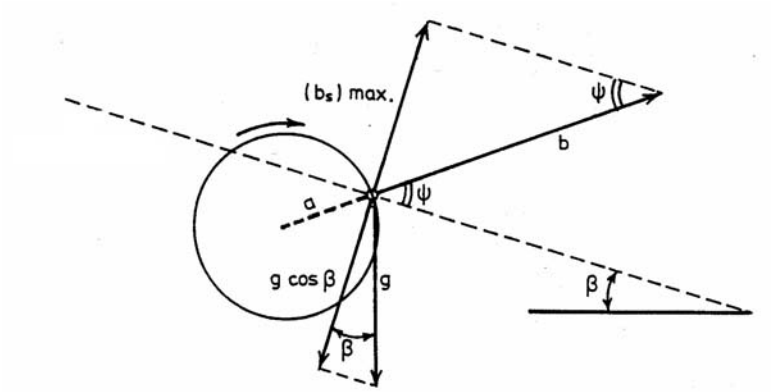

Fig. 1.4.2 - Relationship between centrifugal acceleration b_s and gravity

b_s is the centrifugal acceleration maximum. A single particle can only be thrown upwards when $K_v > 1$. For screening bulk material it is more complicated (mutual friction, moisture, etc.), and K_v should be at least 1.5.

When ψ is the angle between the centrifugal acceleration vector and screen surface then

$$\Psi = \omega \cdot t \qquad (1.4.3)$$

$$b_s = b \cdot \sin(\Psi) = a \cdot \omega^2 \cdot \sin(\Psi) \qquad (1.3.9)$$

A particle is thrown upward when $b_s > g \cdot \cos(\beta)$ and for the value of $\Psi = \Psi_L$ for which this happens applies

$$a \cdot \omega^2 \cdot \sin(\Psi_L) = g \cdot \cos(\beta) \qquad (1.4.5)$$

$$K_v = \frac{a \cdot \omega^2}{g \cdot \cos(\beta)} = K \cdot \frac{1}{\cos(\beta)} \qquad (1.4.6)$$

$$\sin(\psi_L) = \frac{g \cdot \cos(\beta)}{a \cdot \omega^2} = \frac{\cos(\beta)}{K} = \frac{1}{K_v} \qquad (1.4.7)$$

The relationship between Ψ_L and the throw angle α is shown by Eq. 1.4.8. and Fig. 1.4.3.

$$\alpha = 90° - (\psi_L + \beta) \qquad (1.4.8)$$

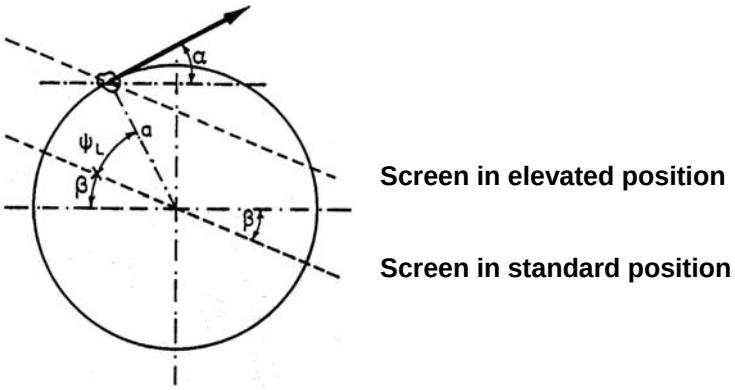

Fig 1.4.3 - Relationship between ψ_L and α.

With the above we are able to calculate α for different combinations of K and β. Besides, the particle trajectory and impact location of a thrown particle can be calculated. This means that a, n and β can now be adjusted to create optimised screening conditions.

Kluge (1971) and Schranz et al. (1958) made those calculations. Results were in reasonable agreement for screening of coarse material. For finer sized feeds, the factors that are neglected in the calculations gain in importance: friction and mutual binding forces. As a consequence considerable discrepancy between theory and practice appear for finer feeds, but nevertheless interesting conclusions can be drawn. It appears that α is strongly correlated to K. When β = 0 en K = 2 then α = 60°. Vibratory screens with circular drive (Fig. 1.4.4a) must be installed under an angle to ensure sufficient transport. This is disadvantageous under certain conditions. Advantage of a circular drive is its loosening effect on the feed. Linear drives ensure easy and sufficient transport on a horizontal surface (Fig. 1.4.4b), but have less loosening effect. As a compromise an elliptic drive can be applied that has an acceleration vector differing in size and direction. Even with a small inclination sufficient transport is guaranteed.

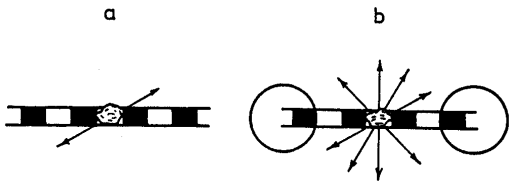

Fig. 1.4.4 - Forces on a particle with linear (a) and circular (b) drive [Schubert, Vol. I].

The value of K_v, as function of α, β, ω and a, is of major importance for the screening process. In general no screening will occur when $K_v<1.5$. When $1.6<K_v<1.8$ the particles will reach the screen when it is in its top position, resulting in minimal size reduction of soft materials such as coal. For materials that are difficult to screen, such as cokes, $2.1<K_v<2.3$ is maintained. For easily screenable material $3<K_v<3.5$ results in the highest capacities. At $K_v\approx3.3$ the flying time of the particle equals the stroke of the screen (or a multiple of it), causing resonance. It occurs when

$$K_v = \sqrt{1+(n\pi)^2} \qquad (1.4.9)$$

The best screening results are obtained at these values. $K_v>>4$ should be avoided, since transport is high and passage probability and therefore efficiency becomes too low. The optimised K_v is determined by feed properties and may vary for different applications. Fig. 1.4.5 shows particle trajectories on the screen deck for various K_v values.

Feed size determines the optimised amplitude and frequency of the vibration at a given K_v:

For loosening of a bed of coarse feed larger amplitudes and lower frequencies are employed. For finer feeds it is reverse.
At constant K_v materials are thrown higher at larger amplitudes and lower frequencies as reverse.

As a consequence for fines screening small amplitudes at higher frequencies are used, and reverse for coarse feeds.

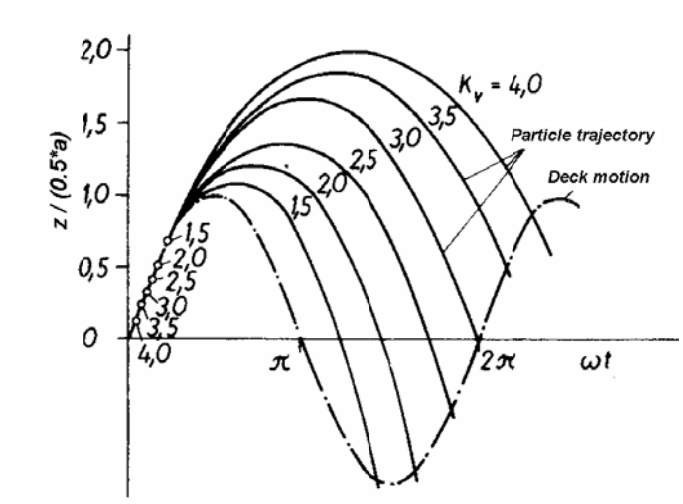

Fig. 1.4.5 - Particle trajectories on a vibrating screen deck at various K_v [Schubert, Vol. I]. r = radius = ½a, z = particle height.

1.5. Screen decks

Numerous types of screen deck (or screen media) are available (Fig. 1.5.1). Differences are mainly in the aperture shape, open area percentage, shape of the mesh sides, mesh construction, and material.

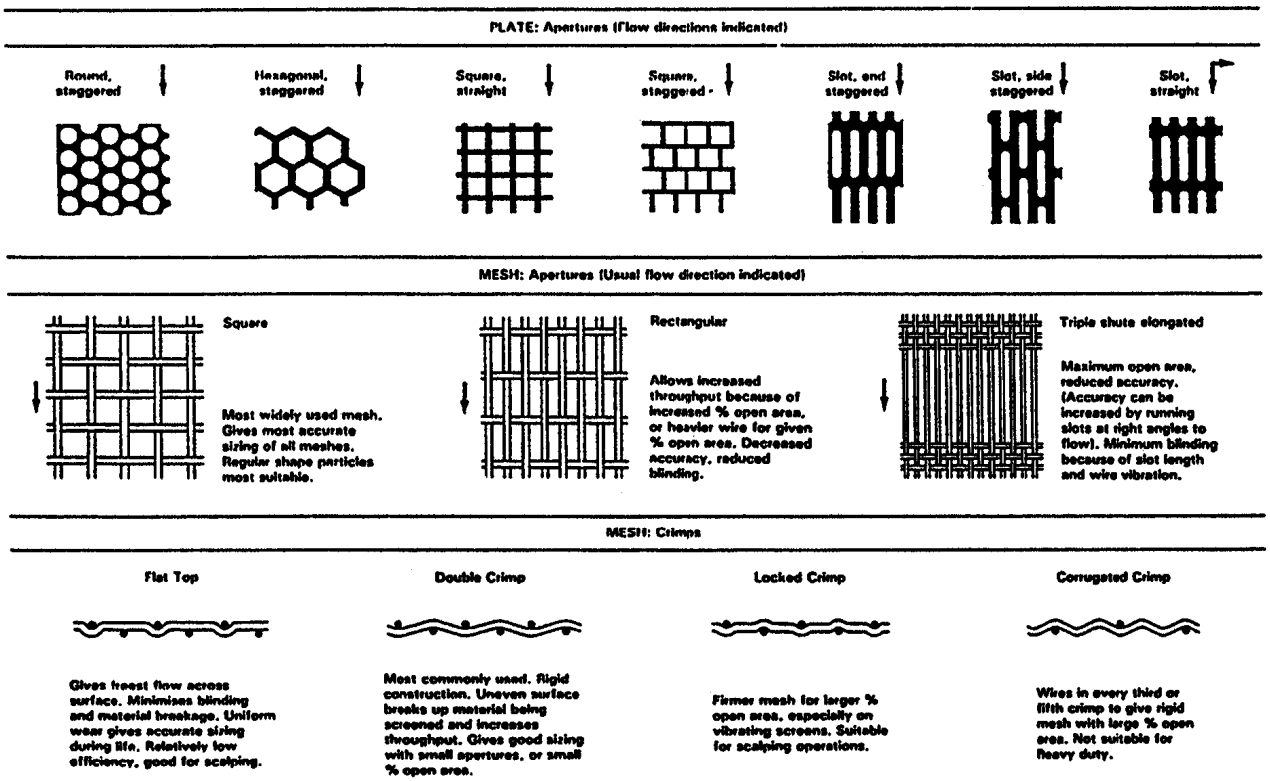

Fig. 1.5.1 - Various perforated plate and woven wire screen decks.

Perforated plate (Fig. 1.5.1, top): wear resistant steel plate with round, square or elongated holes. Normally used on primary (ROM) screens and on classifying screens.

Grizzly rod deck: heavy rods in the direction of flow. Stationary as well as vibrating versions exist. Inclination can be between 35° and 50°. Usually rods have a decreasing width in the direction of flow to prevent blinding or pegging. Spacing 20...300 mm. Typical application: pre-screening of primary crusher feed.

Bar deck: robust steel bars of ≈50 mm diameter in the direction of flow and at right angles to it, making square holes. Applied when robustness is required, for primary screening or coke screening.

Rod deck: about 1m long steel rods with a minimum of 5 mm spacing mounted loosely in slots supported by steel frame bars running across the deck. The rods are free to rotate in slots, preventing build up of bridges of fines. This is enforced by motion of the deck. Screening is not accurate, but this type is very suitable for damp material that is otherwise difficult to clean (5...10 mm). A typical application is dry pre-screening of ROM coal, when only the oversize needs processing.

Wedge-wire deck (Fig. 1.5.2, r): wedge-shaped SS wires, tapering from ≈2mm wide on the surface down to ≈1mm to the bottom, so preventing blinding. Typical spacing is 0.25...10 mm. Typical applications are desliming, draining, rinsing, slurry screening, dewatering, and pre-screening at small apertures. Usually the slots are in the flow direction, but it can be across as in sieve bends (Fig. 1.8.3).

Woven wire screen media (Fig. 1.5.1, middle, bottom)**:** mesh pattern of woven steel wire, with typical apertures 0.2...100mm. Wire thickness is a compromise between open area (efficiency, capacity) and screen deck life (wear). For small apertures screening a feed containing coarse sizes a relief deck below the wire screen may be applied for additional strength. Proper tensioning of the deck is essential to prevent premature failure. After installation it must be retensioned after some hours running and tensioning should be further monitored on a weekly basis.

Polyurethane screening media (Fig. 1.5.2, l)**:** Panels of typical dimensions (305...610)*(305...915) mm and 30...50 mm thickness, with typical apertures of 0.3...100 mm square or slotted 0.3*13 to 20*40. The panels are supported by a steel bar frame. Advantage of the modular construction is that only worn panels need to be replaced instead of the total screen deck. Wedged panels exist as well. Modular polyurethane decks have a somewhat smaller open area as traditional woven wire decks, therefore existing screens may show lower capacity when replacing the deck with PU panels.

Rubber screening media: Applied for heavy duty primary dry screening (absorption of impact) and for fine screening of moist feed, to prevent blinding and pegging (E.g. dry fines screening of ROM coal). Can be mounted in the same modular PU panels, rubber and PU can also be combined in a single screen, the rubber panels absorbing the impact at the feed end.

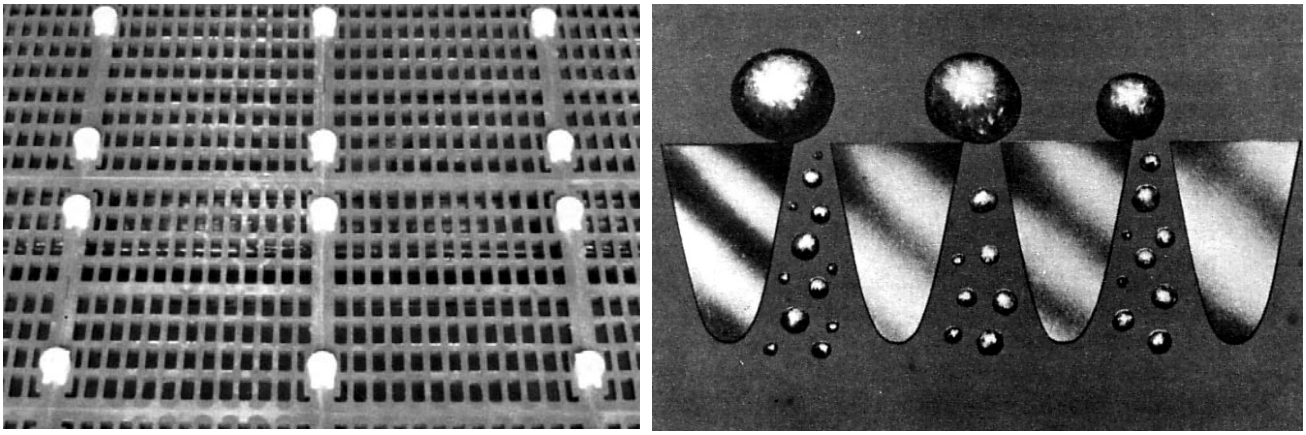

Fig. 1.5.2 - PU Modular deck (l). Detail of wedge-wire deck cross-cut (r) [SACPC / Wills].

1.6. Screening efficiency

1.6.1. Efficiency parameters

Screening efficiency can be expressed in various ways, depending on the objectives of the operation. For coarse fractions the efficiency E can be expressed as:

$$E = 100 \cdot \frac{g_1 G_1}{g_v G_v} \qquad (1.6.1)$$

G_1 is the mass of the oversize and g_1 and g_v are the mass percentages coarse material in the oversize and in the feed G_v. For fines a similar expression applies. However, Eq. 1.6.1 does not fully express the screening result. An expression is needed that includes behaviour of both fractions. **Newton's Classification Efficiency**, E_N, is the most complete. Using the following symbols:

	Fractions		
	mass	*% coarse*	*% fine*
feed	G_v	g_v	f_v
oversize	G_g	g_g	f_g
undersize	G_f	g_f	f_f

$$E_n = 100 \cdot \left[\frac{(G_v - G_f) \cdot g_g}{G_v \cdot g_v} - \frac{(G_v - G_f) \cdot (1 - g_g)}{G_v \cdot (1 - g_v)} \right] \qquad (1.6.2)$$

Applying a mass balance,

$$G_v \cdot g_v = (G_v - G_f) \cdot g_g + G_f \cdot g_f \qquad (1.6.3)$$

applies and by combining Eq. 1.6.2 and Eq. 1.6.3 we obtain

$$E_n = 100 \cdot \left[\frac{(g_g - g_v) \cdot (g_v - g_f)}{g_v \cdot (1 - g_v) \cdot (g_g - g_f)} \right] \qquad (1.6.4)$$

Capacity and efficiency act against each other in screening, therefore efficiency and capacity are a compromise. In practical applications E_n usually varies between 65% and 75%. When it must be increased to 85...90% the necessary screening surface becomes very much larger, because the increase must be generated from the $0.7<x<1.5$ material that is difficult to screen. E_n of a dry laboratory test (Section 2.9) is often not much better than 90%, since fines agglomerate with the coarse fraction.

The efficiencies that are calculated are strongly influenced by the size distribution of the feed. When a large fraction of the material is smaller than 0.5x, high efficiencies are obtained, but it does not mean that the screening is performed under optimised conditions. Therefore Testut (1958) proposed to relate the efficiency to the problematic fraction $0.5D<x<D$. A simple formula for E can successively be applied:

$$E = 100 \cdot \frac{G_f \cdot g_f}{G_v \cdot g_v} \qquad (1.6.5)$$

This expression is rearranged using mass balances to

$$E = 100 \cdot \frac{g_f \cdot (g_v - g_g)}{g_v \cdot (g_f - g_g)} \qquad (1.6.6)$$

Here $g_{v,f,g}$ are the mass fractions in feed, undersize and oversize respectively of material having a diameter D of $0.5D < x < D$. Testut reported $60\%<E<90\%$ for the problematic fraction, which corresponds to 70...90% for all material, which is a bit higher than average, being 65%...75%.

1.6.2. Tromp curve

Instead of a single efficiency parameter the efficiency of an industrial screen can be represented graphically based on sampling and laboratory experiments. A **Tromp curve** shows the **cumulative oversize** as function of size. In other words, a point on the curve shows the percentage of that particular particle size that reports in the oversize. Ideally, below the screen aperture size all percentages should be zero, and above it 100%. The according Tromp curve is represented by the steep straight line at the screen aperture (Fig. 1.6.1). However, in industrial screening practice, curves as shown by the bold line in Fig. 1.6.1 are obtained. The shape of the curve gives immediate insight into screening efficiency, and therefore is frequently applied in routine industrial screening performance monitoring.

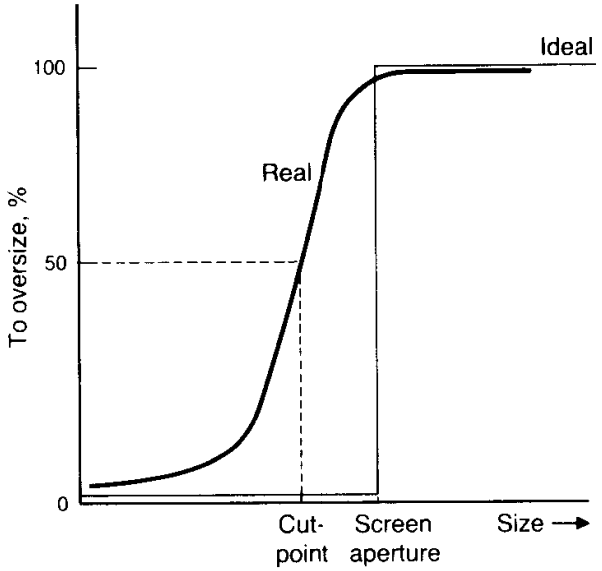

Fig. 1.6.1 - Tromp curve for a screening operation [Wills].

When the curve is available, single quality parameters are derived. The **cut-point**, which is always lower than the aperture size, is the value at 50% (x_{50}). Frequently used is the "**Écart probable**" or E_p:

$$E_p = \frac{x_{75} - x_{25}}{2} \qquad (1.6.7)$$

A disadvantage is that E_p depends on the cut-size (x_{50}), hence screening operations at various x_{50} cannot be compared. In these cases the "**Imperfection**" I can be used:

$$I = \frac{E_p}{x_{50}} = \frac{x_{75} - x_{25}}{2x_{50}} \qquad (1.6.8)$$

Other parameters used are the particle spread H:

$$H = \frac{x_{75}}{x_{25}} \qquad (1.6.9)$$

and the separation sharpness T:

$$T = \tan(\alpha_{x50}) \qquad (1.6.10)$$

Where α is the angle of the curve at d_{50}. It should be realised that the E_p or other parameters obtained from the Tromp curve are not a screen characteristic, but rather indicate the efficiency of a particular screening operation, since besides screen design and vibration, factors like overload, feed size distribution, moisture content etc. have a pronounced effect. Tromp curves and its related efficiency parameters E_p and I are also used for monitoring density separation by replacing the size axis by a density axis.

1.7. Screening capacity

When comparing two screens of mesh sizes D_1 and D_2, the number of mesh openings is inversely proportional to the mesh size squared. Assuming that for both screens the same number of particles passes per unit of time, the masses of the two particlesa relate to (mesh size)^3. As a consequence, screening capacity is proportional to mesh size. Therefore capacity is expressed in tonnes per m^2 and per mm mesh size. It explains why in ore processing screening below 0.2 mm is rarely economic. For dry coal screening this limit is about 5 mm, but can be as smaal as 1 mm occasionally.

The capacity C of a vibratory screen can be estimated with the empirical expression:

$$C = 1.4 \cdot \frac{\rho}{\gamma} \cdot D^{0.6} \qquad (1.7.1)$$

with C the capacity in t/hr.m^2, ρ the material (solid) density in g/cm^3, D mesh size in mm, and γ the fraction of feed particles having $0.5D < x < 1.5D$. Eq. 1.7.1 corresponds to an efficiency for the problematic fraction ($0.5D < x < D$) of approximately 90%. The application of Eq. 1.7.1. is limited to:

- Square mesh openings of a deck with at least 50% open surface.
- $\gamma < 15\%$ (otherwise transport becomes a delimiting factor)
- 0.5 mm < (mesh size) < 250 mm

Moisture has a major effect on capacity. levels between 8% and 10% reduce capacity down to 0.8C, while efficient spraying may increase it up to 1.25C. More empirical expressions are available in the literature (Schubert, 1986).

1.8. Screening equipment

Numerous screen types exist. Grizzlies (for coarse material) and sieve bends (for fines) are stationary screens. Roller screens, trommel screens, reciprocating screens and vibrating screens are based on motion of the screen deck to improve screening kinetics. An overview is given in Fig. 1.8.1. Of the different screen types, vibrating screens are the most important group. Screens are further subdivided according to deck type (Section 1.5).

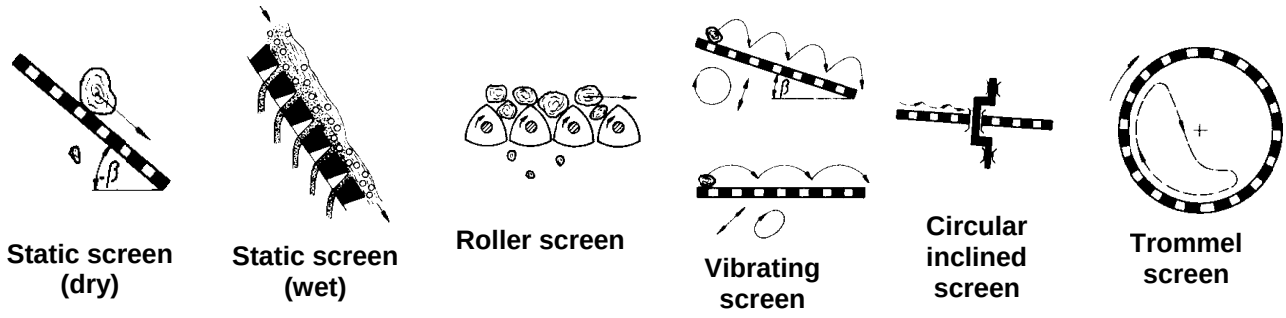

Fig. 1.8.1 - Basic screen types [Schubert, Vol. I].

1.8.1 Static screens

Three types of static screens are frequently applied:

Grizzly: tapered self-relieving parallel bars in the direction of flow, at and angle of 35°...50°. The deck may be vibrated, but more often it is static (Fig. 1.8.2, l). Cut-size 20...300 mm (for coal 50...150 mm). A grizzly is frequently used before a primary crusher to remove undersize (Fig. 1.8.2, r). The material should not be too sticky or damp, and efficiency (E_N) is <75%.

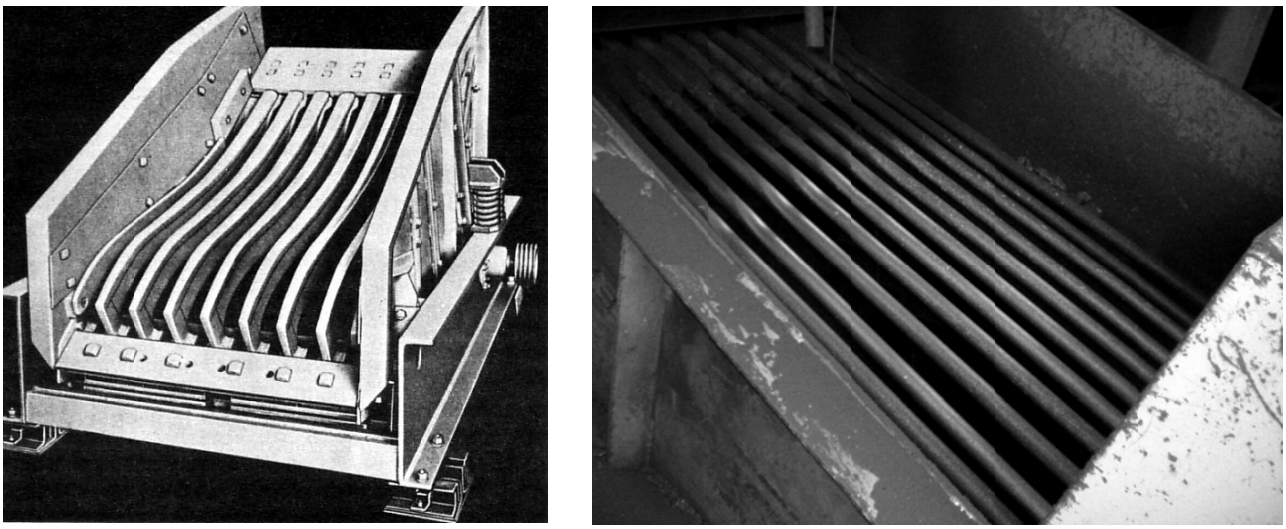

Fig. 1.8.2 - Ore grizzly, schematic (l). 50 mm static grizzly installed directly preceding a jaw crusher at the coal preparation plant of Dr. A. Schäfer Bergbau GmbH, Germany (r) [Wills / TU Delft].

Drain panel: Static screen of standard PU or wedge wire panels having slots with flow direction (SWF). They are usually combined with a vibrating screen down-flow. Drain panels assist in removal of excessive water or fines.

Sieve bend: Static curved wedge wire (usually PU) with slots across the flow (SAF). It was developed by Staatsmijnen in the Netherlands in the 1950's and applied for fine coal. Usually applied for dewatering preceding a vibrating screen. Cut-size ≈1...0.5 mm. Feed (a suspension of fine solids) is directed to the upper part of the curve. The feed is added tangentially and needs to have a constant rate. The curve effects centrifugal forces assisting in the sweeping of water from the suspension. In general cut-size = 0.5*slot size. Decks can be turned when worn. Also rapped sieve bends exist, consisting of vibrated profile wire driven by compressed air valves in order to prevent blinding,.

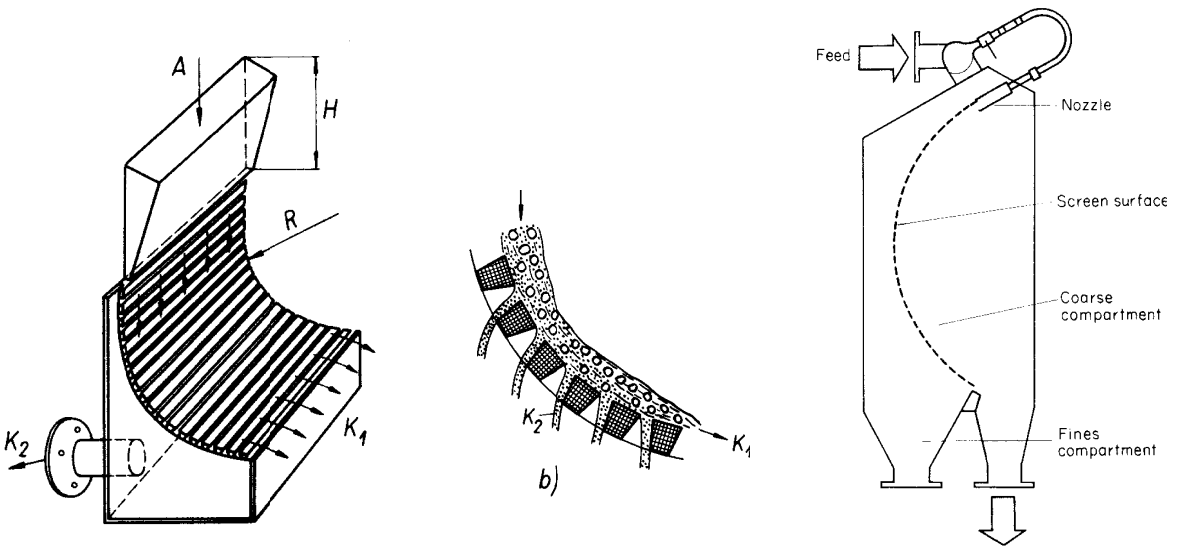

Fig. 1.8.3 - Sieve bend principle [Schubert, Vol. I (l,m) / Wills (r)].

1.8.2. Vibrating screens

Vibrating screens can be subdivided based on differences in motion characteristics (Fig. 1.8.4). Vibrating screens with **linear** (or straight line) **motion** are the largest group. The motion can be generated by an excenter, electro-magnetic drive or double-unbalance drive (Fig. 1.8.5).

Excenters are rarely used anymore. See Fig. 1.8.1; circular inclined screen. They were typically applied for coal screening.

In **double unbalance drives** the amplitude and frequency can be adjusted easily, and therefore have a wide application area. Machines with double-unbalance drives are usually lighter and require less maintenance than other systems (e.g. resonance screens or excenter drives).

Electromagnetic drives are applied for fine to ultra-fine screening (0.1...4 mm). Typical amplitudes are 0.2...2 mm, and frequencies 25...100 s^{-1}. Only the deck is vibrated, the frame is static. The deck is strongly inclined.

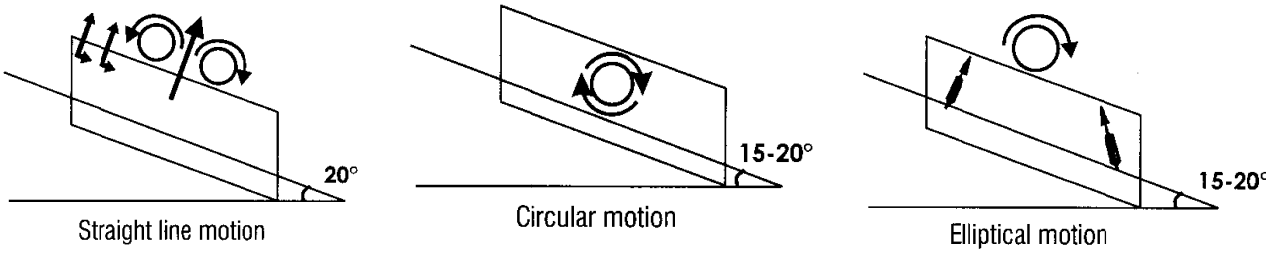

Fig. 1.8.4 - Basic screen motion drives: linear (l), circular (m) and elliptical (r) [SACPS].

The advantage of linear motion is the good control of throw angle and transport velocity. Linear motion effects sufficient transport even on horizontal screens. The low self-cleaning effect is a disadvantage.

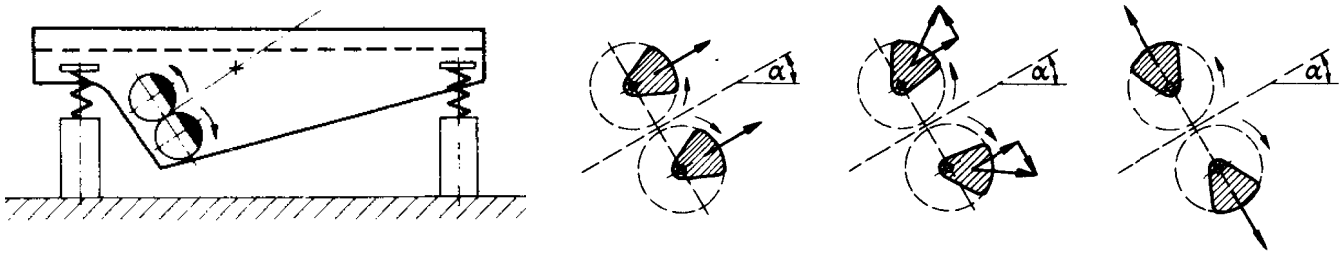

Fig. 1.8.5 - Horizontal linear motion screen (l). Double unbalance drive principle (r) [Schubert, Vol. I].

Circular motion screens are always inclined (12°...25°) to allow transport of the feed. Drives are single or double excenters or a single unbalance drive. Double excenters are used for 40...100 mm amplitude at frequencies of 120...200 min^{-1}. They are insensitive for choking. Often they are only in use in older plants.

Single excenters are used for any size range, having typical amplitudes of 1.5...5 mm and frequencies of 1200...2000 min^{-1}. Single unbalance drives have a frequency 3...5 times the resonance frequency of the screen. Typical amplitudes are 1.5...7.5 mm and frequencies 750...2000 min^{-1}. The amplitude is easily modified by adjusting the excenter weight. Typical screen sizes are 50...1 mm. The advantage of circular motion is the self cleaning effect: a particle stuck into the mesh experiences forces in all directions promoting its loosening. The transport velocity depends on the inclination of the screen, which in general is not easily adjusted.

Elliptical motion screens combine the advantages of linear and circular motion. Elliptical motion is effected by a single unbalance motor and a specific spring configuration, or alternatively by an arrangement of three unbalance motors. Below a more detailed description of the most common vibrating screens, cited from [SACPC]:

Linear motion horizontal screen (Fig. 1.8.5, l): Linear motion (sometimes known as straight line motion horizontal screens) are today the most common and consist of a horizontal screen deck, a drive (being either excitors or vibrator motors) and vertical side plates, all mounted on isolators. The screen can be suspended or root mounted to suit the plant layout. The most commonly used isolators are coil springs, rubber buffers, air fides and Rosta mounts. The screening action is derived from two counter-rotating, eccentric, out-of-balance masses that lift particles off the screen deck at a predetermined angle, in a straight line, and then drop them vertically back onto the screen deck (Fig. 1.8.5, r). This "zigzag" action conveys the material down the screen deck at a constant velocity determined by the angle of the drive, the G-force and the speed of the drive.

Normally the drive is at 45° to the screen deck, which means that a particle will be lifted in a straight line at 45° for the length of the stroke and then dropped vertically onto the screen deck. The stroke length will determine the frequency that a particle will make contact with the screen deck and have an opportunity to pass through the apertures, and also the velocity that the material will move along the screen length. This is one of the reasons why the relationship between aperture size and stroke is so important. If the stroke is too long in relation to the aperture size, the frequency with which particles contact the screen deck could be insufficient, resulting in carry over of undersize and poor efficiency. To change the velocity of material moving over a linear motion horizontal screen where the speed of the drive and G force are fixed, the deck can be inclined up to a maximum of 7° or down by 10°. This will result in an increase or decrease in retention time on the screen deck. An increase in retention time will also, however, increase the material discharge bed depth, which could also result in poor stratification if the discharge bed depth is greater than 4 times the aperture size. The converse is also true, if the velocity increases too much and the discharge bed depth reduces below 2 -3 times the aperture size, particles are not held down on the screen deck and will tend to bounce, resulting in a decrease in efficiency.

Linear motion horizontal screens are normally used on secondary or tertiary applications where the maximum aperture size is limited to approximately 45mm and the particle size to l50mm. The reason for this is that the maximum stroke achievable at 5 G's is approximately 18 mm, which is about the minimum length required for an aperture size of 45 mm The minimum stroke achievable is between 2-4 mm and the minimum aperture size is 0.3 mm, achieved using 4 pole motors rotating at 1440 RPM. The most common applications are sizing, dewatering, desliming, and drain & rinse.

Linear motion inclined screens also use twin counter rotating drives (excitors or vibrator motors, Fig. 1.8.5) but they are positioned at 9 o'clock and 3 o'clock, which results in the material being lifted vertically off the screen deck. For forward motion, the screen has to be inclined downwards a minimum of 15°. The inclination can be varied between 15° and 28° down. The different inclinations, at the same stroke, will increase or decrease the forward velocities accordingly. This type of screen will otherwise operate in the same way as a linear motion horizontal screen. A typical application would be for sizing materials up to an aperture size of 45 mm. The main reason for installing a linear motion inclined screen instead of a linear motion horizontal screen is that with the increased velocity of the inclined screen, higher throughputs can be achieved for the same screen size.

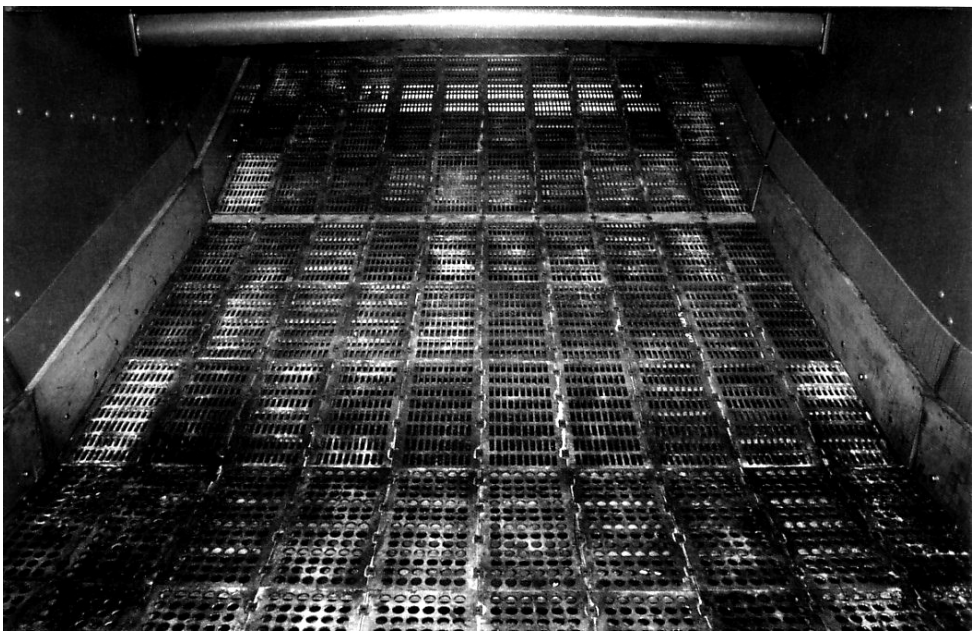

Fig. 1.8.6 - Multi-slope or "Banana" screen for ROM coal with steel and PU modular deck elements [Multotec / SACPS].

Linear motion multislope screen or "Banana" screen (Fig. 1.8.6): Linear motion multislope screens have the same drive action as linear motion horizontal screens but the screen deck consists of a number of sloped sections. Typically the top slope will be at 30 to 35° and the bottom slope 10 to 15°. Screens vary from between two and six slopes depending on the particle size and screening application. The major reason for using multislope screens in place of horizontal or inclined screens is to size large volumes of material with a high percentage of fines in the feed (60% and above). The higher material velocities, especially over the first two slopes of the screen, reduce the material bed depths allowing good stratification and the efficient removal of fines. Typically 60 % of the fines are removed in the first third of the screen. They can also be used in drain and rinse applications where static sieve bends are removed and replaced with a vibrating screen section which will handle the drainage function efficiently, followed by draining and rinsing on the almost horizontal sections. Dewatering applications can also be handled with the top slope being at approximately 20° down and the last slope inclined at 5° up.

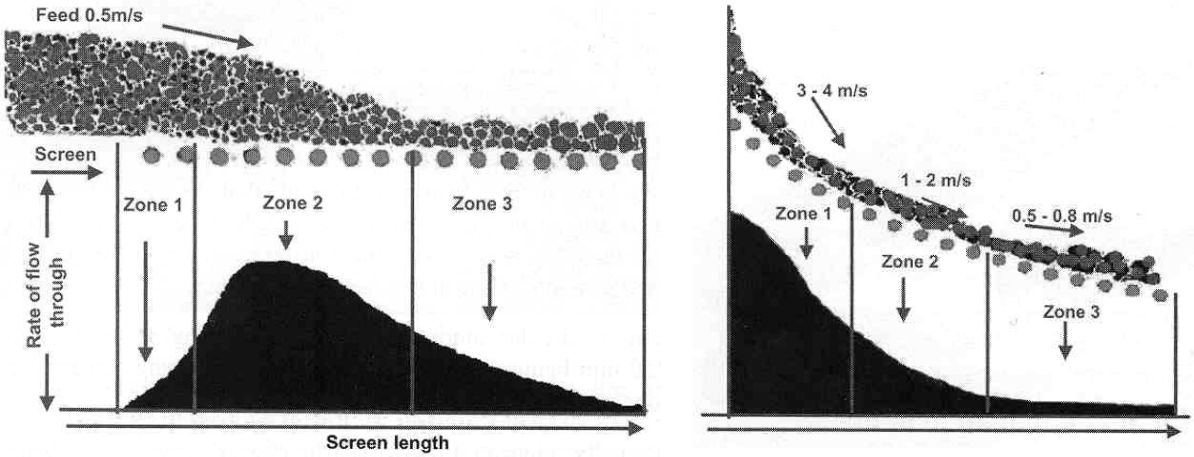

Fig. 1.8.7 - Horizontal (l) vs multislope (r) – comparative screen performance and product flow [SACPS].

Circular motion inclined screen: Circular motion inclined screens have the drive situated on the centre of gravity of the screen. The drive consists of a single eccentric mass rotating clockwise or anti-clockwise depending on the required retention time. The screen is inclined at between 15°...28° down and is varied to suit the required throughput, retention time and screening efficiency. The rolling action of circular motion allows for screening at much larger aperture sizes, up to approximately 250 mm being possible. These types of vibrating screens are normally used only for primary and secondary screening applications.

The drive will normally rotate in a clockwise direction allowing the maximum forward velocity and highest throughputs. However, if carry over of fines occurs, the drive can be reversed, increasing the retention time of the material on the screen deck. This can improve screening efficiencies by reducing the carry over of fines but with the reduced material velocities, the material bed depth will also increase. This could reduce stratification and also decrease screening efficiencies. If this happens, the only alternative is to reduce the amount of feed to the screen. Always try and keep the discharge bed depth between 3 and 4 times the aperture size to maximize screening efficiencies.

Elliptical motion inclined screen: Elliptical motion inclined screens work on the same principle as circular motion inclined screens but their drive is normally situated above or below the centre of gravity of the screen. If the eccentric drive is in the clockwise direction, the material initially moves forward in an elliptical motion, the material bed depth reducing as undersize passes through the screen apertures. Circular motion is experienced underneath the drive followed by a backward elliptical action at the discharge end of the screen, which causes the material bed depth to build up. The converse will apply when the drive is in an anti-clockwise direction. There will be a build up of material feeding onto the screen and a reduction in discharge bed depth as the material discharges off the screen. These types of screens are very cost effective as the drive is often a single vibrator motor, where a linear motion screen would require two motors. The vibrator motors are typically 40% of the cost of a linear motion screen. Even though they are not particularly efficient screens they can be used very effectively for sizing applications where the throughput is low.

Resonance screen: Resonance screens also operate using the same linear motion principles as a linear motion horizontal screen. With most screens, a lot of energy is used up in vibrating the screen, i.e. they require high-power motors. Due to the continuous change in the direction of the motion, much energy is wasted. Resonance screens are designed to reduce the energy requirements, allowing lower power motors to be used. The screen is mounted on flexible hanger strips, which are connected to a balance frame three or four times heavier than the screen itself. The balance frame is mounted on rubber pads. Movement is imparted to the screen by an eccentric drive and connecting rod. A rubber pad connects the rod to the screen. Rubber trippers restrict the movement of the screen and serve to store up energy, which is re-imparted to the screen frame. Hence, any movement given to the screen is transmitted to the balance frame. The throw of the balance frame is less than that of the screen because its mass is so much greater. Any motion thus given to the balance frame sets up vibrations that, instead of being wasted, are imparted back to the screening frame. Thus the loss of energy is reduced to a minimum. In certain types of resonance screen, the deck movement is restricted by a series of stops, which are attached to the deck and operate between buffers attached to the frame. In addition to storing energy, the sharp return motion of the deck imparts a lively action to the deck and hence promotes good screening.

Modular screen: The modular screen is a recent innovation in screening technology. It consists of a number of small linear motion screen modules, each consisting of two internal chassis plates, a twin vibrator motor drive, polyurethane screening media and mounted on Rosta-type isolation mounts. The modules can be placed side by side or in front of each other to form a screen of any size. Stresses are confined to each individual module and thus there is no limitation on screen dimensions. The modules can perform any normal screen duty associated with linear motion, horizontal or multislope configurations. In addition, they are lighter, use less power and are easier to maintain than conventional screens of a similar size.

Omni screen: Another new screen on the market is the Omni screen, which also uses the modular screen concept. It consists of single or double deck modules that have the drives positioned on the outside of the screen plates. The modules vary in width from 1.5 m to 3.05 m wide and 2.44m to 3.05m long. Modules are linked together in length to make up screens of whatever size is required. The advantage of this design is that it uses linear motion and the modular sections can be either horizontal or inclined to form multislope type screens.

Multi-deck screens: Some screens are equipped with more than one deck, and are known as double or triple deck screens, depending upon the number of decks they have. Double deck screens have two different aperture sizes of screen media. The larger aperture media is fitted above the smaller - such double-decked screens are used for pre-screening. Another use is dewatering. The meshes will be of the same order, hence the top deck helps to dewater the larger material and also screens a plus 12 mm (or 5 mm as the case may be) product. Consequently the top deck relieves the bottom deck resulting in the bottom deck being more lightly

loaded than if it had to handle the whole of the feed. It is, therefore, able to function more efficiently. It produces a 12 x 0.5 mm dewatered fraction and a minus 0,5 mm slurry in water.

Screens of two or more decks are rarely used in coal preparation. The major disadvantage of multi-deck screens is that the stroke is sized according to the upper deck aperture size. This is often too large for the bottom deck, resulting in poor screening efficiency as undersize particles are carried over. Multi-deck screens always result in a compromise with regard to the stroke and screen area. The screen area will be determined by largest screen area required. Regularly one of the screen decks is oversized. Ideally single deck screens should be used although this is not always practical. If multi-deck screens are used, try and keep the difference in aperture sizes between the decks to a minimum. Frequently applied multi deck screens are the circular Allgaier screen sets

1.8.3. Non-vibrating moving screens

Trommel screen (Fig. 1.8.8, l): Consists of a rotating trommel in which the cascading feed is fed from the entrance and conveyed by the angle under which the trommel is installed, or by lifter plates. Advantages are the simple (cheap) construction and absence of vibration loads on foundations. Disadvantages are low efficiency, low capacity, low self cleaning effect, and relatively high energy consumption (2...3 times more than vibrating screens). Despite the disadvantages the constructional advantages makes their application favourable for mobile or temporary operations (e.g. on dredges). They were more frequently applied in older plants, and apart from minerals processing operations, today they are extensively used in waste treatment, soil remediation and recycling applications. The material is kept in cascading motion, usually at speeds between 0.25 and 0.45 n_{crit} (see Eq. 1.3.6). Typical diameters are 0.8...1.5 m. They are applied for dry as well as wet screening. By installing several cylinders inside each other several products can be obtained with a single device. Specific capacity per mm mesh size is 0.15...0.2 $m^3/(m^2hmm)$ for dry screening and about 0.28 $m^3/(m^2hmm)$ for wet screening.

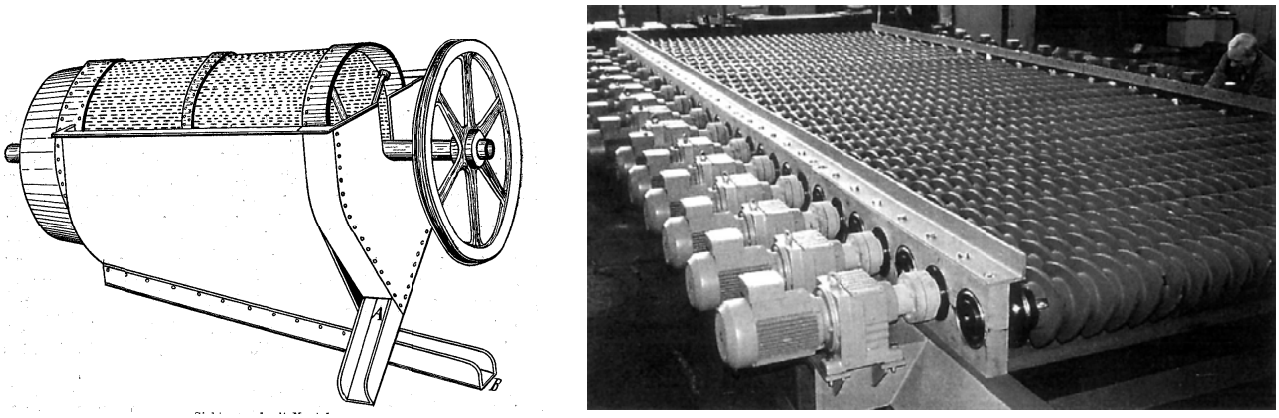

Fig. 1.8.8 - Trommel screen with SWF slots (l). Roller screen (r) [Schennen (l) / SACPS (r)].

Roller screen (Fig. 1.8.8, r): The roller screen consists of a number of elliptical rollers spaced across the screen length. The rollers rotate at a synchronised speed conveying the material down the screen length and allowing the finer particles to pass between the rollers. The elliptical shape of the rollers causes the particles to lift off the screen allowing efficient stratification and fines removal and also moves the material along the screen. The design and positioning of the elliptical rollers maintains a constant gap or aperture between the rollers. The roller-type screen is effective on wet sticky coal (moisture content between 5...20 %) that needs to be screened without the use of water sprays. Conventional vibrating screens would tend to blind on this type of application even using flexible screening media. Typically the roller screen is used on apertures below 10 mm. There are however units that have been developed for handling larger particles.

Screens specifically designed for sticky, moist dry fines, such as the **Mogensen Sizer**, **Flip-Flow** and **NCB's rotating probability screen**, are described in the next section.

1.8.4 Dry fines screening

As already mentioned in Section 2.7 the efficiency of screening is severely affected by moisture content. Already 1 Vol. % moisture may strongly deteriorate the efficiency, due to the formation of water bridges between particles, leading to agglomeration. This causes blinding and the excessive adherence of fines to the oversize. At a certain moisture percentage the point with "maximum stickiness" has been reached. From this point, adding water or drying makes screening easier. For coal this point is on average around 10%, for coarse coal only 1...2% but for fines up to 15...20%. For most rock and ore types the percentages are smaller, depending on rock density compared to coal. For a fair amount of clay being present the stickiness shows variations. In practical terms below 5 mm blinding problems may cause difficulties in industrial screening of moist feed, but applications downto 1 mm using special screen types are known. When screening moist feed is necessary, the problems can be relieved by:

- **Increase the forces** on the particles (increase K_v).
- **Drying** of the feed (needs lots of energy and an additional process step)
- **Adding water** to the feed (unfavourable if downstream dewatering and drying of the products is required)

Screens of high frequency and low amplitude are employed for dry applications. A typical ROM coal already contains 5...10% moisture due to dust spraying. For coal industrial dry screening is not employed below 6 mm. Some machines handle a moist feed rather well, without the need for adding water or drying. They are listed below:

Heated-deck screens: Stickiness is reduced by heating the mesh by electric currents.

Piano-wire decks: Individually tensioned pieces of piano-wire in the direction of flow avoid bridge formation by vibration of the wire. **Harp screens**, **duo-sieves** etc. have a corrugated wire shape and rely on the same principle.

Sta-Kleen decks: Captive rubber balls are mounted below a standard mesh. As the screen vibrates, the balls strike the mesh and destroy any bridges.

Probability screens: Normal screens have an aperture that is already ≈20% more than the effective cut-point. In probability screening apertures even considerably larger than the required cut-point are used. The apertures are staggered, so finally only small particles will pass all decks and report in the undersize. An example is the **Mogensen Sizer** (Fig. 1.8.9, l), having typically 5 staggered screen decks of decreasing aperture, all considerably larger than the cut-point. The staggering of decks are the reason that large particles tend to catch a screen wire and be deflected rather than pass an aperture, and let it report in the oversize even though the aperture would normally allow passage. Only particles small enough will finally pass all decks. Cut sizes can be between 50...0.1 mm. Another example of a probability screen is **NCB's rotating probability screen**, where the rotation speed of a disc with radial orientated rods in fact determines cut-size (Fig. 1.8.9, r). It was especially developed for dry fines pre-screening of ROM moist coal, a 2.4 m diameter disc having a capacity of ≈100 t/h for a <19 mm feed and cut-size of 4 mm.

Liwell Flip-Flow (or **Hein Lehmann**) screening machine (Fig. 1.8.10, l). It consists of two screen cases encased in each other. They are counter current wise oscillated. An elastic, wear resistant deck is alternately connected to the screen via cross beams, causing alternately tensioning and detensioning of the deck at 500...700 min^{-1}, leading to a trampoline-like screening action. The high acceleration forces prevent any pegging and blinding. It screens moist and sticky feed effectively.

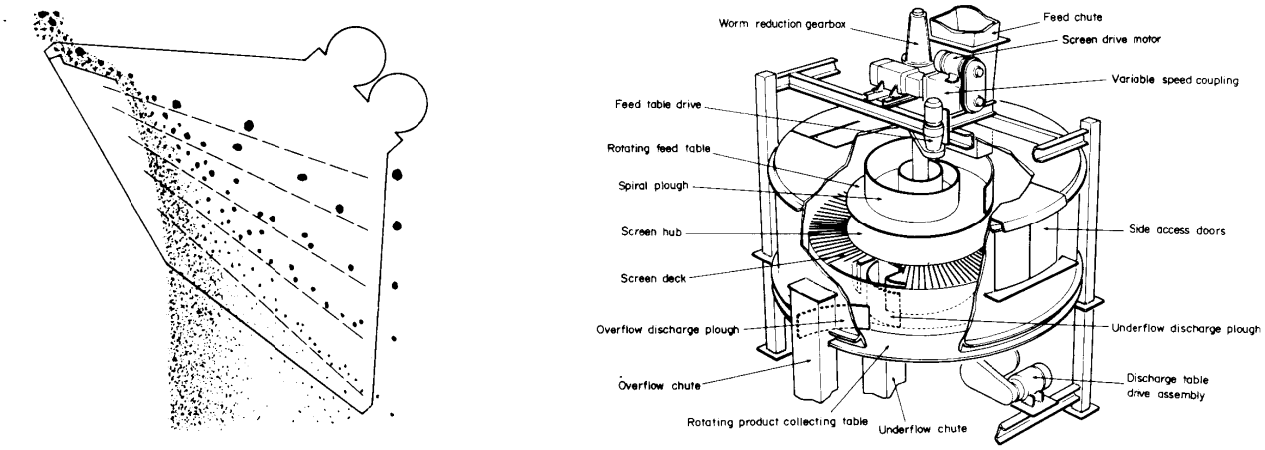

Fig. 1.8.9 - Principle of Mogensen Sizer (l). NCB's rotating probability screen (r) [Wills].

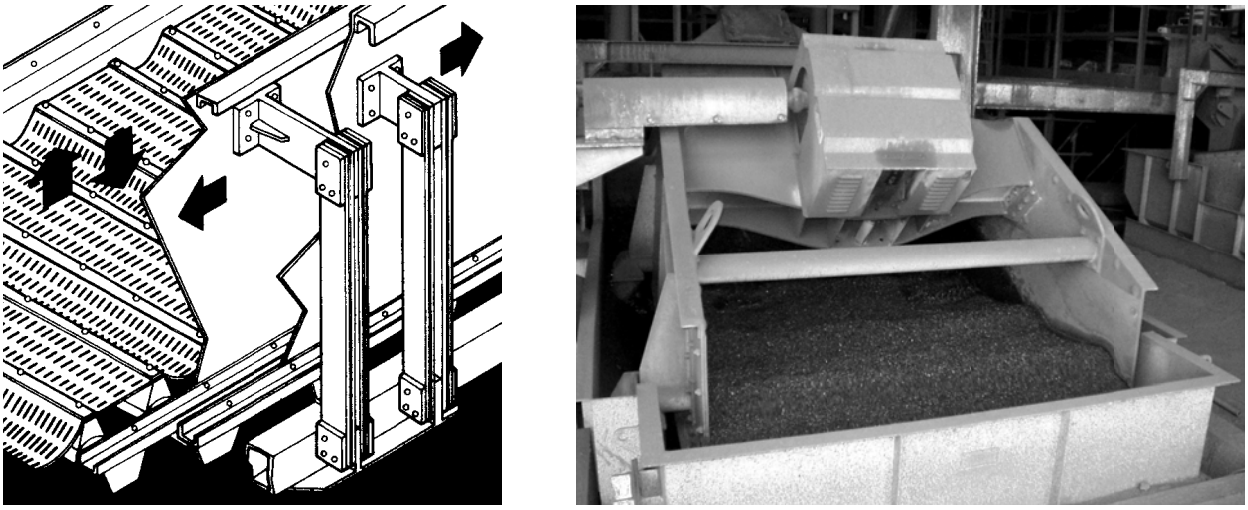

Fig. 1.8.10 - Flip Flow screen (l). Dewatering screen for mid-size coal (r) [Schubert Vol. 1 / TU Delft].

1.8.5 Wet fines screening

Apart from **sizing**, fines are screened for **dewatering**, **slurry cleaning** and **medium drainage**. Usually apertures in the range of 0.25...1 mm are used with wedge wire or fine PU screen panels operated at high-speed and small amplitude. These, and especially slurry cleaning, can be problematic (Fig. 1.8.11, l). A large part of the water quickly drains trough the mesh, leaving behind a thick paste blinding the screen. Addition of **spray-water** is an effective solution.

For first stage **dewatering** of fines linear motion vibrating screens are widely used. They are not very effective, especially when many superfines are present. Screens especially developed for dewatering purposed rely on producing a thick bed of fines, which moves slowly across the screen and compacts while expelling extraneous water, such as the Fordertechnik or Velco Reverse Slope screens (Fig. 1.8.10, r). Apart from being pushed through the screen, moisture may also be driven to the surface. The screen has a section that is inclined downward directly at the feed side and bending sharply upward at a given point, forcing the layer of cake to compress when it is pushed across this angle. Moisture levels of 4...9% lower than conventional screens can be obtained. For coal fines of 0.15...0.5 mm levels down to ≈28% are typical. Fig. 1.8.11, r, indicates obtainable maximum drainage rates as function of open area of the screen deck.

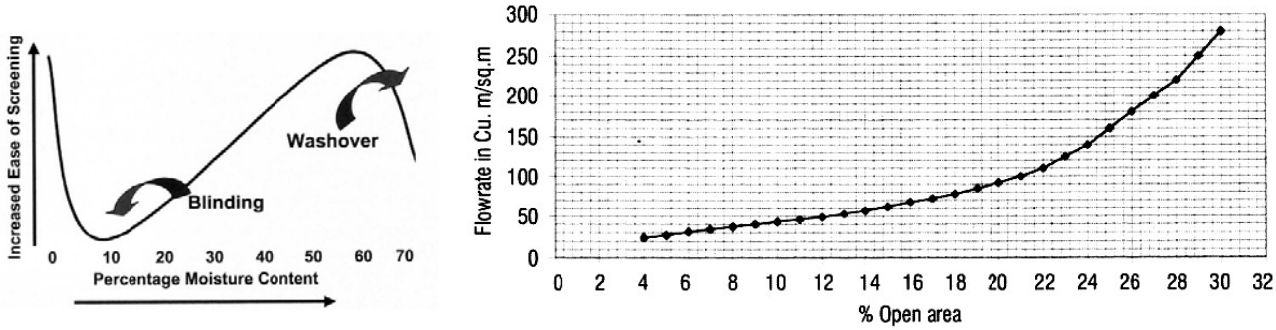

Fig. 1.8.11 - Effect of moisture on screening (l). Drainage rate as function of open area (pulp density ≈1400 kg/m^3 [SACPS].

1.9. Sieve analysis

Laboratory sieving methods are used to determine particle size distribution of a given sample. From top to bottom the particles pass a stack of calibrated sieves with decrementing mesh ($X_1>X_2>X_3>X_4>X_5$, Fig. 1.9.1, l). The sieves are mechanically or alternatively manually vibrated during a fixed time interval. Mechanical sieve shakers usually have a timer (Fig. 1.9.1, r). The weight percentage of each fraction between successive sieves (between m_i and m_{i+1}, Fig. 1.9.1, r) yields the size distribution. Usually test sieving can be carried out between about 75 mm and 38 µm, but exceptionally down to 5 µm with electroformed ultra-fine laboratory sieves. Sieve sets are standardised: ISO 565 (International), ASTM E11, E323 (USA), DIN 4188, 4187 (Germany), BS 410 (United Kingdom), NEN 2560 (Netherlands), GOST 3584 (Russia), Z8801 (Japan) or Tyler's standard screen scale sieve series. They are available in textbooks (e.g. Schubert Vol. I, 1989, p316-319 or SME Vol. 2, 1985, table 13, p30-32). Often only alternating sieves, in which the ratio of adjacent sieves falls in a √2 series, are used. Sieve size is often expressed in mesh size, being the number of square openings in the sieve per linear inch. Most sieve standards guarantee aperture sizes between 5% and 10%.

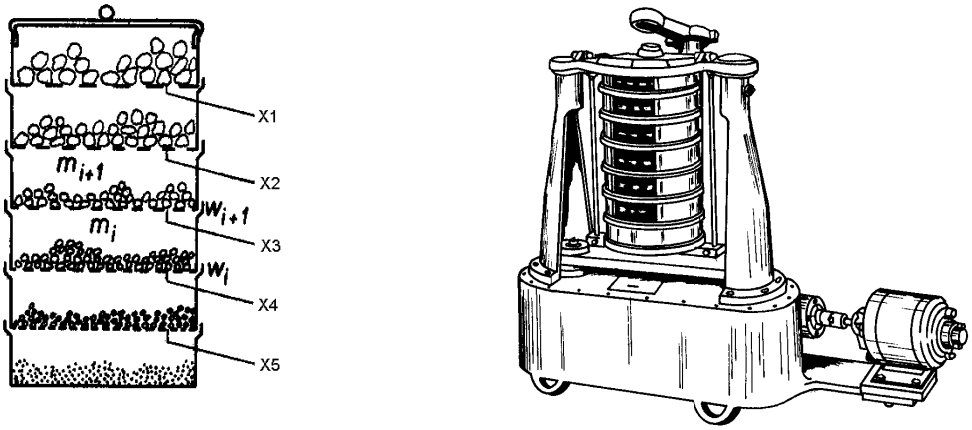

Fig. 1.9.1 – Stack of laboratory sieves (l). Testing sieve shaker (r) [Schumann Vol. I / SME].

The measured particle size d_p of a fraction retained between sieve sizes d_i and d_{i+1} is given by the geometric mean:

$$d_p = \sqrt{d_i d_{i+1}} \qquad (2.9.1)$$

In test sieving, as in industrial screening (Section 2.3) three kinetic regions are distinguished: I=rapid weight loss, II=transition and III=equilibrium (Fig. 1.9.2).

A premature endpoint is reached when the sieves become blinded, e.g. due to agglomeration (upper curve Fig. 1.9.2). This is caused by material that is not properly dried and is around the "maximum stickiness" point (Section 2.8.4), or by unfavourable particle shape. In the latter case the sieving should be stopped periodically to push out the particles sticking into the screen with a brush.

Equilibrium may never be reached sieving some types of soft material or material with brittle sharp edges, due to breakage (lower curve, Fig. 1.9.2). Therefore, a proper endpoint depends on weight, hardness, shape and actual size distribution of the material.

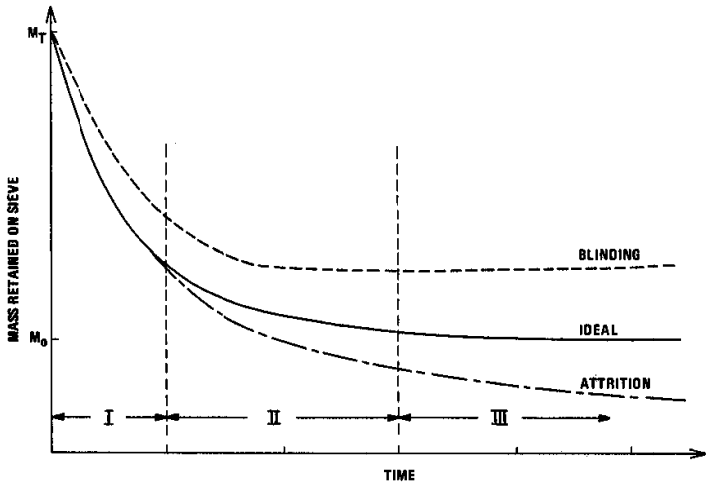

Fig. 1.9.2 – Sieving kinetics [SME].

Sieve analyses are carried out dry, wet or combined. The following combined method (Table 1.9.1 can be used) has been found to provide accurate results, though simplified methods may be applied in routine practice:

1. Take about 500 g of representative sample.
2. Wash it with water on a 38µm (400 mesh) screen to remove ultra-fines, collect the wash water with fines, filter, dry, and determine its weight.
3. Dry all >38µm (400 mesh) material.
4. Select an appropriate series of screens, have them cleaned and weighted. Check if the mesh is undamaged.
5. Place a pan at the bottom of the sieve stack, and pour the dried material onto the top sieve (see Fig. 1.9.1, l).
6. Shake the sieve set(s) mechanically (when available) or manually for a specified time period, usually >20 min.
7. Determine the weight retained on each sieve with a top loading balance (accuracy <0.1 g), subtract the tare (empty) weight of the screen.
8. Repeat 6 and 7, until the difference in weight between two successive intervals is less than 0.5%.
9. Calculate the fraction in each interval, including the washed <38µm material and bottom pan fraction. Round the fractions to the nearest tenth of 1%.
10. The (cumulative) distribution fuction can be plotted, e.g. on Rosin-Rammler paper, after adding all fractions finer than each sieve opening (Fig. 1.9.3).

For ultra-fines sieving (<40µm) specific laboratory equipment and methods are available (Alpine air swept, felvation, etc.).

Table 1.9.1 – Sieving data sheet

Sample ID:_____

Total sieving time:___ min

top X bottom sieve size [mesh or µm]	bottom size [µm]	empty sieve mass, (dry and clean) [g]	sieve + sample mass [g]	nett sample mass [g]	interval fraction [%]	fraction finer than bottom size (cum. undersize) [%]
___ X ___	_____	_____	_____	_____	_____	_____
___ X ___	_____	_____	_____	_____	_____	_____
___ X ___	_____	_____	_____	_____	_____	_____
___ X ___	_____	_____	_____	_____	_____	_____

___ X ___ ___ X ___ ___ X ___ ___ X ___ ___ X ___ ___ X ___ ___ X ___ ___ X ___ ___ X ___ ___ X ___	_____ _____ _____ _____ _____ _____ _____ _____ _____ _____	_____ _____ _____ _____ _____ _____ _____ _____ _____ _____	_____ _____ _____ _____ _____ _____ _____ _____ _____ _____	_____ _____ _____ _____ _____ _____ _____ _____ _____ _____	_____ _____ _____ _____ _____ _____ _____ _____ _____ _____	_____ _____ _____ _____ _____ _____ _____ _____ _____ _____
Bottom pan fines Washed fines Total fines				_____ _____ _____	_____	
Total sample weight				_____		

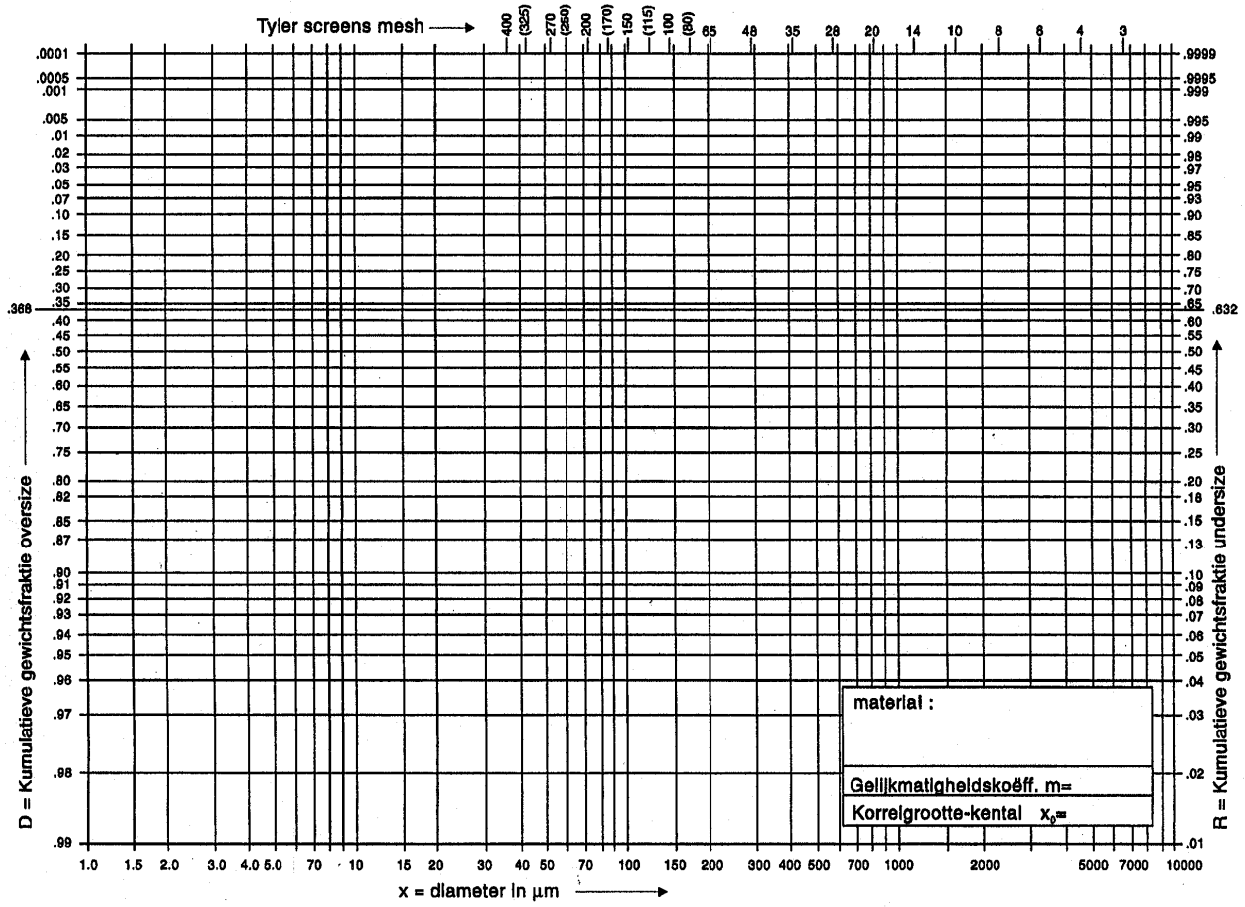

Fig. 1.9.3 - Rosin-Rammler paper for plotting sieve size distribution. Cumulative oversize on left Y-axis, cumulative undersize on right Y-axis, sieve size in µm on lower X-axis, in mesh on higher X-axis.

Typically the size distribution shows a linear appearance on RR scale (Fig. 1.9.3). As a consequence it can be described by only two parameters. Usually these are the gradient being m= tan (α) that indicates the spread of the size distribution and x_0, the cumulative oversize percentage at 36.8% (being 100%*1/e).

1.10. References

England, T. (editor): Coal preparation in South-Africa. The South African Coal Processing Society, 2002.

Fontein, F.J.: Das Bogensieb der niederländischen Staatsmijnen, ein neues Gerät zur nassen Siebung von Feinkohle. Glückauf 91, 27/28, S. 781-786, 1955.

Kluge: Erdöl und Kohle, 4 Jg. H. 11, p 705-11, 1971.

Schranz, Bergholz: Bergbauwissenschaften, 1 Jg, H. 8, p 223-234, 1954.

Schubert, H.: Aufbereitung fester mineralischer Rohstoffe. VEB Deutscher Verlag für Grundstoffindustrie, Leipzig, 1989.
Testut, Revue de l'Industrie Min., Doc. S.I.M. LI, 1958.
Whitby: ASTM Technical Publications No. 234, p 3-23, 1958.

2. CLASSIFICATION

2.1. Introduction

The separation of solid bodies is named grading or classification. It can be defined as splitting up a mixture into two or more fractions, each of which is more uniform in a certain property than the original mixture. When use is made of differences in the velocity of particles in a fluid, we speak of pneumatic or hydraulic classification.

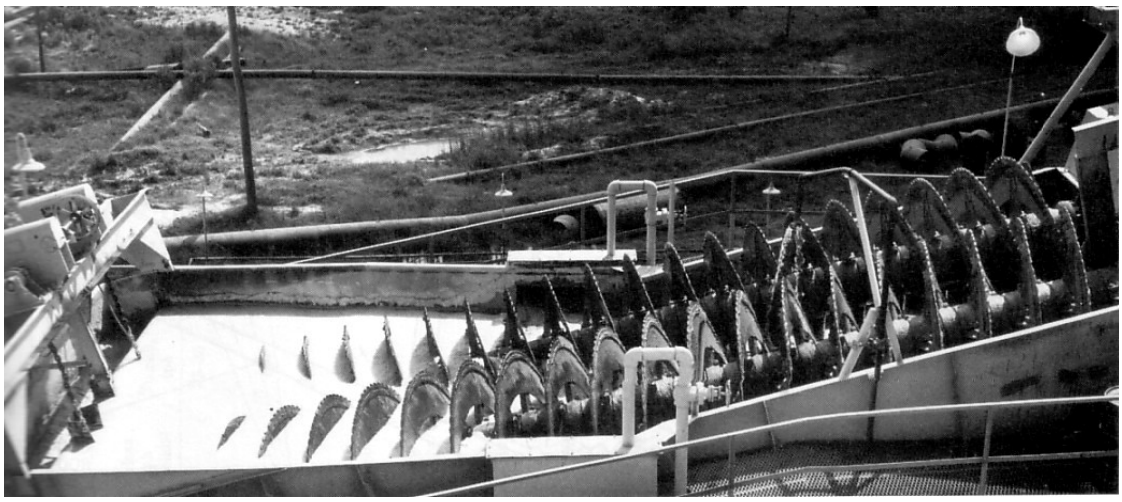

Fig. 2.1.1 - Duplex screw classifier [SME].

In many grinding circuits classifiers separate material fine enough and return oversize product to the mill, hence avoiding overgrinding. Pneumatic classification is sometimes called wind-sifting; it can be carried out in the following ways (Fig. 2.1.2, Rietema et al., 1961):

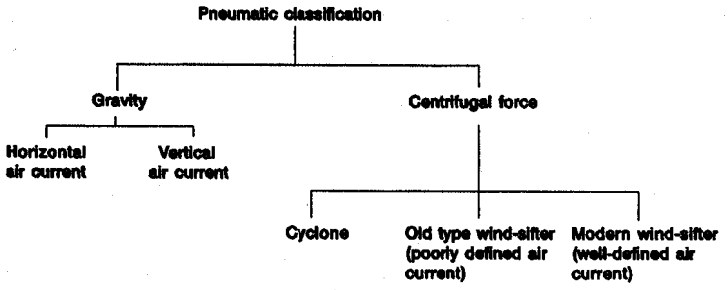

Fig. 2.1.2 - Pneumatic classification.

Classification in an air current is sometimes an attractive technique and it is generally not very expensive. If the particles become small, however, separation from the air flow becomes increasingly difficult and a centrifugal force may be necessary to achieve the desired separation. This can be accomplished in a cyclone, of which the dimensions and operational conditions are so chosen that the fine fraction passes through the overflow and the coarse fraction is obtained in the underflow. Hydraulic classification bears great resemblance to wind-sifting, and it can also be carried out under the force of gravity or by means of a centrifugal force (Fig. 2.1.3).

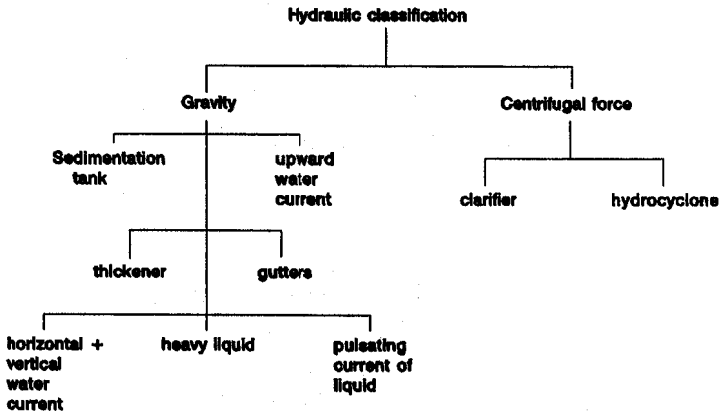

Fig. 2.1.3 - Hydraulic classification.

For understanding the classification mechanism, settlling theory is studied in Section 3.2. Secondly, a number of frequently applied hydraulic and pneumatic classifiers are discussed in Secxtions 3.3 and 3.4. Section 3.5 concludes with cyclone theory and introduces some specific cyclone classifiers.

2.2. Motion of particles through fluids

[From Coulson & Richardson, 1991]

2.2.1 Free settling of spheres

Many processes for the separation of particles depend on the variation in the behaviour of the particles, when they are subjected to the action of the moving liquid. In 1851, Stokes (1851) calculated from purely theoretical considerations, the drag force exerted on a sphere moving at low velocity (laminar flow) in an infinite extend of continuous fluid:

$$F_d = 3\pi\mu d v \tag{2.2.1}$$

where F_d = the drag force
μ = viscosity of the fluid
d = diameter of the sphere
v = velocity of the fluid relative to the particle

In describing physical transport phenomena, it is common to introduce a friction factor f, or drag coefficient, which is defined as:

$$f = \frac{F_d}{EA} \tag{2.2.2}$$

where E is the characteristic energy per unit volume of fluid and A the characteristic area on which the force is considered to act.

The characteristic energy can be taken as:

$$E = \frac{1}{2}\rho_f v^2 \tag{2.2.3}$$

where ρ_f is the fluid density.

The area of a sphere is:

$$A = \frac{1}{4}\pi d^2 \tag{2.2.4}$$

hence Eq. (2.2.2) becomes for laminar flow (Re<1):

$$f = \frac{24}{\mathrm{Re}} \tag{2.2.5}$$

where

$$\mathrm{Re} = \frac{\rho_f v d}{\mu} \tag{2.2.6}$$

is the particle Reynolds number.

At high Reynolds numbers (Re>500, turbulent flow), the flow around the particle shows a constant drag coefficient:

$$f \approx 0.44 \tag{2.2.7}$$

Between the laminar (Re<1) and turbulent (Re>500) regions is a transition zone (1<Re<500), where the drag coefficient can be approximated by:

$$f \approx \frac{18.5}{\mathrm{Re}^{0.6}} \tag{2.2.8}$$

0.5f as function of Re is given in Fig. 2.2.1.

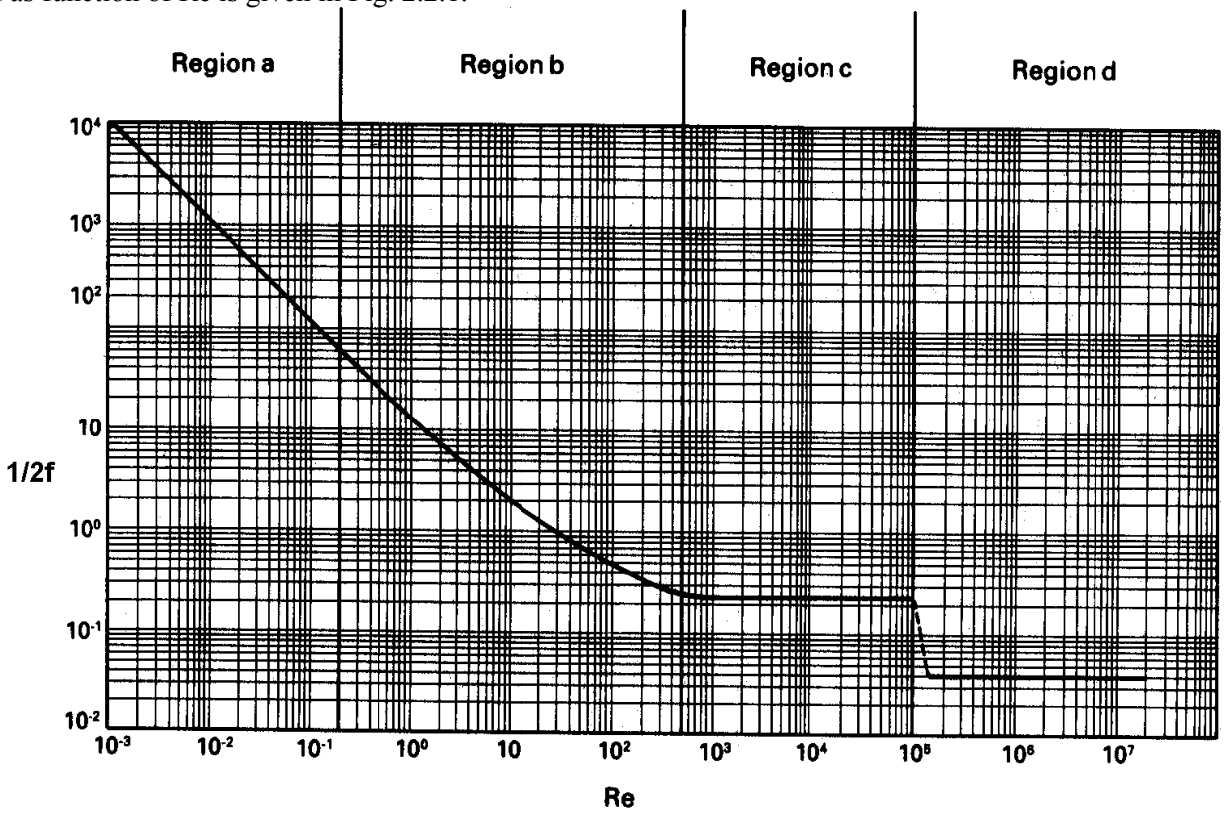

Fig. 2.2.1 – 1/2f as function of Re [Coulson & Richardson]. Region a = laminar, region b = transition, region c = turbulent (region d only rarely occurs in minerals processing applications).

When it is assumed that the settling of a particle is not hindered by the presence of other particles, then expressions can be derived for the terminal falling velocity v_0 of the particle. When the terminal falling velocity of the particle is reached, drag force, gravity and buoyancy force are in equilibrium:

$$F_d = F_g + F_b \tag{2.2.9}$$

or

$$f \cdot \frac{1}{2}\rho v_0^2 \cdot \frac{1}{4}\pi d^2 = \frac{1}{6}\pi d^3(\rho_s - \rho_f)g \tag{2.2.10}$$

from which

$$v_0^2 = \frac{4d(\rho_s - \rho_f)g}{3f\rho_f} \tag{2.2.11}$$

where ρ_s = particle density
g = gravity acceleration

In the laminar region, f = 24/Re. Substitution in Eq. (2.2.11) yields:

$$v_0 = \frac{1}{18}\frac{d^2(\rho_s - \rho_f)g}{\mu} \qquad (2.2.12)$$

Equations for the other flow regions can easily be obtained by substitution of the appropriate equation for f in Eq. (2.2.11).

In systems where centrifugal acceleration is present rather than gravitational acceleration, the equations can be rewritten by replacing the gravitational acceleration g by the centrifugal acceleration $\omega^2 r$, where r is the radius of rotation and ω the angular velocity.

Example 2.2.1

What will be the setting velocity of a 0.4 mm spherical steel particle with density 7870 kg/m^3? The oil density is 820 kg/m^3 and the viscosity 0.01 Ns/m^2.

Solution:

$$v_0 = \frac{1}{18}\frac{(0.4*10^{-3})^2(7870-820)9.81}{0.01} = 0.061\, m/s$$

Check:

$$\mathrm{Re} = \frac{\rho v_0 d}{\mu} = \frac{820*0.061*0.4*10^{-3}}{0.01} = 2.0$$

hence the flow conditions are laminar.

Example 2.2.2

A spherical sand particle with density 2750 kg/m^3 settles freely in water. If the particle Reynolds number is 0.1, calculate the particle diameter. The viscosity of water is 0.001 Ns/m^2, the density 1000 kg/m^3.

Solution:
Using Eq. (2.2.12) gives:

$$v_0 = \frac{1}{18}\frac{d^2(2750-1000)9.81}{0.01} = 9.5410^5 d^2\ m/s$$

The Reynolds number then becomes:

$$\mathrm{Re} = \frac{1000*9.5410^5*d^2*d}{0.001} = 0.1$$

from which d = 4.76 10^{-5} m.

In many cases, the flow regime is not known at the start of the calculation. If it is not known whether the flow is laminar, turbulent or in the transition zone, the terminal falling velocity can be found by computing

$$\mathrm{Re}^2 f(\mathrm{Re}) = \frac{2\rho d^2}{\mu^2 A} F_d = \frac{4d^3\rho_f(\rho_s - \rho_f)g}{3\mu^2}(sphere) \qquad (2.2.13)$$

first. Then the Reynolds number can be read from a graph of $0.5f(Re)Re^2$ against Re (Fig. 2.2.2) and the terminal falling velocity is given by

$$v = \frac{\mu \mathrm{Re}}{\rho_f d} \qquad (2.2.14)$$

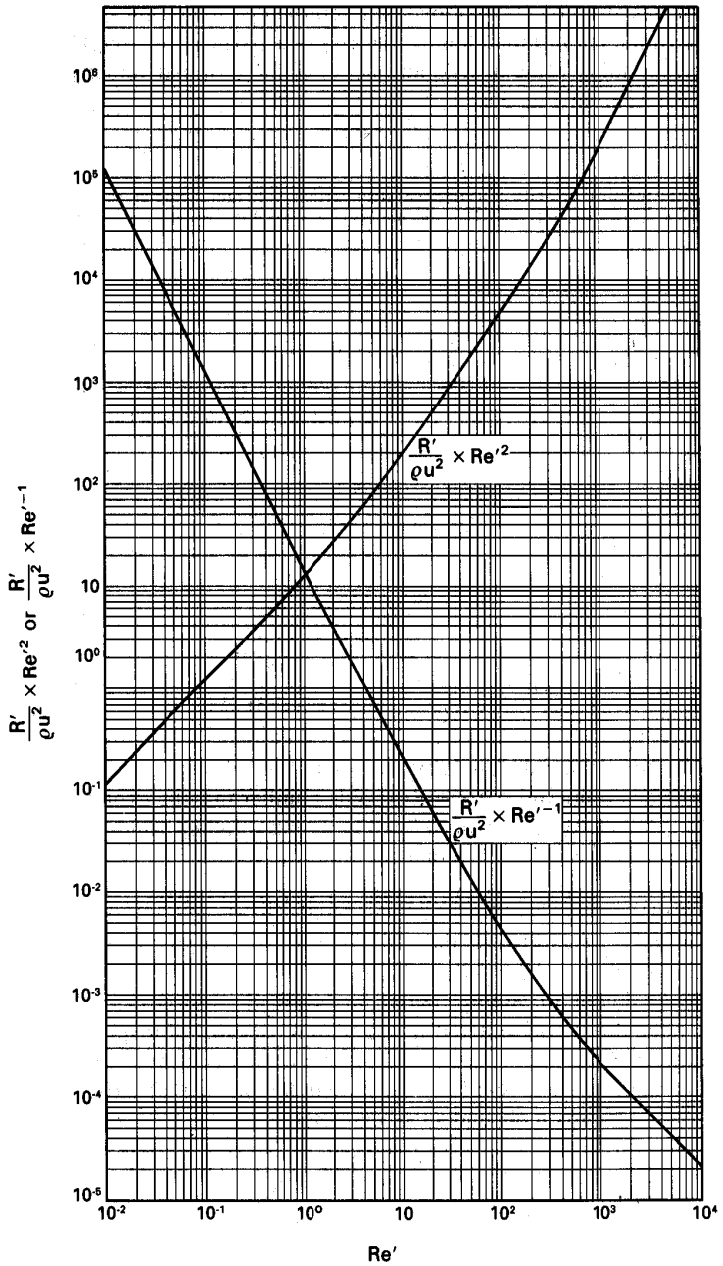

Fig. 2.2.2 – $0.5fRe^{-1}$ (declining) and $0.5fRe^2$ (rising) as function of Re (with $0.5f=R'/\rho u^2$) [Coulson & Richardson].

2.2.2 Effect of shape and orientation on drag

A spherical particle is unique in that it presents the same surface to the oncoming fluid, whatever its orientation. For non-spherical particles, however, the orientation must be specified before the drag force can be calculated. The experimental data for drag can be correlated in the same way as for the sphere by plotting the drag coefficient f against the Reynolds number. The diameter of the particle is now defined as the diameter of the circle, having the same area as the projected area of the particle, and is therefore a function of the orientation, as well as the shape of the particle. The curve for f against Reynolds can be divided again in a laminar region, turbulent region and transition region. In the laminar region, the flow is entirely streamline and practical data suggests a correlation of the form:

$$f = \frac{K}{\mathrm{Re}} \qquad (2.2.15)$$

The constant K varies somewhat according to the shape and orientation of the particle, but always has a value of about 24.

In this region, a particle falling freely under the action of gravity, will normally move with its longest surface parallel to the direction of motion. In the transition region, a freely falling particle will tend to change its orientation as the value of the Reynolds number changes and some instability may be apparent. In the turbulent region, the particle will tend to fall so that it is presenting the maximum possible surface to the oncoming fluid. Typical values of f in this region are shown in Table 3.2.1.

Table 2.2.1 - Friction coefficient for non-spherical particles [Coulson & Richardson].

Thin rectangular plates, planes perpendicular to direction of motion		
length/width =	1-5	f =1.2
	20	1.5
	infinity	1.9
Cylinders with axes parallel to the direction of motion		
length/diameter =	1	f =0.9
Cylinders with axes perpendicular to the direction of motion		
length/diameter =	1	f =0.6
	5	0.7
	20	0.9
	infinity	1.2

It should be noted that the friction coefficients for non-spherical particles are higher than the value 0.44 for a spherical particle.

2.2.3 Other correction factors

A number of other factors may have to be considered when treating the flow of particles through a fluid. The most important one is hindered settling, which will be discussed in a later chapter. Although generally not important in full size operations, a wall effect may be significant in laboratory testing. This problem arises because the moving particle pulls fluid along with it, and in the vicinity of the stationary wall, the fluid movement is slowed, resulting in an apparent increase in drag coefficient.

The drag forces computed with formula 3.2.2 relate to steady motion, i.e. the particles are assumed to have constant speed. If the particles are accelerated, the difference between the gravity and buoyant force on the one hand and the drag force on the other is used for the acceleration of the particle and part of the fluid around it:

$$F_g + F_b - F_d = m_p a + m_f a \qquad (2.2.16)$$

where m_p = mass of particle
m_f = mass of accelerated fluid (added mass)

For laminar flow and spherical particles the volume of the fluid that is accelerated amounts to half the volume of the particle.

2.2.4 Fluidisation and sedimentation

Hydrodynamically there is little difference between fluidisation and sedimentation, both can be considered as an expanded packed bed where the particles are free to move relative to one another. Fluidisation and sedimentation are distinguished by whether the fluid or solid moves relative to the containing vessel. If a fluid is passed through a bed of unrestrained particles, the pressure drop will increase until a point is reached where the pressure drop and weight just counteract the buoyancy forces. Provided the bed is free flowing, it will start to behave like a boiling liquid. Such a bed is said to be fluidised. If the fluid velocity is increased further, the bed continues to expand and eventually, as the terminal velocity is approached, the particles are entrained in the fluid. The minimum fluidisation velocity is the velocity where the bed just starts to be fluidised. Above this minimum velocity, the pressure drop increase is negligible as the velocity increases. With smooth particles, the point of minimum fluidisation is not a sharp feature. Irregularly shaped particles may cause a peak on the Δp-ν curve, due to particle interlocking (thin line in Fig. 2.2.3).

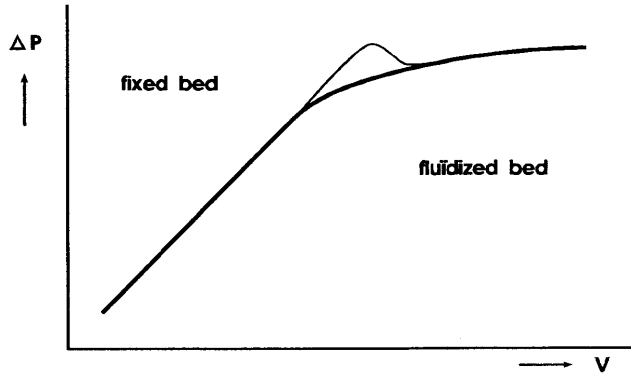

Fig. 2.2.3 - Pressure drop vs superficial velocity in a fluidised bed.

Sedimentation or hindered settling represents the opposite of fluidisation. Generally the particles accelerate rapidly and settle at their terminal velocity, producing an interface between the clear liquid and the slurry. As the particles settle, an interface between settled and settling particles rises from the bottom. Eventually the two interfaces meet, after which the settled particles go through a process of compression, which involves very slow settling.

The pressure drop for flow through a fixed bed has been determined empirically. It can be described by the Ergun equation:

$$\frac{\Delta P}{H} = \frac{1-\varepsilon}{\varepsilon^3 d_{vs}}\left(\frac{150(1-\varepsilon)\mu v_s}{d_{vs}} + 1.75\rho v_s^2\right) \qquad (2.2.17)$$

where ΔP = pressure drop
H = height of the bed
ε = volume of voids/volume of the bed
v_s = superficial velocity, the average linear velocity of the fluid if no particles were present
d_{vs} = the volume surface diameter of the particle = $6V_p/S_p$
V_p = volume of the irregular particle
S_p = surface area of the irregular particle

For the gas flow through a fluidised bed, an equation similar to the Ergun equation has been found:

$$\frac{\Delta P}{H} = \frac{1-\varepsilon}{\varepsilon^3 d_{vs}}\left(\frac{200(1-\varepsilon)\mu v_s}{d_{vs}} + 3.0\rho v_s^{\,2}\right) \qquad (2.2.18)$$

An alternative and better approach to fluidisation and sedimentation of uniform spherical particles is to use empirical relationships. One of the most widely known is the one by Richardson and Zaki (1954, 1961):

$$\frac{v_f}{v_0} = \varepsilon^n \qquad (2.2.19)$$

where v_f = falling velocity of suspension with respect to a fixed horizontal plane (sedimentation), or superficial velocity (fluidisation)
v_0 = terminal velocity of a single particle at infinite solution

The exponent n can be approximated by Table 2.2.2:

Table 2.2.2 – n as function of Re_p

n	Re_p
4.65	<0.2
$4.35Re^{-0.03}$	0.2-1
$4.45Re^{-0.1}$	1-500
2.4	>500

where Re_p, is the Reynolds number based on terminal velocity:

$$Re_p = \frac{d\rho_f v_0}{\mu} \tag{2.2.20}$$

2.2.4.1 Flux curves

In some situations, in stead of considering the settling rate ν, it is more useful to consider the flow rate of particles per unit area, the solids flux ψ, which is given by:

$$\psi = Cv \tag{2.2.21}$$

where ψ = mass flux of particles
C = concentration, mass per unit volume

Since 1 - C/ρ_s = ε and ν can be represented by Eq. (2.2.19), the solids flux becomes:

$$\psi = v_0(1-\varepsilon)\rho_s \tag{2.2.22}$$

which results in the characteristic flux curve for sedimentation, shown in Fig. 2.2.4.

It can be seen that a low solids flux occurs at low solids concentrations, when few particles are present, and at high concentrations, when settling becomes severely reduced by hindrance effects.

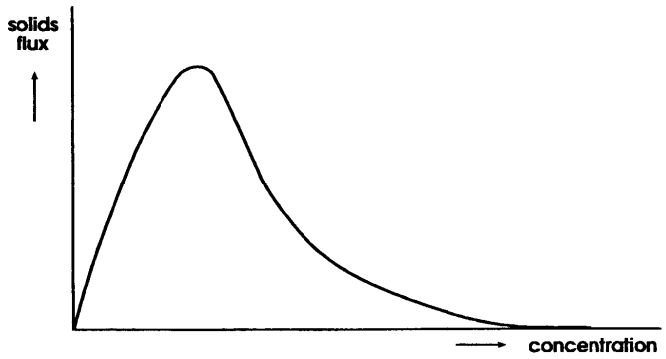

Fig. 2.2.4 - Sedimentation flux curve.

2.2.4.2 Settling ponds

Some mineral processing units behave like an ideal settling pond. Essentially this is a pond in which slurry is fed at the one side and the overflow at the other side of the pond contains a much lower solids content. This is illustrated in Fig. 2.2.3.

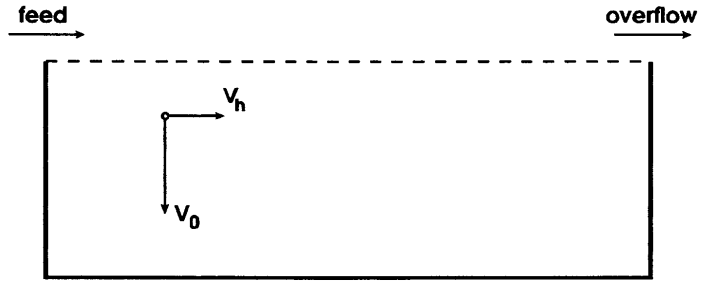

Fig. 2.2.3 - Velocity components of a particle in a settling pond.

The particles have a horizontal velocity component equal to the horizontal liquid velocity; they are also subjected to gravitational settling forces and thus have a vertical velocity component as well. The limiting size of a particle is that which can just settle the depth of the pond during passage. The time t_0 to settle the depth H of the pond is:

$$t_0 = \frac{H}{v_0} \tag{2.2.23}$$

which is also equal to the residence time τ, the time to travel the length L of the pond:

$$\tau = \frac{L}{v_h} \tag{2.2.24}$$

However,

$$v_f = \frac{F_v}{WH} \tag{2.2.25}$$

where F_v = volumetric flow rate of the slurry
W = width of the pond
H = height of the pond

resulting in

$$v_0 = \frac{F_v}{WL} = \frac{Fv}{A_t} \tag{2.2.26}$$

where At = surface area of the pond.

This shows a significant feature of settling ponds; the ability to capture a particle is <u>independent</u> of the depth of the pond. In practice, concentration gradients and non-ideal plug flow conditions will exist, resulting in a required area being greater than the conventional area. The areal efficiency η is defined as:

$$\eta = \frac{\text{theoretical surface area}}{\text{actual surface area}} * 100\% \tag{2.2.27}$$

Values of η are usually in the order of 50-100%, at higher concentrations and flow rates, η may be significantly lower.

2.3. Hydraulic classifiers

Three different hydraulic classifiers are distinguished:

- Clearing cones
- Mechanical classifiers
- Rising current classifiers

They are discussed in the next sections 2.3.1 to 2.3.3.

2.3.1 Clearing cones

The design principle is that the coarse fraction is withdrawn with the minimum amount of liquid, while the fines pass with the mass of liquid to the overflow (Fig. 2.3.2, left). Its basic design is over 200 years old, but it is still widely applied in e.g. sand classification and coal slurry thickening. In square classifiers the feed usually is added to one end, while in cone classifiers it is fed centrally. Wall angle should not exceed 30^o to the vertical to prevent settling on the sides. Design objective is to maintain laminar flow conditions inside. Clearing cones are applied for feed sizes up to 3 mm, with cut sizes 0.025...0.1 mm. Automated withdrawal mechanisms for the settled coarse material, operating at constant rate, are important for sufficient separation sharpness. Better results are obtained with multi-stage cells (Fig. 2.3.1).

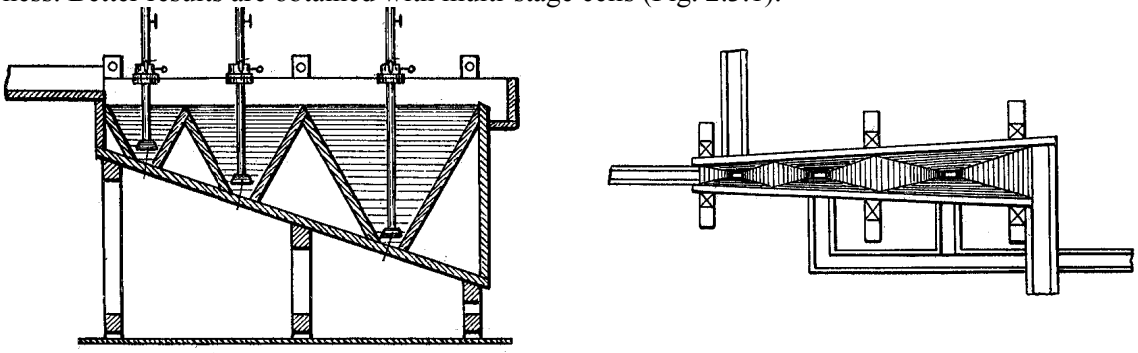

Fig. 2.3.1 - 19th century "Harz" horizontal classifier [Schennen].

2.3.2 Mechanical classifiers

Mechanical classifiers have an elongated, inclined settling basin with an approximately central feed (Fig. 2.3.2, r). A screw mechanism (Fig. 2.3.3), or in other variants an oscillating rake (Fig. 2.3.4), slowly conveys the settled material upward, while the fines are carried over a weir. A classifier may contain more than one screw or rake (duplex mode, Fig. 2.3.3). They are mainly applied in grinding circuits, combined with ball mills (Chapter 3), but also for desliming and dewatering of sands or sandy products. Capacity is proportional to width of the settling through. Inclination of the through is limited by the backflow properties of the sand. It is 10^o...15^o for rake classifiers and 14^o...18^o for screw classifiers. The latter have a continuous conveying action, which permits a higher inclination angle. For the same reason they are preferred in ball mill grinding circuits, since in less floor space they are able to carry the sand higher for return into the mill. Therefore usually screw classifiers are preferred and rake classifiers are only operating at older plants. In modern grinding circuits, mechanical classifiers are more and more replaced by cyclones for fines classification in the 50...250 μm range (Section 2.5) and screens for larger cut-sizes in the mm range (Chapter 1). However, especially screw classifiers remain important in many circuits for classification at larger cut-sizes (mm range).

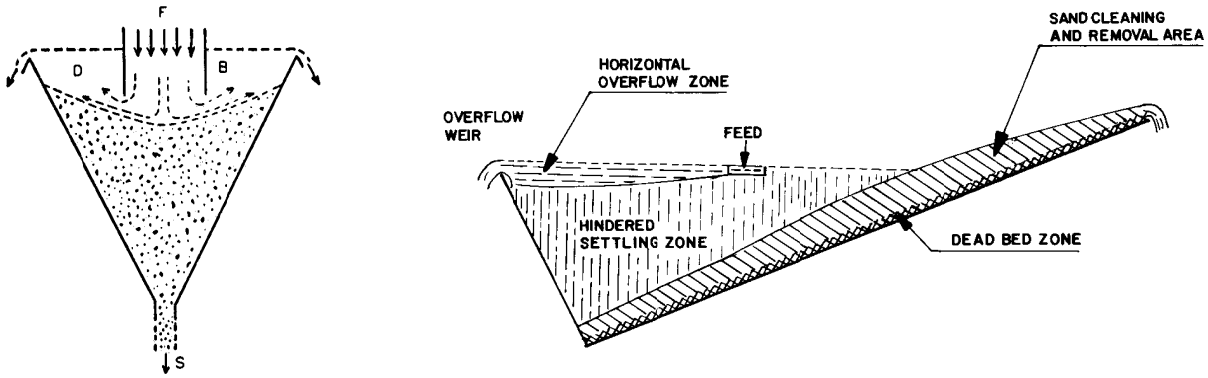

Fig. 2.3.2 - Settling cone principle, F=feed, B=feed cylinder, D=classificvation zone, S=spigot discharge (l). Principle zones of mechanical classifier (r) [Wills / SME].

Typical through lenths of screw classifiers are 3...12.5m at widths of 0.75...6.5m. The higher the overflow weir, the smaller the cut size. When the screw is fully submersed in the lower end, cut sizes down to 100µm are possible.

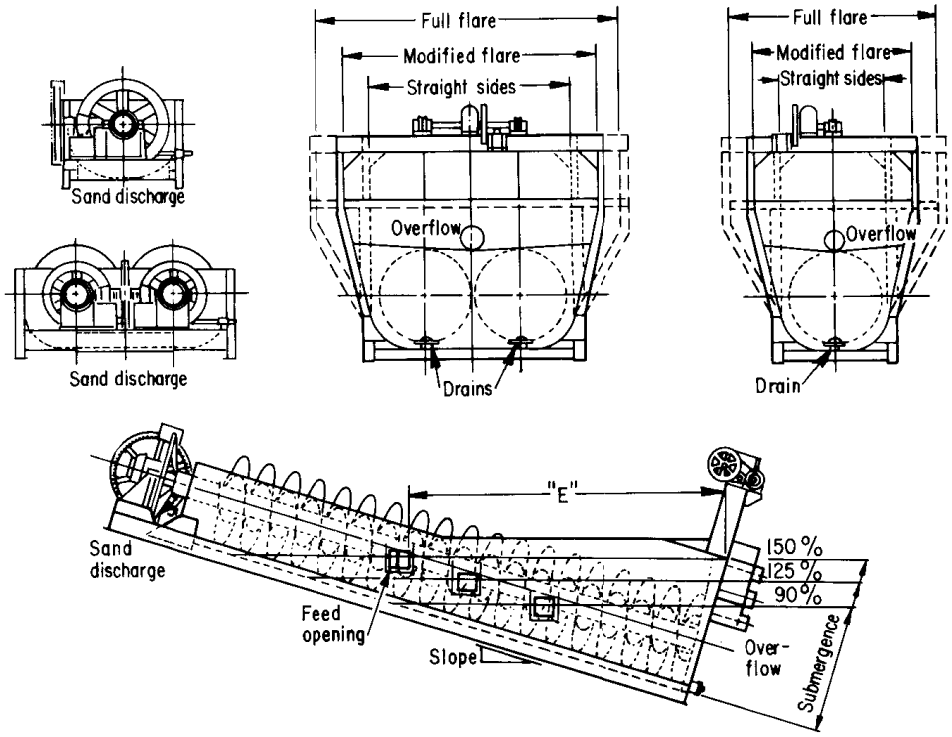

Fig. 2.3.3 - Single and duplex screw classifier design [SME].

The overflow solids capacity of screw classifiers with an average weir height is given by the following empirical expression [Published in Schubert Vol. I, from an earlier Russian reference]:

$$C_{s\_over} = 4.55 N_S D_S^{1.765} k_d k_\rho k_\beta k_D \text{ t/h} \qquad (2.3.2.1)$$

where N_S is the number of screws (see Fig. 2.3.5), D_S screw diameter, and $k_{d,\rho,\beta,D}$ correction factors. $k_\rho=\rho/2700$, valid for $2000<\rho<5000$ with ρ the solid density in kg/m^3. The other factors are given in Table 2.3.1 ... 2.3.3.

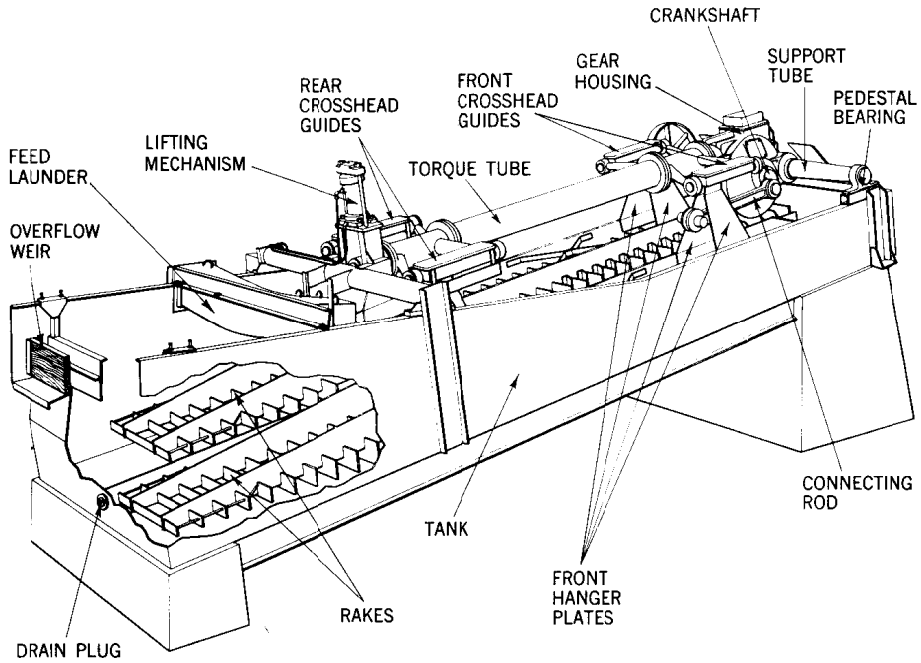

Fig. 2.3.4 - Rake classifier [SME].

Table 2.3.1 - Correction factor particle size classifier overflow k_d

d_{95} over-flow [mm]:	1.17	0.83	0.59	0.42	0.30	0.21	0.15	0.10	0.074
% < 0.074 in overflow	17	23	31	41	53	65	78	88	95
% < 0.045 in overflow	11	15	20	27	36	45	50	72	83
Standard over-flow dilution[1] for ρ=2700 kg/m^3 = m_l/m_s	1.3	1.5	1.6	1.8	2.0	2.33	4.0	4.5	5.7
mass% solids overflow	43	40	38	36	33	30	20	18	16.5
k_d	**2.5**	**2.37**	**2.19**	**1.96**	**1.70**	**1.41**	**1.0**	**0.67**	**0.46**

Table 2.2.2 - Correction factor bottom inclination k_β

ß in ^{o}	14	15	16	17	18	19	20
$k_ß$	**1.12**	**1.10**	**1.06**	**1.03**	**1.00**	**0.97**	**0.94**

Table 2.2.3 - Correction factor k_D for the real desired dilution relative to the reference dilution (Table 3.2.1, 4th row).

ρ_s [kg/m^3]	$\frac{(m_l/m_s)_{real}}{(m_l/m_s)_{stand}}$	0.4	0.6	0.8	1.0	1.2	1.5	2.0
2700		**0.60**	**0.73**	**0.86**	**1.00**	**1.13**	**1.33**	**1.67**
3000		**0.63**	**0.77**	**0.93**	**1.07**	**1.23**	**1.44**	**1.82**
3300		**0.66**	**0.82**	**0.98**	**1.15**	**1.31**	**1.55**	**1.97**
3500		**0.68**	**0.85**	**1.02**	**1.20**	**1.37**	**1.63**	**2.07**
4000		**0.73**	**0.92**	**1.12**	**1.32**	**1.52**	**1.81**	**2.32**
4500		**0.78**	**1.00**	**1.22**	**1.45**	**1.66**	**1.99**	**2.56**
5000		**0.83**	**1.07**	**1.32**	**1.57**	**1.81**	**2.18**	**2.81**

The coarse (settled) fraction capacity is given by:

$$C_{s\_settled} = 5.45 N_S D_S{}^3 n_s (\rho / 2700) k_\beta \text{ t/h} \qquad (2.3.2.2)$$

where n_s is the rotation speed of the screw in min^{-1}.

[1] This is the dilution of the reference situation, not the specific situation that is calculated.

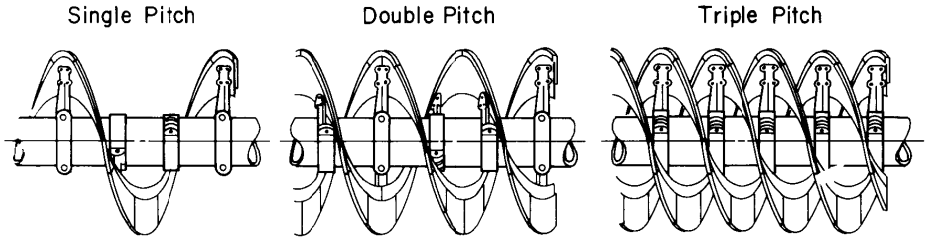

Fig. 2.3.5 - Pitch number variants of a screw classifier [SME].

2.3.3. Rising current classifiers

The most simple rising current classifier is a straight vertical tube through which water is pumped upward, having a feed sluice in the middle, coarse withdrawal at the bottom, and fines overflow at the top. In this way a separation based on differences in settling velocity can be obtained. For materials of equal density and approximately equal shape it act as a classifier. More advanced systems have controlled withdraweal of underflow and are specifically designed to create either fluidisation conditions, or a more diluted flow (Fig. 2.3.6). Typical cut sizes are 0.4...2.5 mm. Separation sharpness usually is $1.4<E_p<2.2$ (see Eq. 1.6.7 and Fig. 1.6.1). Single units can be combined in larger multi stage classifying units. Typical applications are dredging sand classification (e.g. off-shore sand dredging) or other applications in industrial minerals.

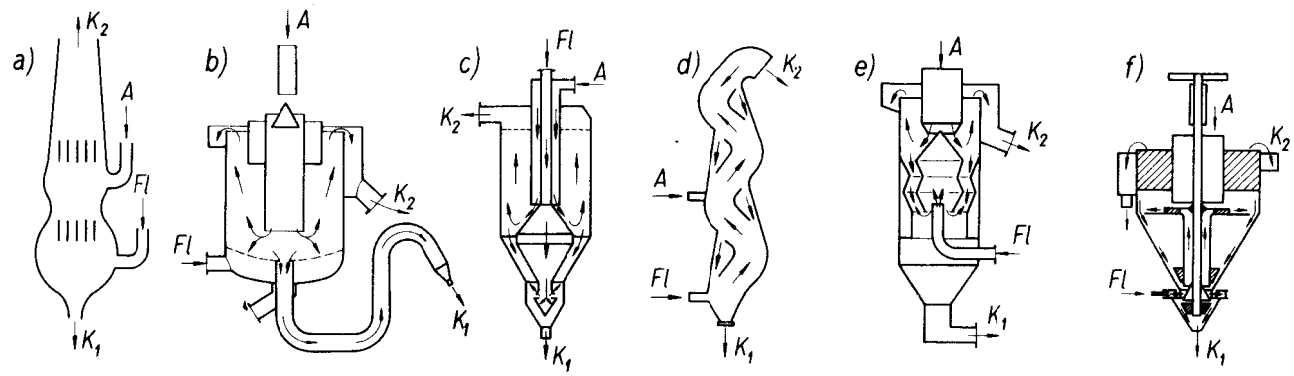

Fig. 2.3.6 - Several hydraulic rising current classifiers, A=feed, Fl=water inflow, K_1=coarse product, K_2=fines product [Schubert Vol. I].

2.4. Pneumatic classifiers

Pneumatic classification or (wind-)sifting is typically applied for cut sizes about 5...500 μm, and occasionally up to several mm, or even several cm for very light material (fibers, foils etc.). Pneumatic classification can be subdivided in the operations:

Homogeneous and constant supply of feed to the separation zone
The separation process
Separating air from the coarse and fine products

The necessary air is supplied as fresh air, is recirculated, or a combination. The air flow needs to be monitored by measurement and controlled.

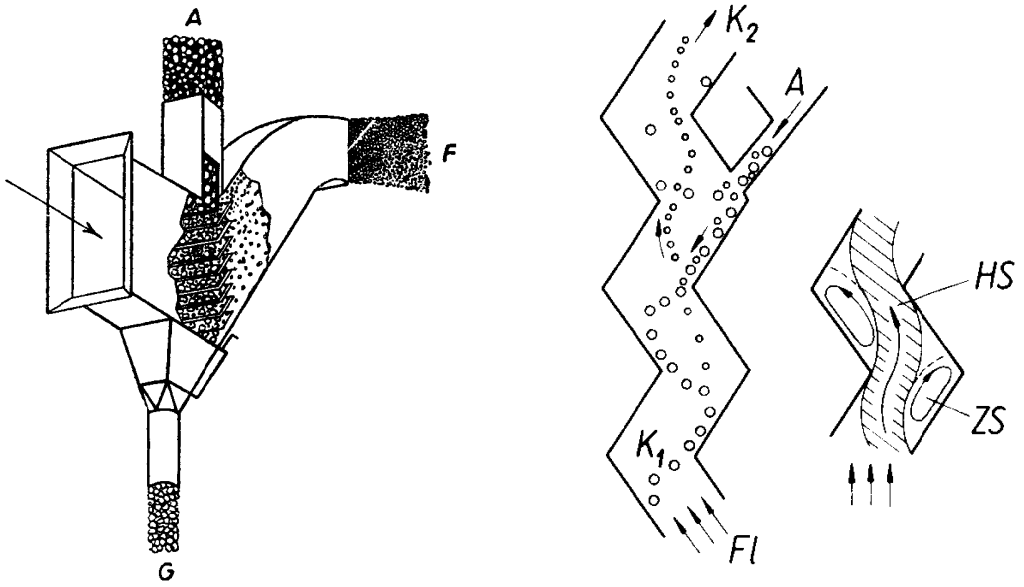

Fig. 2.4.1 - Pneumatic classifiers: cross flow classifier, A=feed, F=fines, G=coarse (l), Zig-Zag windsifter principle (r) A=feed, K_1=fines, K_2=coarse, FL=air input, HS=main stream, ZS=circulating flow [Schubert Vol. I].

The capacity of a sifter is estimated by:

$$C_{sift} = Auc_s = A\partial v_{CS} c_s \qquad (2.3.3.1)$$

with A=cross sectional area of sifter, u=air velocity, c_s=solids concentration of sifter air, v_{CS} stationary settling velocity of the cut-size particle, and $\delta=u/v_{CS}$. At smaller cut sizes, the design must be such that high δ values are obtained in order to have sufficient troughput, e.g by applying a centrifugal force field or high-velocity cross flow. Air solids concentrations are typically 0.5 kg/m^3 with a range 0.2...5 kg/m^3. Horizontal cross flow classifiers are applied for cut sizes 0.2...0.6 mm with c_s<1.5 kg/m^3 (Fig. 2.4.1, left). Typically $\delta\approx0.5$ for this type.

Zig-Zag classifiers can be considered as a sequence of single cross flow classifiers (Fig. 2.4.1, right). In every corner a circulating flow of material is generated (at "ZS"), catching the unsuspended solids and returning it cross-wise in the main air flow ("HS"). Though a single stage has poor efficiency, with the multi-stage arrangement 1.2<E_p<1.7 can be obtained for cut sizes 0.1...10 mm.

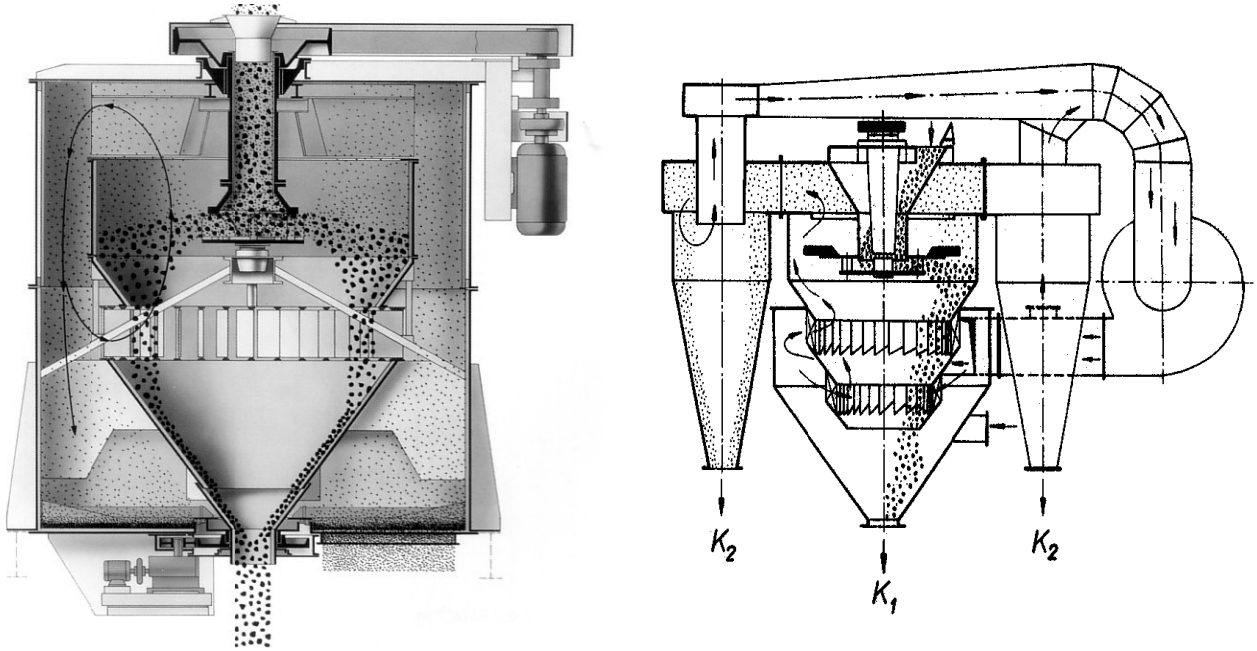

Fig. 2.4.2 - Classifier with spinning distribution table and internal air circulation (l) and external circulation (r). A=feed, K_1=coarse, K_2=fine [Humboldt Wedag / Schubert Vol. I].

In classifiers of the type shown in Fig. 2.4.2 the feed is added from a rotating table into the air. The separation principle is very much similar to a cross flow classifier. The cut size can be modified by changing the rotation speed and the design of the spinning table. Fig. 2.4.2, left, shows internal air circulation, right external air circulation with cyclones. The advantage of the latter configuration is better control and higher separation sharpness. They are frequently applied in dry grinding circuits for cement clinker and for fine coal classification. Typical cut sizes are 0.05...0.6 mm at sharpness $1.5<E_p<3.0$. The largest air classifiers for ground cement clinker have diameters up to 8 m at capacities of about 500 t/h. Table 2.4.1 shows typical data regarding applications in cement and coal classification.

Table 2.4.1 - Capacity data of typical sifter applications [Schubert Vol. 1].

Cement	Cut size ≈90µm, 60%<90µm	
Sifter diameter [m]	Capacity [t/h]	Power draw [kW]
1.5	5...6	4...6
2.5	15...20	7...15
3.5	30...60	20...40
5.0	50...120	50...75
Coal	Cut size 500µm, ≈25%<500µm	
Sifter diameter [m]	Capacity [t/h]	Power draw [kW]
1.5	≈14	≈6
2.5	≈75	≈16
3.5	≈150	≈30

Besides the basic designs described above numerous other designs are applied, specifically designed for certain types of material and classification objectives.

Fig. 2.4.3 – Centrifugal classifier ("deduster") for raw small coal can handle dry as well as moist feed

2.5. Cyclones

[From Coulson & Richardson, 1991]

The use of hydrocyclones has the advantage of simplicity and flexibility, so that the results may be modified by altering operating conditions. As opposed to many other types of equipment, hydrocyclones are better for classifying than for clarifying. The reason is that the high shearing stresses in a hydrocyclone promote the suspension of the particles and oppose flocculation. A disadvantage is that both the coarse and fine fractions are obtained as suspensions of fairly high dilution. Moreover, the viscosity of the fluid should not be too high.

2.5.1 Centrifugal separation

The rate of settling in a fluid can be greatly increased if centrifugal rather than gravitational forces are employed. In the cyclone separator (Fig. 2.5.1), the fluid is introduced tangentially into a cylindrical vessel, clean fluid is taken off through a central outlet at the top. The solids are thrown outward against the cylindrical wall of the vessel and are collected in the conical base.

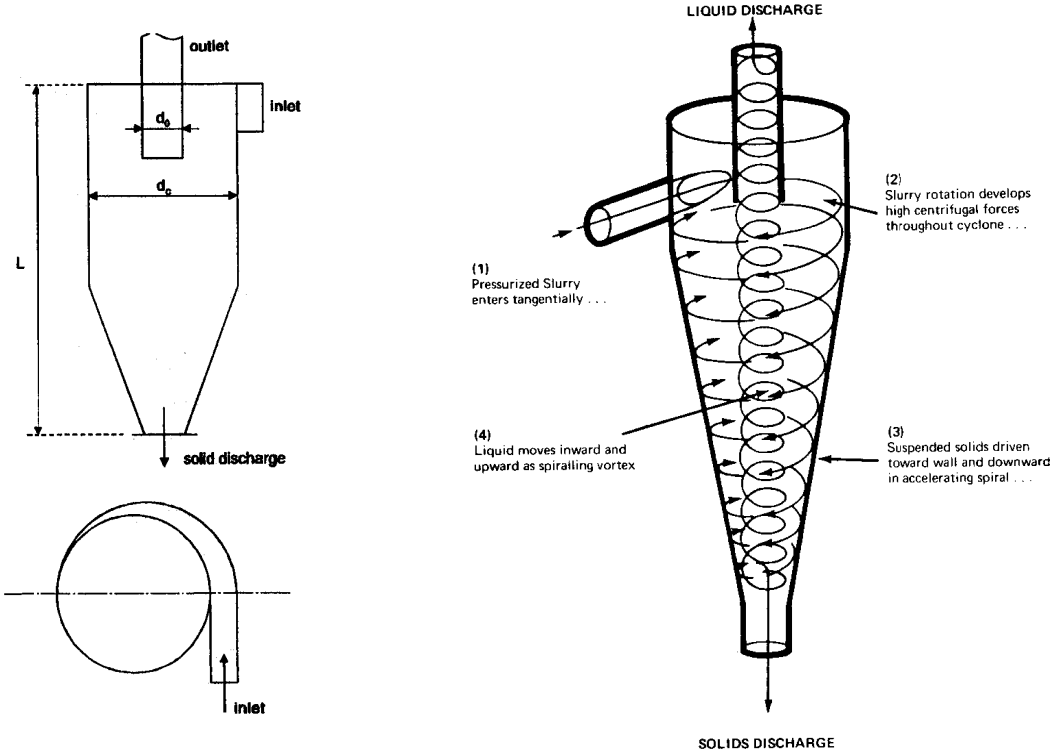

Fig. 2.5.1 - Schematic diagram of a cyclone separator (l) and fluid flow(r) [r: SME].

This separator is very effective, unless the fluid contains a large portion of particles less than 10 μm in diameter. The fluid in the cyclone moves spirally downward, gradually approaching the central portion of the separator and then rises and leaves through the central outlet at the top (Fig. 2.5.1, r). The tangential component of the velocity of the fluid appears to predominate throughout the whole depth, except within a highly turbulent central core of diameter about 0.4 times that of the fluid outlet pipe. The radial component of the velocity acts inwards, and the axial component is away from the fluid inlet near the walls of the separator but is in the opposite direction in the central core.

Pressure measurements indicate a relatively high pressure throughout, except for a region of reduced pressure corresponding to the central core. Any particle is therefore subjected to two opposing forces in the radial direction, the centrifugal force which tends to throw it to the walls and the drag of the fluid which tends to carry the particle away through the fluid outlet. Both of these forces are a function of the radius of rotation and of the size of the particles, with the result that particles of different sizes tend to rotate at different radii. As the outward force on the particles increases with the tangential velocity and the inward

force increases with the radial component, the separator should be designed so as to make the tangential velocity as high as possible and the radial velocity low. This is generally effected by introducing the fluid at a high tangential velocity and making the height of the separator large. The radius at which a particle will rotate within the cyclone corresponds to the position where the net radial force on the particle is zero. The two forces acting are the centrifugal force outwards and the frictional drag of the fluid acting inwards.

Let's consider a spherical particle of diameter d rotating at radius r. Then the centrifugal force is:

$$\frac{mu_t^2}{r} = \frac{\pi d^3(\rho_s - \rho_f)u_t^2}{6r} \qquad (2.5.1)$$

where m = mass of the particle
u_t = tangential component of the velocity of the fluid
ρ_s = particle density

lt is assumed that there is no slippage between the fluid and the particle in the tangential direction. If the radial velocity is low, the inward radial force due to friction will, from Eq. (2.2.1) be equal to $3\pi\eta du_r$, where η is the viscosity of the fluid and u_r is the radial component of the velocity of the fluid. The radius r, at which the particle will rotate at equilibrium, is then given by:

$$\frac{\pi d^3 \rho_s u_t^2}{6r} = 3\pi\eta d u_r$$

or

$$\frac{u_t^2}{r} = \frac{18\eta}{d^2(\rho_s - \rho_f)}u_r \qquad (2.5.2)$$

When the density of the particle is large compared with that of the fluid, u_o, the free falling velocity of the particle, is given by Eq. (2.2.12) as:

$$u_0 = \frac{d^2 g(\rho_s - \rho_f)}{18\eta} \qquad (2.5.3)$$

Substituting in Eq. (2.5.2):

$$\frac{u_t^2}{r} = \frac{u_r}{u_0} g$$

or

$$u_0 = \frac{u_r}{u_t^2} rg \qquad (2.5.4)$$

Thus the higher the terminal falling velocity of a particle, the greater the radius at which it will rotate and the easier it is to separate. If it is assumed that a particle will be separated provided it tends to rotate outside the central core of diameter $0.4d_0$, the terminal falling velocity of the smallest particle which will be retained is found by substituting $r = 0.2d_0$ in Eq. (2.5.4), i.e.

$$u_0 = \frac{u_r}{u_t^2} rg \qquad (2.5.5)$$

In order to calculate d_0, it is necessary to evaluate u_r and u_t for the region outside the central core. The radial velocity u_r is found to be approximately constant at a given radius and to be given by the volumetric rate of flow of the fluid divided by the cylindrical area for flow at the radius r. Thus if G is the mass rate of flow of the fluid through the separator and ρ is its density, the linear velocity in a radial direction at a distance r from the centre is given by:

$$u_r = \frac{G}{2\pi r L \rho} \qquad (2.5.6)$$

where L is the length of the separator.

The tangential velocity is found experimentally to be inversely proportional to the square root of the radius at all depths. Then if u_t is the tangential component of the velocity at radius r, and u_{t0} is the corresponding value at the circumferenee of the separator:

$$u_t = u_{t0}\sqrt{\frac{d_c}{2r}} \qquad (2.5.7)$$

Further it is found that u_{t0} is approximately equal to the velocity with which the fluid enters the separator. If these values for u_r and u_t are now substituted into Eq. (2.5.5), the terminal falling velocity of the smallest particle which the separator will retain is given by:

$$u_0 = 0.2\frac{Gd_0 g}{\pi\rho L d_c u_{t0}^{\ 2}} \qquad (2.5.8)$$

If the cross-sectional area of the inlet is A_i, $G = A_i\rho u_{t0}$ and:

$$u_0 = 0.2\frac{A_i^{\ 2} d_0 \rho g}{\pi L d_c G} \qquad (2.5.9)$$

A small inlet and outlet therefore result in the separation of smaller particles, but as the pressure drop over the separator varies with the square of the inlet velocity and the square of the outlet velocity, the practical limit is set by the permissible pressure drop. The depth and diameter of the body should be as large as possible, because the former determines the radial component of the fluid velocity and the latter controls the tangential component at any radius. In general, the larger the particles, the larger should be the diameter of the separator because the greater is the radius at which they rotate.

Because the separating power of the separator is directly related to the throughput of the fluid, the cyclone separator is not very flexible, though its efficiency can be improved at low throughputs by restricting the area of the inlet, and hence increasing the inlet velocity. Generally, however, it is better to use a number of cyclones in parallel and to keep the load on each approximately the same.

Because the vertical component of the velocity in the cyclone is downwards everywhere outside the central core, the particles will rotate at a constant distance from the centre and move continuously downwards until they settle in the conical base. Continuous removal of the solids is desirable so that the particles do not get entrained again in the fluid stream due to relatively low pressures in the central core. Entrainment is reduced to a minimum if the cyclone has a deep conical base of small angle.

Example 2.5.1.

A cyclone separator, 0.3 m in diameter and 1.2 m long, has a circular inlet 75 mm in diameter and an outlet of the same size. If the gas enters at 1.5 m/s, at what particle size will the theoretical cut occur?
Viscosity of air 0.018 mNs/m^2
Density of air 1. 3 kg/m^3
Density of particles 2700 kg/m^3

Solution:

The cross sectional area $A_i = (\pi/4)(0.075)^2 = 4.42*10^{-3}$ m^2 . The mass flow rate of the gas becomes then

$$G = 1.5*4.42*10^{-3}*1.3 = 8.62*10^{-3} \text{ kg/s.}$$

Using Eq. (2.5.9) the free-falling velocity u_0 can be calculated:

$$u_0 = \frac{0.2*(4.42*10^{-3})^2*0.075*1.3*9.81}{\pi*1.2*0.3*8.62*10^{-3}} = 3.83*10^{-4} \text{ m/s}$$

Use is now made of Stokes law (Eq. 2.5.3) to find the particle diameter:

$$d = \sqrt{\frac{u_0 18\mu}{g\rho_s}} = \sqrt{\frac{3.83*10^{-4}*18*0.018*10^{-3}}{9.81*2700}} = 2.17*10^{-6} \text{ m} = 2.17 \text{ μm}$$

2.5.2 Optimum cyclone dimensions

There is no unique design manual for cyclones. The design is generally based on experiments by numerous authors. However, summarizing these experimental results leads to the following set of guidelines for the dimensions in liquid-solid cyclone systems:

$$\frac{l}{d_c} = 0.4 \quad \frac{L}{d_c} = 5 \quad \frac{d_i}{d_c} = 0.28 \quad \frac{d_0}{d_c} = 0.34 \qquad (2.5.10)$$

in which:

d_c = cyclone diameter
1 = length of vortex finder
L = length of the cyclone
d_i = inlet diameter
d_0 = diameter of overflow outlet

The vortex finder is the portion of the overflow pipe projecting into the cyclone (Fig. 2.6.1, l). The manner in which the total length of the cyclone is divided over the cylindrical and conical sections is not highly critical. lt appears that some preference must be given to a cone that is as long as possible, and that the top angle of the conical section should not exceed 30^o. lt should be noted that these data are only valid if an air core can develop in the centre of the cyclone.

2.5.3 Pressure drop in a cyclone

The resistance of a cyclone to the fluid flow is expressed by the flow resistance coefficient α, which can be expressed as:

$$\alpha = \frac{Q}{A_f \sqrt{2g \frac{\Delta p}{\rho}}} \qquad (2.5.11)$$

in which Q = cyclone capacity, m^3/s
A_f = area of the feed opening, m^2
g = gravity acceleration, m/s^2
Δp = pressure drop across the cyclone, N/m^2
ρ = density of the fluid, kg/m^3

Another important factor for the cyclone is the Reynolds number:

$$\mathrm{Re} = \frac{\rho v_f d_c}{\mu} \qquad (2.5.12)$$

where v_f = feed velocity
d_c = cyclone diameter
μ = fluid viscosity

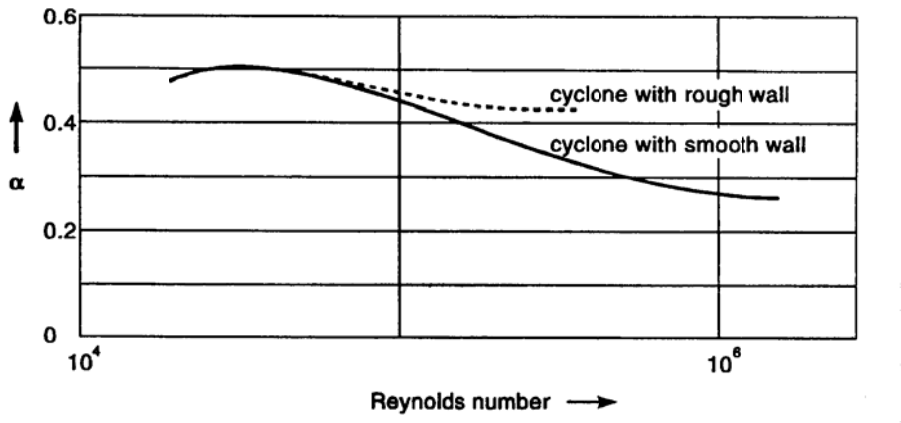

Fig. 2.5.2 - Resistance coefficient as a function of the Reynolds number

The resistance coefficient a for a certain cyclone is only dependent on the Reynolds number and the wall roughness. At higher Reynolds number the flow resistance coefficient u decreases as is shown in Fig. 2.5.2.

2.5.4 Cyclone efficiency and the classification curve

The efficiency of the cyclone separator is greater for large than for small particles and increases with the throughput until the point is reached where excessive turbulence is created. If the cyclone is designed to separate a definite particles size, a cyclone efficiency may be defined as the mass fractions of the particles of that size that is separated in the cyclone. It can be expressed as a Tromp curve (Section 1.6.2, Fig. 1.6.1), and derive Ecart probable (Eq. 1.6.7) or Imperfection (Eq. 1.6.8) from it.

For cyclones the Tromp curve for classification indicates the percentage of particles of a given particle size reporting in the apex (conical base) discharge, leaving out of account in the calculation the solids in the feed which are contained in a volume which comprises just as much liquid as is present in the apex discharge (Fig. 2.5.3).

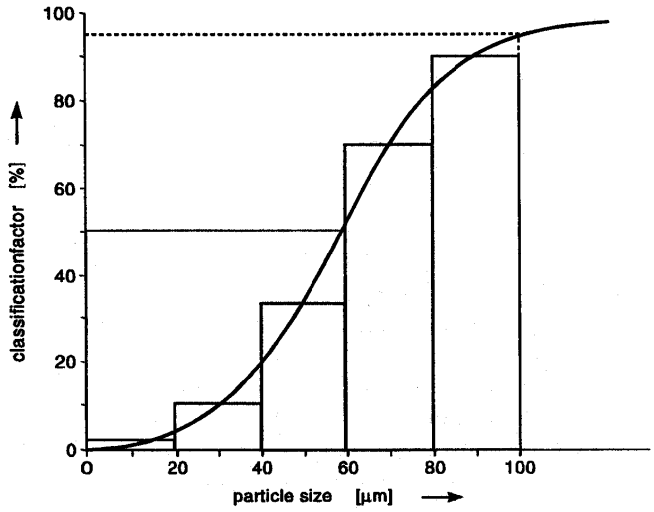

Fig. 2.5.3 - Cyclone Tromp curve.

A good classification curve is steep, which means that a relatively small amount of coarse material will end up in the overflow fraction and only a small amount of small particles will be discharged through the apex. A term that is often used is "separation size". lt relates to the size of particles of which 95% is caught. The 95 percent value is chosen arbitrarily, since the point of 100% is difficult to determine.

Unfortunately, different authors use different methods for representing cyclone performance. Wills (1988) for example, represents cyclone efficiency by the performance or separation curve, which is in essence the same as the classification curve. He defines the "cutpoint" or “separation size" as that point on the partition (or Tromp) curve for which 50% of particles in the feed of that size report to the underflow, i.e. particles of that size have an equal chance of going either with the overflow or underflow. This point is referred to as the d_{50} point.

Many mathematical models of hydrocyclones include the term "corrected d_{50}" taken from the "corrected" classification curve. lt is assumed that in all classifiers, solids of all sizes are entrained in the coarse product liquid by short-circuiting in direct proportion to the fraction of the feed water reporting to the underflow. For example, if the feed contains 16 t/hr of material of a certain size, and 12 t/hr report to the underflow, then the percentage of this size reporting to the underflow and plotted on the normal partition curve is 75 percent. However, if 25 percent of the feed water reports to the underflow then 25 percent of the feed material will short-circuit with it, therefore 4 t/hr of the size fraction will short-circuit to the underflow; and only 8 t/hr leave in the underflow due to classification. The corrected recovery of the size fraction is thus

$$\frac{12-4}{16-4} * 100\% = 67\%$$

The uncorrected partition curve can therefore be corrected by utilising the equation:

$$y' = \frac{y-R}{1-R} \qquad (2.5.14)$$

where y' is the corrected mass fraction of a particular size reporting to the underflow, y is the actual mass fraction of a particular size reporting to the underflow, and R is the fraction of the feed liquid which is recovered in the coarse product stream. Fig. 2.5.4 shows uncorrected and corrected classification curves.

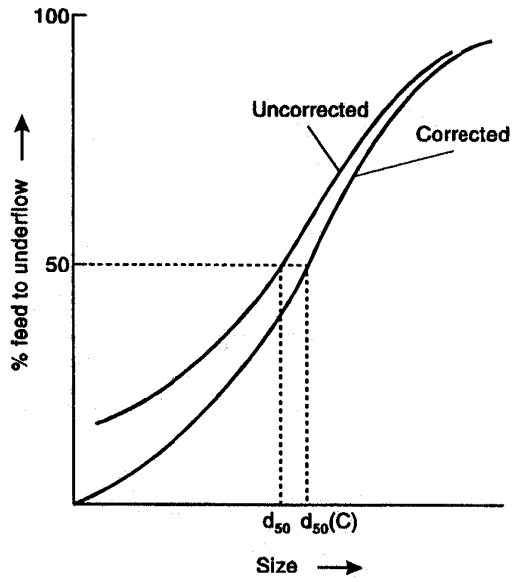

Fig. 2.5.4 - Uncorrected and corrected classification curves.

2.5.5 Influence of different variables on hydrocyclone operation

Designing cyclones is, as said before, generally based on experimental data. It is therefore useful to show some of the trends that follow from the investigations of a large number of researchers.

(1) cyclone diameter

For the same pressure at two cyclones, the separation size is proportional to the square root of the cyclone diameter, when both cyclones are having the same geometric shape. If, for example, a cyclone with a diameter of 350 mm gives for sand a separation size of 60 microns, then for the same sand a cyclone of 100 mm gives a separation size of 1 (100/350) * 60 = 32 microns. Increasing the diameter for big cyclones has a smaller effect on the particle size than would follow from this rule. Also, there is a lowest Reynolds number for cyclones. This lowest number depends on the shape of the cyclone. If this lowest Reynolds number is reached, a decrease in cyclone diameter will result in an increase of the separation size.

(2) feed pressure

The capacity of a cyclone is proportional to the square root of the feed pressure. If at 1 atm pressure the capacity of a cyclone is 25 m^3/hr, then at a pressure of 2 atm the capacity is $\sqrt{2} * 25 = 35\ m^3$/hr. The separation size is inversely proportional to the fourth root of the feed pressure. Hence at 16 times higher pressure the particle size of separation is reduced by a factor of two.

(3) cone angle

It is difficult to quantify the effect of the cone angle in the form of an equation. Generally it can be said though that increasing the cone angle leads to an increase of the separation size. Decreasing the cone angle leads to an increase in wall area. This results to a higher number of the flow resistance coefficient α and in a decrease of the capacity. A cyclone with a high cone angle has the disadvantage, however, of wearing out more rapidly.

(4) feed and overflow dimensioning
In general, reduction of the cyclone openings results in a decrease of the separation size. In principle, the feed opening should not be larger than 1/3 of the cyclone diameter. For products with low density <1500kg/m^3) the feed opening should not exceed 1/5 of the diameter.

(5) density of the particles
The classification of material with a density larger than about 2500 kg/m^3 can be calculated according to Stokes law, which means that the separation size is inversely proportional to the square root of the density of the solids minus the density of the liquid. For example, if a cyclone classifies quartz (density 2650 kg/m^3) at 60 microns, then it will classify magnetite (density 5000 kg/m^3) at

$$60\sqrt{\frac{2650-1000}{5000-1000}} = 38 \text{ microns}$$

(6) viscosity of the fluid
The separation size is proportional to the square root of ν, the kinematic viscosity ($\nu=\rho_l\eta$, with ρ_l the liquid density and η the dynamic viscosity). Consequently, a two times higher viscosity gives a 12 times bigger particle size of separation.

(7) feed concentration
At low feed concentrations the separation size remains about constant, but at higher feed concentrations the size of separation increases. By recirculating part of the overflow or part of the apex discharge to the feed, the size of separation can be effectively influenced.

(8) shape of particles
The shape of the particles is an important factor in the separation. For the same cyclone, particles with the same density, but different shape will be separated at different sizes. For example, disk shaped particles which carry a relatively large amount of liquid, behave as if they had a lower density and are therefore classified at a coarser size than might be expected from their real density. For this reason it is always advisable to carry out a classification test before determining the size of separation.

(9) cyclone efficiency
The foregoing sections gave a qualitative description of the impact of cyclone parameters on cyclone efficiency. However, also more quantitative descriptions exist. Bradley (1965) e.g., lists different equations to calculate the cutpoint d_{50}. The oldest one is that of Dahlstrom:

$$d_{50} = \frac{13.7(d_0 d_i)^{0.68}}{Q^{0.53}(\rho_s - \rho_l)^{0.5}} \qquad (2.5.15)$$

where d_{50} is the cutpoint (μm), d_0 is the overflow diameter (cm), d_i is the inlet diameter (cm), Q is the total flow rate *(m^3/h)*, ρ_s is the specific gravity of the solids and ρ_l is the specific gravity of the fluid. Equations like this one is, however, are not directly applicable to industrial cyclones, since most of the work was carried out on dilute slurries using very small diameter cyclones.

Plitt (1976) has developed a mathematical equation for large diameter cyclones operating at high solids content. The equation for cut-size is:

$$d_{50} = \frac{14.8 d_c^{0.46} d_i^{0.6} d_0^{1.21} e^{0.063V}}{d_u^{0.71} h^{0.38} Q^{0.45} (\rho_s - \rho_l)^{0.5}} \qquad (2.5.16)$$

where d_{50} is the "corrected" d_{50} (μm), d_c, d_i, d_0 and d_u are inside diameters of the hydrocyclone, inlet, vortex finder and apex, respectively, V is the volumetric percentage of solids in the feed, h is the distance from bottom of the vortex finder to the top of the underflow orifice (cm), Q is the flow rate of the feed slurry (m^3/hr), and ρ_s and ρ_l are the density of the solids and liquid respectively (g/cm^3).

Example 2.5.2.

The collection efficiency of a cyclone is 45 % over the size range 0-5 μm, 80% over the size range 5-10 μm, and 96 % for particles exceeding 10 μm. Calculate the efficiency of collection for the following dust:

weight distribution	50%	0-5 μm
	30%	5-10 μm
	20% above 10 μm	

Solution:

For the collector:

size(μm)	0-5	5-10	>10
efficiency(%)	45	80	96

For the dust:

weight(%)	50	30	20

Basis 100 kg dust, weight at inlet (kg)

22.5	24.0	19.2	total = 65.7 kg

overall efficiency = (65.7/100)*100 = 65.7 %

2.5.6. Cyclone design

Cylindrical – conical single cyclones with cone angle 10^o...20^o are the most common types (Fig. 2.6.1). Today most manufactures prefer involuted feed entries (Fig. 2.6.1, right: middle & bottom) instead of tangential inlets (Fig. 2.6.1, right: top). Involuted entries reduce turbulence and enable operation with higher slurry densities. Larger cyclones (0.25...1.6 m diameter) are usually made from steel with an inner liner, often made from rubber or plastics. Smaller cyclones are often made fully from Polyurethane or ceramics.

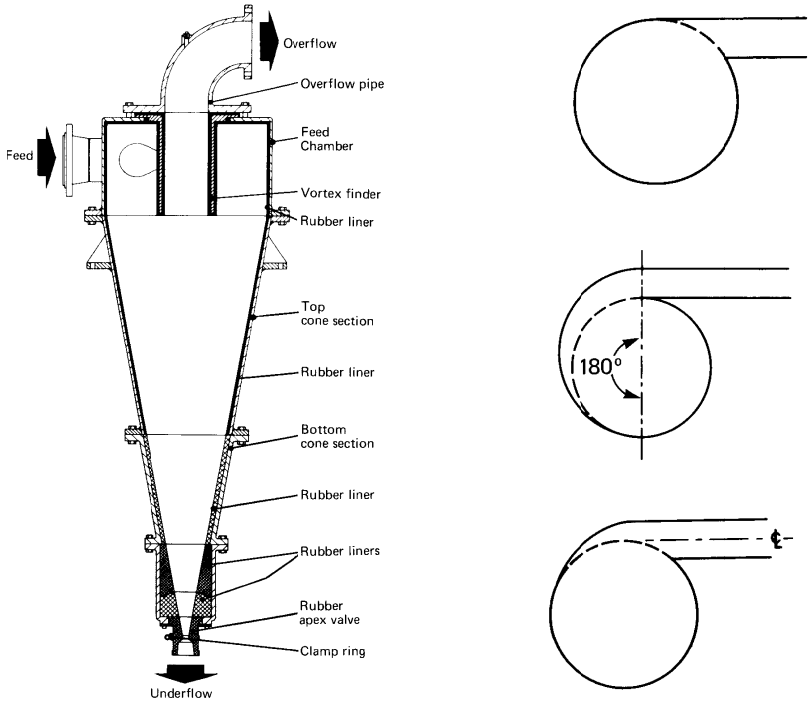

Fig. 2.6.1 - Typical cyclone construction (l). Feed entry design (r) [SME].

Cyclone outlets are sensitive for intensive wear, and therefore usually easily exchangable (Fig. 2.6.2). Some models have adjustable outlet diameters. The centrifugal force field is a multiple of gravity, therefore orientation of the cyclone can be any (horizontal, vertical, or inclined).

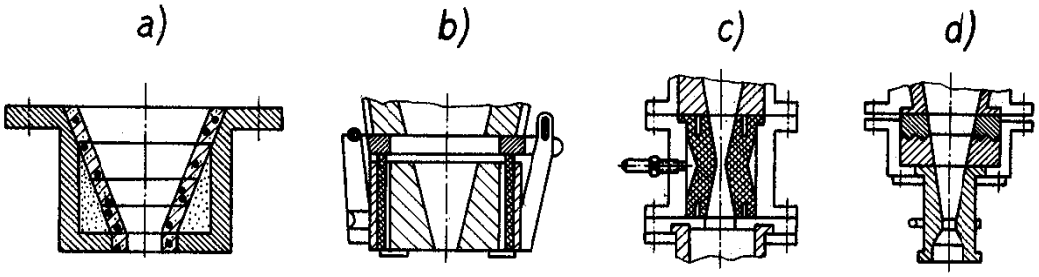

Fig. 2.6.2 - Cyclone outlet design with: a - ceramic liner, b - exchangable rubber liner, c - rubber liner with adjustable cross section by pressure, d – manually adjustable liner [Schubert, Vol. I].

Applications needing small cut sizes need small diameter cyclones that each have a relatively small capacity. Therefore several cyclones are combined in a bank to save space (Fig. 2.6.3, l). The same is applied for high capacity applications in large grinding circuits (Fig. 2.6.3, r).

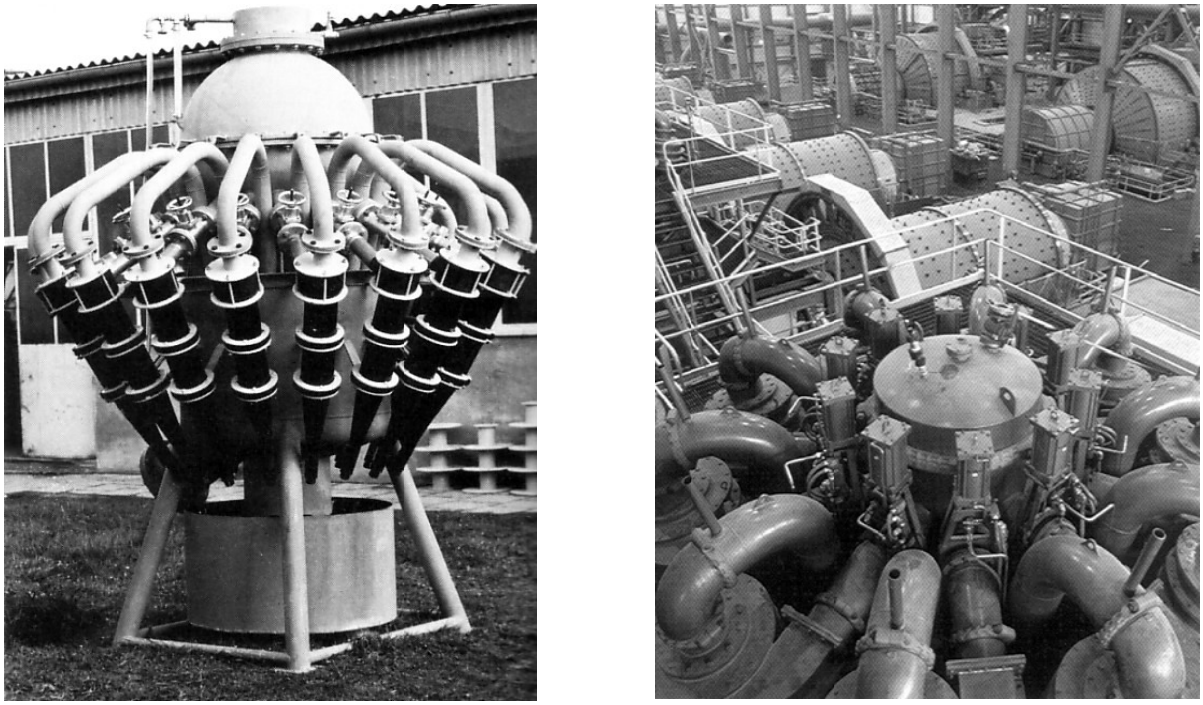

Fig. 2.6.3 - Bank of cyclones for small cut sizes (l), or high capacity in a grinding circuit (r) [Amberger Kaolinwerke / Krebs Engineers].

Fig. 2.6.4 gives an example of a typical cyclone range that is applied in the mining industry for grinding circuits. Cyclone diameter ranges from 254...838 mm with according cut sizes ranging from 40...220 µm (assuming $2500<\rho_s<3200$ kg/m^3). The relationship between pressure drop and capacity of these cyclones is given in Fig. 2.6.5. As said, higher capacities are obtained by installing banks of multiple cyclones (Fig. 2.6.3, right).

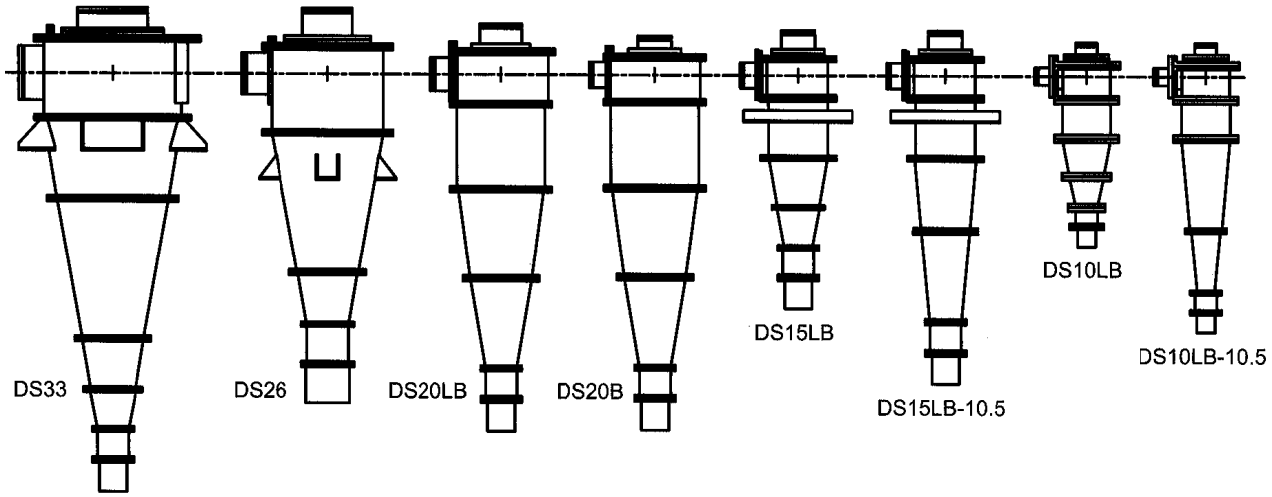

Fig. 2.6.4 - Krebs cyclone range from 838...254 mm diameter [Krebs Engineers].

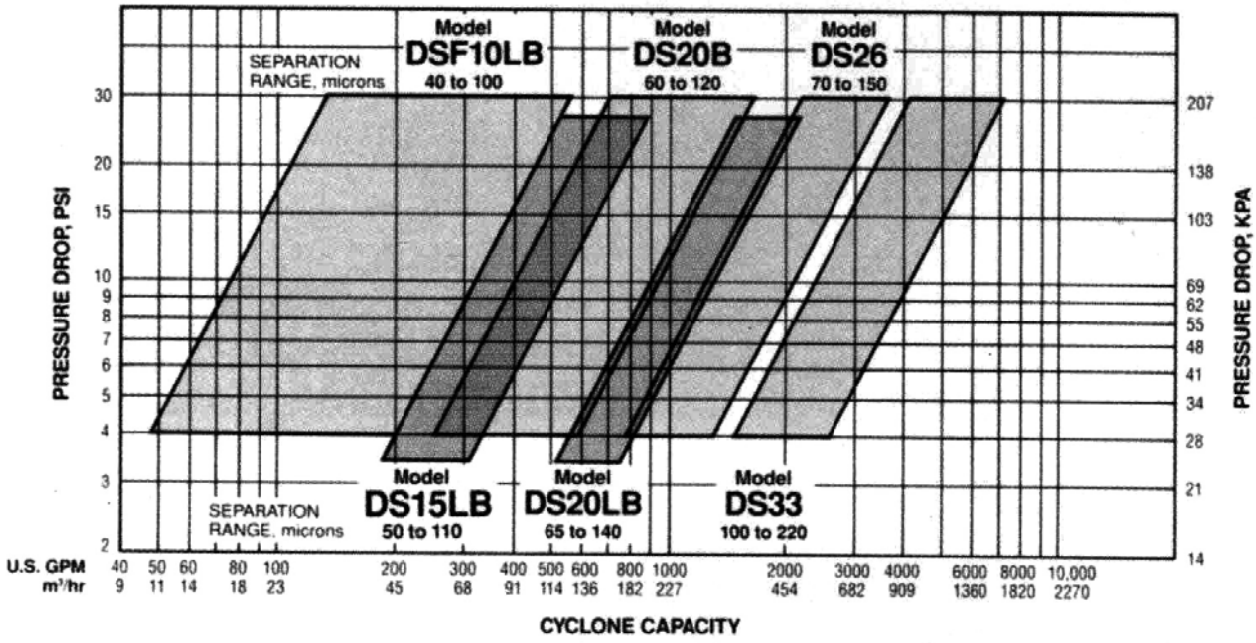

Fig. 2.6.5 - Cyclone performance chart [Krebs Engineers].

2.6 References

Bradley, D. The hydrocyclone. Pergamon Press, Oxford, 1965

Concha F, Almendra E.R. Settling velocities of particulate systems, 2. settling velocities of suspensions of spherical particles. International Journal of Mineral Processing, 6 (1979) 31-41.

Coulson, J.M., Richardson, J.F.: Chemical Engineering, Vol. 2. 4th edition. Pergamon press, Oxford,1991.

Plitt, L.R. A mathematical model of the hydrocyclone classifier. CIM Bull., 69, 114, dec 1976

Richardson J.F., Zaki W.N. Sedimentation and Fluidisation: Part I Trans.Inst.Chem.Engrs, Vol. 32, 1954.

Richardson, J.F. and Meikle, R.A. Sedimentation and fluidisation, part 3 Trans. Inst. Chem. Eng., 39, 348-356, 1961

Rietema, K. and Verver, C.G. Cyclones in Industry. Elsevier Publishing Company, 1961

Stokes, G.G, Mathematical and physical papers, Trans. Cambridge Phil. Soc. 9, part II, 51ff, 1851

Wallis G.B. A simplified one-dimensional representation of two-component vertical flow and its application to batch sedimentation. Symposium on the interaction between fluids and particles. London 20-22 june 1962.

Wallis G.B. One-dimensional two-phase flow. McGraw-Hill Book Company, New York. 1969.

Wills, B. A. Mineral processing technology. Pergamon Press, 4th edition, 1988

3. SIZE REDUCTION

3.1. Introduction

The first step in size reduction of rock is mining. In this, rock of infinite size is reduced to transportable material not larger as 200...1000 mm. For hard rock in general drilling and blasting is the only practical method. From Fig. 3.1.1, left, it is clear that by means of blasting no uniform particle size distribution can be generated. Larger lumps from the slabbing zone are generated parallel with fines from the compression zone directly surrounding the charge. An alternative method is sawing in regular blocks. It avoids generation of a distributed particle size, but is only applied for decorative stone because of its high costs and low production capacity. Examples of cutting are the quarrying of marble or granite, or soft limestone blocks as building material ("Mergel" in Dutch South-Limburg).

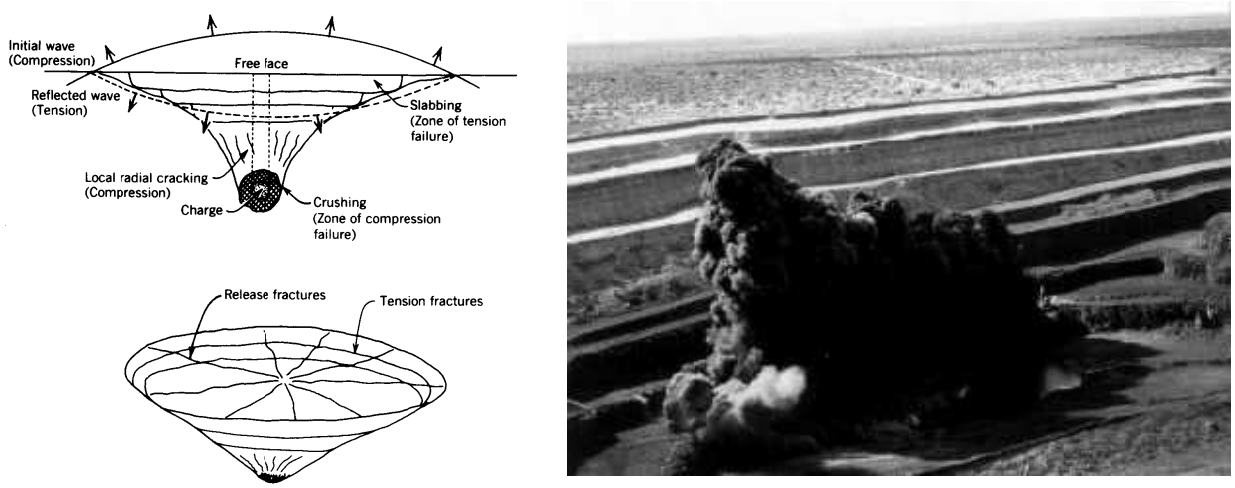

Fig. 3.1.1 - Principle of size reduction by means of blasting for hard rock. Blasting in an open pit manganese mine [Hartmann (l), TU Delft (r)].

Medium and soft rock types (coal, gypsum etc.) can be cut. This gives a more uniform size distribution and more continuous production. Besides, negative effects of explosions are avoided (safety hazard, exhaust gases, higher costs). Therefore recent developments in mining equipment are focussed on cutting methods for rocks of increasing hardness. Besides rock properties, the cutting method has a pronounced effect on particle size distribution. In coal mining the average particle size has decreased considerably due to the replacement of hand-held pneumatic hammering (conventional mining) to continuous miners (Fig. 3.1.2).

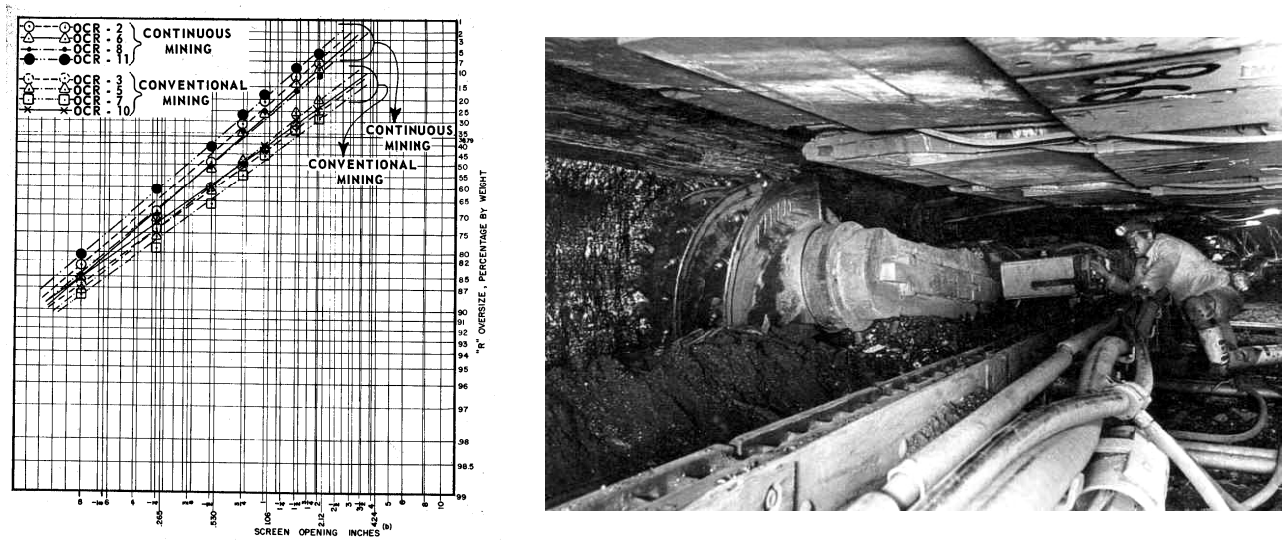

Fig. 3.1.2 - Size reduction of continuous mining and traditional mining compared (right). Cutting by means of continuous mining in an underground coal mine (longwall mining system) [Mitchell (l) /DSK (r)].

During mining rock is usually crushed only fine enough for transportation. Further size reduction is carried out near or in the processing plant. Here crushing reduces particle size of the rock. It is accomplished by compression against rigid surfaces. It is carried out until the material is fine enough for grinding (usually between 10 and 25 mm), which is accomplished by abrasion or impact of rock by the free motion of unconnected media such as rods, balls, or pebbles (Fig. 3.1.3 right). Crushing is performed in several stages with reduction ratios ranging from 3 to 6 per stage. This ratio is the maximum size of feed relative to the maximum size of the product. Tumbling mills are used for grinding, and comprise the last stages of size reduction, also known as comminution. Worldwide over $3*10^9$ tonnes of minerals are comminuted per year. This amount will increase due to decreasing cut-off of ore and increased use of raw materials (Fig. 3.1.3 left). In ore preparation size reduction typically comprises 5% to 15% of the mine-to-metal processing costs.

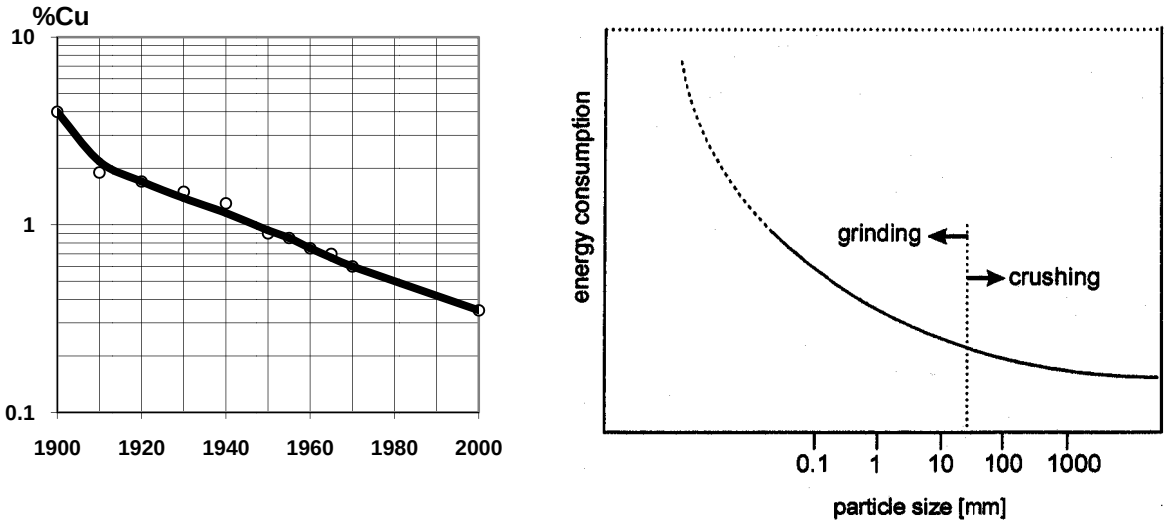

Fig. 3.1.3 - Average copper content of ore in the U.S.A. (left) and energy consumption as function of particle size (right).

The most important reasons for crushing and grinding are as follows:

- Liberation of a valuable component from a sterile matrix, such as iron ore from gangue rock (Fig. 3.1.4). It can be achieved by size reduction (comminution). Note that the crushing and grinding has as objective the liberation of minerals, not size reduction as such.
- Promotion of a more rapid chemical reaction by increasing the reaction surface, e.g. pulverised coal.
- Production of a material with desired treatment-, use-, or storage properties, such as food products, cement, pigments, railroad or concrete gravel etc.

The desired particle size varies for the different applications, some examples:

copper ore	max. 200 µm
gravel for road construction	max. 10 cm
coal	max. 15- 50 mm

For ore, grains of the valuable component are chemically bound to the surrounding gangue mineral. Size reduction involves the rupture of these bonds. Mechanical fracture of a particle occurs, if a stress exceeding the fracture strength of the material is applied. For practical reasons in industrial size reduction compressive force or impact is used to fracture ore particles.

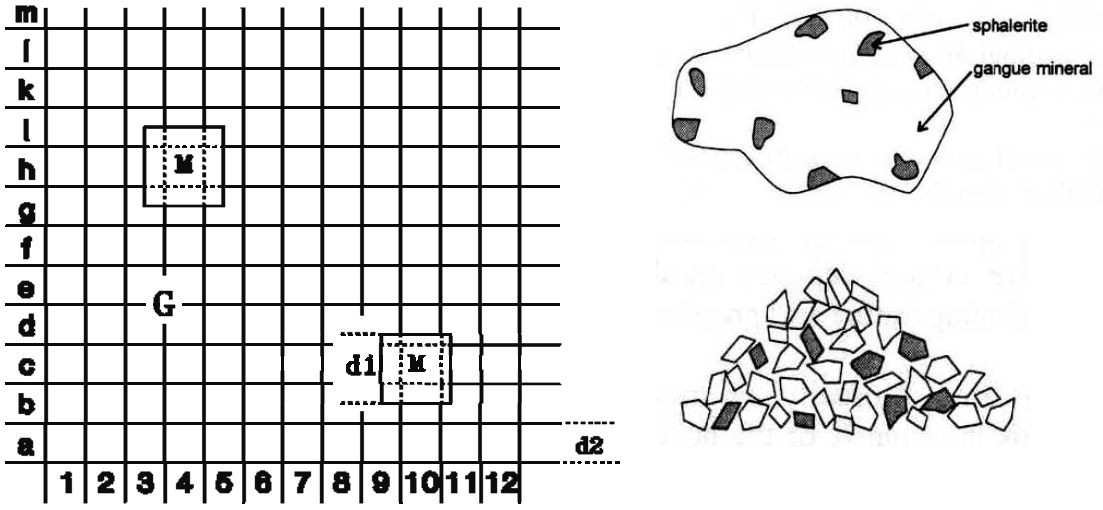

Fig. 3.1.4 - Principle of liberation: G=gangue mineral, M=valuable mineral, d1=grain size, d2=liberation size.

Most rock types are brittle, and during crushing release stress energy mainly by crack propagation (Fig. 3.1.5, right). Crack propagation is also inhibited by encounters with other cracks or grain boundaries. Therefore fine-grained rocks are usually tougher than course-grained rocks. The required energy for comminution is reduced in the presence of water. Often the cohesive and adhesive forces that are operative inside the various mineral phases and between the grain boundaries are of comparable strength. Therefore in most cases preferential rupture along the boundaries of the mineral grains during size reduction cannot be obtained. This has important consequences:

- Full liberation of minerals is practically impossible. Always some gangue material will be attached to the mineral grains, and mineral is lost as small fragments attached to gangue fragments.
- The actual size of the liberated mineral is considerably smaller than the original grain size in the rock. This is an important drawback, because the costs of separation progressively increase with declining particle size. Nevertheless, grain size of the mineral as present in rock (d1) determines the liberation size (d2) in comminution.

When crushed a particle falls into two distinct size classes; coarse particles resulting from the induced tensile failure, and fines from compressive failure near the points of loading or by shear at projections (Fig. 3.1.5, right).

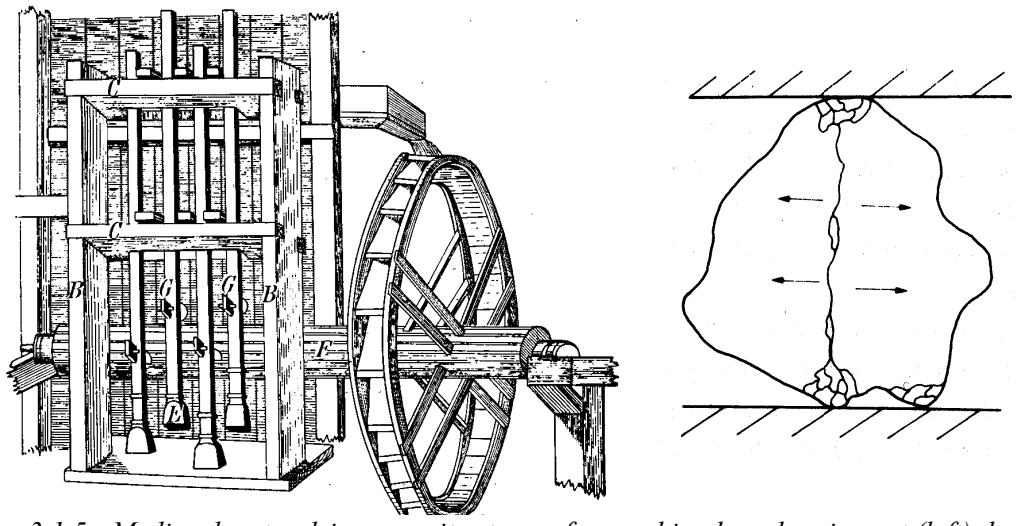

Fig. 3.1.5 - Medieval water driven gravity stamps for crushing based on impact (left), being a successful automation of hand hammer breaking. Fracture by pressure (right) [Schennen (l) / Wills (r)].

Comminution is an energy intensive operation. In ancient times, besides animal traction, streaming water provided energy for ore mills (Fig. 3.1.5, left). Today about 3.5% of the world's electric energy is used for crushing and grinding, of which (0.6 % in the ore dressing industry. Indeed, up to 200 tonnes of ore need to be crushed and grinded for the recovery of 1 tonne of copper metal. The world's largest copper mine, Escondida in Chile (9% of the global copper production), has a mill capacity of 237500 tonnes per day. In many applications the grinding stage takes most energy. This stage is usually carried out wet, though dry applications exist as well (cement, lime, iron ore etc.). In the design of comminution circuits generation of fines, which is material smaller than the required product size, should be minimised.

3.1.2. Liberation

Ideally the minerals should be liberated as shown in Fig. 3.1.4, right. This is however only possible when the grain boundaries are weaker than the material itself, which is in many applications not the case. In practice the model shown in Fig. 3.1.4, left, is more realistic, especially for many metallic run-of-mine ores. After crushing and grinding many free gangue material remains, while combined grains and some pure mineral grains represent the valuable components. It is the task of successive mineral concentration stages to recover the valuable components by gravity separation, magnetic separation, flotation or other methods.

At progressing size reduction the degree of liberation of a given mineral in a host rock improves. The rate at which it improves depends on type, volume concentration and properties of the minerals present, and on their texture and shape. Quantification of this process is of high economic and technical relevance, since it determines the maximum obtainable grade and recovery, as well as the required crushing and grinding effort. Also downstream it determines the required classification in size ranges: which size range can be processed together on a single line, and how many different lines of different size intervals give the best techno-economic performance. In other words: when the feed is classified in more size ranges, the technical separation result improves. However, the resulting increase in yield must bring more than the costs of changing screen apertures and treatment costs of a larger number of size classes. The techno-economic optimum can be determined by liberation (washability) analysis and flow sheet simulation. The liberation analysis (or washability in coal preparation terms) is the clue to this optimisation.

Numerous models describing binary liberation have been developed. They can be easily extended to multi-phase systems (more than 2 different minerals) by successively considering each mineral apart and considering the others as host rock. Based on the models of Meloy a number of conclusions can be drawn when we assume:

- The particles are of type 1, 2 or 3 only (Fig. 3.1.6).
- The particles are geometrically similar, also at progressing size reduction
- These is no selective (easier) breakage of inter-mineral contacts. This is usually true for magmatic and igneous deposits, but sedimentary deposits often show easier breakage along the mineral boundaries.

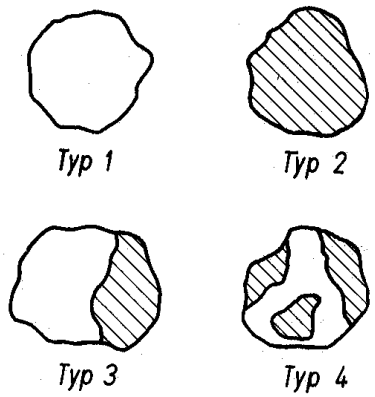

Fig. 3.1.6 – Types of liberation, type 1, 2 = free, type 3 = simple combination, type 4 = complex combination: two or more separate volumes of mineral [Schubert].

The main conclusion of the theories is that the degree of liberation, expressed in the volume percentage of minerals unliberated (U) and liberated (L) is inversely proportional to particle size.

$$\frac{d_1}{d_2} = \frac{L_2}{L_1}$$

Assume L=60% or 60% of the valuable mineral is free at average particle size d. When we reduce the average size to 0.5d, then L=80%, and to 0.25d, then L=90%.

It is important to consider the downstream concentration processes when analysing the required degree of liberation. For density and magnetic concentration, the volume ratios of mineral to host rock in a particle are determining, while for flotation, leaching, dissolution or electrostatic concentration, only the mineral phases that are exposed to the particle surface are determining. As a consequence, in the latter the volume ratios in the unliberated particles do not give the correct picture of concentration possibilities (See the enclosed volume in type 4, Fig. 3.1.6).

Liberation analysis (washability)

The degree at which the mineral is intergrown in the host rock, as well as liberation of the mineral in particles of a given size class, can be determined by direct inspection. The particles can be moulded in a carrier (usually epoxy) and cut in slices and polished. For microscopy also thin section can be made. Digital imaging techniques enable the measurement of linear or planar ratios of the visible mineral relative to the rock, on condition there is sufficient contrast (Fig. 3.1.7, left). In some cases contrast can be increased by applying surface treatment or chemicals. These measurements give a value for L and U directly, however they are too optimistic. When considering only a linear or planar section of a combined particle, there is a considerable probability that the section shows only one type of mineral (Fig. 3.1.7., right). Therefore these determinations require geometric correction. Gaudin's method (below) can be applied for this.

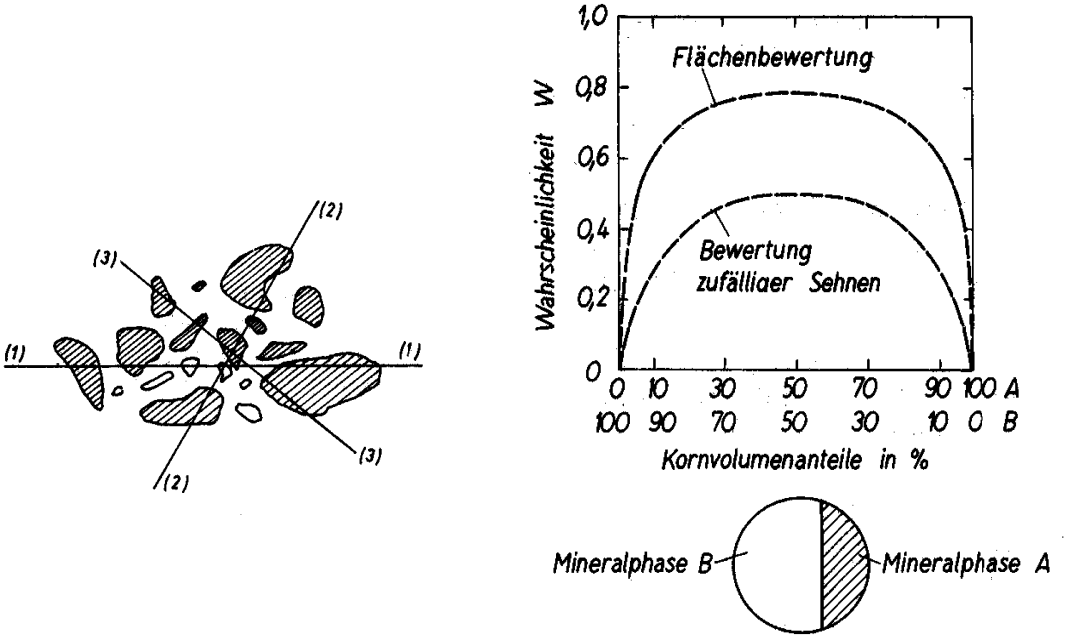

Fig. 3.1.7 – liberation analysis by direct inspection. The linear or planar observations (left) are too optimistic and require geometric correction (right). W gives the probability that indeed two phases are observed in a random section of a combined particle. The lower curve is for linear sections, the upper for planar sections.

From the sections, of each particle the average size and ratio of mineral to host rock can be determined by digital imaging. When this is not available it can be done by hand as well, but this is quite laborious. The particles are classified in narrow size ranges i. For each, L_i is given by:

$$L_i = \frac{N_{fr}}{N_{fr} + N_{eq}}$$

With N_{fr} the number of free particles within size range i, and N_{eq} the number of equivalent particles in size range I, as determined based on measurement of the sections. N_{eq} is the volume (estimated from area or length as observed) of all unliberated mineral in i added up, divided by the average particle volume of i. When linear or planar sections were used for the determination of N_{fr} and N_{eq}, a geometric correction needs to be applied for L_i using Fig. 2 and the following equation[2]:

$$L_i = \frac{N_{fr} - N_{eq}\left(\frac{1}{W} - 1\right)}{N_{fr} + N_{eq}\left(1 - \left(\frac{1}{W} - 1\right)\left(1 - \langle V_M \rangle\right)\right)}$$

N_{fr} and N_{eq} are those as determined from the planar or linear sections and V_M is the estimated average volume fraction of the valuable mineral. W is determined by Fig. 2, right (note that V_M=A in Fig. 2). The total liberation percentage L of the sample is now composed of those of all size classes i together:

$$L = \frac{\sum L_i m_i c_i}{< c >}$$

m_i is the mass fraction of size class I, c_i the mass fraction of valuable mineral in I, and <c> the average mass fraction of valuable mineral in the total sample. <c> and c_i can be determined analytically or directly from imaging.

Liberation (or washability) curves

The liberation of a given feed material can be systematically investigated by first classifying into size classes, and successively by determining the distribution of the mineral phase in each size fraction. This method is standard routine in coal preparation where the heavier mineral phase "ash" is considered (all mass left after the coal is burned), but can be equally well applied for any other mineral combination. The density of average pure ash is around 2.6, and that of pure coal around 1.3. Therefore, since ash content is proportional to density, the liberation of ash can be determined by density analysis. By laboratory density analysis the cumulative floats are collected and analysed on ash content after incrementally increasing liquid density from about 1200 kg/m^3 to over 2200 kg/m^3 in steps of e.g. 100 kg/m^3. The resulting data can be plotted and result in curves as given in Fig. 3.1.8.

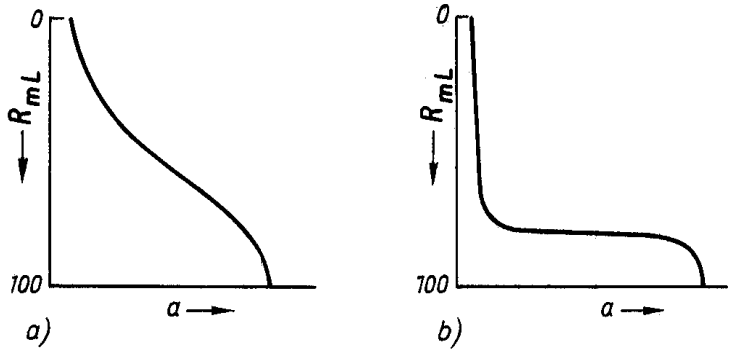

Fig. 3.1.8 – Mineral phase, in this case coal ash content "a" (x-axis), is plotted against the cumulative total mass recovery of floats (y-axis). It is more evenly distributed in the poorly liberated material of the left curve, compared to the well liberated material of the right curve.

As example, a coal having an ash content of 20% is considered. When the ash is perfectly liberated, which is never the case in practice, the first 80% would float of during the density analysis without bringing out any ash: from 0% to 80% on the y-axis, "a" would be 0%. When the density of the ash is reached, at once it would all float and the curve would jump to 100% ash. Thus the liberation curve looks like a horizontal step. In the other extreme, all particles have the same ash content and there is no liberation. The curve is a vertical line at 20% ash content.

[2] This is not needed for volumetric (tomographic) imaging, e.g. based on X-ray transmission, or methods based on density, susceptibility etc.

In practice curves similar to those shown in Fig. 3.1.8 are obtained. To the left a coal showing a poor washability (poor liberation), to the right a coal having good washability. Typically the curve starts at a minimum ash content of 2 – 5 % and a maximum of 75 – 95%. Pure coal phase and ash phase will show residual finely dispersed content of the other phase, which will not be liberated at all at the given size range. The washability (or "ease of concentration") of different coal types can be compared by looking at the curves *for the same size interval only.* When different size classes of the same coal are considered they will show better washability for the smaller sizes (move gradually from the shape of type a towards type b in Fig. 3.1.8).

Coal washability curve

Coal sample ID: Example

Lower size: 5 mm Upper size: 25 mm

Column:	1	2	3	4	5	6	7	8	9	10	11	12	13
	Density class	X-(density)		**Mass %**	Cum. Mass %	**Ash %**	Ash %	Cum. mass	Cum. ash	Average ash	Cum. Mass	Cum. Ash	Average ash
	kg/m^3			**of class**	of class	**of class**	share of total	floats	in floats	in floats	sinks	in sinks	in sinks
	lower	upper	average		Y-axis	X1				X2			X3
	0	1300	650	49.4%	49.4%	1.7%	0.84%	49.4%	0.84%	1.7%	100.0%	17.83%	17.8%
	1300	1400	1350	20.6%	70.0%	5.3%	1.09%	70.0%	1.93%	2.8%	50.6%	16.99%	33.6%
	1400	1500	1450	6.3%	76.3%	15.6%	0.98%	76.3%	2.91%	3.8%	30.0%	15.89%	53.0%
	1500	1600	1550	4.0%	80.3%	26.8%	1.07%	80.3%	3.99%	5.0%	23.7%	14.91%	62.9%
	1600	1800	1700	2.9%	83.2%	39.5%	1.15%	83.2%	5.13%	6.2%	19.7%	13.84%	70.2%
	1800	2000	1900	2.2%	85.4%	59.8%	1.32%	85.4%	6.45%	7.5%	16.8%	12.69%	75.6%
	2000	2200	2100	2.5%	87.9%	71.3%	1.78%	87.9%	8.23%	9.4%	14.6%	11.38%	77.9%
	2200	10000	6100	12.1%	100.0%	79.3%	9.60%	100.0%	17.83%	17.8%	12.1%	9.60%	79.3%
	10000	Sum:		100.0%			**17.83%**	**ash % in feed**					

Fig. 3.1.9 – Coal washability form. The washability curve is given by column 6 plotted on the X-axis against 5 on the Y-axis.

In the example given here it is shown how a washability curve (Fig. 3.1.10, solid line, left) can be constructed from laboratory sink-float data and ash analysis (the shaded columns in Fig. 3.1.9 are the data acquired in the laboratory). Besides, cumulative ash in the floats (lower dotted curve) and sinks (upper dotted curve) are shown in the same graph. The total mass recovery in the floats as function of density is shown in the right curve. Often both curves are combined in a single diagram.

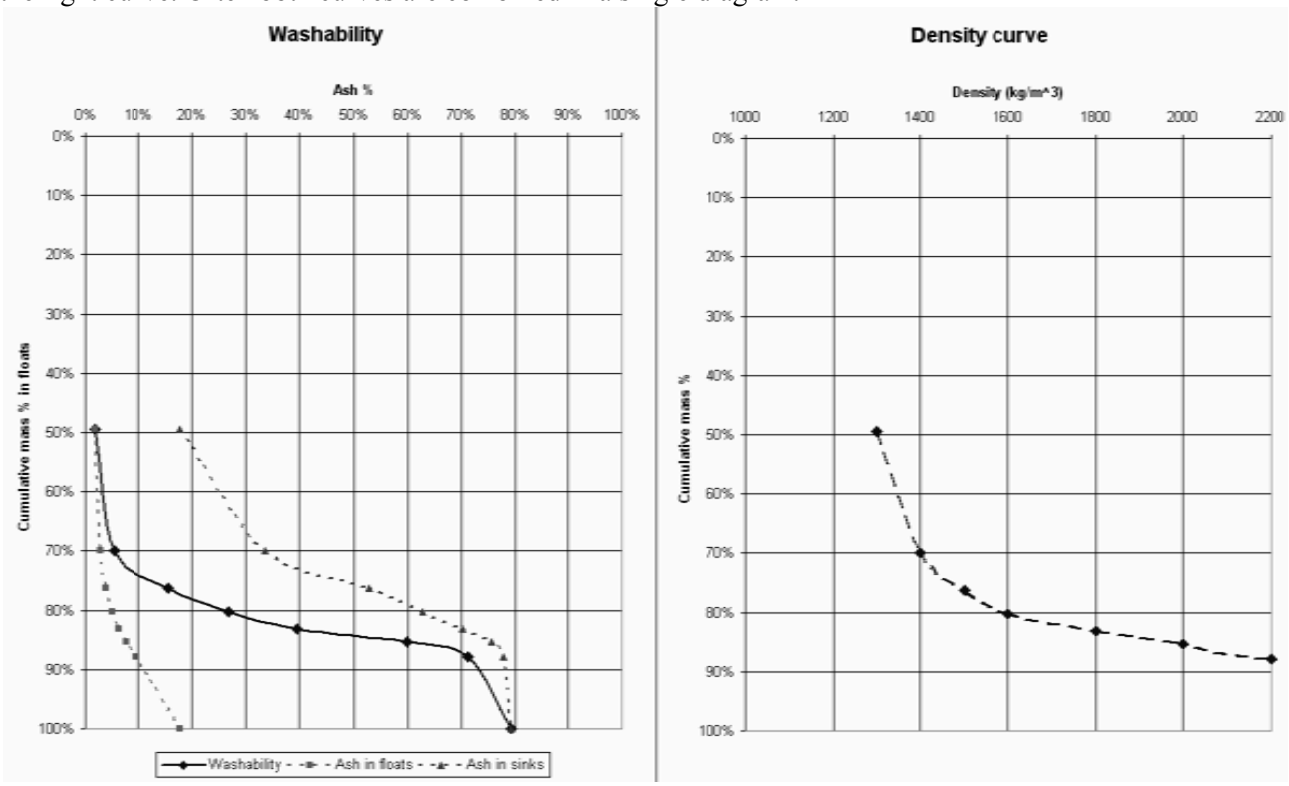

Fig. 3.1.10 - Washability and density curves

The practical value of the curves is illustrated with an example. Of the considered size fraction, it is decided to set the cut density of a heavy medium separation vessel at 1600 kg/m^3. From the right curve it is directly determined that the mass recovery is 80%. From the left curve it is read that at 80% mass recovery the ash percentage of the coal will be 5% and of the waste about 63%.

3.2. Crushing

Primary (coarse) crushing is usually carried out on the mine site itself in order to save transport costs. Two important crusher types are distinguished: Jaw crusher (Fig. 3.2.1 and 3.2.2) and gyratory crusher (Fig. 3.2.3). In both crusher types fracture of rock is achieved by compressing two massive armoured crushing blocks together. The crushing surfaces are usually made of manganese steel and are arranged such that the input opening is larger than the discharge opening due to a predetermined nip angle (angle between the crushing blocks). As a result, large particles can only pass the crusher after fracture. In this type of equipment, size of the input and output openings determines the reduction ratio. Scalping screens (a screen removing all sizes smaller than the top crusher product size) may be installed ahead of the crusher to remove undersize material and fines.

Jaw crushers consist of two more or less plane crushing surfaces that are pushed together periodically with a typical stroke of 10 – 25 mm at the set opening and 4 – 6 mm at the gape (feed opening). Gyratory crushers, on the other hand, consist of a vertical concave cone in which a conical mantle gyrates. Jaw crushers are usually applied at low throughputs or when the feed occasionally contains material that obstructs the crusher: they are easier to maintain and take apart. At high throughputs, gyratory crushers are more cost effective at equal capacity, and have the advantage that they can be directly fed from a truck. A jaw crusher always requires a special feeder. A choke feed is the operation of a crusher with a completely filled chamber.

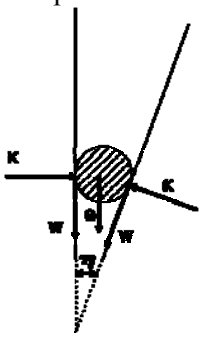

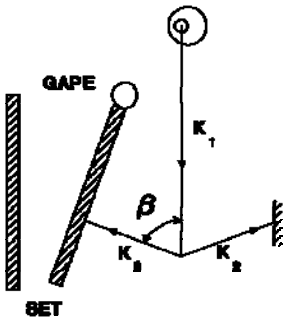

$$K_2 = \frac{K_1}{\cos\beta}$$

$\beta \rightarrow 90^\circ$

$\cos\beta \rightarrow 0$

$K_2 \rightarrow \infty$

Negligible weight G relative to other forces
K = crushing force
W = friction force

$K \cdot (1 - \cos(\eta)) - W \cdot \sin(\eta) = 0$

$$\frac{W}{K} = \tan(\varphi) \quad \text{(Friction angle)}$$

$K - K \cdot \cos(\eta) - W \cdot \sin(\eta) = 0$ (1)
$K \cdot \sin(\eta) - W - W \cdot \cos(\eta) = 0$ (2)
$W \leq K$ boundary case $W = K$ (3)

$$\frac{W}{K} = \frac{1-\cos(\eta)}{\sin(\eta)} = \frac{2\sin^2\left(\frac{\eta}{2}\right)}{2\sin\left(\frac{\eta}{2}\right)\cos\left(\frac{\eta}{2}\right)} = \tan\left(\frac{\eta}{2}\right)$$

hence: $\eta < 2 \cdot \varphi$

Fig. 3.2.1 - Overview of forces in a jaw crusher.

Jaw crushers, invented by Blake in 1858, are employed for middle hard and hard rock (Fig. 3.2.2). The Blake type is still widely used. Other types vary in the method of transferring breaking forces, but are in essence the same (Dodge, Universal, Krupp, Gauldie etc.). They have an intermittent breaking action, contrary to cone crushers that continuously exert breaking. Heavy flywheels are present at both ends of the driving shaft; one of them is connected with V belts to the driving motor. The nip angle should be small enough in order to prevent the rock from slipping upwards under compression. Nip angles should be as high as possible for a maximum reduction ratio. In theory critical nip angles vary between 22^o and 33^o depending on the material, but in practice nip angles between 16^o and 20^o for hard rock and between 18^o and 22^o for middle hard material are common.

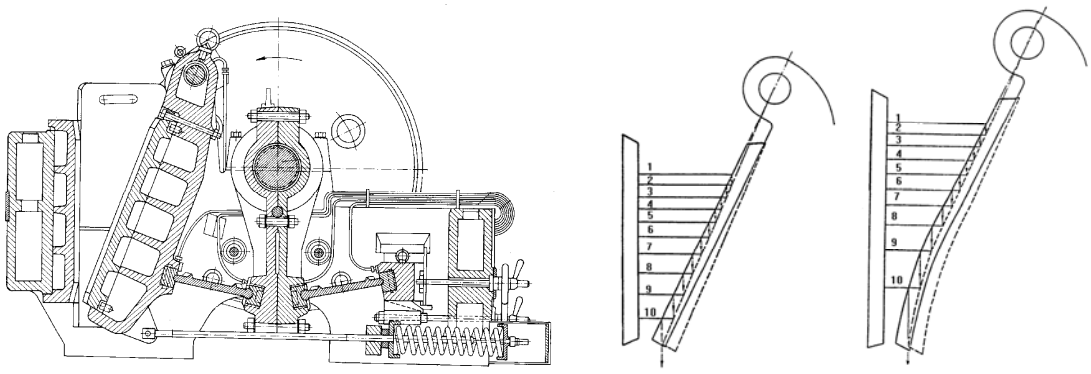

Fig. 3.2.2 - Cross section of "Blake" primary jaw crusher (left) and two jaw geometries (right) [SME].

An optimised stroke frequency (n, usually expressed in ^{1}/min) is essential for proper operation of a jaw crusher. If n is too high, the material has insufficient time to fall downwards. If n is too low, the material densifies between the jaws. In both cases capacity will decrease.

Large primary jaw crushers: n=140 ... 180 min^{-1}, feed opening dimensions: gape<1.8m, width<2.5m, set opening <0.4m. Max. capacity <1100 m^3/h.

Medium sized primary crushers: n=180 ... 250 min^{-1}, stroke length 15 ... 25 mm.

Smaller secondary crushers: n=275 ... 400 min^{-1}, stroke length 10 ... 12 mm.

Jaw crushers may choke when too much material accumulates near the set. For smaller crushers, curved plates are applied for a better volume distribution and decreasing nip angle as the material becomes finer (Fig. 3.2.2, right). Constant feed rate is needed for proper operation and to prevent choking. A choked jaw crusher cannot be started and must be emptied before re-start, which is a labour intensive procedure.

The maximum feed size is approximately (0.8 ... 0.9)G, with G the gape. The width of the feed opening, W, is usually >1.6G. Capacity of a crusher is often expressed in m^3/h, which is readily expressed in t/h by multiplying with the rock density in g/cm^3. Capacity is delimited by the smallest cross section at the set, which is S*W (S=set). Within certain limits the capacity of the crusher is variable by changing S. Table 3.2.1 can be used to estimate jaw crusher capacity, unit mass and electric power.

Table 3.2.1 - Jaw crusher capacity [Schubert Vol. I].

	small					*medium*					*large*	
W	315	400	500	630	800	900	1000	1250	1600	1800	2200	mm
G	200	250	315	400	500	630	630	900	1250	1400	1600	mm
S_{min}	25	30	40	45	60	80	75	120	180	190	230	mm
S_{max}	60	70	80	95	130	160	160	230	320	320	330	mm
V_{min}	**2**	**3**	**9**	**14**	**27**	**40**	**50**	**90**	**150**	**230**	**270**	**m^3/h**
V_{max}	**4**	**10**	**16**	**30**	**60**	**80**	**100**	**170**	**270**	**380**	**520**	**m^3/h**
Mass	3	4	6.5	10	20	28	30	60	120	170	240	t
Power	6	9	13	18	35	50	50	75	110	130	160	kW

W=width, S=gape, S=set, V=volume capacity

Gyratory crushers have the same application as jaw crushers, their main difference being the fact that the crushing action is continuous. An eccentric cone is rotated in a funnel shaped opening (Fig. 3.2.3). The largest stroke is at the set opening. Similar to the Blake jaw crusher, the crushing action is effected by exerting pressure. The set can be varied by hydraulically lifting or lowering of the spindle (central axis with the cone). The hydraulic system also protects against unbreakable material. In this case the spindle lowers permitting the object to pass the set. The spindle automatically returns into its original position. Starting the crusher with a full crushing chamber and a choke feed is possible. The feed can be directly dumped from a mine truck or shovel.

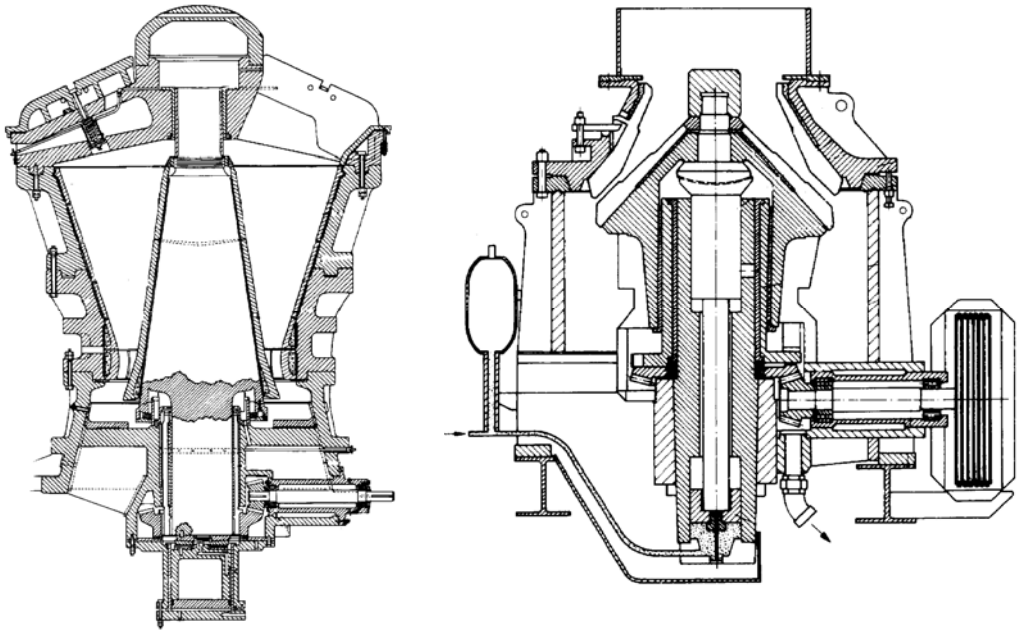

Fig. 3.2.3 - Cross-section of gyratory (left) and cone crusher (right) [SME].

For an equal maximum feed size the capacity of a gyratory crusher is about 4 times that of a jaw crusher. The capacity V can be estimated with the following expression (in m^3/h):

$$V = 0.8 D^{2.5} S$$

D is the lower diameter of the crushing cone (in m) and S the set (in mm). A selection chart for large gyratory crushers is given in Table 3.2.2:

Table 3.2.2 - Selection of large gyratory crushers [Schubert Vol. I].

D_f	1000	1250	1600	2000	2500	3150	mm
G_f	315	400	500	630	800	1000	mm
S_{min}	40	50	70	80	100	120	mm
S_{max}	80	100	140	160	200	240	mm
Mass	15	22	40	65	85	150	t
Power	45	55	75	90	130	170	kW

D_f=total diameter feed opening, G_f=radial width of feed opening, $S_{min,max}$=set

The design of **cone crushers** is in principle similar to gyratory crushers. They are employed as secondary crusher. Crushing action is more based on impact rather than on pressure. Hence they have a faster rotating speed of the cone, which usually varies between 300 and 600 min^{-1}. The effective nip angle is smaller as for a gyratory crusher and may decrease to the bottom (as with the curved jaw crusher shape, Fig. 3.2.2, right). Reduction ratios are 15 ... 20. The maximum feed size can be up to 250 mm for a large crusher, and the product size can be as small as 3 mm for a small one. The stroke length is several times more than the set, contrary to gyratory crushers where it is reverse. Cone crushers have a much wider crushing cone with a side angle of 30^o at the top to 50^o at the lower end. For gyratory crushers this angle is constant (60^o ... 75^o).

If for primary crushing a jaw crusher or a gyratory crusher is selected depends on several factors. An overview:

Jaw crusher advantages

- Little head room required, favourable for underground crushing
- Easy replacement of worn parts
- Easy adjustment of set opening

Jaw crusher disadvantages

- Expensive, heavy foundations necessary due to intermittent crushing action

- Emergency stopping impossible due to fly wheels
- Re-start with choked crushing chamber impossible
- Flat objects may pass uncrushed
- A special feeder for constant feed rate is needed to prevent choking

Gyratory crusher advantages

- Very high capacities (up to 8000 t/h)
- High energy efficiency
- Costs of foundation lower (continuous crushing action)
- Less choking problems
- Less sensitive for unbreakable material (no fly wheels)
- Direct feeding from different sides with 200 – 300 tonne mine dumpers is possible
- Irregular feed and choke feed no problem
- Emergency stop possible, no fly wheels
- Re-start with filled crushing chamber is possible

Gyratory crusher disadvantages

- Complex construction
- Feeding with soft material is impossible (rule of thumb: "if it can't be screened, it can't be gyratory crushed")
- High wear of bearing
- Specific shape of the crushing plates: turning of liner plates is impossible, higher replacement costs.

At an equal top feed size, jaw crushers are cheaper than gyratory crushers, however at an equal capacity gyratory crushers are cheaper than jaw crushers. The final choice is determined by the relationship between feed opening and capacity. At a low mine capacity and large top feed size, jaw crushers are more favourable. Today most high capacity ore mines exclusively employ gyratory crushers.

Toothed, slowly rotating **roll crushers** are frequently applied in primary crushing of coal, e.g. in underground longwall mines, as well as for other sticky or soft minerals (sedimentary iron ores, salt). The teeth move at a linear speed of about 100 m/min. Fig. 3.2.4, left, shows a single roll crusher, but two and even multiple roll configurations exist as well. The long teeth act as feeders and split the larger lumps. The shaft bearings may be spring mounted to protect against uncrushable objects (example: steel roof supports). Top feed size should not exceed half the roll diameter. Maximum roll diameter is 2.5 m at a width of 2.5 m. Maximum top feed size is about 2000 mm, and maximum capacity >2000 t/h. Crushing action is mainly by pressure, and in some specific designs also some shear or impact. Low investment and small space requirements make this crusher very effective for smaller or underground operations. As with all roll crushers, undersize material in the feed may still be crushed further, which is a disadvantage.

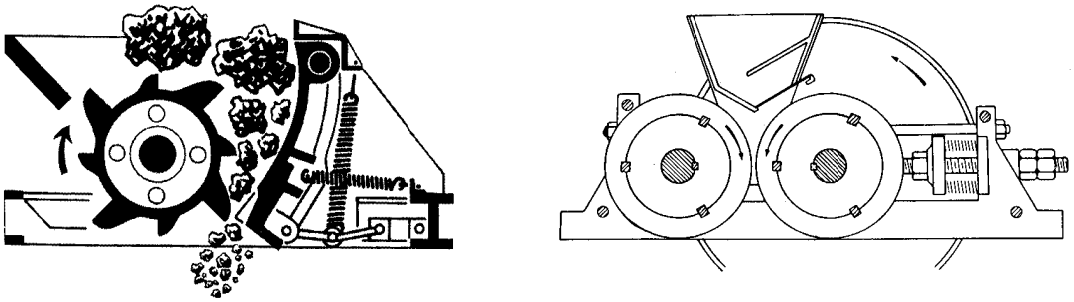

Fig. 3.2.4 - Toothed single crushing roll (left), double crushing roll with flat surface (right) [SACPS (l), Wills (r)].

Roll crushers or **High Pressure Grinding Rolls (HPGR)** for hard rock are widely applied in the cement industry (over 500 applications) and are typically used as **secondary crusher** (Fig. 3.2.4, right), typically preceding a ball mill. In this application the capacity of the ball mill can increase up to 30% when preceeded by a HPGR and considerable energy savings, up to 50%, were obtained. For ore grinding the energy use is

typically between 1 and 2 kWh/t, depending on the hardness. Application of roll crushers is particularly favourable for crushing friable, sticky, frozen, and less abrasive feeds, such as limestone, coal, chalk, gypsum, salt, phosphate, and soft iron ores.

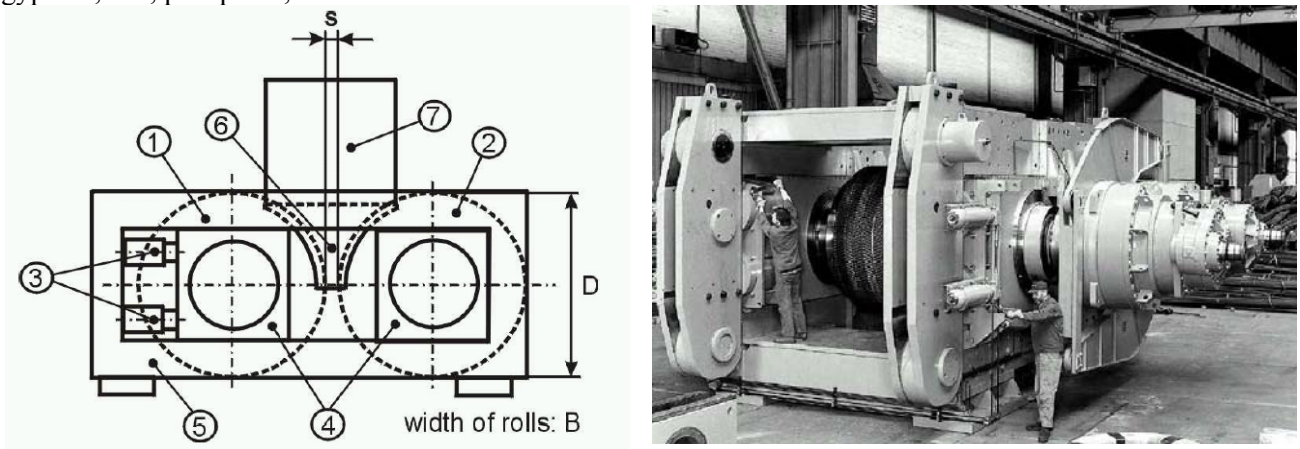

Fig. 3.2.4b – Main HPGR components and picture: 1=floating roller, 2=fixed roller, 3=hydraulic pressure pistons, 4=bearing house, 5=machine frame (can be opened for maintenance), 6=cheek plates, 7=feeding bin.

Most HPGR have a diameter (D) to width (W) ratio close to 1.0 and rolls of up to 2 m diameter. The total press force can be adjusted using a hydraulic system. Machines of different roll geometry can be compared by considering the specific pressing force p=F/D*W. In ore grinding pressure forces typically exceed 2 N/mm^2 and can be up to 6 N/mm^2. Due to geometrical constraints of the rolls reduction ratios exceeding 5:1 are rarely used. However, the high pressure grinding force causes numerous micro-cracks, reducing the costs of downstream grinding and favourable for processes such as leaching. Roll crushers for coarse feed often have corrugated surfaces or a teeth arrangement, while a smooth surface is employed for finer crushing.

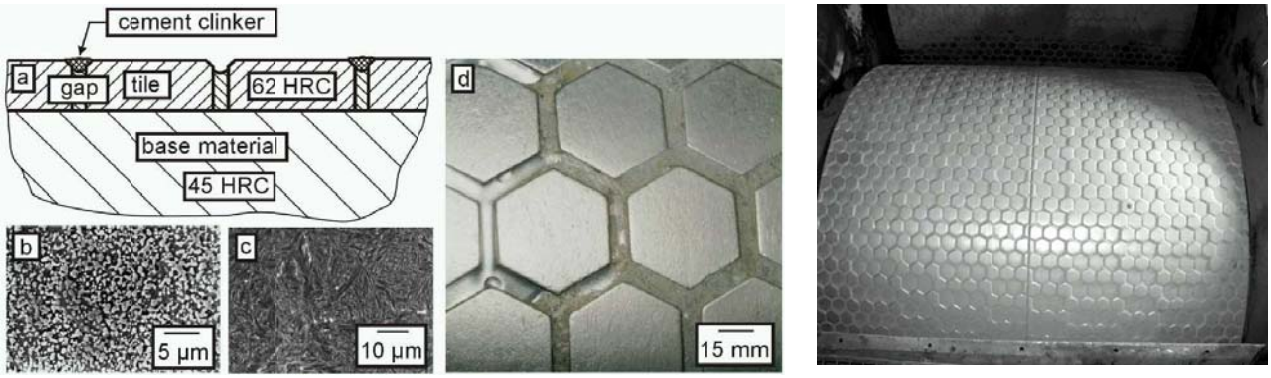

Fig. 3.2.4c – Hexadur liner design, micro structure and surface appearance. The roll shown in the right had a stand time of 7500 h in a cement plant (D=1400 mm, B=1200 mm).

Wear of roll surface, which usually consists of a manganese exchangeable “tyre”, can be high, but newly developed liner material, e.g. “Hexadur” have a very good stand time on rock of considerable hardness (Fig. 3.2.4c). Roll crushers cannot handle choke feed and must be “starvation fed”, since there is no provision for the swelling of broken material in the crushing chamber. Some unbreakable oversize may escape the rolls due to action of the springs or cylinders that push the rolls towards each other.

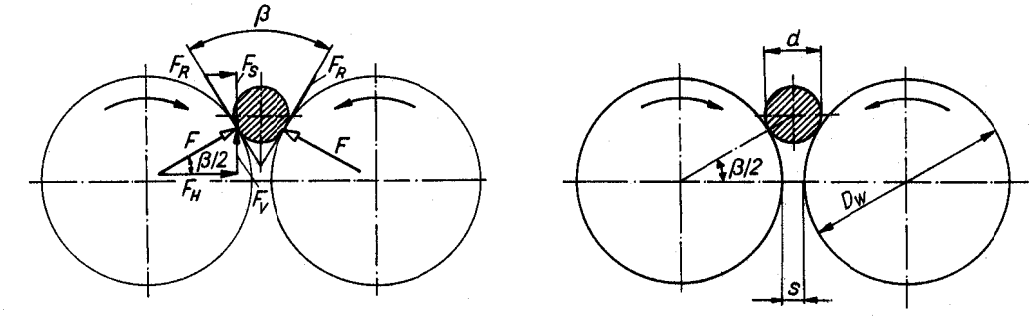

Fig. 3.2.5 - Forces on a particle in a roll crusher [Schubert Vol. I].

The reduction ratio of a roll crusher (N) is determined by S, the set opening (distance between the rolls) and the roll diameter D_w. The top feed size is limited by the roll diameter. If the top feed size is too large, the angle of friction is insufficient to "draw" the feed into the rolls and the material simply stays lying on top of the rotating rolls. This is most unfavourable employing smooth surfaces, for which the theoretical maximum feed size can be determined.

Consider the horizontal component F_H and vertical component $F_V=F\sin(ß/2)$ of the radial contact force F (Fig. 3.2.5, left). F_V acts against the "drawing-in" of the particle that is caused by the tangential friction force $F_R=\mu F$ (μ: friction co-efficient, usually around 0.3). The vertical component of F_R, $F_S=F_R\cos(ß/2)=\mu F\cos(ß/2)$ is opposed to F_V. Condition for the particle's drawing in is:

$$F_S > F_V$$
$$\mu > \tan\frac{\beta}{2} \qquad (3.2.1)$$

For average flat rolls μ≈0.3, hence ß≈30°. In practice the top feed size d_0 should fulfil (Fig. 3.2.5, right):

$$\frac{D_w + S}{D_w + d_0} = \cos\frac{\beta}{2} \qquad (3.2.2)$$

with S the set opening and D_w the roll diameter. From this follows

$$D_w = \frac{d_o \cos\frac{\beta}{2} - S}{1 - \cos\frac{\beta}{2}}$$

or

$$D_w = \frac{d_0 - S\sqrt{1+\tan^2\frac{\beta}{2}}}{\sqrt{1+\tan^2\frac{\beta}{2}} - 1}$$

For total drawing in of the top feed size $\tan(ß/2)<\mu$, therefore:

$$D_w \geq \frac{d_0 - S\sqrt{1+\mu^2}}{\sqrt{1+\mu^2} - 1} \qquad (3.2.3)$$

For a reduction ratio of 4:1 and for μ=0.3 $D_w>67s$ and hence $D_w>17d_0$, while for a reduction ratio of 8:1 $D_w>158d_0$. Hence, for larger reduction ratios the roll diameter becomes excessively large, with consequently higher costs and space requirements. In practice N=3...4 for a flat roll surface and N<8 for a toothed surface. $D_w\approx 20d_0$ for a flat surface, $D_w\approx 10..12d_0$ for a profiled surface and $D_w<10d_0$ for a toothed roll. Roll crusher capacity C_r in t/h is given by:

$$C_r = 3.6vW'S\rho f 10^{-3}$$

v is the tangential velocity of the roll surface [m/s], W' is, for flat roll surfaces the roll width W [mm], for toothed surfaces about 0.5...0.6 the roll width, S the set opening [mm], ρ the material density [g/cm^3], and *f* a materially dependent constant between 0.1 and 0.3.

Advantages of roll crushers

- Low energy consumption
- Simple construction and trouble free operation
- Easy maintenance and repair, especially for fines crushing
- Handles frozen, sticky or agglomerated feed
- Uniformity of product
- Often the most economic solution in the 3...10 mm range
- Simultaneous heat transfer via the rolls is possible

Disadvantages of roll crushers

- Low reduction ratio
- Low capacity in relation to its unit dimensions (not compact)
- Continuous feed rate is necessary, no choke feed

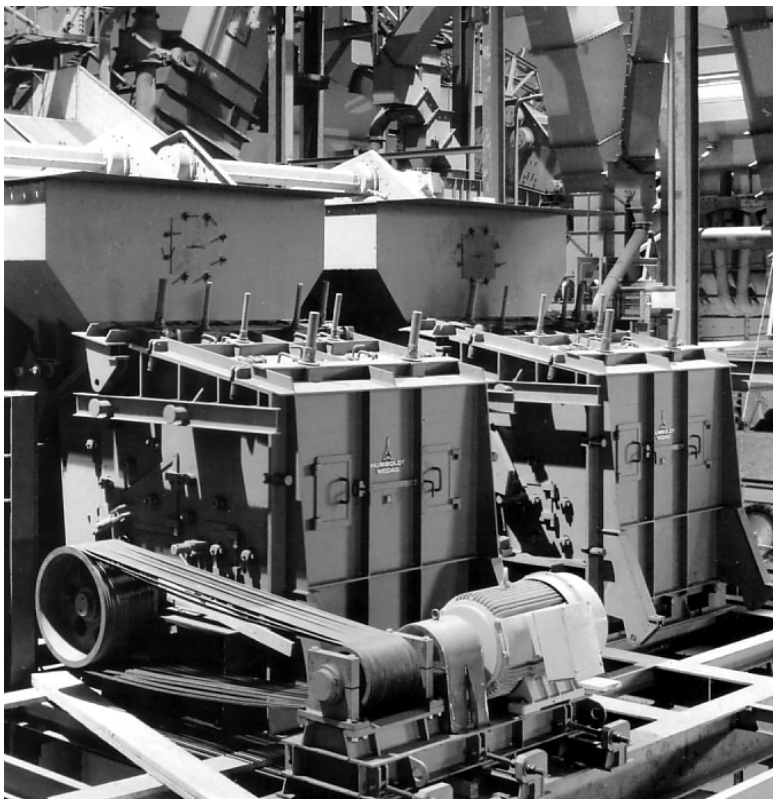

Fig. 3.2.6 – Impact crusher for fine coal [Humboldt Wedag].

For friable materials with low abrasiveness **impact crushers** (Fig. 3.2.6, 3.2.7) or **hammer crushers** (also swing hammer crushers, hammer mills, or cage mills, Fig. 3.2.8) are employed, e.g. for coal, limestone, gypsum, salt, sticky ore etc. Both crushers show similarity in principle and the difference is not always clearly defined. There is a wide variation in impact crusher design, often optimised for specific materials. Important difference is the presence of a bottom screen or "cage" in a hammer crusher (but it is not always installed), and the main crushing action mechanism, which is more between rotor and screen or on the rotor for hammer crushers, instead of on the rotor and rotor plate itself for impact crushers. There is less free space for the material in hammer crushers. Hammer mills can handle more sticky, agglomerating or ductile material.

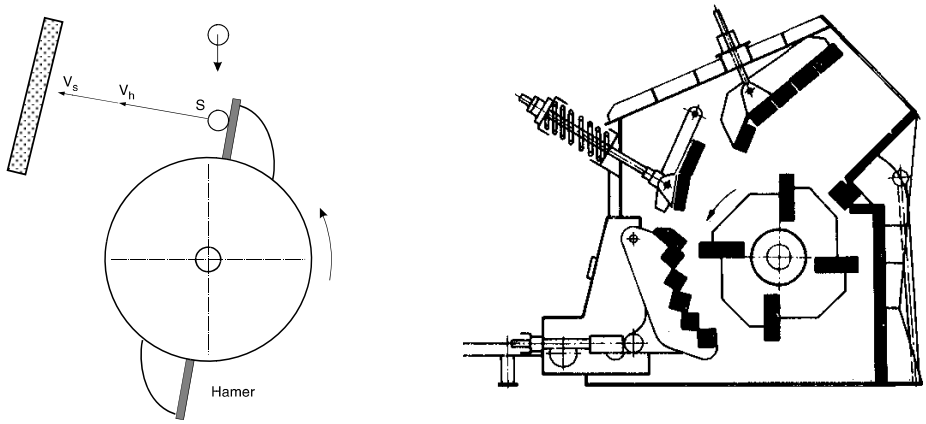

Fig. 3.2.7 - Principle (left) of an impact crusher (right) [Schubert Vol. I (r)].

In **impact crushers** or **impactors** breakage is achieved on the rotor and rotor plate by impact (Fig. 3.2.7, left). An advantage of impact crushers is the reduction ratio that can be as high as 40:1. Size reduction down to 100 μm is possible. The rotation speed is typically between 500 and 3000 rpm (tangential rotor speed 20...60 m/s). Large impact crushers can handle a top feed size of up to 1.5 m with capacities of typically around 1500 m^3/h. Disadvantage may be more excessive fines generation relative to other crusher types and the excessive crushing of undersize feed. Wear will be excessive if silica content exceeds 15%. The distance between rotor and rotor plate is an essential design parameter. For a finer sized product this should be

smaller because of the shorter deceleration distance of fines after impact from the rotor. The braking distance s_0 of a fine particle in air is calculated with

$$s_0 = \frac{v_r d_p^{\,2} \rho_p}{18\eta}$$

where v_r is the starting speed, obtained after collision with the rotor, d_p the particle diameter, ρ_p its density and η the viscosity of air at the ambient temperature inside the crushing chamber. This formula is only valid in the laminar flow regime (Re<1). By adjusting impact plates the crusher can be adjusted to a specific feed. The maximum feed size is 60...1500 mm. When no bottom screen is installed impact crushers can be used for selective size reduction in case one mineral has a different strength than the others. Capacity of impact crushers is given in Table 3.2.3.

Table 3.2.3 - Capacity of heavy duty ("H") and lighter impact crushers ("L") [Schubert Vol. I].

	H	*H*	*H*	*H*	*H*	*H*	*H*	*L*	*L*	*L*	*L*	*L*	*L*	
D_r	630	800	1000	1250	1600	2000	2500	630	800	1000	1250	1600	2000	mm
W_r	630	800	1000	1250	1600	2000	2250	630	800	1000	1250	1600	2000	mm
d_{max}	300	400	500	700	1000	1400	1500	60	80	100	150	250	500	mm
V_{max}	**25**	**40**	**65**	**150**	**310**	**540**	**1000**	**8**	**25**	**50**	**75**	**125**	**390**	**m_3/h**
V_{min}	**10**	**20**	**35**	**60**	**125**	**270**	**460**	**16**	**15**	**25**	**45**	**70**	**125**	**m_3/h**
Mass	3	6	10	20	40	75	115	2	4	6	12	24	50	t
Power	30	45	70	130	200	550	1200	16	30	50	80	140	300	kW

D_r=rotor diameter, W_r=rotor width, d_{max}=top feed size, $V_{max,min}$=Capacity

Advantages of impact crushers

- High reduction ratio
- Easy adjustable to variable feed material or different applications
- Lower capital costs in comparison to jaw, gyratory or roll crushers
- Small head room requirements
- Selective crushing possible in some cases

Disadvantages of impact crushers

- Constant feed rate required
- Only crushing of soft or middle hard rock
- No material that tends to agglomerate should be fed
- High wear (especially on rotor edges), and the need to use advanced wear resistant materials

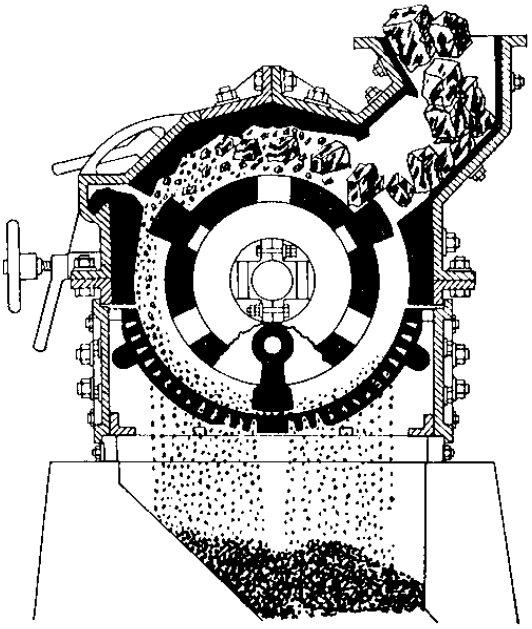

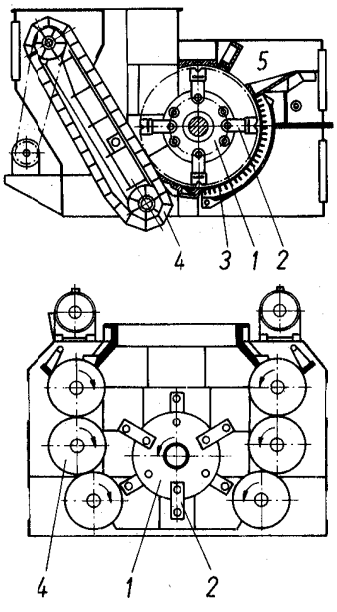

Fig. 3.2.8 - (Swing) hammer crusher (left) and two versions with a moving crusher plate, e.g. for sticky ore (right, 1=rotor, 2=hammer, 3=cage, 4=crushing plate, 5=compartment for uncrushable material,such as tramp iron) [Wills (l) / Schubert Vol. I (r)].

Hammer crushers (lighter versions are also known as **hammer mills** or **cage mills**) have a wide application field and are especially suitable for size reduction of sticky and agglomerating material (Fig. 3.2.8). Rotor speeds are similar as those of impact crushers (20...60 m/s tangential rotor speed). The reduction ratio is usually limited to 10...15. A bottom screen or cage is usually installed ensuring a defined top product size. A special compartment may be present to catch unbreakable material. For sticky feed the impact plates are replaced by impact belts or rolls that remain clean (Fig. 3.2.8, right). In recycling technology similar crushers are known as shredders, where they are especially designed and used for size reduction of object containing (ductile) metals such as scrapped cars, electric waste etc.

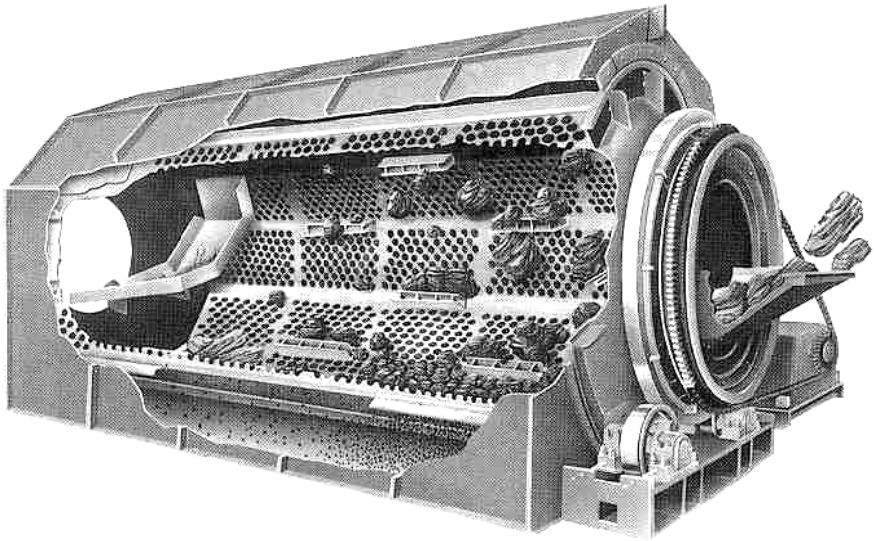

Fig. 3.2.9 - Rotary coal breaker [SACPS].

Rotary breakers are employed for treatment of large tonnages of coal (Fig. 3.2.9). They are not suitable for crushing of hard rock. The rotation speed is 12 – 18 rpm with a diameter of 3...4 m and length of typically 4...10 m. Maximum feed size is about 1100 mm and capacity of the larger units approximate 2000 t/h. The size of the perforation is the size to which the coal is to be broken. Large pieces of shale do not break as easily as coal and are discharged at the end, effecting a pre-concentration ("selective crushing"). The broken coal is quickly removed, so there is little generation of fines. Rotary coal breakers are typically installed for handling run-of-mine washery feed, since they control top size and reduce the need for sorting operations due to partial shale removal. Maintenance and operating costs are relatively low and they are generally cheaper than gyratory or jaw crushers. A disadvantage is that, when present, clayey material may form balls and plug the perforations.

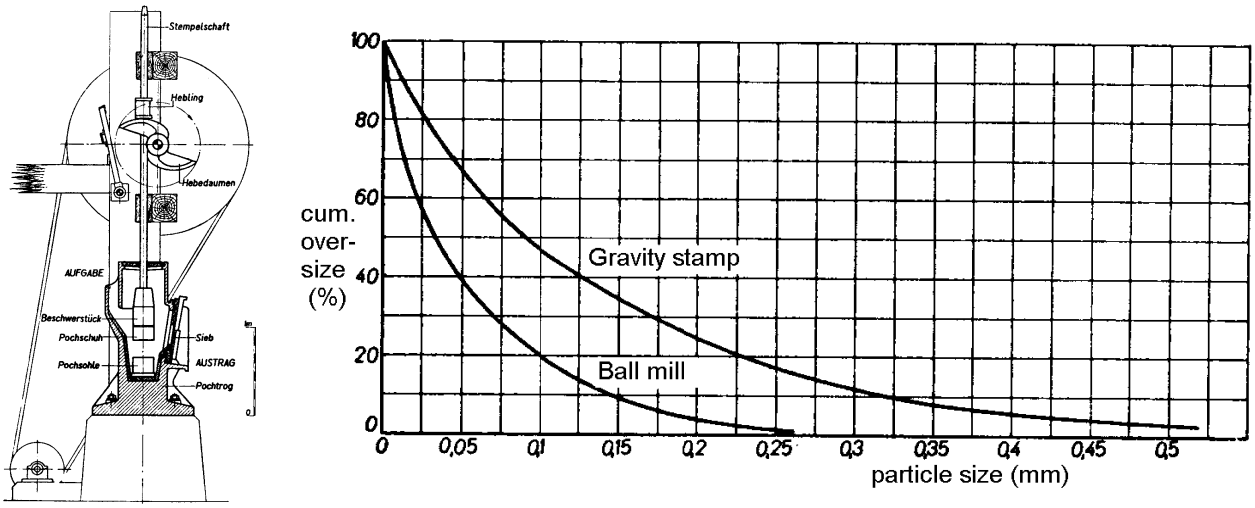

Fig. 3.2.10 - Gravity stamp (left). Comparison of product size distribution of gravity stamps compared to ball mills (right).

Breaking by **hand hammers** or **hand sledges** may, besides laboratory work, occasionally be used to break ore through grizzlies, or to break oversize lumps for crushers that are too small. ≈4 kg sledges are used for soft rock or for work on high altitude, ≈5 kg for average service, and 6...7 kg for hard rock. Design of a crusher plant should be such that hand breaking is unnecessary, since in general its operation is with certainty uneconomic. Hand held or crane mounted **pneumatic hammers** may be used to crush soft and medium hard rock and coal.

Gravity stamps (Fig. 3.1.5, 3.2.10) became obsolete in the first half of the 20th century, but may occasionally be in use at older and small-scale operations. Weight of the stamps could be up to 1000 kg, though 250...750 kg was more common. Drop height was usually 14...20 cm at typically 60...120 drops/min. Capacity ranged from 2...30 t/24h for each stamp, depending on rock type, stamp weight and bottom screen, with apertures (and hence product top size) from 0.5...10mm. The advantage of stamps is the low investment cost for small-scale operations, since crushing and grinding are combined. Therefore it can be seen occasionally in small-scale gold mining operations even today. Further it can handle ore with metallic (pure) copper that is uncrushable in jaw or rotary crushers. The product of a gravity stamp is too inhomogeneous for flotation. Wet operation was more common than dry operation. **Ball breaking** is a variant in which a heavy, multi-tonne ball or block is dropped from several meters height on a large piece of material. It is practiced for primary breaking of large slag from e.g. steelworks or during demolition operations. Armoured plates should be installed around the drop point to prevent the crushed particles spreading away with high speed.

3.3. Grinding

A typical metallic ore is usually crushed downto approximately 5...25 mm. Often this is still insufficient for liberation of the metalliferous minerals. Therfore further size reduction downto approximately 100 μm is necessary, which is effected by means of grinding. Besides liberation, grinding is equally essential in iron making, cement production, preparing pulverised coal fuel and numerous other applications. The majority of grinding operations rely on impact and shear of the material with special grinding media inside the mill, which often consists of a rotating drum. The following mills are distinguished, based on differences in grinding media:

Tumbling mills:

- Ball mill (steel balls)
- Rod mill (steel rods)
- Tube mill (rods&balls, or balls only)
- Pebble mill (hard, rounded rocks, e.g. flint stone or porcelain)
- Autogeneous mill (large pieces of ore)
- Semi-Autogeneous (SAG) mill (Large pieces of ore and steel balls)

Other mill types:

Roller mill, pan mill

Vibratory mill

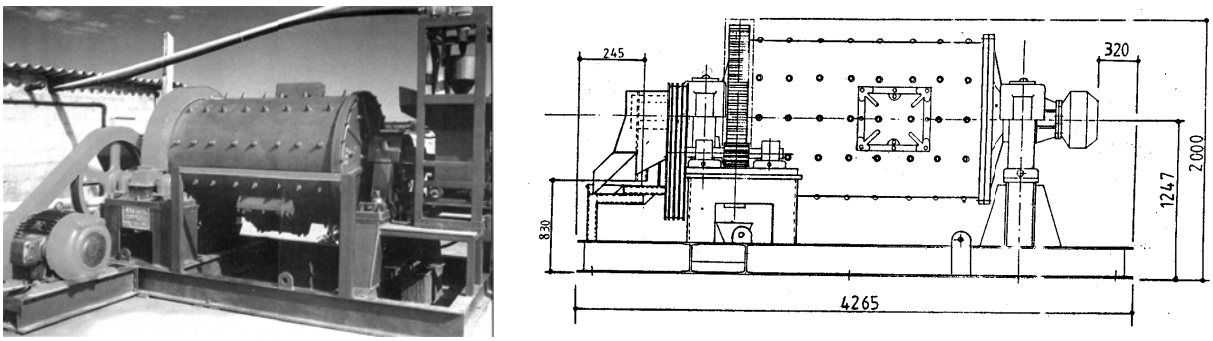

Fig. 3.3.1 - ABJ open discharge ball mill for small gold mining operations:1.2m diameter, 1.5m long, 31 RPM, wave liner, 27 kW power consumption, 2-3 tons of <20mm feed per hour [Waltkru Holdings Ltd].

Tumbling mills have a cylindrical or conical body that rotates around a horizontal axis (Fig. 3.3.1). A cross section with typical terminology is shown in Fig. 3.3.3, left. Tumbing mills can be employed dry as well as wet. Most ore grinding is wet, while in other areas mostly dry grinding is applied (Chemical engineering, ceramics industry, cement, food).

Advantages of wet grinding:

Less energy consumption per tonne of product

No dust generation

Moist feed does not need to be dried prior to grinding (contrary to dry grinding)

Disadvantages of wet grinding:

Higher wear of grinding media and liner

Corrosion

Product is wet and must be dewatered

Some products are not allowed to contact water (cement!)

The fill rate φ_m of the grinding medium is given by

$$\varphi_m = \frac{V_m}{V_M} = \frac{m_m}{\rho_m (1-\varepsilon_m)} \frac{1}{V_M} \qquad (3.3.1)$$

V_m is the total volume of grinding media inside the mill, including porosity, V_M the inside mill volume, m_m the media mass, and ρ_m its density. ε_m is the porosity between the grinding media, which is about 0.4 for balls and 0.2 for rods. The fill rate of the feed, φ_v, is given by

$$\varphi_v = \frac{V_v}{V_M} = \frac{m_v}{\rho_v (1-\varepsilon_v)} \frac{1}{V_M} \qquad (3.3.2)$$

with V_v the feed volume, m_v the feed mass, ρ_v its density and ε_v feed porosity. The effective fill rate, φ_v', indicates the fraction of the inter-media porosity that is filled with feed:

$$\varphi_v' = \frac{V_v}{V_m \varepsilon_m} = \frac{\varphi_v}{\varphi_m \varepsilon_m} \qquad (3.3.3)$$

In practice it appears that φ_v'=0.6...1.1 is an optimum value.

An optimised motion of the grinding media is essential for the efficiency of the mill. It is influenced by

Mill rotation speed

Mill diameter

Shape and size of the media

Medium fill rate φ_m

Liner profile

Handling properties (flow behaviour) of the feed

Ball mills are usually shorter than rod mills and have a diamater that is not much smaller than its length. For large mills the diameter can be up to 6 meters. Feed of a ball mill can be as large as 25...40 mm for friable materials, but is usually no larger than 10 mm. Reduction ratios are in the range of 20:1 ... 200:1. the largest balls have ≈130 mm diameter.

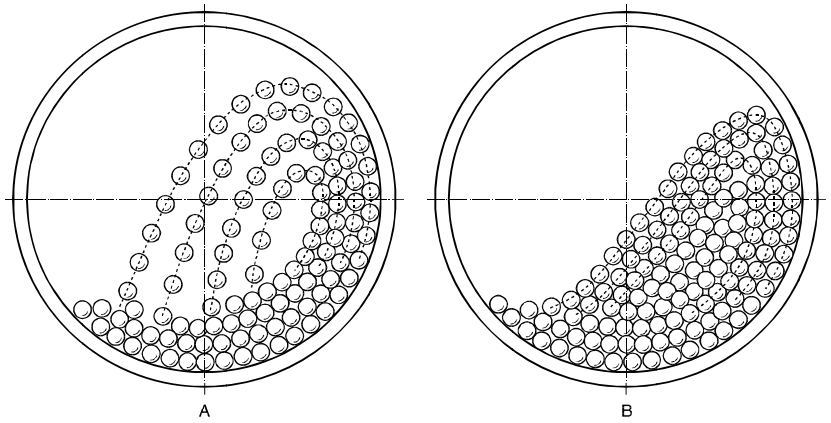

Fig. 3.3.2 - Motion of grinding media A=Cataracting, B=Cascading.

Cataracting (Fig. 3.3.2A) occurs at higher rotation speeds as cascading and is mainly applied in ore grinding, where fines production is undesireable. It also occurs when profiled liners are employed (compare with Fig. 3.2.8, rotary coal breaker). The grinding media are lifted by the lined wall of the mill and return in free fall to the bottom. Grinding action is due to impact of the falling media and due to pressure and shear during upward motion.

Cascading (Fig. 3.3.2B) is employed for ultra-fine grinding, e.g. pigments, and occurs at slower rotation and flat surfaced liner. It is characterised by the rolling motion of the media. The core of the media body remains inactive. Grinding action is due to pressure, shear and friction. The pressure load on the feed grains is determined by mill diameter D_{mill}, average height h of the media indside the mill (depending on φ_m) and density of the grinding media ρ_m:

$$P = \rho_m g h \qquad \text{with } h \text{ proportional to } D_{mill}$$

At intermediate rotation speeds cataracting and cascading occur combined. Excessive wear is problematic on a flat liner surface when slip occurs. When the rotation speed n is too high, the media start centrifuging and there is no grinding action. n_{crit} is the citical speed when centrifuging starts. For every mill and feed there is an optimised rotation speed n_{opt} for maximum efficiency, which is relatively low for cascading and higher for cataracting.

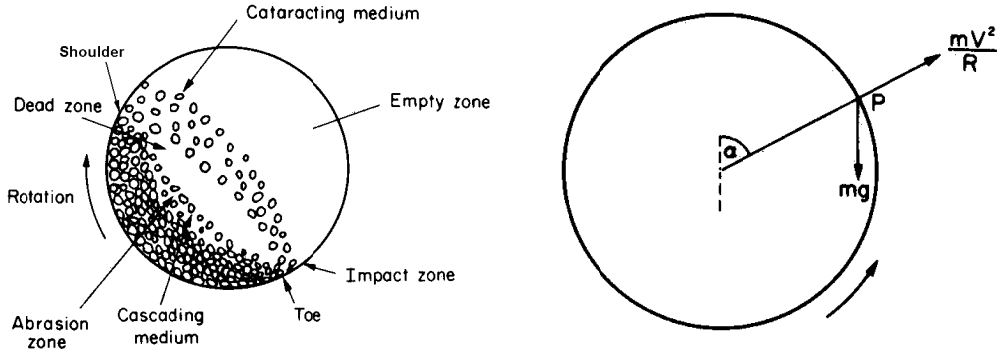

Fig. 3.3.3 - Ball mill terminology (left), mill critical speed determination n_{crit} (right) [Wills].

The critical speed n_{crit} can be determined as a function of mill and media characteristics by means of a force balance in radial direction. The forces in tangential direction consist of support from lifted grinding balls, with no nett effect of gravity. We assume flat liners. When weight of the grinding ball or rod just balances the centrifugal force

$$\frac{mv^2}{R} = mg\cos\alpha \qquad (3.3.4)$$

applies with m mass of the grinding body, v its linear velocity, and g the gravity acceleration. Taking ball or rod diameter into account (D-d)/2 is the radius of the outermost path with D the mill diameter and d the rod or ball diameter. Thus

$$\cos\alpha = 0.0011 n^2 \frac{D-d}{2} \quad (3.3.5)$$

The critical speed n_{crit} is obtained when the balls or rods cannot fall even from the very top of the mill, where $\alpha=0$ and hence $\cos\alpha = 1$. Then

$$n_{crit} = \frac{42.3}{\sqrt{D-d}} \text{ rev/min} \quad (3.3.6)$$

Hence, the larger the mill diameter, the lower n_{crit}. In practice $n_{opt}=0.6...0.8\ n_{crit}$ with $\psi=n/n_{crit}$ the "specific rotation speed".

Design of the liner profile is essential for the grinding media trajectories, as shown in Fig. 3.3.4. Current research pays special attention on mill performance as function of liner profile and liner wear.

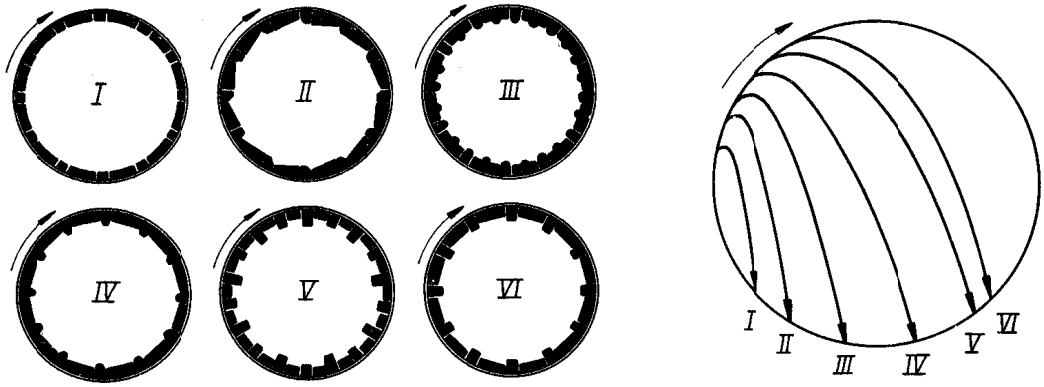

Fig. 3.3.4 - Effect of liner type on ball trajectories. n=constant for I...VI [Schubert Vol. I].

Due to friction and impact between grinding media and wall of the mill wear occurs and mounting **wear resistant liner** is a necessity. Wear may comprise up to 50% of the operational costs of a mill. The type of liner is chosen taking the following into account:

Profile, determines lifting of the grinding bodies (Fig. 3.3.4).
- Cataract: coarse feed, large lifters
- Cascade: fine feed, small grinding media, small or no lifters

Cost price of the wear resistant liner: High investment, low maintenance, or reverse.
Method of liner construction. A favourable method reduces maintenance time and costs considerably.

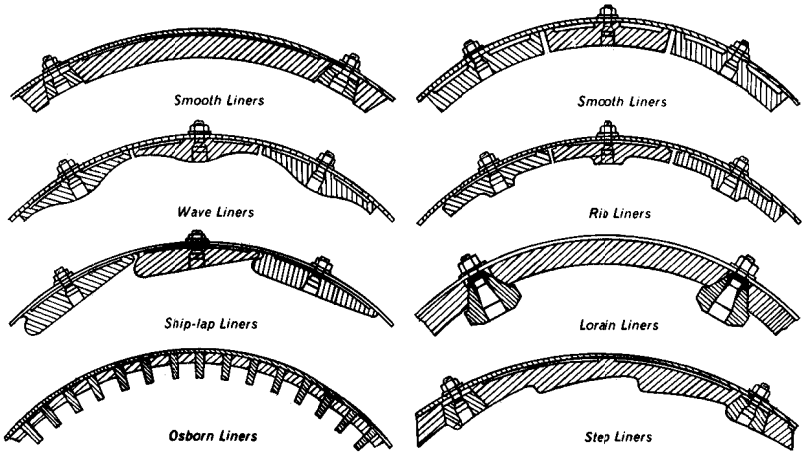

Fig. 3.3.5 - Some liner types and lifter design [Wills].

Frequently used liners are shown in Fig. 3.3.5. Wave liners are often applied in rod mills. A wide variety of liner materials is applied.

Wear resistant steel alloys (Cr-, Mn-, Ni-, Mo-, Va-) of 50...150 mm thickness

Rubber (only when lifters are present to avoid slip). Less noise and easy installation (leight weight).

Grinding mills are fitted with a **gear/pinion assembly** to the driving motor (see Fig. 3.3.1 right, 3.3.6).

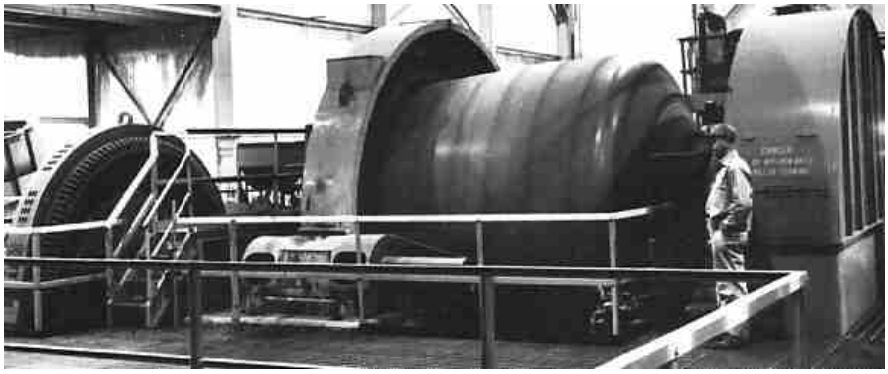

Fig. 3.3.6 - Ball mill with gear/pinion assembly (middle) and driving motor (left) [SME].

Internal length L and diameter D of a mill largely affect:
- Power consumption
- Grinding efficiency (D affects impact intensity)
- Residence time distribution of ore grains
- Mill capacity

The **power consumption** of a tumbling mill can be estimated using an empirically determined expression:

$$P = 8.44 K_T K_\varphi K_\phi L D^{2.5} \qquad \text{[kW]} \quad (3.3.7)$$

The constant 8.44 includes grinding media density (and assumes steel), K_T is a factor determined by a specific type of mill (1.0 for wet overflow discharge, 1.13 for wet grate discharge and 1.25 for dry discharge, see Fig. 3.3.10), K_φ is determined by medium fill rate φ (usually 30%...50%) and K_ψ by the specific rotation speed ψ (n/n_{crit}, usually 65%...85%). K_φ and K_ψ are given in the diagram of Fig. 3.3.7. Summarising,

$$P = f(\rho_m, \varphi, \phi, L, D^{2.5}) \qquad (3.3.8)$$

P is practically independent of particle size distribution and feed rate. Hence, for P it does hardly matter if there is ore in the mill or not. Given constant grinding media and a fixed φ, with the mill internal volume $V_m = \pi/4\ D^2 L$ we can write

$$P = C_1 D^{2.5} L = C_2 V_m D^{0.5} \qquad (3.3.9)$$

where C_1 and C_2 are constants. For the mill capacity m' in t/h:

$$m' = C V_m D^{0.5} \qquad (3.3.10)$$

with C a constant. Mill capacity is proportional to power consumption.

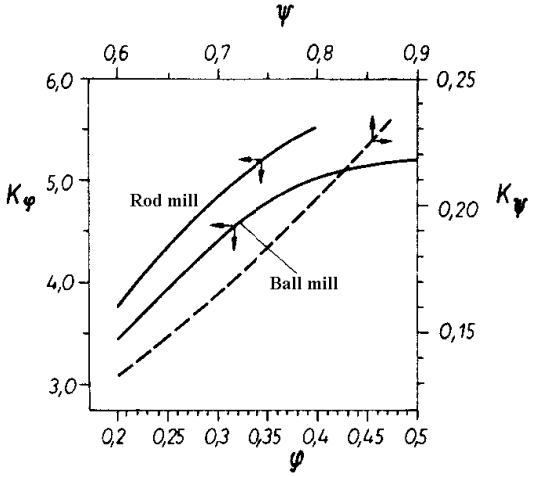

K_φ is read as function of φ_m (medium fill rate) using the solid lines for ball or rod mill.

K_ψ is read as function of ψ (n/n_{crit}, the specific rotation speed) using the dashed line.

Fig. 3.3.7 - Determination of K_φ and K_ψ [Schubert Vol. I].

Several special devices are used for feeding a tumbling mill. The feeder type depends on whether dry or wet grinding is employed, and whether the mills operate in closed or open circuit. Dry mills are usually fed with a vibratory feeder. Fig. 3.3.8 gives three common feeders for wet grinding.

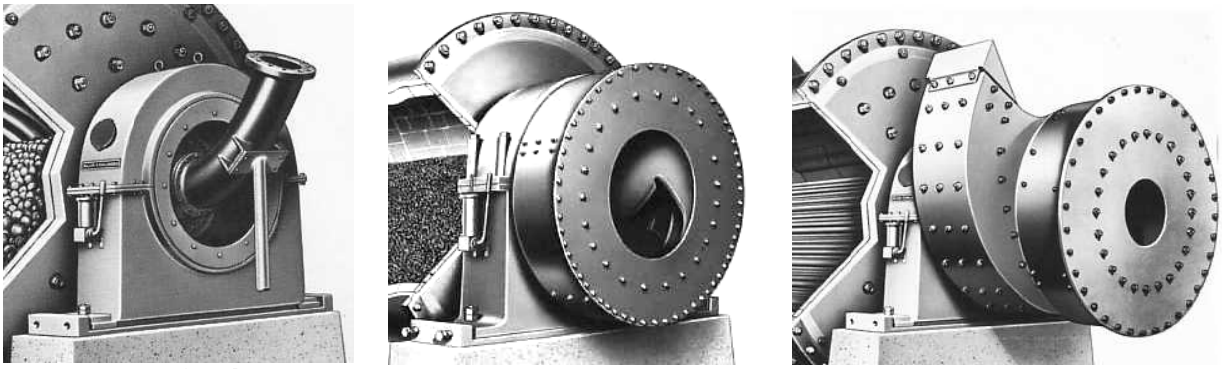

Spout feeder **Drum feeder** **Drum-scoop feeder**

Fig. 3.3.8 - Mill feeders [SME].

A **spout feeder** is often applied for open circuit rod mills or mills in closed circuit with hydrocyclone classifiers. The curved chute gravity-feeds the slurry into the mill.

A **drum feeder** has an internal spiral that carries the feed to the inside of the mill. It requires less headroom as a spout feeder. It allows convenient addition of grinding balls.

A (combined) **drum-scoop feeder** is generally used for wet grinding in closed circuit with a screw or rake classifier (Chapter 2). New material is directly fed into the drum. The scoop picks up the classifier sands for regrinding.

Sometimes double **scoop feeders** (without drum) are used for finer-sized feeds.

Moisture effects the grinding efficiency to a great extend. For an optimised efficiency the feed should have good handling (flow) properties. For dry feeds it should be below 4Vol%. For wet feeds it should be higher than 45 Vol%. The intermediate range 4 Vol%...45 Vol% should be avoided: water bridges between the particles will form due to capillar forces, causing agglomeration. This effect strongly increases with decreasing particle size, especially < 1 mm. Also sticking to the mill internal surface occurs. The optimised moisture content for wet grinding is 50 Vol% ... 55 Vol% for coarse feeds, and 55 Vol% ... 70 Vol% for fine feeds.

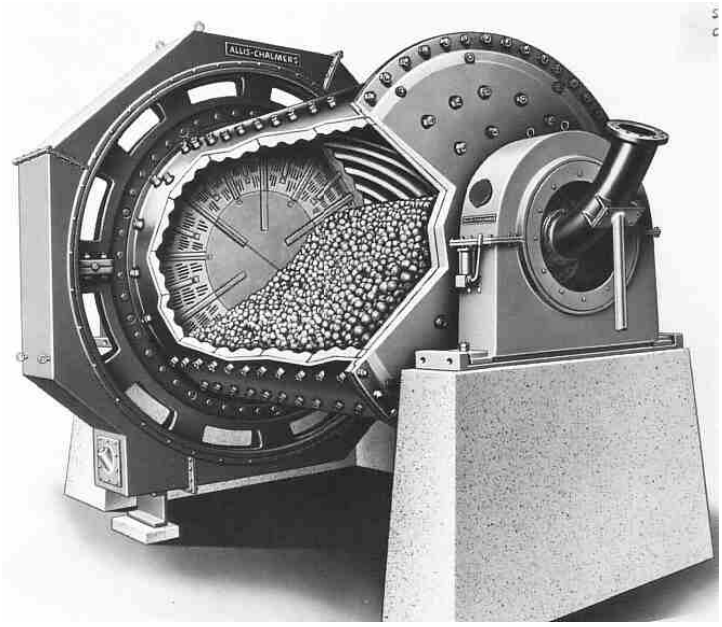

Fig. 3.3.9 - Ball mill with spout feeder and grate discharge [SME].

Usually L/D proportion for ball mills is between 1 and 2. The largest models have L=10m, D=6.5m with P=8100 kW, however optimal results were obtained with D not exceeding 5.5 m. The optimised L/D proportion and ball diameter is largely determined by the d_{80} (80% cumulative undersize diameter) of the feed:

d_{80} of feed [mm]	*max. ball size [mm]*	*L/D*
5...10	60...90	1,00...1,25
0.9...4	40...50	1.25...1.75
very fine	20...30	1.50...2.50

The residence time, and hence grinding efficiency of the material is largely determined by the design of the **discharge**.

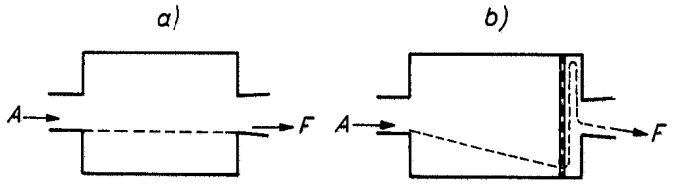

Fig. 3.3.10 - a=overflow discharge, b=grate discharge (A=feed, F=product) [Schubert Vol. I].

An **overflow discharge** (Fig. 3.3.10a) can be used for ball as well as rod mills. The outlet opening has a larger diameter as the inlet. Residence time is relatively long. An overflow discharge is characterised by an essentially trouble-free operation. A disadvantage is possible over-grinding for minerals that are particularly sensitive for it.

In a **grate discharge** mill a screen is installed before the outlet (Fig. 3.3.9 and 3.3.10b). The ground material passing the screen is elevated into the outlet opening via lifters on the mill inside behind the screen. In general, due to the rapid product discharge, residence time of the material is shorter than in an overflow discharge mill. A grate discharge is unsuitable for ultra-fine grinding: the relatively small grinding balls would otherwise blind the sceen. A grate discharge mill produces a coarser product of narrower size width compared to an overflow discharge. A grate discharche cannot be applied for rod mills, otherwise the rods would damage the screen. A disadvantage is the approximately 15% higher energy consumption per tonne relative to an overflow discharche.

Grinding ball diameter is determined by:

Grinding surface: the number of ball-material contact points should be as large as possible.

On pressure load the **catching angle** between the coarsest feed particle and the balls should be sufficiently small (see crushing roll principle, Fig. 3.2.5, right).

On impact load the **kinetic energy** should be sufficient to crush the particle on cataracting.

For a large grinding surface many small balls are needed, for a good catching angle and kinetic energy larger balls are more favourable. Therfore in practice there is an optimised ball size distribution. Bond established an expression for d_0, the largest ball diameter to enter the mill:

$$d_0 = C\sqrt{d_{80}}\left(\frac{\rho_v W_i}{\phi}\right)^{1/3} D^{-1/6} \text{ (mm)} \qquad (3.3.11)$$

with C=0.024 for steel balls, d_{80} relates to the mill feed size and ρ_v to its density. W_i is the Bond work index of the feed (see Section 3.5 for determining W_i) and Φ a characteristic property of the rock to be ground.

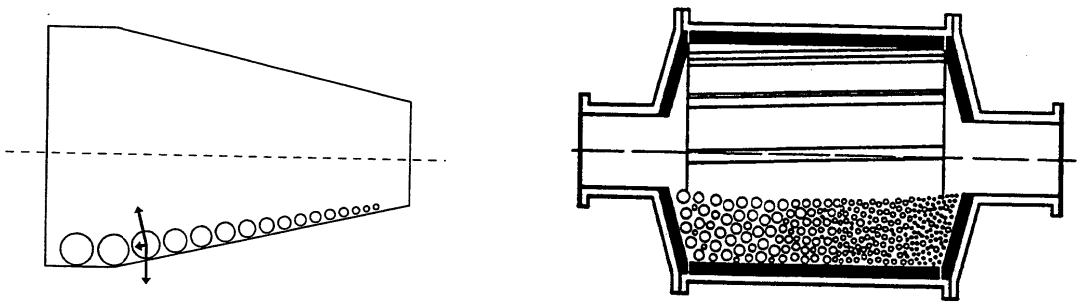

Fig. 3.3.11 - Size segregation of grinding balls due to specific mill design: conical mill shape (left) or spiral twist in liner profile (right).

In practice only the largest grinding balls are routinely added. Only when a mill is filled for the first time a predetermined size distribution must be fed. Wear effects the desired size distribution automatically. Typical steel wear from the media is between 100 and 1000 g per tonne of product, in exceptional cases even up to 3000 g/t.

For ball mills optimised operating parameters are φ=40%....45%, ψ=0.65...0.8 and for the feed d_{80}<10mm. For a >10 mm feed ball mills will not grind efficiently. Any desired fineness of the product can be obtained by giving it sufficiently long grinding time (large residence time).

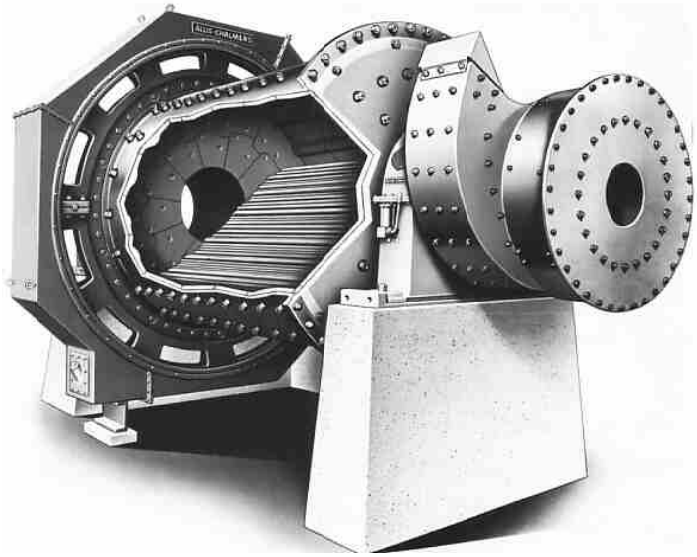

Fig. 3.3.12 - Rod mill with overflow discharge [SME].

The length of a **rod mill** (Fig. 3.3.12) is usually longer as its diameter, typical L/D values are 1.4...1.6. At least L>D in order to prevent the rods from disarranging. The maximum length is limited by the stiffness of the rods: if their diameter <100mm and L>6 m they tend to bend, which should be avoided. The rods serve as crushing medium. For their diameter the same arguments as already discussed for ball mills apply, however rod diameter is less critical as ball diameter. The largest rod mills have L=6.1m, D=4.6m, and P=1700 kW. Usually they are of the overflow discharge type, though rarely central or end peripheral discharge are applied.

Rod mills generate a more uniformly sized product than other tunbling mills and minimise fines (particles that are smaller than the required product size). Apart from grinding, the rods effect classification of the feed (Fig. 3.3.13).

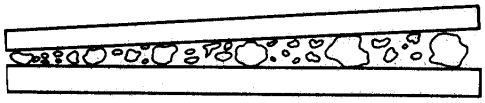

Fig.3.3.13 - Principle of rod mil. Feed from the right, the material flows towards the left [Wills].

In this way only the coarsest material is crushed repeatedly and there is no overgrinding. Due to their classifying effect, rod mills are usually employed in open circuit. Top feed size can be a little larger as for ball mills and should have a d_{80}<25mm. Product size is usually d_{80}=5...0.5 mm, which is considerably coarser as a ball mill product. Optimised φ=35%...45% and ψ=55%...75%. Summarising, rod mills have a coarser feed and product as ball mills. Therefore in many grinding circuits the first stage comprises a rod mill, the second a ball mill.

Autogeneous mills have the same working principle as rod or ball mills, however a coarse lump-sized fraction of the feed serves as grinding media. The wall of the mill is equipped with liners to prevent slip with the feed and to promote cataracting. Some mills have additional breaking plates. Three basic types of AG mills exist: **pebble (PAG) mills**, (conventional) **autogeneous (AG) mills** and **semi-autogeneous (SAG) mills**.

1. Pebble mills are usually fed with fines, e.g. the product of a rod mill. They are only rarely applied for a primary grinding stage. The grinding media consist of classified coarse fraction (usually 25...60 mm), e.g. as taken from the ore flow between a primary and secondary crusher. L/D ratio is similar to ball mills, therefore ball mills can be converted to pebble mills. The pebble size is selected based on the principle that the pebble mass should be equal or larger than the ball mass of a conventional ball mill for the same feed. As example, if for secondary grinding steel balls of diameter 20...40 mm would be needed, the pebble diameter should be 25...60 mm if the pebble density is in the range of 2800...4900 kg/m^3. When applied as primary grinding stage pebbles up to 250 mm can be used. Fill rate: 0.35<φ<0.5 and specific rotation speed 0.6<ψ<0.9. A typical application of pebble mills is the grinding of hard gold ore in South-Africa.

2. Autogeneous mills usually have a coarse feed (200...300 mm), e.g. the product of a primary jaw or gyratory crusher. The coarse feed in the range 100...300 mm serves as grinding media. The grinding mechanism is the crushing due to impact of larger particles on finer ones. The product is typically 3...5 mm, but can be as fine as 0.1 mm, which is fine enough for feeding a flotation circuit. Hence very high reduction ratios (60<N<1000) and one-stage grinding is possible. Because of the low investment costs (70...95% those of ball mills), simple flowsheet (1 stage grinding) and relatively low wear (no steel media) they have been frequently applied since the 1980's. For fine grinding (0.1...1 mm) energy consumption becomes excessively high. Autogeneous mills always operate in cataracting mode. The fill rate is lower compared to other tumbling mills (φ<0.3). This is necessary to prevent gradually slowing down of particles in a thick layer of fine product, which is unfavourable. Mill diameter is considerably larger than other tumbling mills (up to 12.2 m), and L/D is smaller (L/D<0.3).

Dry autogeneous mills or Aerofall mills are frequently applied for one-stage grinding circuits and have high reduction ratios (feed <900 mm, product >80 μm). They operate in closed circuit with a wind-sifter, and can also be employed in semi-autogeneous mode (with added steel balls).

3. Semi-autogeneous (SAG) mills are similar to conventional AG mills and have similar feeds, the difference being the addition of 3...10% steel balls (Fig. 3.3.14). They are especially employed when otherwise the coarse fraction would break too easy and the largest lumps, needed for effective grinding, become depleted. Especially the intermediate sizes not easily break, therefore balls are added.

Fig. 3.3.14 - Svedala's giant 12.2m (internal) diameter, 20 MW SAG mill at Cadia Hill gold/copper Mine, New South Wales, Australia, is world's largest grinding mill (left). Another SAG mill with gear and pinion drive (right) [Svedala (l) / TU Delft (r)].

Fig. 3.3.15 shows a conventional SAG mill design (left) and a design where the mill is supported by multi-shoe hydrodynamic bearings (right). The advantage of the latter is the simpler construction, avoidance of massive castings and easier access to the mill.

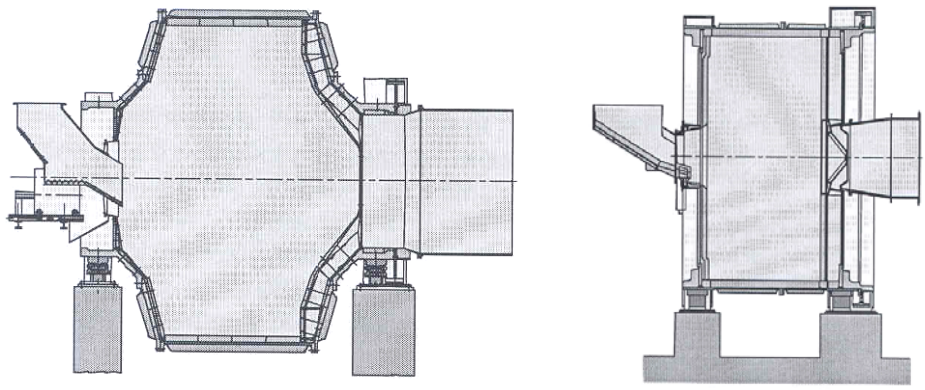

Fig. 3.3.15 - Conventional (left) and shell supported (right) SAG mill design [Krupp Polysius AG].

Advantages of autogeneous mills

- Simple flow sheet
- Lower operational costs as ball mills
- Less contamination of product with Fe^{3+} (less steel consumption), favourable for flotation efficiency
- Increased breaking along grain boundaries when ore minerals are stronger than the matrix due to lower impact load compared to ball mills. This results in optimised liberation and more efficient flotation (better adherance of air bubbles).

Disadvantages of autogeneous mills

- Not suitable for all ore types
- Autogeneous mills cannot be designed using lab-scale tests results alone: expensive pilot scale testwork is necessary (scaling up).
- Higher energy consumption for fine grinding
- Higher slimes generation may occur due to attrition, which may cause high reagent use in downstream flotation stages
- Capacity per unit of mill volume is lower, due to lower density of grinding media and lower φ
- At a variable ore body supply of ore that grinds autogeneously may be problematic

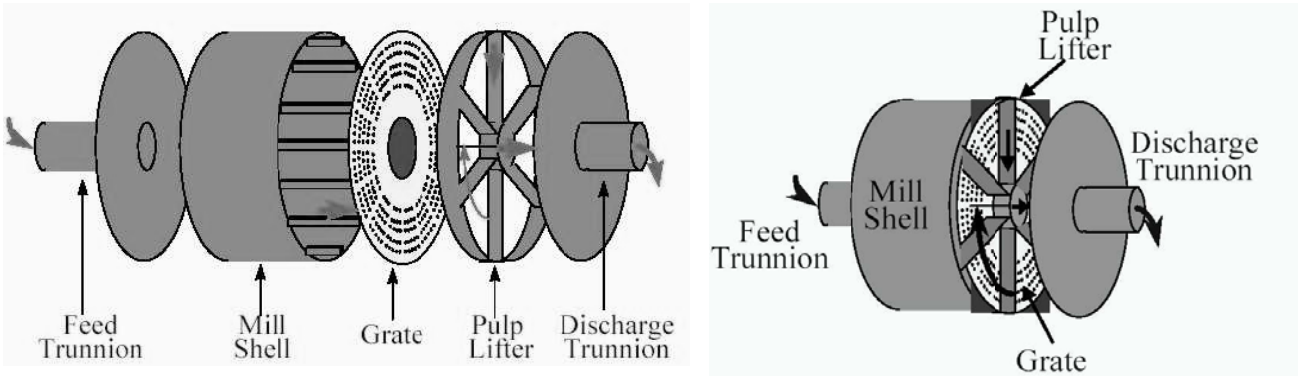

Fig. 3.3.15b – Schematic view of a SAG mill with arrangement of pulp lifters [Latchireddi, 2005].

The efficiency of a SAG mill depends on the charge motion and, especially for the larger mills, on the efficiency at which the ground material is removed from the mill. The latter depends on grate design and pulp lifter design. The presence of a slurry pool should be prevented (Fig. 3.3.15c), which can be

accomplished by employing optimised pulp-lifter devices. The performance of a SAG mill is controlled by monitoring power draw, throughput and in addition by employing acoustic sensors mounted on the outside shell.

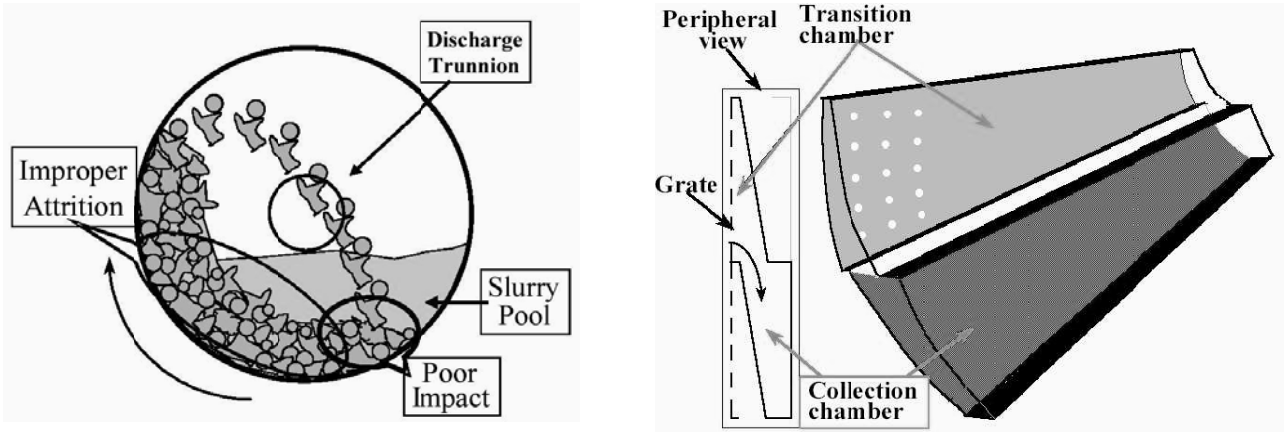

Fig. 3.3.15c – Adverse effect of slurry pooling on grinding process in a SAG mill (l), Twin Chamber Pulp Lifter (TCPL) (r) [Latchireddi, 2005].

SAG mill control

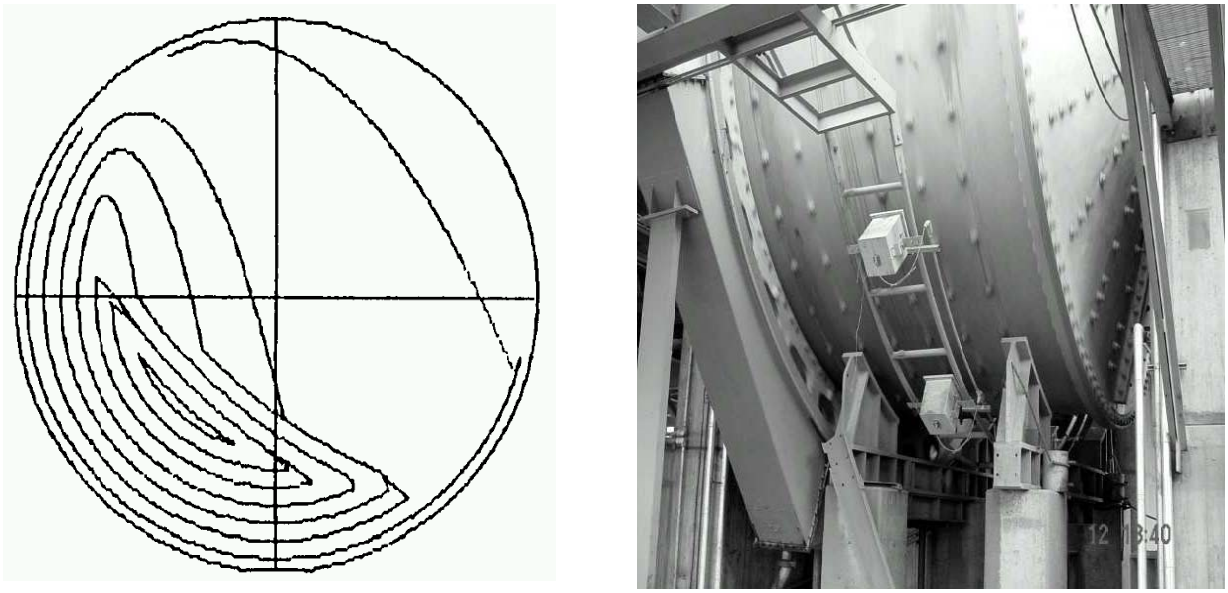

Fig. 3.3.15d - SAG mill ball trajectories landing on the load and striking the mill liners (l); Microphones of the Imactmeter on the shell of the SAG mill [Almond, 2005].

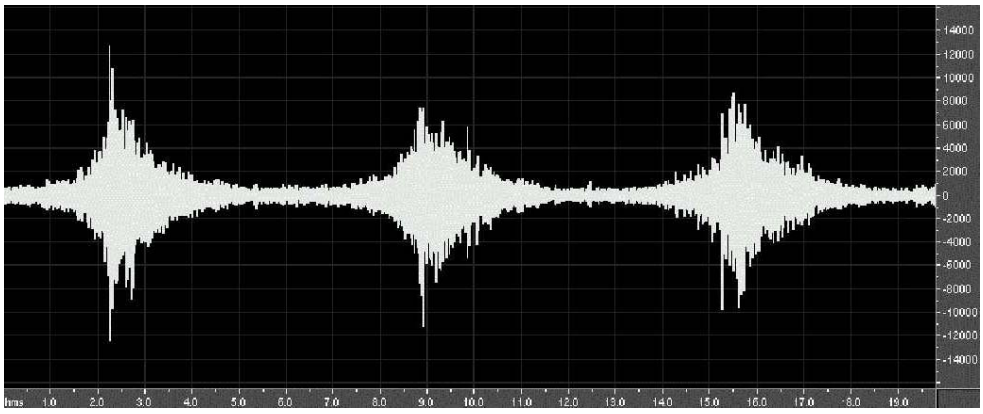

Fig. 3.3.15e – Sound trace used to determine load position during mill revolution. The load Toe is nearest to the highest amplitude points [Almond, 2005].

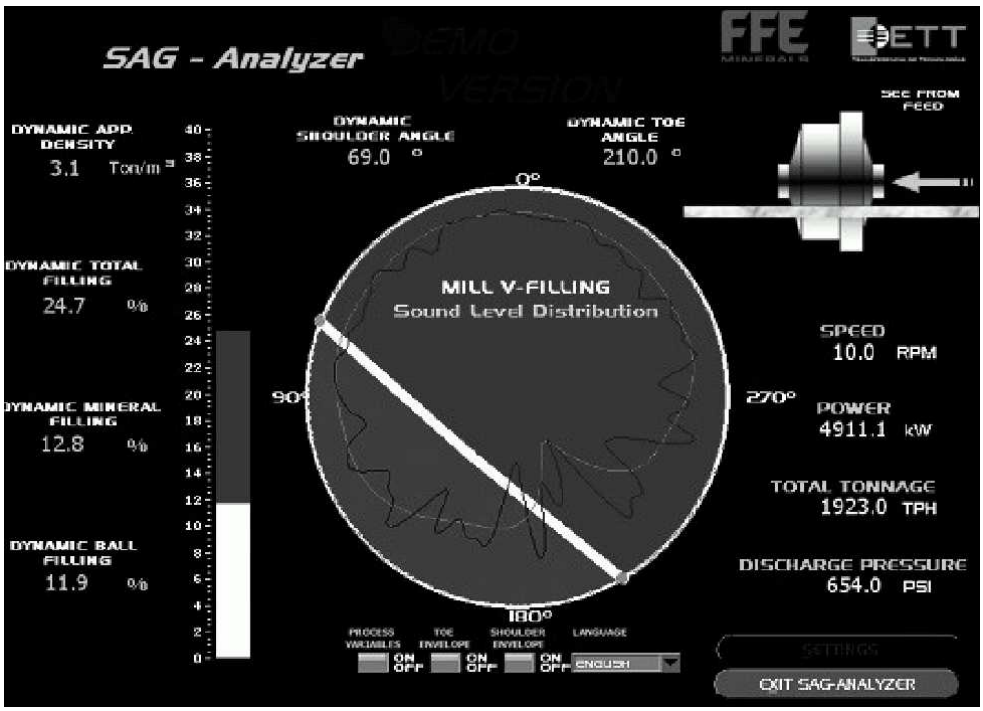

Fig. 3.3.15f – SAG analyzer display screen showing mill filling based on acoustic signal and other process data [Almond, 2005].

Tube mills have a very large L/D ratio (L/D=2.5...8). The mill can be divided into compartments, for example the first having rods, the second balls, or both having balls of decreasing diameter towards the outlet (Fig. 3.3.16). They are for example used for clinker grinding in the cement industry. The largest tube (ball) mill is a dry grinding mill, having D=6.2 m, L=25.5 m and is powered by a 11.2 MW ring motor. It runs on shell mounted bearings and is installed at a North American gold mine.

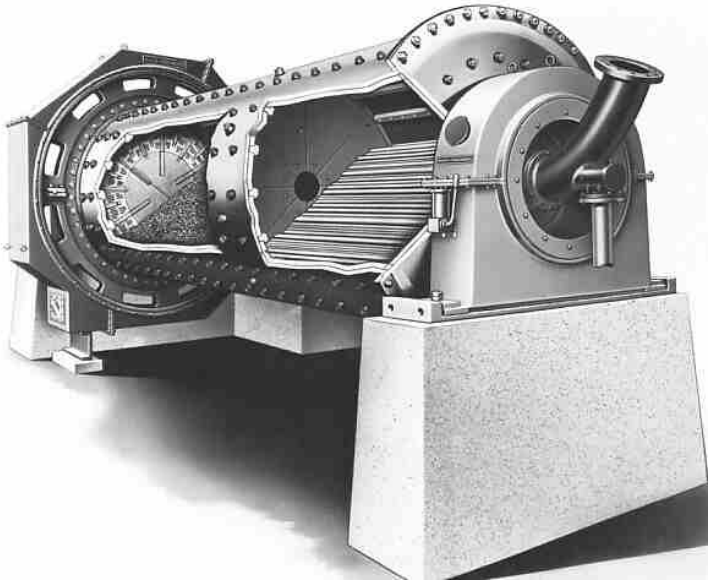

Fig. 3.3.16 - Tube mill with rod and ball compartment [SME].

Roller mills are employed for dry grinding of medium-soft materials, e.g. coal, cement clinker etc. They have a lower energy consumption as conventional mills, but show excessive wear for harder materials. There are several variants of which the **pan mill**, or **table-and-roller mill** is most well know (Fig. 3.3.17, 3.3.18). In it, ground material spilling over the edge of the table is air-carried into a classifier that returns coarse particles for further grinding. It is possible to combine drying and grinding employing roller mills. Some roller mills are also used for mixing (Chili mill, Fig. 3.3.17, right).

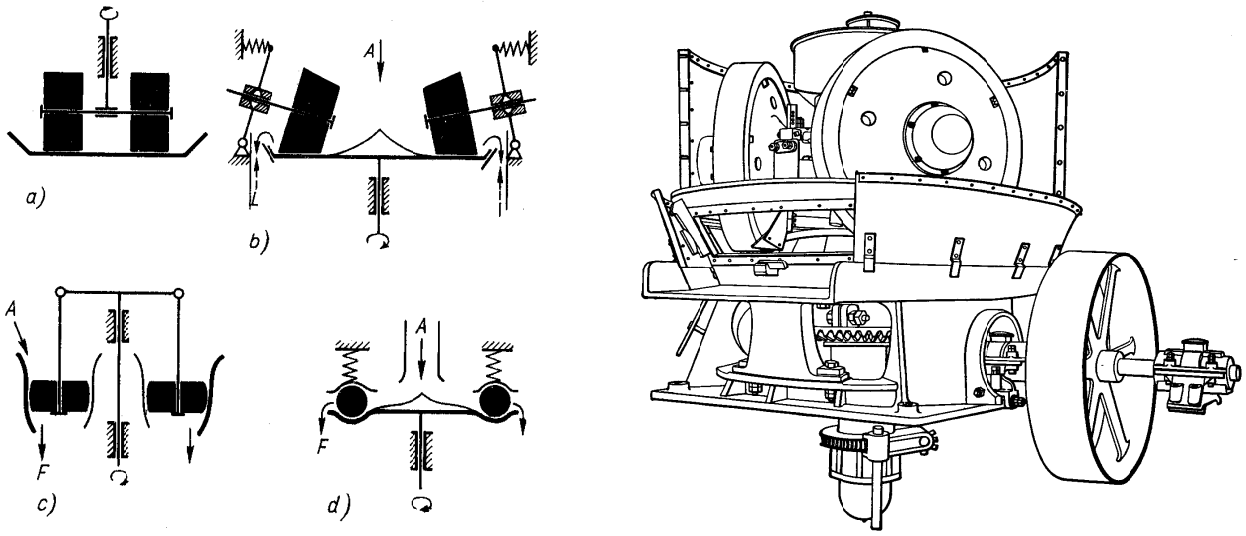

Fig. 3.3.17 - Principle design of roller mills: a,b=pan mills, c=ring roller mill, d=ring ball mill (left). Garfield Chili mill (right) [Schubert Vol. I / Source unknown].

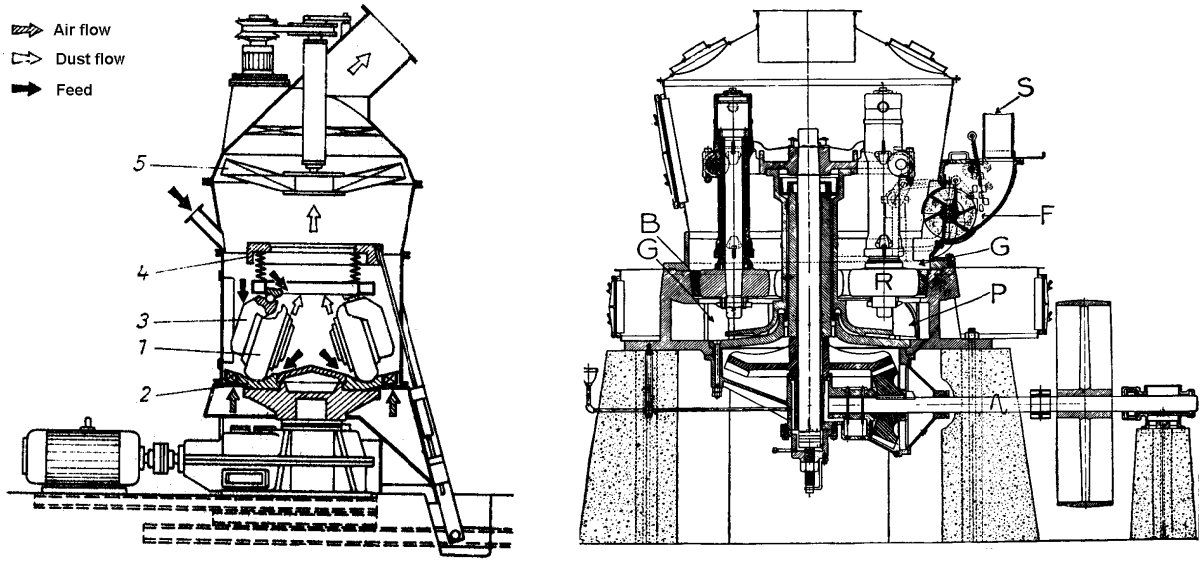

Fig. 3.3.18 - Dry pan mill with integrated air classification (left) and Raymond dry centrifugal roller mill (right)[Schubert Vol. I / Source unknown].

Vibratory mills are employed for ultra-fine grinding (downto ≈10 μm) of a wide variety of materials. Both continuous and batch mills are used (Fig. 3.3.19). The grinding chamber is 60%...80% filled with grinding media (balls) and vibrated with an excenter drive. The vibration is transferred from chamber wall onto the balls, hence the grinding mechanism is predominantly impact. Dry as well as wet grinding are employed. Typical applications include pigments, ceramic raw materials, metal powder etc. Batch vibratory mills are frequently applied in the laboratory for sample preparation (e.g. XRF analysis etc.).

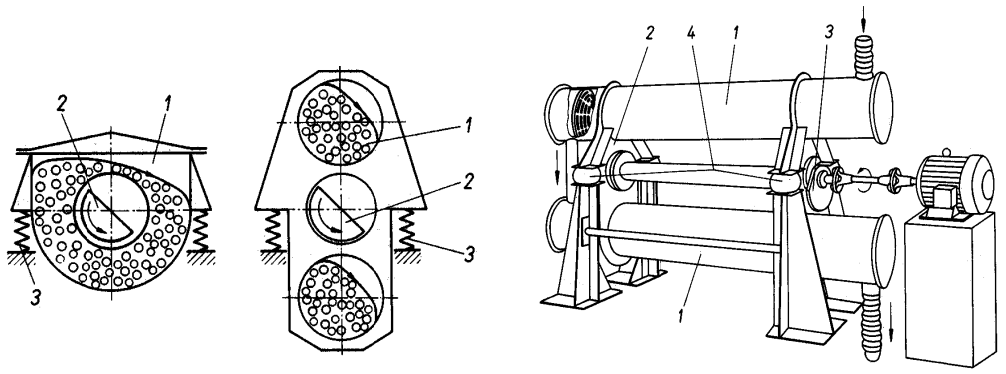

Fig. 3.3.19 - Batch vibratory mill (left), continuous vibratory mill (middle and right) [Schubert Vol. I].

A variety of other mills for ultra-fine grinding exist, e.g. based on air jets (Microsizer, Majac jet etc.). Their application is mainly in industrial minerals applications, chemical engineering, pharmaceutical industry, and food processing. More can be found in the literature regarding powder technology.

3.4. Size reduction theory

Size reduction theory provides insight in the crushing and grinding process. This is important for engineering tasks, such as predicting the electric power consumption and particle size distribution, dimensioning of the mill, flow sheet design, minimisation of liner wear, and process control. It is often said that grinding is an extremely inefficient process in terms of energy consumption. If, as is often maintained, the total mechanical work expended within a grinder is considered the energy input and the useful energy is taken as that converted to surface energy in the newly ground product, then grinding can be nothing but a very inefficient process, probably of the order of 0.1 to 1 percent. Since, however, size reduction can probably never be accomplished without some permanent lattice rearrangement occurring in the crushed material to absorb energy, a better definition of efficiency might include this term, in which case efficiency values might be expected to be between 1 and 2 percent. Finally, it can be argued that deformation energy, even though most of it is ultimately converted into heat, performs a necessary service, for without being deformed, actual materials certainly will not fracture. Deformation may thus be considered an activation step. The efficiency, if deformation energy is included, then attains a respectable figure, perhaps as much as 20 to 50 percent. Size reduction theory is extensively discussed in the course “Fysische chemie van de vaste stof“ (TA3200-05) by Dr. Jack Voncken.

3.5. Mill power draw

3.5.1. Predicting power draw of rock samples

Power consumption (or power draw) is one of the major factors determining grinding costs. Essential is the relationship between mass-specific grinding energy W_m (J/kg) and the size reduction Δd (communition result). Experimentally it is known that W_m is proportional with Δd and hence with d_0 (product size) at constant Δd. From this an empirical relationship is derived:

$$dW_m = -C\frac{1}{d^n}d(d) \qquad (3.5.1)$$

with C a constant and d_n the diameter after n grinding cycles. **Rittinger** (1867) stated that the necessary grinding energy is proportional to the additional new area per unit mass ΔA_m (ΔA_m=ΔA/m) that is created during grinding, considering the splitting of a cube with sides d_1 into smaller cubes with sides d_2:

$$W_m = C\Delta A_m$$

and with n=2 in Eq. 3.5.1.

$$W_m = C\left(\frac{1}{d_2} - \frac{1}{d_1}\right) \qquad (3.5.2)$$

can be derived. Rittinger's expression fits fairly well for 10 μm < d_0 < 1000 μm, the fine grinding range (Fig. 3.5.1). **Kick** (1885) stated that W_m is proportional to the reduction ratio:

$$W_m = C \ln\left(\frac{d_1}{d_2}\right) \qquad (3.5.3)$$

Kick's expression fits approximately for d_0>10mm, hence in the crushing range (Fig. 3.5.1, left). Eq. 3.5.3 can also be derived from Eq. 3.5.1. using n=1. Based on experiments, **Bond** (1952) derived:

$$W_{Bm} = C_B\left(\frac{1}{\sqrt{d'_{80}}} - \frac{1}{\sqrt{d_{80}}}\right) \qquad (3.5.4)$$

where d'_{80} is the 80% cumulative undersize of the product, and d_{80} the 80% cumulative undersize of the feed. d_{80} and d'_{80} must be given in μm. Eq. 3.5.4. can also be derived from Eq. 3.5.1. using n=1.5. Bond's expression is valid for the typical ball and rod mill grinding range: 100μm<d_0<10mm (Fig. 3.5.1).

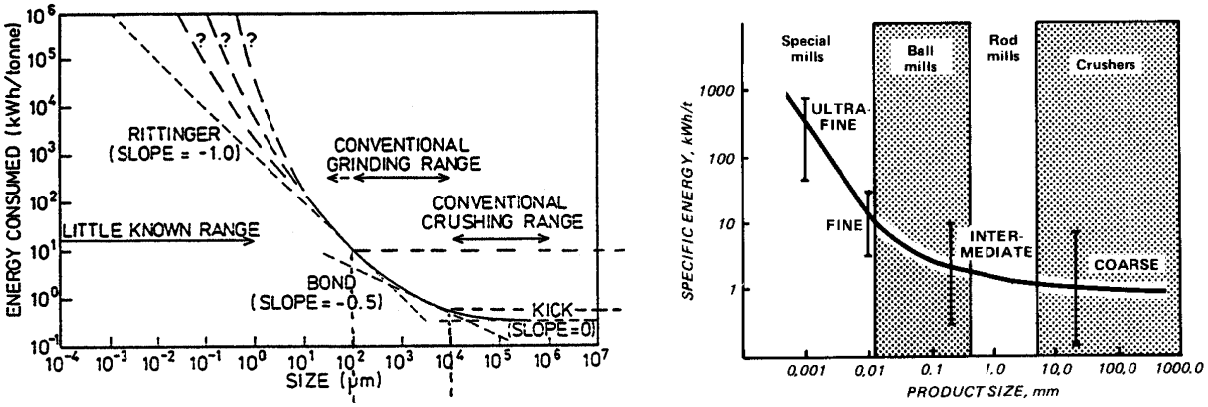

Fig. 3.5.1 - W_m as function of size [SME].

When W_{tm}, the total energy that is necessary to reduce a particle of infinite size to d'_{80}, is considered, the second term in Eq. 3.5.4. approaches zero and

$$W_{tm} = C_B \frac{1}{\sqrt{d'_{80}}} \qquad (3.5.5)$$

is obtained. Taking W_{tm}=W_{im}, where W_{im} is known as Bond's work index, with d'_{80}=100μm in Eq. 3.5.5. we obtain

$$C_B = W_{im}\sqrt{100} \qquad (3.5.6)$$

Substituting Eq. 3.5.6 into 1.5.4 we obtain

$$W_{Bm} = W_{im}\sqrt{\frac{100}{d'_{80}}}\,\frac{\sqrt{d_{80}} - \sqrt{d'_{80}}}{\sqrt{d_{80}}} \qquad (3.5.7)$$

W_{im} is a material specific constant that can be determined experimentally using a specially designed laboratory mill (see text books for procedures). It is defined as the theoretical work to reduce 1 short ton (st or 907 kg) of a material of infinite size (d_{80}=∞) down to d_{80}=100μm (multiply with 1.1025 for metric tonnes!). Some indicative values of W_{im} are given in Table 3.5.1.

Table 3.5.1. Indicative values of Bond's work index W_{im}

Material	W_{im} [kWh/st] *average*	W_{im} [kWh/st] *range*
Quartz	12.8	6.8...22.1
Cement clinker	4.2	1.4...8.8
Limestone	11.1	3.3...27.6
Bauxite	5.3	2.5...12.2
Iron ore	10.0	2.3...33.6
Copper ore	12.4	1.8...40.2
Molybdenum ore	12.5	5.8...18.6

Lead ore	15.5	11.0...21.8
Shale	10.6	5.8...19.0
Gypsum	6.9	4.3...11.7

The wide ranges of W_{im} for the different materials in Table 3.5.1. indicate the necessity to establish W_{im} experimentally case by case. During mill operation W_{im} may be determined routinely to adjust plant settings under feed fluctuations, e.g. mining different sections of an ore. After establishing W_{im}, mill design is pursued as follows:

Determine W_{im} (see Section 3.5.2)
Determine size distribution of the feed d_{80} and product d'_{80} of the grinding stage to be designed
Calculate W_{Bm} in [kWh/t] by using Eq. 3.5.7. and correcting for metric tonnes: W_{Bm}[kWh/t] = 0.907 W_{Bm}[kWh/st].
Determine power of the motor using $P=W_{Bm}Q$ (Q in t/h)
Determine L and D, e.g. by using Eq. 3.3.7 and Fig. 3.3.7.

3.5.2. Experimental determination of Bond's work index W_{im}.

Small-scale laboratory or bench scale grinding tests on representative samples are necessary in order to establish W_m. Only then mill dimensions for a new plant can be determined or existing mills monitored. Initially grinding tests were simple open-circuit tests. The procedure was as follows:

Size reduction below a specific d_{80}
Determine size distribution (set of screens)
Grind in a defined laboratory mill for a fixed time interval
Determine new size distribution
(When needed) repeat 2, 3 and 4 until required d'_{80} is obtained

Various reference ores were set as standard for comparison. Mill dimensions were determined comparing the ore with these reference ores, being harder or softer than these. The disadvantage of open circuit test grinding is that many ores are inhomogeneous. As a consequence, the desired particle distribution is easily obtained with test grinding, however the softer minerals may be concentrated in the fines and the harder ones stay in the coarse fraction. Therefore the Bond grindability test in closed circuit is preferred. A closed circuit means that the mill product is sized with a classifier: the undersize is the grinding circuit's final product and the oversize is returned to the mill and added to the feed (Fig. 3.5.2, see also the sections about grinding circuits further on). The Bond test assumes a circulating load of 250%, hence 2.5 times more material is returned to the mill from the classifier as oversize compared to the circuit's feed. It gives the work index from which the power draw of an industrial ball mill of 2.44 m diameter can be predicted. For other mill diameters conversion factors are available in the literature. The ball mill grindability test is suitable for size ranges of 5...0.2 mm.

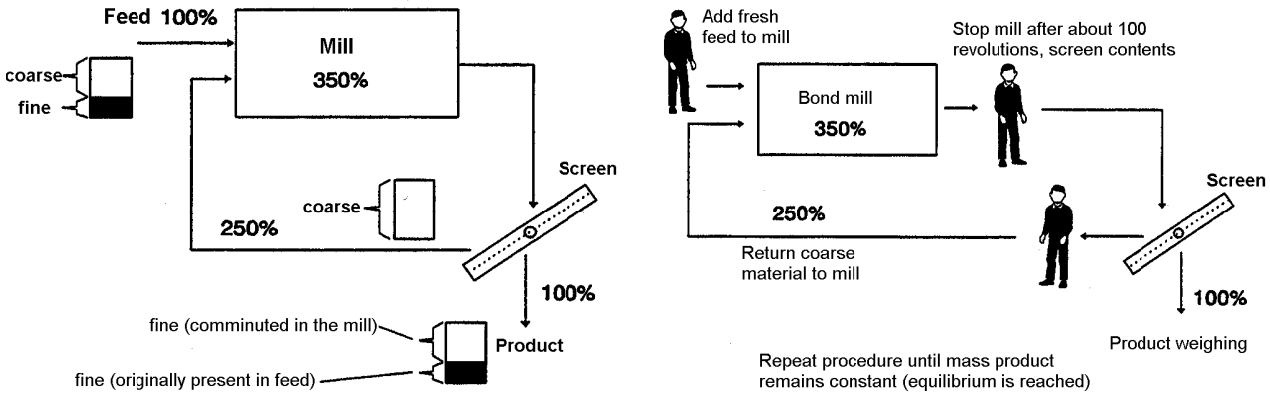

Fig. 3.5.2 - Schematic view of continuous mill (left). Simulation of continuous mill with Bond's test (right).

Ball mill grindability is determined with a horizontal mill having D=L=0.305 m (12 inch) and rotation speed n=70 rpm. Grinding media comprise 285 balls of total mass 20.125 kg of the sizes given in Table 3.5.2. Distribution of ball mass (right column) is readily calculated from the total mass of the media, ball diameter (middle column) and required number of balls as given by Bond.

Table 3.5.2. Grinding media characteristics of Bond's grindability mill.

Number of balls	Diameter [mm]	Diameter [inch]	Mass [g]
43	37	1.45	8806
67	30	1.17	7209
10	25	1.00	672
71	19	0.75	2009
94	15	0.61	1429
285			**20125**

Bond's wok index procedure, as applied at the Comminution Laboratory of the Faculty of Applied Earth Sciences of Delft University of Technology, is given on the next page.

Bond's work index determination

The following procedure must be maintained. Before starting, make sure all equipment is available and clean. You will need: jaw crusher, roller mill, (both for feed preparation), dry screening sets, Bond mill, and a balance. It is advised to wear safety goggles, hearing protection and dust mask.

1. Crush about 4 kg feed sample down to <0.83 mm (20 mesh) with jaw crusher (first stage) and roller mill (second stage).
2. Select screen size X for which W_{im} must be determined. Examples 0.208 mm (65 mesh) or 0.417 mm (35 mesh).
3. Determine size distribution of the crusher product (balance and screen set). Include the screen of mesh size X in the screen set. This is the feed of the Bond mill. Use Table 3.5.4, feed columns. The sieving procedure given in Section 1.9 can be used.
4. Take 700 cm^3 of ore and determine its mass. This is M_{feed}. Put it into the mill. Later, exactly this mass must be fed to the mill for each cycle.
5. Select the initial number of rotations (n_{in}). Indicative values: n_{in}=100 for fine grinding (0.208 mm = 65 mesh); n_{in}=50 for coarse grinding (0.417 mm = 35 mesh).
6. Close the mill, put in horizontal position, set counter to 0, start the mill.
7. Stop the mill after having reached the required number of rotations n_i (n_i=n_{in} for the first cycle). Turn the mill upside, vertically. Replace the lid by the basket. Turn the mill downwards vertically, collect the grinded material, and switch on the mill until it is empty.
8. Screen the material at the size selected at (4). Use two larger screens on top to reduce excessive mechanical load on the selected screen.
9. Determine mass of the oversize, and add feed material (<0.83 mm = 20 mesh) until you reach again M_{feed}.
10. Determine mass of the undersize of the ground material. In the feed material (<0.83 mm = 20 mesh) there already was a percentage of material <X. Use the size distribution, determined at 2, to determine this percentage and calculate the mass of the material <X as originally present in the feed.
11. Determine the following and add to Table 3.5.3:
    a. Number of revolutions of the mill (n_{in})
    b. Mass of the undersize ($M_{<Xtotal}$ column)
    c. Mass of the undersize that already was present in the feed ($M_{<Xfeed}$)
    d. Subtract c from b and put to ($M_{<Xnett}$) column.
    e. Calculate grindability G_{bp}=($M_{<Xnett}$)/n_{in} and put in the right column, being the mass of the newly generated <X material per revolution.
12. At step (8) original (<0.83 mm = 20 mesh) feed material was added. Calculate the mass of the percentage of this material <X and add to the next row of Table 3.5.3 at the ($M_{<Xfeed}$) column.
13. Calculate the Ideal Potential Product with IPP=M_{feed}/3.5. Bond's method assumes that except the 100% feed in the product, there is a circulating load of 250%, hence totalling 350% or a factor 3.5.
14. Calculate the number of revolutions for the next cycle with n_i=(IPP-$M_{<Xfeed}$)/G_{pb}. $M_{<Xfeed}$ was determined at step (11).
15. Repeat step 5...13. G_{pb} will increase or decrease. After it has reached its highest or lowest point, do another two cycles to verify the validity of the maximum or minimum.
16. Determine size distribution of the product of the final cycle using balance and screen set (use Table 3.5.4). The sieving procedure given in Section 2.9 can be used.
17. Plot both size distributions from Table 3.5.4 on Rosin Rammler paper (Fig. 3.5.3). Determine from both d_{80}.
18. Calculate the (laboratory) work index W_{im} in kWh/t from

$$W_{im} = \frac{49.1}{X^{0.23} G_{bp}{}^{0.82} \left(\frac{10}{\sqrt{d'_{80}}} - \frac{10}{\sqrt{d_{80}}} \right)} \qquad (3.5.8)$$

with X the size determined at (4), G_{pb} the average of the G_{pb}'s of the three lowest or highest cycles, d_{80} the 80% cumulative undersize of the feed and d'_{80} of the final product. See Section 3.5.1 for determination of the power draw and mill dimensions based on W_{im}. Note that Eq. 3.5.8 gives the value per metric ton (1000 kg). Many literature date give values pere short ton (1 st = 907.2 kg).

Table 3.5.3 Bond Index results, Cycle progress table.

Cycle No.	Number of revolutions	M<Xtotal [g]	M<Xfeed [g]	M<Xnett [g]	G_{bp} [g/rev]
1					
2					
3					
4					
5					
6					
7					
8					
9					

Feed d_{80}= ____ μm

Product d'_{80} = ____ μm

G_{pb} = _____ g/rev

W_{im} = _____ kWh/t (Eq. 3.5.8)

Table 3.5.4 Bond index results, size distribution tables of feed and final product (to be used for RR paper, Fig. 3.5.3).

Mass of feed = _____ g

% smaller as X in feed = _____ %

Ideal Potential Product (IPP) = _____ g

Screen [μm]	Screen [mesh]	Feed [g]	Feed [%]	Feed [Cum. %]	Product [g]	Product [%]	Product [Cum. %]
	Total:						

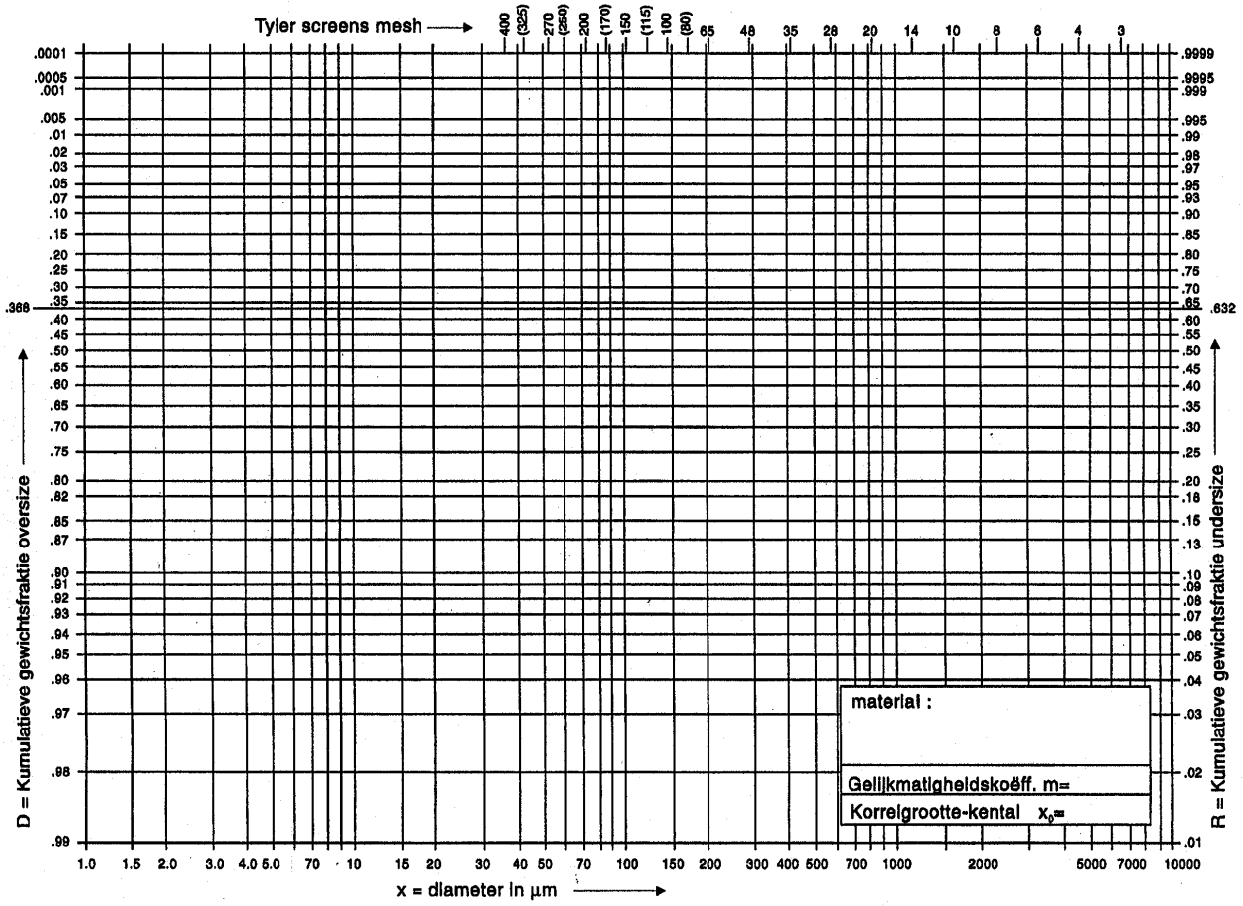

Fig. 3.5.3a - Size distribution of Bond mill feed (Rosin-Rammler paper).

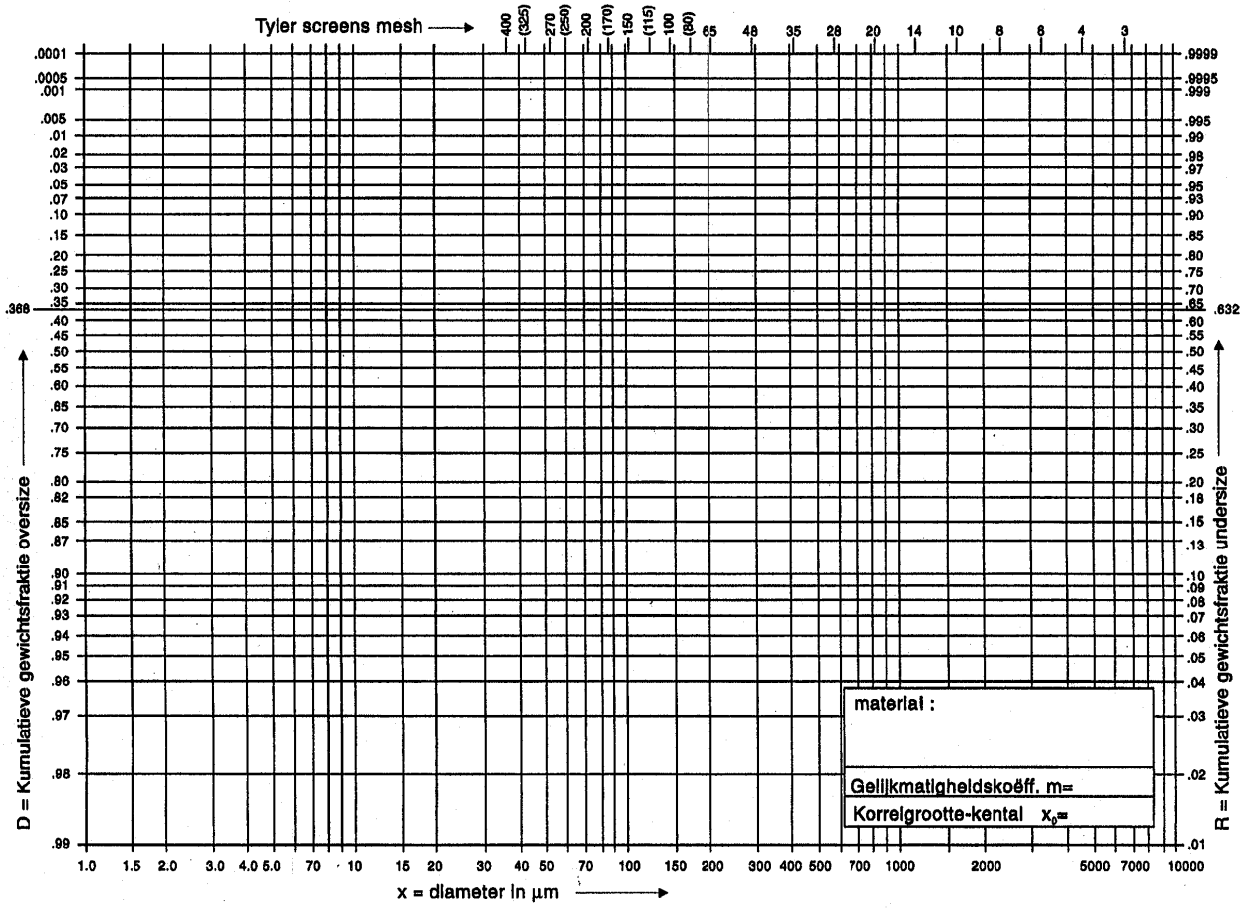

Fig. 3.5.3b - Size distribution of Bond mill final product (Rosin-Rammler paper).

3.5.3. Grinding efficiency

Bond's and Rittinger's relationship show an increase in W_m (mass specific grinding energy) at a decreasing particle size (Fig. 3.5.1). For fines, the fundamental reason is the increasing depletion of Griffith flaws at decreasing sizes (see Section 1.4). For the intermediate size range up to 10 mm the decrease is caused by the difference between individual load of particles (crushers, >10 mm) and collective load (grinding). In the latter case much energy is lost due to friction. Friction losses increase with decreasing size.

The **efficiency** η of comminution can be defined in different ways (see also Section 1.4.1):

Consider the increase in surface energy ($2\gamma\Delta A$) and relate to the consumed grinding energy W_m:

$$\eta_1 = \frac{2\gamma\Delta A}{W_m} \approx 0.1...1\%$$

If in addition to the increase in surface energy, structural changes of the flaws are included: $\eta_2 \approx 1...2\%$
If losses due to plastic deformation are also included: $\eta_3 \approx 1...12\%$
When all energy, excluding friction, that is needed for size reduction (W_v) is related to grinding energy W_m: $\eta_4 = W_v/W_m$

The latter efficiency definition applied for some size reduction equipment gives:

	η_4 (%)
roll crusher	70...100
impact crusher and mills	25...40
roller mill	7...15
ball mill	6...9
pneumatic stream mills	1...2

Losses are due to:
Plastic deformation of particles
Plastic deformation of crusher/mill and media surface
Friction
Elastic deformation not leading to breakage
Kinetic energy of material
Machine wear
Generation of noise and vibration

Fig. 3.5.4, left, shows typical generalized curves from practice illustrating what occurs to mill power draw (W_m) as product size changes during grinding of an ore with constant work index W_{im}. Fig. 3.5.4, right, illustrates typical relationships between W_m and feed tonnage when ore with a varying work index is treated in a rod, ball, or SAG mill.

The **grinding medium** has a significant effect on the grinding energy W_m. For crushing it is always air, but grinding is employed wet as well as dry. From grinding experience it is known that:

$W_{wet} \approx \frac{1}{3} W_{dry}$
$W_{wet} > W_{wet}$ + Grinding aids
$W_{dry} > W_{dry}$ + Grinding aids

Grinding aids are surface-active chemical agents that lower surface energy γ. For dry grinding they lower interaction forces between particles (dispersion effect) resulting in:
No agglomeration (better dispersion, looser packing op particles)
No sticking to the mill wall and media

As grinding aids certain alcohols, amines and fatty acids of intermediate chain length (to ensure sufficient spreading over the large material surface) appeared favourable. For wet grinding they have similar effects, but the mechanism is of more complex nature involving ion-ion interaction, electrical double layer, pH etc. In water there is a better dispersion and less friction, due to which water as medium has a similar effect as grinding aids for dry grinding.

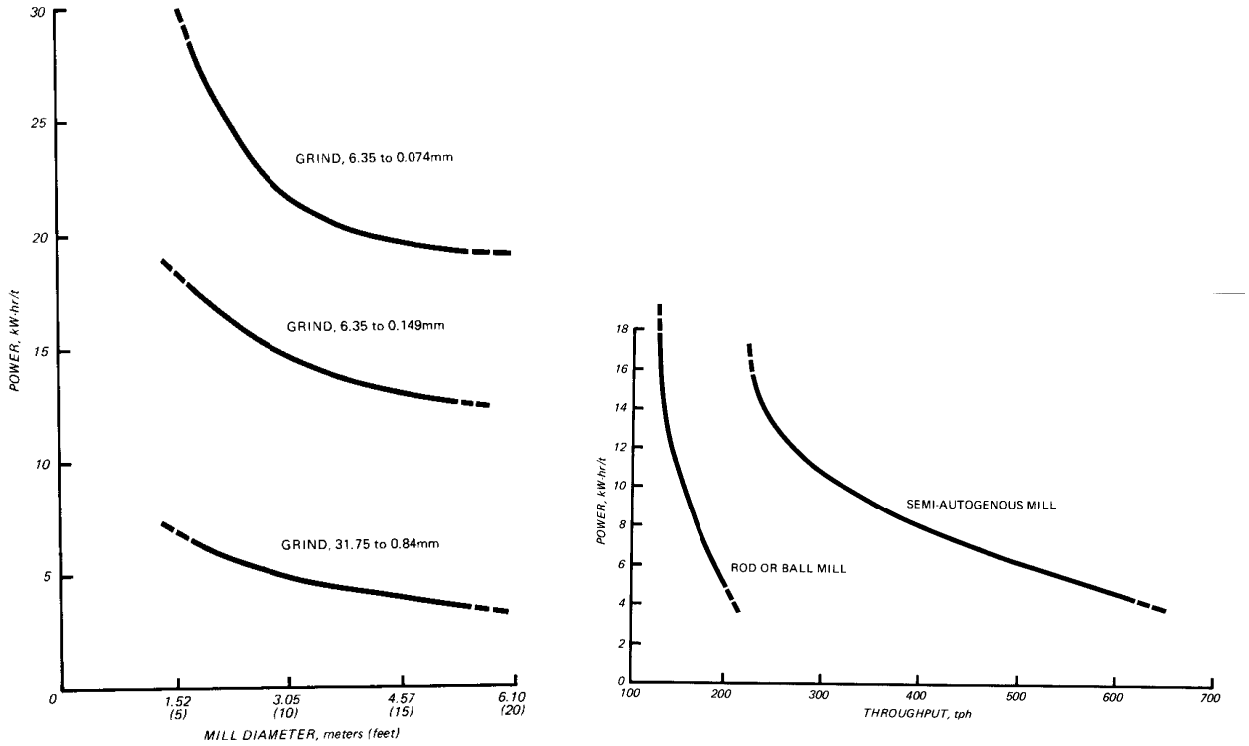

Fig. 3.5.4 - W_m as function of mill diameter for three different Δd (left). W_m as function of throughput for ore of various W_{im} for rod/ball mill and SAG mill (right) [SME].

3.6. Grinding circuits

A grinding circuit is the total system designed for communition of material down to a specific size. It may comprises several unit processes, such as crushers, rod mills, ball mills, screens and classifiers. A distinction is made between open and closed grinding circuits. Open circuits are the most simple configurations, where the mill outlet is simply the same as the circuit product. In closed circuits mill outlet is classified and the oversize returned to the mill. A further distinction is made in dry and wet circuits. Most sulfidic ore grinding is wet, iron ore can be dry or wet, and cement dry. Fig. 3.6.1 shows a typical wet circuit for the grinding of sulfidic ore with typical reduction ratios (n) indicated per unit. Many different circuit designs exist. experience learns that they need to be taylor made for a specific application. It may be that the same circuit has good performance for one ore, but is totally unsatisfactory for another. Proper understanding of the grinding and classification mechanism and a good, experimentally determined, characterisation of the ore is essential for designing effective circuits.

Traditionally rod and ball mill circuits are predominantly used in wet ore grinding. In the latest decades there is a trend to apply AG and SAG mills instead of secondary, tertiary crushing and primary grinding. In modern wet closed circuits cyclones are the predominant size classifiers, however srew classifiers still have an important place. For the coarser sizes screw classifiers are more and more replaced by screens. Most dry grinding circuits are closed loop using a pneumatic classifier.

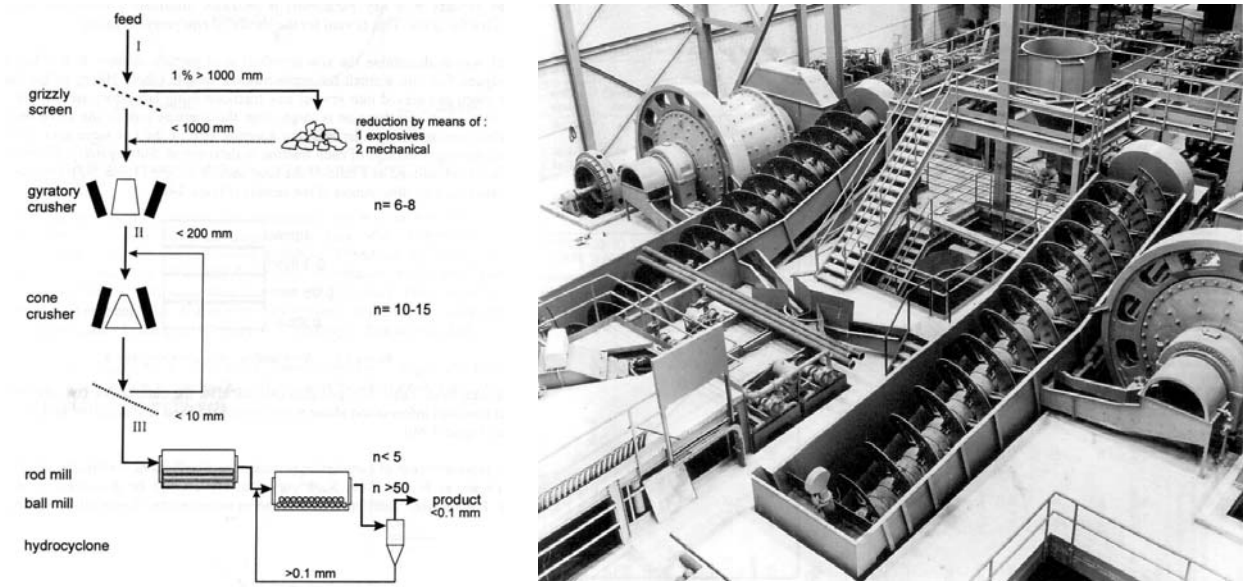

Fig. 3.6.1 - Typical wet closed loop grinding circuit for sulfidic ore(l). Ball mill – screw classifier wet closed loop circuit with two parallel lines (r) [TU Delft / SME].

3.7. Wet grinding circuit flow sheets

In this section an overview is given of wet grinding circuit flowsheets, based on the description by Mular et al., 1982.

3.7.1 Wet open circuits

In **wet open circuits** water and ore are fed to the mill and the final product is direcly discharged without classification. (S)AG, pebble, rod, ball or tube mills may be operated open circuit (Fig. 3.7.1, Fig. 3.7.2, left). Tube mills (Fig. 1.3.16), often compartimented, are especially suitable for open circuit operation. A typical application is limestone grinding in wet cement plants. Two mills in series may give comparable results (Fig. 3.7.1, r). Advantages of wet open circuits are:

Minimum equipment requirement (low investment)
High pulp density. This is favourable when the mill product is leached, e.g. in uranium and gold-silver ores.

Further their application is particularly favourable when:
Reduction ratio, n, is only small
Size reduction to a coarse natural grain size, e.g. grinding of cemented sandy rock
Flotation middlings are returned to the mill
Particle size distribution is uncritical (over- and undersize can be tolerated)

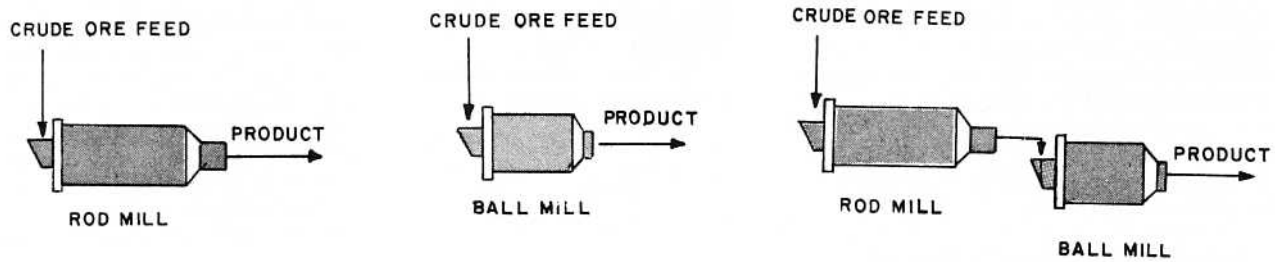

Fig. 3.7.1 - Wet open circuit flow sheets [SME].

3.7.2 Single-stage wet closed circuits

Wet closed circuits efficiently produce a product with controlled top size and minimum overground material, and are therefore most commonly applied in mineral processing. The classifier (cyclones in Fig. 3.7.2) returns the oversize into the mill.

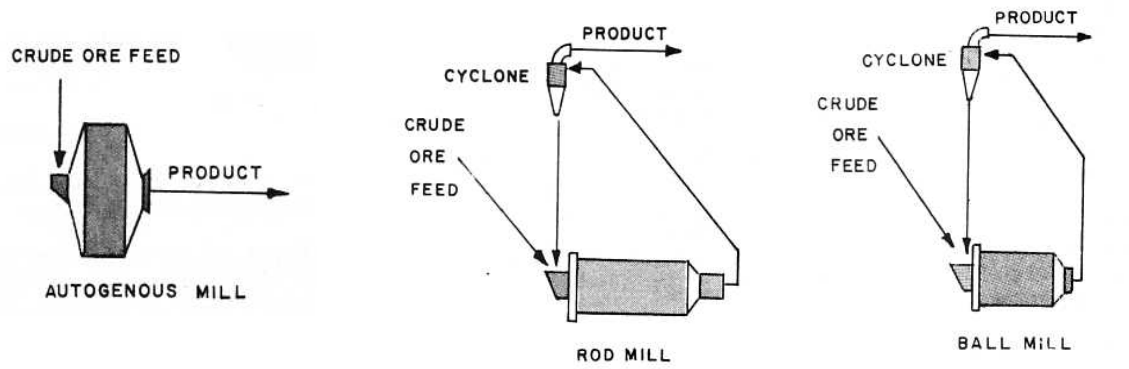

Fig. 3.7.2 - AG mill open circuit (left). Rod and ball mill single stage closed circuit (middle & right) [SME].

Single-stage closed circuits can be used with all type of mills and wet classifiers. Applications are primary grinding and regrinding. Single-stage primary rod or ball mill grinding is typically applied for tertiary crushed ore. Sometimes (S)AG mills are used for direct grinding of primary crusher output to final product size (Section 1.3). The benefits are simplicity and hence low investment and maintenance costs. Disadvantages may be low flexibility and lower grinding efficiency (= higher energy consumption).

3.7.3 Multi-stage wet open circuits

Multi-stage wet open circuits have two or more mills and one or more classification stages. Advantages compared to single-stage circuits are a better optimisation for a specific application and higher efficiencies.

Rod/ball mill 2-stage closed circuits are traditionally the basic ore grinding circuit following two- or three-stage crushing (Fig. 3.7.3, left). Power draw per tonne of the ball mill stage is about twice that of the rod mill, hence often two ball mills are applied downstream a single rod mill.

Ball/ball mill 2-stage closed circuits are mainly used when application of a rod mill is unpractical or less economic (Fig. 3.7.3, right). This circuit requires less floor space and has higher interchangeability of parts.

Rod/pebble mill 2-stage closed circuits may be applied for various ore types. A typical application is the grinding of gold ore. The higher capital costs of a pebble mill (per unit of capacity) may be compensated by the lower grinding media cost, which in some cases can be screened from the feed or domestically purchased at low cost.

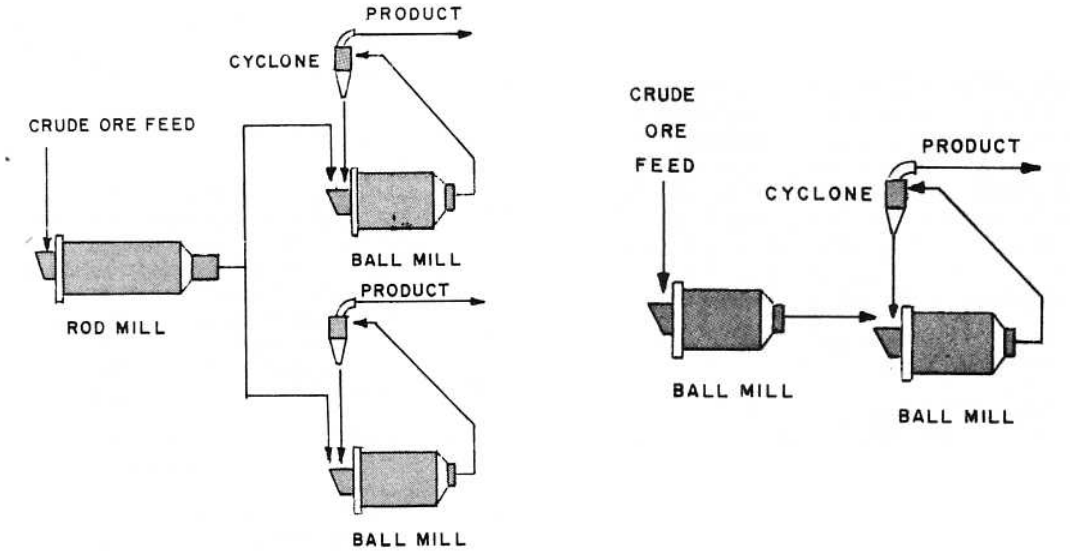

Fig. 3.7.3 - Rod/ball mill 2-stage closed circuit (left). Ball/ball mill 2-stage closed circuit (right) [SME].

2-stage circuits with **2-stage classification** may be applied for better grinding control and less overgrinding, albeit rarely (Fig. 3.7.4, left). Two-stage wet closed circuits with **intermediate treatment** are favourable when some degree of concentration is already possible at relatively coarse sizes (Fig. 3.7.4, right). A typical application is the grinding of magnetite ore. In this case the intermediate concentration saves considerable grinding effort. Instead of magnetic concentration, gravity separation can be applied as well. Examples are gold, lead-zinc, copper ore and barite.

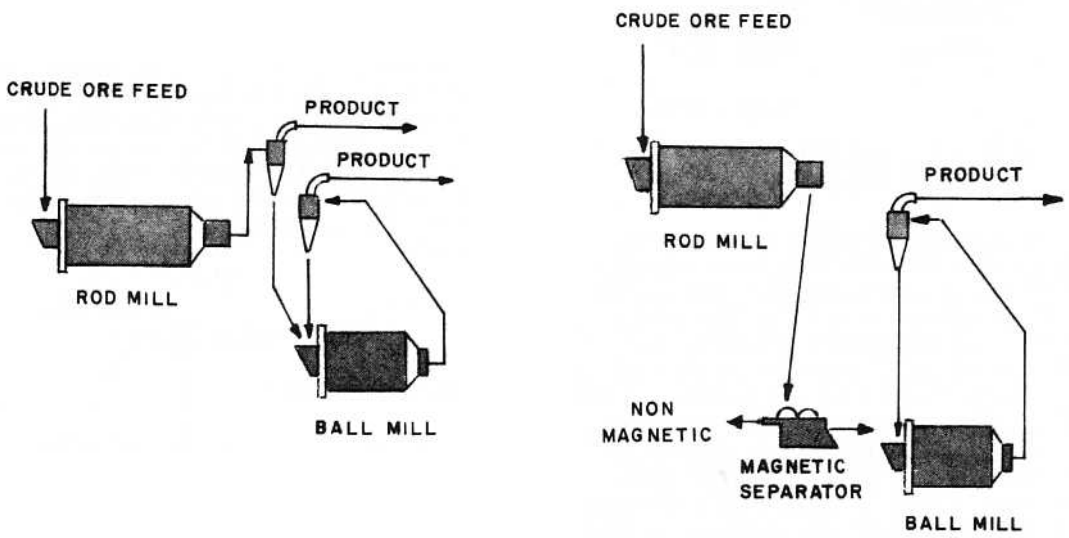

Fig. 3.7.4 - 2-stage wet closed circuit with 2-stage classification (left) and with intermediate treatment (right) [SME].

AG mill–screen-pebble mill–classification circuits are used to grind ore without steel media (Fig. 3.7.5, left). Run-of-mine or primary crusher product is fed to the AG mill. The screen separates the pebble grinding media, an intermediate size for return to the mill, and an undersize ball mill feed. The pebble media and undersize are fed to the pebble mill for fine grinding.

ABC circuit: An **AG mill-Ball mill-Crusher-classification** circuit is designed to screen out the ≈25mm to ≈75mm fraction as oversize from the outlet that will not grind autogeneously (Fig. 3.7.5, right). Part of it is crushed and returned to the AG mill. The undersize is fed to a ball mill – classifier circuit. The advantage is a reduction in grinding media consumption and a more efficient use of them.

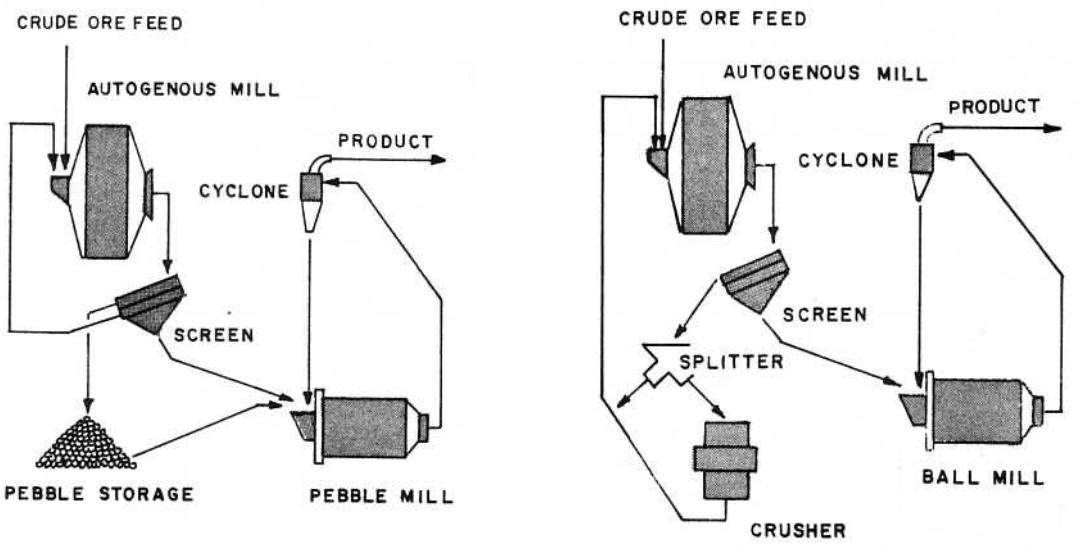

Fig. 3.7.5 - Autogeneous and pebble mill wet closed circuit grinding (l). ABC circuit: Autogeneous-, Ball mill, Crusher, classification circuit [SME].

A **SAG mill-ball mill-classification** circuit is popular because of favourable economics. It replaces secondary and tertiary crushing and screening. Primary crusher product is directly fed to the SAG mill where it is reduced to about 19...13 mm (Fig. 3.7.6, left). The SAG mill product is further reduced in a ball mill-classification circuit down to product size. The grate discharge (Fig. 1.3.10, right) of a SAG mill effects an "internal" classification. Ports in the grate allow a limited amount of smaller, worn, balls and coarse ore to pass to a magnet that removes the balls for use in the ball mill or for discarding. The remaining coarse ore returns to the SAG mill.

3.8. Dry grinding circuit flow sheets

The largest dry grinding operations are for iron ore and cement. Other important applications are the grinding of pulverised coal fuel for firing boilers, and the grinding of industrial minerals like barite, clay, feldspar, silica, talc etc.

Rod mill, ball mill, tube mill, pebble mill –classification closed circuits are the prevalent type of dry circuits, applied for a wide variety of materials. The flow sheet is similar to the one shown in Fig. 3.7.3, right.

Dry (S)AG-classification closed circuit grinding is applied for iron ore grinding, though recently wet grinding gains in popularity (Fig. 3.8.6, right). Both AG and SAG mills are used, depending on ore characteristics. Air classifiers are described in Chapter 2.

Dry roller mill-classification closed circuits are mainly applied for pulverised coal or barite for drilling mud. In coal grionding the operation can be combined with drying by heating the air. The circuit is similar as the one shown in Fig. 3.8.6, right.

Impact mills can be operated open circuit or in closed circuit with screens or air classifiers.

A **hammer mill** has an internal screen to control top product size, and therefore is generally operated open circuit (Fig. 3.2.7, left).

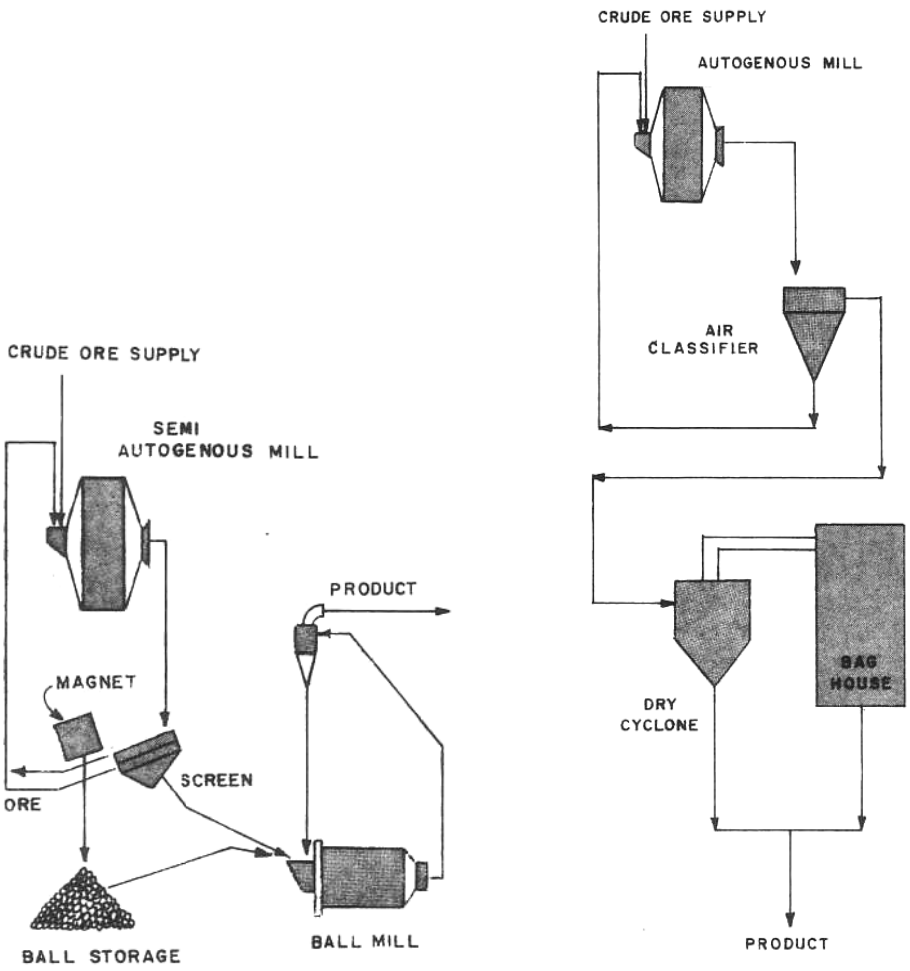

Fig. 3.8.6 - SAG mill-ball mill circuit (left). AG dry grinding circuit (right) [SME].

3.9. Determination of the circulating load

In closed grinding or crushing circuits the returned material is the circulating load. It may vary between 100% and 800% of the feed. The overall mill capacity initially increases at an increasing circulating load (Fig. 3.9.1). This is effected by the better avoidance of overgrinding, and hence saving of energy. The available energy is better spend on reduction of size only down to the required level. When the circulating load is too high, excessive dimensions of the equipment and an overall reduction of the capacity per mill may result. The optimisation of circulating load is therefore important and requires some calculation. The method below can be applied for one-stage crushing as well as grinding circuits where the sizing is carried out by means of screens or classifiers.

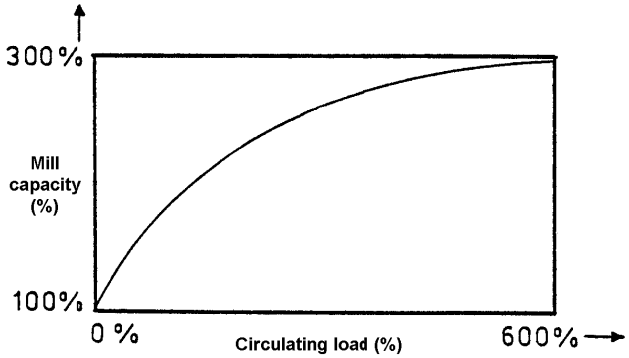

Fig. 3.9.1 - Capacity as function of circulating load.

The particle size distribution of the feed will already contain material fine enough for the product and may pass the size reduction stage. Fig. 3.9.2 shows a simplified flow sheet where F is the circuit feed, R is the

coarse fraction to be returned, B the crusher or mill product (hence classifier feed) and P the product of the circuit.

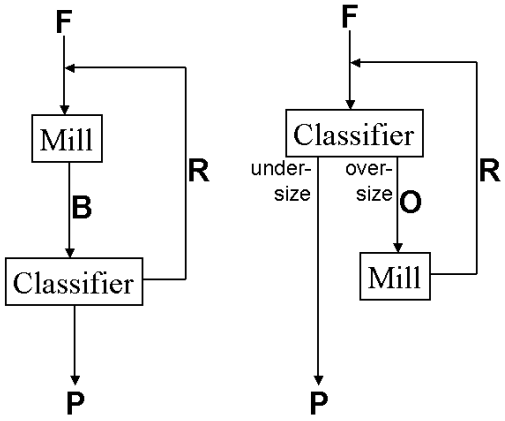

Fig. 3.9.2 - Closed circuit grinding.

C, the circulating load is defined as percentage of the feed:

$$C = 100\% \frac{R}{F} \qquad (3.9.1)$$

C can be considerable, as mentioned. When the mill generates a product that contains a fraction r of material that is too coarse for the product, and when the classification efficiency is E, finally an equilibrium will develop with

$$R = \frac{r}{E} + \frac{r^2}{E^2} + \ldots + \frac{r^n}{E^n} \qquad (3.9.2)$$

R<1 and r/E<1, hence Eq. 3.9.2 converges and with n $\rightarrow\infty$ it follows:

$$R = \frac{r/E}{1 - r/E} \qquad (3.9.3)$$

For instance, R≈0.33 with r=0.2 and E=0.6, the classifier needs to process at a capacity of B=1.33F t/h. In practice monitoring of B is important to detect undesired changes and look for the cause of it to be able to correct in time. B could be determined directly by continuously weighing, but this is not always practical, especially not in wet circuits. Then F, B, R, and P are sampled and a screen analysis is made, determining the undersize fractions f_i, b_i, r_i en p_i of the applied mesh size m_i. From a mass balance it follows that

$$\begin{aligned} F &= P \\ B &= P + R \\ Bb_i &= Pp_i + Rr_i \end{aligned}$$

and hence

$$C = 100\% \frac{R}{F} = 100\% \frac{p_i - b_i}{b_i - r_i} \qquad (3.9.4)$$

In practice this calculation is made using more than one mesh size m_i. When they all indicate approximately the same C, the system is in steady state. In the other case the data can not yet be used to control the proces.

The flowsheet of Fig. 3.9.2, left is improved by directly classifying the feed before milling. This is shown in Fig. 3.9.2, right. With O the classifier oversize, it is obvious that in this case

$$\begin{aligned} F &= P \\ O &= R \\ Ff_i + Rr_i &= Oo_i + Pp_i \end{aligned}$$

More detailed procedures are available in the literature, e.g. Weiss, 1985, pp.30.7.

3.10. Process control

In plant operation typical control objectives are (Wills, 1988):

Maintaining constant product size at maximum throughput
Maintaining constant feed rate within a limited product size range
Maximise production per unit time in conjunction with downstream processing (e.g. flotation)

Of a typical rod/ball mill closed wet circuit only **feed rate** and **water addition** can be varied independently (Fig. 3.10.3). Feed rate is usually controilled with variable speed feeders combined with weightometers. Grinding medium charge is controlled by monitoring power draw of the mill. When it drops, fresh grinding media must be added. Flow rate and density can be monitored by magnetic flow meters and nuclear density gauges. Besides, sump level is monitored continuously.

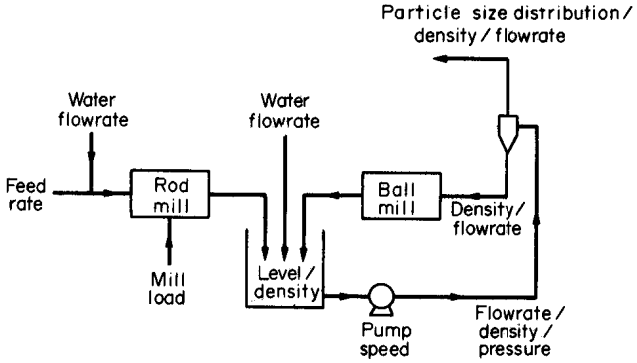

Fig. 3.10.3 - Control variables of a rod/ball mill closed wet circuit [Wills].

Changes in feed rate initiate a slow progessive change in which the final equilibrium represents the maximum product response, while **changes in classifier water addition** initiate an immediate maximum response with only a relatively small equilibrium product response. Increasing water addition increases circulating load and sump level.

If **constant product size** at **constant feed rate** is required, only the classifier water addition can be manipulated, resulting in volumetric and density fluctuations in the cyclone overflow.

Maximum throughput at constant product size allows manipulation of both feed rate and classifier water. It is therefore frequently applied. In fact this means a fixed product size set-point and a circulating load set-point just below the maximum tonnage constraint. Two control strategies are applied:

Product size is controlled by ore feed rate, and circulating load by classifier water addition.
Product size is controlled by classifier water, and circulating load by ore feed rate.

The optimum stategy choice depends on many factors and is variable from case to case. In general if particle size response must be fast, then it is controlled by classifier water, whereas if for a fast mill throughput response is more important, then product size is controlled by ore feed rate.

3.11. Modelling crushing and grinding

Both in the design and the operational stage of a given operation it is necessary to have simulation models for prediction of:

- particle size distribution of the product at a given feed
- capacity
- power draw
- wear pattern

The models are used for automatic process control and for mill design.

Two important modelling approaches are discussed: matrix modelling and discrete element modelling (DEM). Matrix modelling is especially useful for simulation and control. DEM modelling provides powerful simulations about grinding kinetics, power draw and the effect of mill design (e.g. liner profile selection).

3.11.1. Matrix modelling

A matrix model considers the grinding process as a number of consecutive size reductions or grinding stages. The product of a stage is the feed for the next. During grinding, the change in particle size distribution of the material can be studied as function of the number of consecutive stages. The longer it is ground, the finer the comminuted material. Discrete functions describing size distribution and grindability are assumed.

A grinding stage can be defined as a specified number of mill revolutions, or as a specified time interval. Each stage comprises two operations:

Selection of particles for crushing. Each particle has a specific probability of being crushed during a grinding stage.
Breakage of the selected particles.
Often a third operation is considered (closed circuit grinding):
Classification of the particle population after crushing

Selection of material for crushing is represented by **selection function** S_i. S_i indicates the percentage of fraction i of the feed that is indeed crushed during a single stage.

For describing the crushing result, crushing function B_{ij} is used. B_{ij} is a distribution function and indicates the percentage of fraction j of the feed that transfers to a smaller fraction i of the product as a consequence of fracture during a single grinding stage.

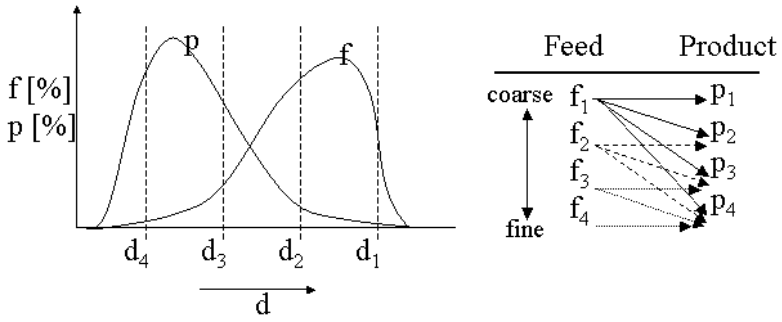

Fig. 3.11.1 - Product and feed material described in matrix format, with $0<d_4<d_3<d_3<d_1$ (left). Size reduction of a single stage (right).

The model is based on a matrix description of particle size distribution of feed and product. At least 4 different size classes d_i should be defined (i=1...4), representing the particle size range of both feed and product. d_1 represents the largest size class and d_4 the smallest. The feed is described as a vector **f** (with $\Sigma f_i=100\%$ and $f_i=m_i/\Sigma m_i$) where each element f_i is the percentage of the feed mass having that size interval, expressed in the geometric mean of top and bottom size of the fraction, or $SQRT(d_{top}*d_{bottom})$:

$$\vec{f} = \begin{bmatrix} f_1 \\ f_2 \\ f_3 \\ f_4 \end{bmatrix}$$

The product vector **p** (with $\Sigma p_i=100\%$) is described accordingly:

$$\vec{p} = \begin{bmatrix} p_1 \\ p_2 \\ p_3 \\ p_4 \end{bmatrix}$$

More than 4 size classes allow more accurate modelling, on condition such data are indeed available. A grinding matrix X can describe the size reduction of the feed **f** to product **p**:

$$\begin{bmatrix} x_{11} & 0 & 0 & 0 \\ x_{21} & x_{22} & 0 & 0 \\ x_{31} & x_{32} & x_{33} & 0 \\ x_{41} & x_{42} & x_{43} & x_{44} \end{bmatrix} \begin{bmatrix} f_1 \\ f_2 \\ f_3 \\ f_4 \end{bmatrix} = \begin{bmatrix} p_1 \\ p_2 \\ p_3 \\ p_4 \end{bmatrix}$$

x_{ij} is the percentage of class j of the feed that transfers to class i of the product. As matrix equation it is **X*f=p**. It fully describes the grinding process when **X** is known. **X** is composed of:

Matrix **S** describing **particle selection**
Matrix **B** describing **breakage function**

Matrix **S** selects the part of **f** that is crushed in a single stage:

$$\begin{bmatrix} s_1 & 0 & 0 & 0 \\ 0 & s_2 & 0 & 0 \\ 0 & 0 & s_3 & 0 \\ 0 & 0 & 0 & s_4 \end{bmatrix} \begin{bmatrix} f_1 \\ f_2 \\ f_3 \\ f_4 \end{bmatrix} = \begin{bmatrix} s_1 f_1 \\ s_2 f_2 \\ s_3 f_3 \\ s_4 f_4 \end{bmatrix}$$

or **S*f**. In words; the percentage of material that is indeed crushed may vary depending on the size class of the feed. In general a higher percentage of the coarser classes is crushed relative to the finer ones, hence $s_1 > s_2 > s_3 > s_4$. **S*f** is crushed according to breakage function **B**. (**I-S**)***f** is the material that remains uncrushed during the same stage (**I** is the unity matrix).

The part of **f** that is selected for breakage by **S** is crushed according to the breakage function **B**. Matrix **B** is determined by the following formula, which is a modified Rosin-Rammler function:

$$B_{xy} = \frac{1 - e^{-x/y}}{1 - e^{-1}}$$

Without classification the model for a grinding process is as follows:

$$\begin{bmatrix} b_{11} & 0 & 0 & 0 \\ b_{21} & b_{22} & 0 & 0 \\ b_{31} & b_{32} & b_{33} & 0 \\ b_{41} & b_{42} & b_{43} & b_{44} \end{bmatrix} \begin{bmatrix} s_1 & 0 & 0 & 0 \\ 0 & s_2 & 0 & 0 \\ 0 & 0 & s_3 & 0 \\ 0 & 0 & 0 & s_4 \end{bmatrix} \begin{bmatrix} f_1 \\ f_2 \\ f_3 \\ f_4 \end{bmatrix} + \begin{bmatrix} 1-s_1 & 0 & 0 & 0 \\ 0 & 1-s_2 & 0 & 0 \\ 0 & 0 & 1-s_3 & 0 \\ 0 & 0 & 0 & 1-s_4 \end{bmatrix} \begin{bmatrix} f_1 \\ f_2 \\ f_3 \\ f_4 \end{bmatrix} = \begin{bmatrix} p_1 \\ p_2 \\ p_3 \\ p_4 \end{bmatrix}$$

or **B*S*f** + (**I-S**)***f** = **p**. Calculation example (3rd row): $p_3 = B_{31}S_1f_1 + B_{32}S_2f_2 + B_{33}S_3f_3 + (1\text{-}S_3)f_3$. It can be rewritten as (**B*S** + **I-S**)***f** = **X*f** = **p**.

Matrix **C** describing **classification** of the population after each grinding stage

To define classification matrix C we introduce the feed of the classifier as **q**, the fine product as **p** and the coarse fraction as **C*q**. The fine product of the classification is given as (**I-C**)***q** = **p**, or

$$\begin{bmatrix} 1-c_1 & 0 & 0 & 0 \\ 0 & 1-c_2 & 0 & 0 \\ 0 & 0 & 1-c_3 & 0 \\ 0 & 0 & 0 & 1-c_4 \end{bmatrix} \begin{bmatrix} q_1 \\ q_2 \\ q_3 \\ q_4 \end{bmatrix} = \begin{bmatrix} p_1 \\ p_2 \\ p_3 \\ p_4 \end{bmatrix}$$

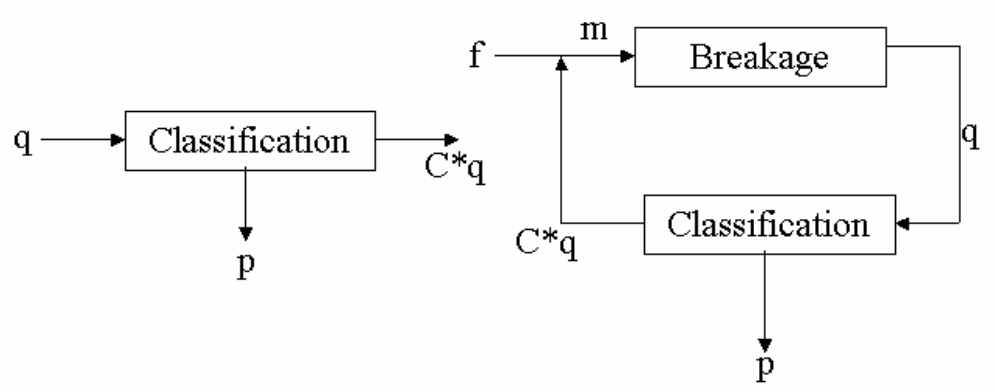

Fig. 3.11.2 - Classification function (left) and closed circuit grinding (right).

For closed circuit classification connected to a mill the following is obtained (Fig. 3.11.2):

p = (**I-C**)***q**
q = (B*S + I-S)*m
p = (**I-C**)*(**B***S + **I-S**)***m**
m = **f** + **C***q**
m = **f** + **C***(**B***S + **I-S**)***m**
f = [**I - C***(**B***S + **I-S**)]***m**
m = [**I - C***(**B***S + **I-S**)]$^{-1}$***f**

and thus **p = (I-C)***(**B***S + **I-S**) * [**I - C***(**B***S + **I-S**)]$^{-1}$ * **f = X*f**. The matrix equation for repetitive grinding steps becomes:

p$_1$ = **X*f**
p$_2$ = **X*p$_1$** = **X*X*f**
p$_3$ = **X*p$_2$** = **X*X*X*f**
... **...** **...**
... **...** **...**
... **...** **...**
p$_n$ = X*p$_n$ = X^n*f

The overall matrix equation describing the grinding process becomes

p$_n$ = **X^n*f**

with **X** = (**I–C**)*(**B***S + **I-S**) * [**I - C***(**B***S + **I-S**)]$^{-1}$

3.11.2. Discrete Element Modelling

Discrete element modelling (DEM) follows the trajectories and spins of all particles and media and predicts their interactions with each other and with the mill. Particles of many different sizes and densities interacting with complex shaped lifters and liner can be simulated. Important are a fast and robust algorithm, adequate collision model and geometrical description of the mill. 2D and more powerful 3D DEM simulation models are available. Currently industrial 3D simulations with up to 500,000 particles are possible in reasonable

times on single processor workstations. We give a summary of the description of the 2D DEM method as described by Cleary (1998).

DEM simulates collisional interactions of all particles with each other and with their environment (mill inside surface). For all objects the equations of motion are solved. Besides, boundary geometry of liner and, when present, lifters needs to be modelled. Simpler models solely model spherical particles and media. Arbitrary shaped objects can also be modelled, e.g. by discs or super quadrics of general form:

$$x^n + \left(\frac{y}{A}\right)^n = s^n \qquad (3.11.2.1)$$

n determines sharpness or blockiness, smoothly changing from a circle to a square as n increases. A is the aspect ratio with semi-major axis s. With A up to 10:1 and sharpness up to 20 many essential elements of real particle shapes are captured. The particle population is subdivided into groups, with each diameter, density, aspect ratio, sharpness and material properties specified. These properties can be distributed uniformly, normally or specified (e.g. Rosin-Rammler) as required.

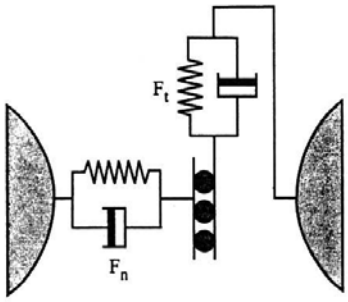

Fig. 3.11.3 - Spring and dashpot contact force model (normal direction) and incrementing spring and dashpot limited by sliding friction (tangential direction) [Cleary].

Collisional forces are determined by the amount of particle overlap Δx, v_n the normal, v_t the tangential relative velocities. A linear spring-dashpot model can be used for the collisions (Fig. 3.11.3). The normal force F_n consists of a spring to provide the repulsive force and a dashpot to dissipate a proportion of the relative kinetic energy:

$$F_n = -k_n \Delta x + C_n v_n \qquad (3.11.2.2)$$

k_n, the stiffness of the spring in normal direction, determines the maximum overlap (typically 0.1...1% with $10^6<k_n<10^7$). The normal damping coefficient C_n is chosen to give a required coefficient of restitution ε:

$$C_n = 2\gamma\sqrt{m_{ij}k_n} \qquad (3.11.2.3)$$

with

$$\gamma = -\frac{\ln(\varepsilon)}{\sqrt{\pi^2 + \ln^2(\varepsilon)}} \qquad (3.11.2.4)$$

and

$$m_{ij} = \frac{m_i m_j}{m_i + m_j} \qquad (3.11.2.5)$$

m_{ij} is the reduced mass of particles i and j with masses m_i and m_j respectively. It can be derived from the analytical solution of Eq. 3.11.2.2 for two particles. In general the same values for ε are used.

The tangential force is given by

$$F_t = \min\left\{\mu F_n, k_t \int v_t dt + C_t v_t\right\} \qquad (3.11.2.6)$$

where the integral of v_t over the collision behaves as an incremental spring that stores energy from the relative tangential motions and represents the elastic tangential deformation of the contacting forces. μ is the friction coefficient, C_t the tangential damping coefficient. The dashpot dissipates energy from the tangential motion and models the tangential plastic deformation of the contact. The total F_t (given by the sum of the elastic and plastic components) is limited by the Coulomb frictional limit at which point the surface contact shears and the particles begin to slide over each other. A DEM algorithm has three essential parts:

A search grid is used to periodically build a particle near-neighbour interaction list. The boundary objects appear as virtual particles. Using only particle pairs in the near neighbour list reduces the force calculation to an O(N) operation, where N is the total number of particles.

The collision forces on each of the particles and boundary objects are evaluated efficiently using the near-neighbour list and the spring-dashpot interaction model (Fig. 3.11.3), and then transformed into the simulation frame of reference.

All the forces on each of the objects and particles are summed and the resulting equations of motion are integrated:

$$\dot{\vec{x}}_i = \vec{u}_i \qquad \dot{\vec{u}}_i = \sum_j \vec{F}_{ij} + \vec{g} \qquad (3.11.2.7)$$

$$\dot{\theta}_i = \omega \qquad \dot{\omega} = \sum_j M_{ij} \qquad (3.11.2.8)$$

where $\mathbf{x}_i$, $\mathbf{u}_i$, and $\mathbf{F}_{ij}$ are position, velocity and collision forces on particle i, θ_i and ω_i are the particle orientation and spin produced by the moments M_{ij}, and $\mathbf{g}$ the gravity vector.

The integration scheme is a second order predictor-corrector. Between 20 and 50 time steps are required to accurately integrate each collision, hence a small Δt is needed (10^{-3}...10^{-6} s), given by

$$\Delta t = \min\left(\frac{\pi}{25}\sqrt{\frac{k}{m_{ij}(1-\gamma^2)}}, 0.1\frac{d_{\min}}{n_s U_{\max}} \right) \qquad (3.11.2.9)$$

where U_{max} is the maximum particle velocity, d_{min} the smallest particle diameter and n_s the number of time steps between searches.

After running a DEM simulation the positions, velocities, orientations and spins of all particles and objects are know. Before these disordered data can be interpreted they need to be binned, possibly smoothed and displayed in an informative way. The smoothing is necessary due to the discrete nature of the particles, resulting in extremely spiky data. Fig. 3.11.4 shows a 2D simulation of a 5m-diameter ball mill with uniformly distributed steel balls between 50 and 200 mm and ten times more rock particles (of circular shape) between 5 and 50 mm at variable rotation speed. The motion of the charge can be studied in detail as function of mill design and rotation speed.

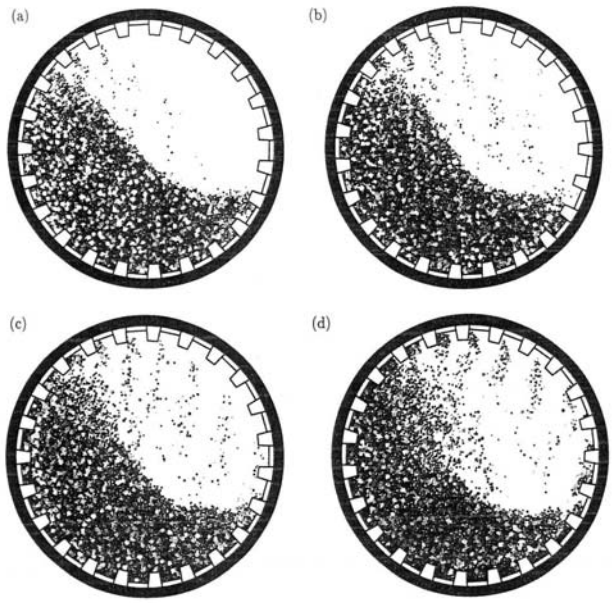

Fig. 3.11.4 - "Snap-shot" of simulation output of SAG mill with a charge of rocks and balls. ψ=0.6 (a), ψ=0.7 (b), ψ=0.8 (c), ψ=0.9 (d) ($\psi=n/n_{crit}$) [Cleary].

Power draw and torque of the mill can be predicted (Fig. 3.11.5). To the left the instantaneous power draw during 3 minutes is shown, having an average of 300 kW per meter mill length (white line in the middle). The irregular and high frequency fluctuations reflect a highly impulsive and unsteady flow of the charge. Fig. 3.11.5, right, shows variation of torque and power with mill speed ψ. At increasing ψ, as the amount of cataracting and then centrifuging increases, the balance of the charge improves and the torque required to

maintain the asymmetric charge position drops steadily. The power (being the product of torque and mill speed) consequently has a much rounder peak centred on ψ=90% before dropping sharply above 105%.

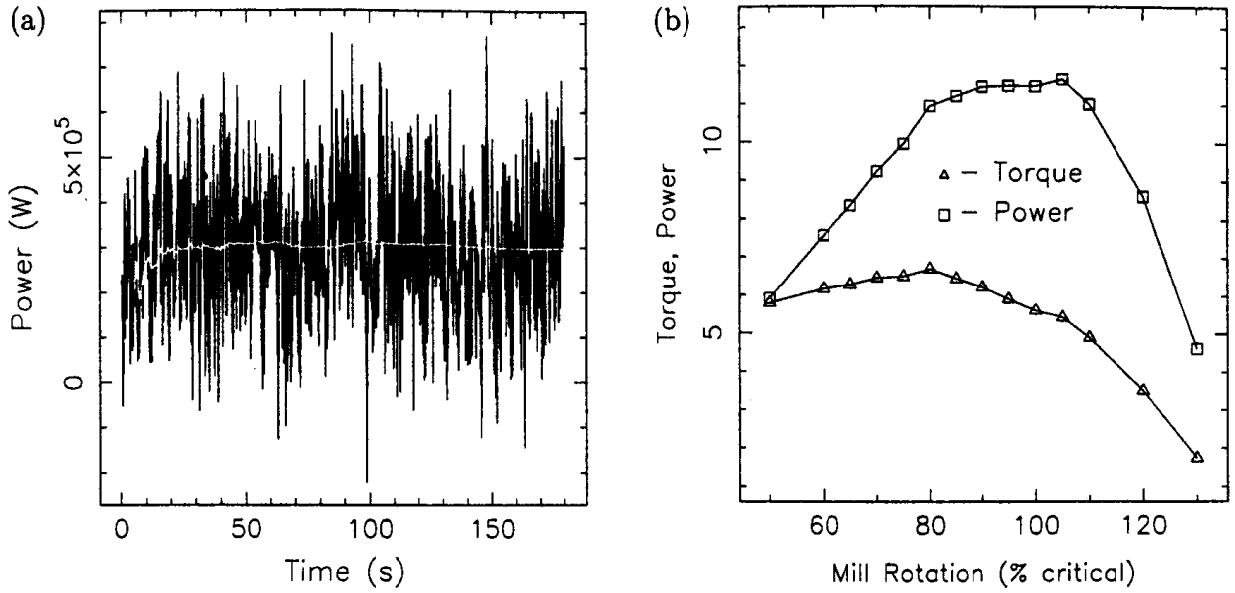

Fig. 3.11.5 - Power draw for ψ=0.8 (a). Average torque and power as function of ψ (mill rotation, % critical) [Cleary].

In Fig. 3.11.6 the difference between spherical and non-spherical balls is shown (the latter with A=0.5...1 and n=2...5, Eq. 3.11.2.1). Though qualitatively appearing similar, there are key differences that are also visible:

When the charge is flowing down the upper half of the free surface, the non-circular material is forced to dilate, producing a higher void fraction in the upper region.

Because of this the free surface is raised compared to the circular material, which in turn raises the height of the cataract.

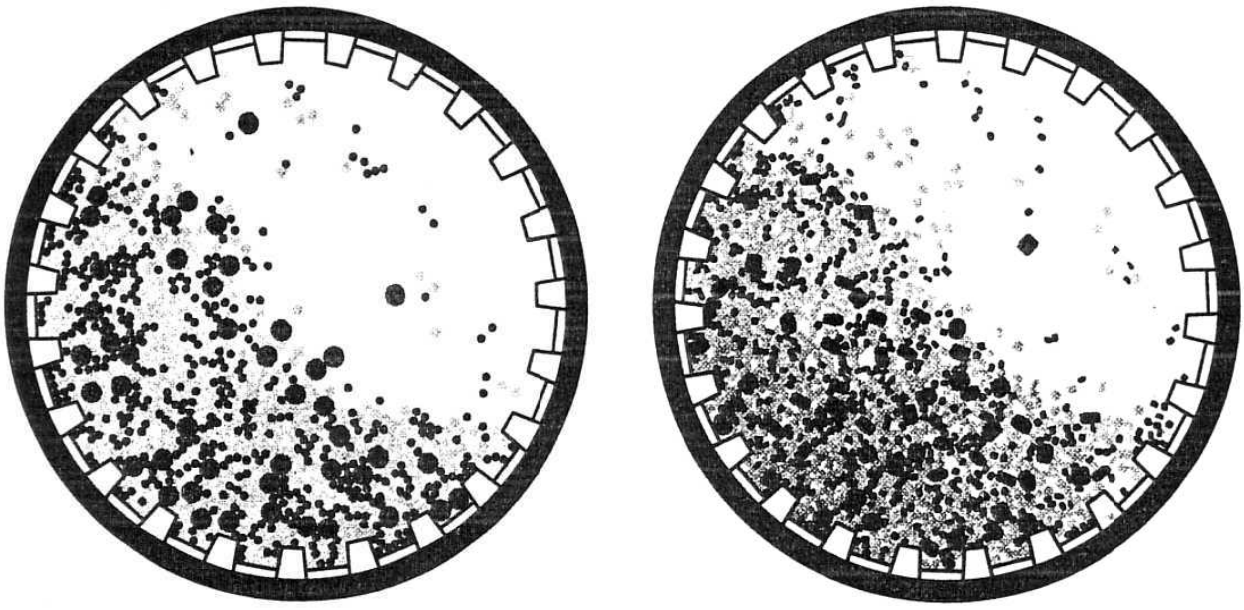

Fig. 3.11.6 - Charge with circular particles (left) and with non-circular particles (right) [Cleary].

Liner and lifter wear predictions can be made from DEM collisional data collected in specific object bins. Particle impact speeds and liner hardness are used to estimate the wear produced by each impact. The wear information is collected around the entire mill, and averaged for all lifters, since the mill is symmetric. Fig. 3.11.7, left, shows a lifter and its bins for ψ=0.6 (a) and 0.8 (b) after 5000 hours of operation. The highest wear occurs around the upper corners of the lifter bar.

Modelling the actual size reduction in a full-scale mill by DEM would involve tracking particles <100μm, but length scales and the huge number of particles are prohibitive at present. Therefore DEM is used to calculate breakage related properties such as rate of particle-particle and particle-wall shear and normal work. They are indicators of the breakage and attrition and so allow comparison of comminution performance for different mill configurations. Fig. 3.11.7, right, shows another DEM output: the intensity of collisions. It increases to the bottom, reflecting increasing weight of material above that must be supported. The collisional forces are slightly higher in the surface-avalanching region. There is a higher force area at the base of the avalanching/shearing in the upper part of the charge, where additional force must be applied to halt the downward flow of this material. A high intensity region in the lower right is caused by the cataracting material impacting heavily on the liner and on the tail of the charge. Attrition and breakage rates can be inferred from such collisional force data.

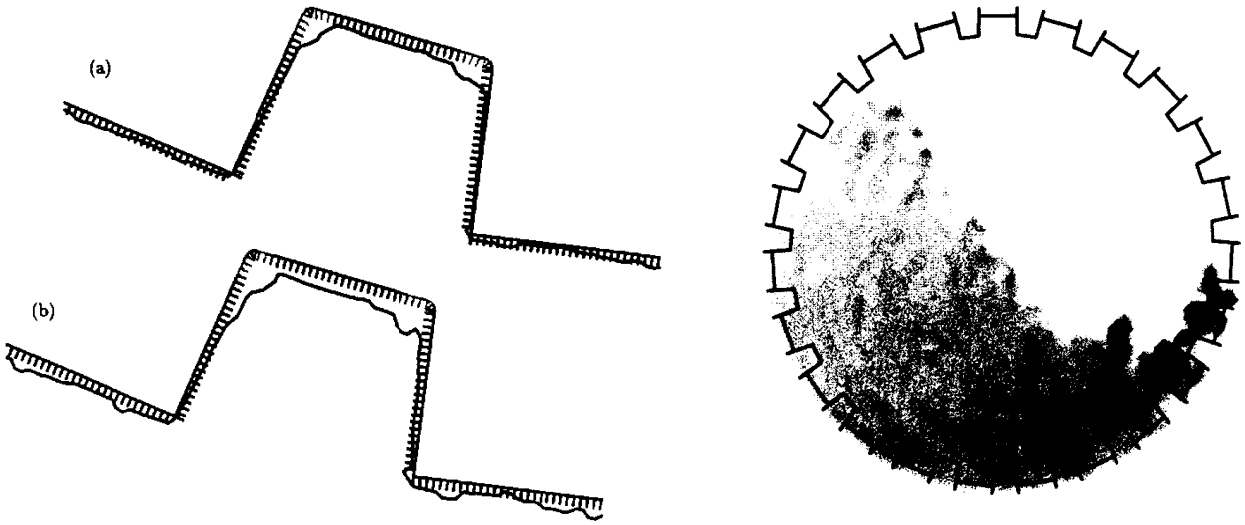

Fig. 3.11.7 - Left: liner shape after 5000 hours operation as predicted by DEM for ψ=0.6 (a) ψ=0.8 (b). Right: collision intensity within the ball mill [Cleary].

DEM of tumbling mills allows prediction of charge profile, segregation state, power draw, torque, liner wear and collision force distribution. However, substantial work is required to validate the predictions, and future research in predicting size reduction remains a significant challenge.

3.12. References

Agar and Charles: Trans. SME 220, 390-4, 1961.

Bwalya, M.M.; Moys, M.H.: The use of DEM in predicting grinding rate. Proc. XXII Int. Min. Proc. Congr., Cape town, 2003.

Cleary, P.W.: Predicting charge motion, power draw, segregation and wear in ball mills using discrete element methods. Min. Engng, Vol. 11, No. 11, pp 1061-1080, 1998.

Cleary, P.W.: DEM as a tool for design and optimisation of mineral processing equipment. Proc. XXII Int. Min. Proc. Congr., Cape town, 2003.

England, T. (editor): Coal preparation in South-Africa. The South African Coal Processing Society, 2002.

Fry, T.C.: probability and its engineering uses, van Nostrand, New York.

Fuerstenau: Trans. SME 220 1961 pp. 395-6.

Gilvarry et al.: Trans. SME 220 1961, 380-9.

Hukki: Trans. SME 220, 1961, 403-8.

Knecht, J.: World's biggest shell supported SAG mill – experience and concept. Publication from Krupp Polysius AG

Lienau: Jnl. Franklin Inst., April, May, June 1936.

Lynch, A.J.: Mineral crushing and grinding circuits. Elsevier, Amsterdam, 1977.

Mishra, B.K.; Rajamani, R.K.: Simulation of charge motion in ball mills. Part 1: Experimental verifications. Int. J. of Min. Proc., 40 p 171-186, 1994

Mular, A.L., Jergensen, G.V.: Design and installation of comminution circuits. SME, New York, 1982.
Powel, M.S.; Nurick, G.N.: A study of charge motion in rotary mills, part 1 – Extension of the theory. Min.Eng. Vol. 9, No. 2, p 259-268, 1996
Powel, M.S.; McBride, A.T.; Govender, I.: Application of DEM outputs to refining applied SAG mill models. Proc. XXII Int. Min. Proc. Congr., Cape town, 2003.
Schubert, H.: Aufbereitung fester mineralischer Rohstoffe. VEB Deutscher Verlag für Grundstoffindustrie, Leipzig, 1989.
Schumann: Min. Eng. Febr. 1960.
Taggart, A.F.: Handbook of mineral dressing. John Wiley & Sons, New York, 1956.
Weiss, N.L.: SME Mineral Processing Handbook. SME, 1985; pp. 30.7.
Wills, B.A.: Mineral processing technology. Pergamon press, Oxford. 1988.

4. AGGLOMERATION

[This Chapter is a shortened reproduction of Chapter 11, Vol. 1 (Weiss et al.) by Fred D. DeVaney]

Introduction

The term agglomeration is used to describe processes whose goal is to form balls, briquettes, nodules, flakes, or other sized shaped particles from loose, usually fine, incoherent particles. In practice it includes such varying processes as the briquetting of coal dust and other substances, the balling and induration (heating) of such nonmetallics as cement, fluorspar, lightweight aggregates, etc. Agglomeration processes are of particular value to the iron and steel industry where the nature of the primary reduction process, the blast furnace, requires for best results a burden essentially free of fines. This is a change that has taken place since about 1960. Prior to that time many fine unsized ores were fed to the furnace. The development of the pelletizing process gave to the industry a chemically controlled closely sized product that increased the production rate and reduced the costs so much that unsized fines are seldom used in modern furnaces. Steel plants produce many fine sized waste products such as fine dust (fine ore coke and gangue) and mill scale. These products, which have a valuable iron content, are usually sintered directly at the plant for reuse. Fine sized ore concentrates are usually pelletized at the mine and shipped as pellets to the steel plant. Common practice in some areas producing natural high grade ores is to screen the ore at the mine to about 10 mm. The oversize is shipped “as is” and constitutes blast furnace feed. The <10 mm fraction may be shipped to the steel plant where it may he sintered or otherwise agglomerated. At some mines the fines may be pelletized prior to shipment. With the development of large ocean ore carriers, and with the transportation of slurried concentrates or fines, a trend has developed of constructing large pelletizing plants or other types of agglomeration plants near large consumption centers (i.e. in the Netherlands or in Japan) where ores of many types are brought together, ground if necessary, blended, and agglomerated.

4.1. Briquetting

Coal briquettes

Briquetting press in action

Briquetting is one of the most common methods of agglomeration. Large tonnages of coal, coke and charcoal, quicklime, phosphate ore, iron ore, mill scale, blast furnace flue dust, sponge metals, cast iron turnings, salt, and many other substances are briquetted. Either by use of a suitable binder or with sufficient pressure, possibly in conjunction with high temperature. Nearly any fine solid material can be made into reasonably strong briquettes.

Various types of operations and of presses are included in the general category of briquetting. These are (1) briquetting, (2) compaction, extrusion, and (4) tableting.

Definition and Types of Presses

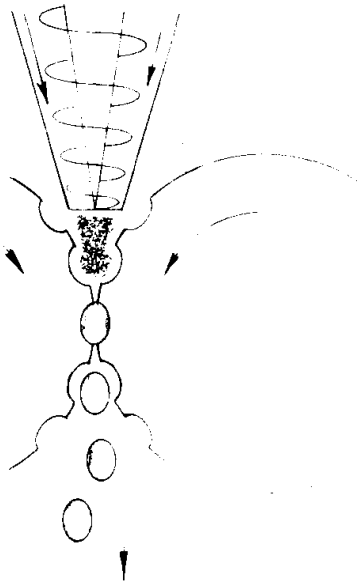

Fig. 1. Roll briquetting press, screw feed.

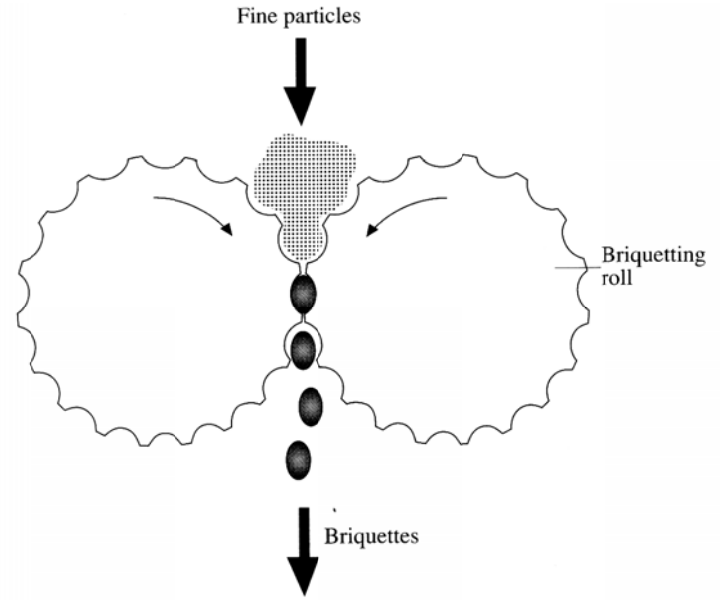

Fig. 2. Roll briquetting press, gravity feed [Woolacott and Eric].

1) Briquetting. Formation of pillow, almond, cylindrical or other geometrically shaped pieces from finely divided solids by means of mechanical compaction. Roll type presses (Figs 1 and 2) are most frequently employed, though ring roll presses have also been used to a limited extent (Fig 3).

2) Compaction. A closely related operation to make flakes or sheets by compressing fine material between either smooth or corrugated rolls These flakes are often broken up into particles of the desired size (coarser than the original material) by an operation known as granulation.

3) Extrusion. Forcing finely divided solids through a cylindrical die to make cylindrical briquettes or pellets Small pellets (e.g., 10 mm in diameter with 10 mm length or smaller) are made by extruding material through many small holes with a roller (Fig. 4). Larger briquettes are made by extruding the feed material through a single cylinder using a press or a reciprocating plunger as in Fig. 5.

4) Tableting. This operation uses cylindrical dies to form short, cylindrical shapes or pills, like aspirin tablets. Tableting machines, shown schematically in Fig. 6, are often complex, using opposing punches to press the tablets evenly from each side and having a complicated sequence of operations to measure, feed, compress, and eject each tablet at high rates of speed.

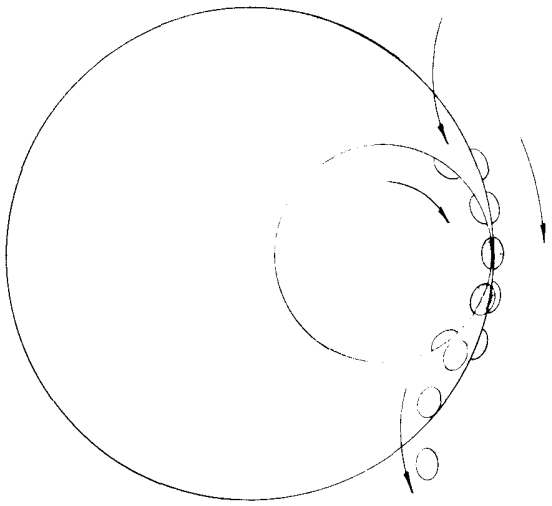

Fig. 3. Ring roll briquetting press.

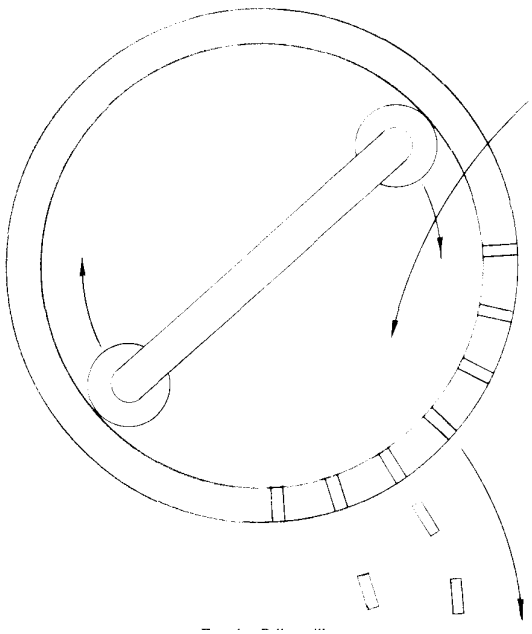

Fig. 4. Pellet mill.

Briquetting; Roll Type Machine

This section is primarily directed toward making briquettes with roll-type machines, but much of it will be pertinent to the other compaction operations. Roll-type machines are the most widely used briquetting and compaction devices in the mineral industries because they can agglomerate large tonnages of solids at relatively low cost.

Mechanism of Briquetting

Flow of Material. The material to be briquetted must be reasonably free-flowing, both to feed into the press at a uniform rate and, even more importantly, to allow the particles to move together during compaction into a dense close-packed arrangement where the compressive and shear stresses are distributed reasonably uniformly throughout the briquette's interior.

If internal friction of the material is too great, some parts of the briquette are insufficiently compacted, with parts of the mold or pocket remaining unfilled, while other parts get overcompacted, with broken grains and tension cracks resulting due to excessive pressure and elastic springback on release of the pressure.

Lubricants can be blended with the feed material to make it more free-flowing, particularly when under compression. Water is the most common lubricant, but other liquids and solids are often used also in proportions typically ranging from 0.5% to 2%, with fine or porous particles requiring the larger proportions. Some typical briquetting lubricants are water, stearic acid, calcium of magnesium stearate, paraffin waxes, minerals oils, dry starch, graphite and molybdenum disulfide. Most binders also serve as lubricants. At the high pressures required to briquette many minerals and metal powders, the solid lubricants such as graphite or the metal sterates are more effective than oils or liquid lubricants.

Binding Action. A number of physical and chemical mechanisms serve to bind solid particles together when they are compacted into a briquette.

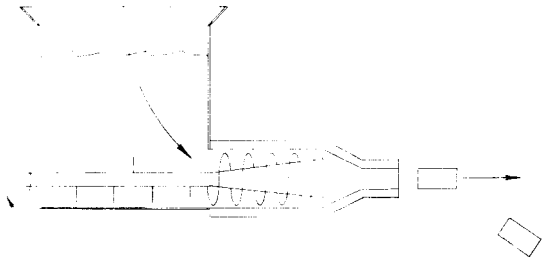

Fig. 5. Screw type extrusion press.

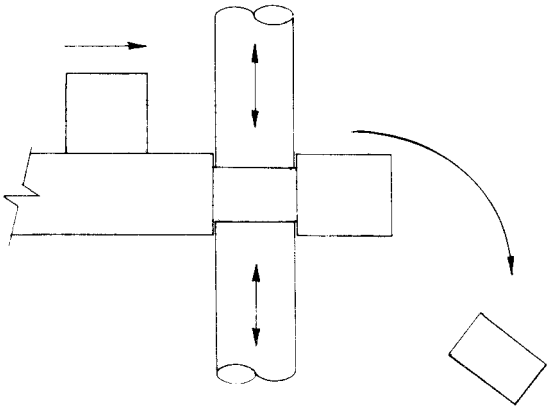

Fig. 6. Tablet press.

A *binder* mixed with the fine solids may act as an adhesive, sticking to the surface of each particle and holding adjacent particles together by the binder's surface tension. In this case the binder exists as a film, and as it must coat each particle, thorough mixing is required to make it function properly. Water often acts as a binder in this manner as well as providing lubrication, and so do resins and other sticky materials.

Mixing the solids with a higher content of a tacky viscous fluid (particularly one that subsequently hardens due to cooling or chemical action) provides a matrix which cements the particles when they are pressed together. Pitches and resins usually act as matrix binders as do mixtures of molasses and lime, spent sulfite liquor, and other "sticky" fluids.

Proportions of matrix binders needed to make satisfactory briquettes depends on the fineness of the solid particles, their porosity, and density. Coal can be briquetted effectively when mixed with 6% pitch, while some fine porous chars require as much as 30% pitch for proper briquetting. In order to coat the particles uniformly, the mixture must be heated to the softening point of the pitch; usually 50°C to 70°C.

The principal characteristics needed by matrix-type binders are sufficiently low viscosity for proper mixing, a tendency to stick to the solid particles, and enough viscosity to hold the particles together after the mixture is pressed into briquettes. Pitches (i.e., coal tar pitch or asphalts) are usually heated to make them fluid enough for mixing, and the finished briquettes are allowed to cool to harden the matrix of binder and so impart strength to the briquette. Subsequent processing steps required of the briquettes may dictate more specific binder requirements.

Some binders have a solvent action and dissolve materials from the surface of the particles to form "solution bridges" which become solid bonds after the solvent evaporates, although the surface tension of the solution must hold the "green" briquette together until it dries. For example, 0.5% to 2% moisture is sometimes used to bond water soluble salts.

While binding action has to be fast enough to enable the briquette to hold together as soon as it falls from the press, many binders do not develop their full required strength until the curing or post treatment takes place. Evaporation of a solvent-type binder, as noted previously, is one example of post treatment. Chemical action involving crystallization or polymerization may also strength a binding substance, particularly a matrix-type binder.

It is difficult in some instances to distinguish the specific effect that a useful briquette additive may have. Water, for example, acts as a lubricant when added to clays and it also facilitates bonding. In other cases, it may function as a coolant, such as when a low melting organic material is briquetted.

Binderless Briquetting. In recent years, improved presses capable of high pressures use the fact that certain solids "weld" together when compressed at high temperature or even at room temperature in order to briquette without binders. Crystals of alkali halides, particularly sodium chloride, tend to become plastic and flow under high shear stress. High pressures will bond them together. At higher temperatures, many other solid substances behave similarly and, in general, higher temperatures make solids less brittle and elastic and

so permit binderless briquetting of a wider range of materials and the use of lower briquetting pressures. In general, alkali metal salts, salts of calcium and magnesium, free metals, and plastic materials readily bond without binders, while use of higher temperatures and pressures permit binderless briquetting of many other mineral substances.

Compaction enhances the sintering action of high temperatures, probably by forcing fused zones of a heterogeneous solid into close contact. Thus, a small quantity of finely divided flux is sometimes mixed with an ore to aid hot briquetting. Use of dolomite or lime help briquette steel mill scale is an example Fluxing is probably involved in the hot briquetting of oxide ores such as hematite.

Iron ore can generally be briquetted at lower temperatures and pressures as its state of oxidation is lowered by reduction.

Similarly, metals can be bonded into briquettes more readily than their oxides Thus, clean cast iron or steel turnings briquette readily, but formation of an oxide film by exposure to the weather makes the material unsatisfactory to briquette. However, before briquetting, the cutting oil on turnings must be removed, usually by heating to 120°C, but also by thorough washing, as the oil interferes with the metal-to-metal bonds formed by high pressure contact.

Action of Roll Presses. Several concepts are useful for understanding the practical application of roll presses.

Briquetting Pressure. In a roll-type press the actual pressure is indeterminate since the effective area against which the rolls press cannot be measured As a useful working definition or approximation, the pressure is often assumed equal to the force between the rolls divided by the projected area of one horizontal row of briquettes. This projected area is equivalent to the roll width times the circumferential pitch of the pockets. With flat-faced compaction rolls the pressure is approximately equal to the force between the rolls divided by a multiple of two to five times the thickness of the strip of compacted material.

The shear stresses induced as a briquette moves past the point if tangency of the rolls cause the particles to move into a more closely packed arrangement and thus provides more effective action than static pressure applied as in a cylindrical die.

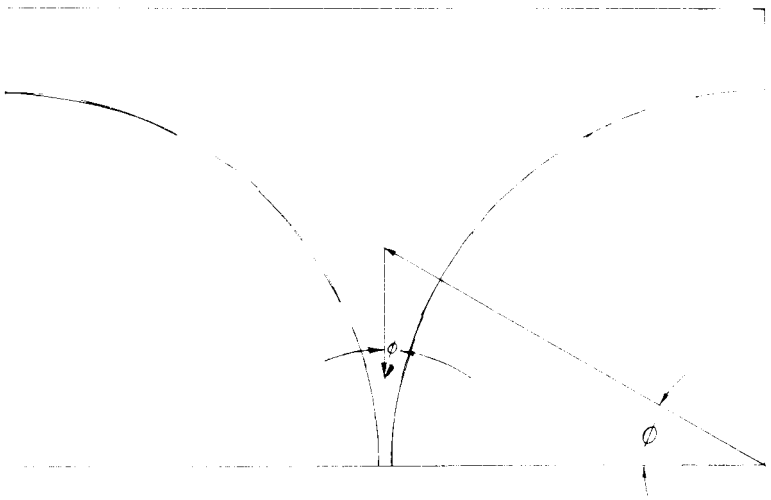

Fig. 7. Angle of nip.

Angle of Nip. This is the angle Φ in Fig 7 below which the rolls sieze the feed material and compress it. Tan(Φ) is equal to the coefficient of sliding friction between the roll's surface and the feed material The rolls will therefore slide past the feed material which is in contact with them above the angle Φ; below Φ, the material moves at the same rate as the roll surfaces and is carried between them and compressed.

Thus, to make a given size briquette there is a minimum roll diameter when gravity feed is used. Too small a roll diameter will not allow enough material to fall into the space included within the angle of nip so that the pockets in the rolls are not filled and the feed material does not get pressed sufficiently.

Also, with gravity feed it may be necessary to meter or limit the flow of feed, as too large a roll diameter can cause too much material to be drawn in, and this will spread the rolls excessively and make briquettes which are unduly thick with large web or seam areas. This Situation produces much fine material.

Force feeding of the rolls with a variable speed tapered screw, as in Fig. 1, enables the proper amount of feed material to be metered or pushed between the rolls; it also permits use of smaller diameter rolls turning at higher speeds than is possible in a given case with gravity feed alone.

Movement of Rolls. Roll loading and the resulting briquetting pressure are controlled by forcing the rolls together with adjustable springs or by hydraulic pressure (using an accumulator with the fluid kept under nearly constant pressure by a confined gas above a flexible diaphragm). Briquette presses are sometimes rated by the force necessary to spread the rolls, with up to 350-ton machines (roll 90 cm diameter).

Generally the force pressing the briquette rolls together is best adjusted to the minimum needed to make satisfactory briquettes when the feed rate is just enough to spread the rolls apart slightly. In this way, the full roll loading bears on the briquettes, and any minor variations in feed rate can be tolerated without resulting in either unfilled pockets or the tension cracks from excessive pressure. Properly adjusted, the rolls should be spread from 1.5 mm to 10 mm, depending on their diameter and the size of the briquettes, and the movable roll will be observed to oscillate or "work" in and out slightly as it rotates.

Discharge of Briquettes. For satisfactory performance briquettes must discharge cleanly from the roll pockets. Briquettes will not discharge properly if the feed material adheres to the rolls, if the pockets are too deep, if excessive binder is used, or, in some cases, if too much or too little pressure is applied. When the feed material adheres to the rolls, use of a lubricant may be helpful.

Performance of Briquette Machines

Briquetting equipment is developing toward larger capacities, greater pressures, and higher roll speeds. For a given capacity, machinery is becoming more intensive—that is, smaller and faster. Feed preparation is becoming more elaborate, too, particularly with use of higher temperatures and controlled atmosphere. For the high roll speeds, preliminary deaeration or densification by pressing the material between smooth rolls or by compressing with tapered screws is often employed just ahead of the briquetting rolls themselves. This precompression reduces the porosity of the feed material and the tendency of the gases pressed out of the pore spaces in the feed to blow back against the stream of incoming feed material and so cause irregular feeding of the briquette machine. Deaeration is particularly helpful when very fine particles are to be briquetted.

High rates of production require careful metering of feed to the rolls, and the use of force feeding is now rather general (Fig. 1).

Some briquette machines have the roll centerlines arranged in a vertical plane with a horizontal screw used for force-feeding. This configuration allows the feed material to drop directly into the scroll of the screw feeder at right angles to its axis without interference from the drive shaft.

Power requirements for briquetting depend on the compressibility of the feed and on the pressures used. They cover a wide range:

- Mixing (where binders and/or lubricants are used): 1.5 to 7.5 kW/t feed
- Feeding: 0.4 to 4 kW/t feed
- Briquetting: 1.5 to 20 kW/t feed

Roll maintenance is one of the largest cost items in briquetting. With abrasive materials, high temperatures, and/or corrosive conditions, roll wear can be considerable. In practice, roll life varies from about 400 to 30,000 hr or more. Actually, in briquetting organic solids such as di-methyl-terephthalate, rolls have lasted ten or more years, while extremely abrasive materials such as glass batch mixtures still await the

development of rolls which have an economical life. As the rolls wear, the pockets enlarge and the briquette production rate rises. However, with wear, the joint or web between the two halves of a briquette gets wider, and more fines are produced along with the briquettes. The generation of fines varies from about 5% with new rolls fed properly to as much as 30%, with the higher figure indicating worn rolls and cheek pieces. (Cheek pieces are the guards at the edge of the rolls which prevent the material from escaping to the sides.) It is generally necessary to screen fines from the briquettes and recycle them back through the rolls. Many briquette machines are equipped with replaceable segments for the wearing surfaces of the rolls. These are quick and less expensive to replace and they can also be made of harder steel than is possible when the wearing surface or pockets is a tire shrunk onto the supporting roll.

Since briquette machines are usually driven at constant speed, their production rate is also constant. Most installations therefore consist of two or more machines in parallel with variations in load accommodated by stopping one machine periodically. This practice requires surge storage of feed material upstream from the briquetting operation The process downstream from the briquette machines must also be able to handle changes in the flow of material as the machines are stopped and started.

Specification of Briquetting Machinery

Though the general principles of briquetting are fairly clear, to assess suitability for a particular application and to specify specific equipment usually requires an actual test. Fortunately, unless the pretreatment is complex, material can be readily tested in a meaningful manner on pilot scale facilities available in the laboratories of most manufacturers of briquetting machinery. If binders are not required, as little as 10 kg of material may be sufficient to supply all of the data necessary to specify a commercial size briquette machine. It is important to recognize that the briquette machine has only one function: to apply pressure to the material. If pressure alone will produce a satisfactory product, it is necessary to determine only what pressure is required. The manufacturer then need only know, in addition, the required rate and briquette size.

If pressure alone will not produce a satisfactory product, the conditions must be altered by adding binders or lubricants, increasing temperature, or otherwise establishing suitable process conditions to permit pressure to bind the fine particles together. A preliminary indication of how well a given material can be briquetted is also often possible by compressing the fines in a cylindrical die using a hand press. This procedure is particularly useful when briquetting is part of a bench-scale process development study. Other laboratory tests of the feed material can be helpful as well, but their use is not yet general.

The size and specifications for briquette machines or compactors to provide a desired output can be estimated as follows:

$$\textit{Volume of briquettes per revolution} = \pi DWT$$

where D is roll diameter (in m), W is effective roll width (width of the briquette pockets, in m), and T is the mean thickness of the briquettes or the thickness of a compacted strip. Thus the output of a roll press will be:

$$Q = \pi DWTN\rho$$

where Q is in kg per min, N is rpm, ρ is density in kg/m^3.

Values of T can be estimated from the correlation given in Table 1 which relates briquetting pressure, roll diameter, and briquette size. These data approximate most briquetting situations. (The periphery of corrugated compaction rolls may have 20 to 30% more corrugations than Table 1 indicates). Note that use of lower pressures on a given machine can permit making larger briquettes. Roll speeds range in practice from about 5 to 100 rpm.

Table 1. Approximate Relation of Briquetting Pressure, Roll Diameter and Briquette Size

Briquetting pressure (tons/cm^2)	*Approx. no of pockets in one row around periphery of roll*	*Ratio D/T**
Low. < 1	36	30
Medium, 1-4	48	40
High, >4	72	60

*D is diameter of roll and T is mean thickness of briquettes

Table 2 shows capacities of typical briquetting machines for making salt (NaCl) briquettes having a density of 2165 kg/m^3 and a roll speed of 25 rpm. In most briquetting operations the actual yields closely approximate the calculated capacity rates as the webs between the briquettes and the leakage of uncompacted material past the rolls are not included in the calculations.

Table 2. Typical Briquette Machine Capacities

Roll diameter (mm)	Effective roll width (mm)	Maximum force between rolls (tons)	Appr. Capacity* (t/hr)
130	50	10	0.15
305	76	25	1.2
380	102	50	2.5
457	152	100	5.5
610	203	150	12.5

*For salt, with briquette density of 2165 kg/m^3, roll speed is 25 rpm, and D/T = 60.

In a typical compacting process, however, the yield of granular product of the desired size may be anywhere from 20% to 90% or more of the calculated throughput, depending upon the range of mesh sizes in the final product and the mechanical properties of the compacted material. The balance of the material is screened out and recycled to the granulator for further grinding or sent to the compactor for agglomeration.

Typical Briquetting Processes

There is no way to subdivide into consistent categories the vast number of materials that are briquetted commerically. However, a division based upon the approximate briquetting pressure illustrates the great range of conditions that these materials require. The briquetting pressure is assumed to equal the roll force divided by the projected area of one horizontal row of briquettes.

Low Pressure Processes (<1 t/cm^3). Many materials can be successfully briquetted at pressures under 1 t/cm^3. These include earthy iron ores, oil and other shales, laterites, phosphate ores, clayey bauxite, and materials in general that are plastic in nature and have high moisture contents (5 to 20%). Materials that are briquetted with matrix-type binders such as coal-pitch mixtures and pitch-ore mixtures also fall into this category. The mechanism of the briquetting process here is primarily one of pressing readily cohesive materials into suitable shapes with comparatively little change in density. Energy requirements are normally 1 to 5 kWh per ton of briquettes, and roll costs usually range from €0.20 to €1.00 per ton of product. Lubricants are not normally used with low pressure briquetting processes.

Medium Pressure Processes (1 to 4 t/cm^3). Sodium and potassium chlorides as well as most typical ionic solids can be briquetted or compacted in this range of pressures. Oxides of calcium and magnesium are briquetted at the high end of this pressure range, whereas many organic solids are briquetted at the low end. The briquetting mechanism in this case is plastic flow of the crystals combined with crushing and rearrangement of the particles: thus, substantial changes in density occur during the briquetting process. These materials are mostly briquetted dry although small additions of moisture, 0.1% to 2%, or film-type binders are frequently employed to assist the process. Lubricants are generally beneficial but their use is often restricted by cost or the purity requirements of the briquettes. Typical energy requirements are 5 to 15 kWh per ton briquettes, and roll costs vary widely from a few €ct to €1.00 or more per ton.

High Pressures (>4 t/cm^3). High-pressure briquetting with roll-type machines is comparatively recent in origin and is still undergoing extensive development. Chips and machine turnings of aluminium, brass, bronze, cast iron, and steel are briquetted at normal temperatures in this range of pressures. The highest pressures used commercially with roll-type machines are for briquetting titanium chips, with calculated pressures of about 10 tons per cm^2. Metal chips and powders, sponge iron, iron ore, and steel mill dusts, as well as other ores and flue dusts, can also be briquetted hot in this range of pressures. In these cases the temperature of the material is usually over 500°C in order for the briquettes to achieve the required strength and density. Maximum briquetting temperatures of about 1000°C are imposed by limitations in materials of construction for the rolls and feeder parts. Energy requirements are generally 15 to 30 kWh per ton of briquettes, and roll costs usually range from €0.50 up to €2.50 per ton as a maximum acceptable cost. Lubricants are frequently employed and the briquetting rolls may be cooled by a water spray if their surface temperature exceeds about 400°C. The use of high temperatures and pressures adapts briquetting to many additional materials, and additional development work can be expected to extend further the use of this method of agglomeration.

4.2. Partial fusion: sintering and nodulizing

Sintering and nodulizing are used for agglomeration of fine minerals through partial fusion for production of indurated agglomerates which are irregularly shaped. Continuous sintering is performed by combustion of solid fuel within a quiescent bed of blended fines using a travelling grate processing system. Continuous nodulizing is performed by firing a tumbling bed of fines using external burner combustion in a rotary kiln operation. Sinter s generally characterized as a crushed and graded structure of porous, cellular solids: nodules are generally characterized as relatively dense, ungraded, rounded masses ranging from large nodular halls to finer sandy structured particles. Sintering is the dominant process for agglomerating minerals, exceeding 300 million tpy of worldwide production and increasing annually, whereas nodulizing, excluding portland cement manufacture, is much less than 10% of this production and appears to be declining.

Both these systems of mineral agglomeration are applied in metallurgical fields for beneficiating furnace burdens by agglomeration of ore minerals for improvements of structure as well as for coincidental desulfurization and devolatilization. Sintering and nodulizing are also applied in the minerals field for production of nonmetallic materials such as lightweight aggregates, portland cement clinker, and special dead-burned fluxes and refractories. in addition to direct processing of minerals, sintering and nodulizing are applied for reclamation, upgrading, and recycling of waste dusts and sludges in metallurgical operations.

4.3. Pelletizing (feed preparation and balling)

Fig. 8. Iron ore pellets

The term pelletizing in the mineral industry refers to processes in which fine concentrate or ore is rolled in a damp condition into balls which are then fired or indurated until they become hard (Fig. 8). Pelletizing consists basically of rolling fine moist ore or concentrates into balls and then firing these into hard pellets. These processes, of which there are several variations, came into commercial use in the late l950s, and their use has had a fast worldwide growth ever since. Prior to that time many fine unsized ores were fed to the blast furnace. The development of the pelletizing process gave to the industry a chemically controlled, closely sized product that increased the production rate and reduced the costs so much that unsized fines are now seldom used in modem furnaces. In 1976 the world pelletizing capacity was estimated on 162 million tons, with an additional 68 million tons under construction, making a total potential capacity of 230 million tons.

This section only highlights the feed preparation and balling of pellets, or in other words the production of "green pellets". Balling is usually a preparatory operation preceding some subsequent pyrometallurgical processing such as drying and induration. A notable exception is the use of balling to render fine powders dust free and free-flowing. The induration (firing) of pellets is covered by (pyro)metallurgical literature.

Balling principles

The term balling is that unit operation wherein finely divided powders are formed into larger agglomerates by the use of water or other liquid in balling drums or disks. Various types of binders are frequently used in addition to the liquid. The forces that hold together a green ball are:

1. capillary forces in the liquid film
2. adhesional and cohesional forces
3. attraction between solid particles by van der Waal and electrostatic forces
4. mechanical interlocking of the granular particles

There is an important influence of the capillary forces of the liquid film in binding together the fine particles forming a green ball. A green ball of mineral particles acts as system of fine capillaries. It can be demonstrated that in a capillary tube the menisci are drawn in opposite directions by the surface tension. This results in a negative pressure on the liquid column corresponding to an equal positive pressure on the surface of the tube. These forces are believed to be among the major ones influencing the growth and strength of green balls of mineral particles.
An optimum amount of liquid is necessary to produce maximum green ball strength. Sufficient liquid should be present to fill completely the void space among the particles, but not so much as to wet excessively the exterior surface. It can be demonstrated that excessive liquid weakens the capillary forces by submerging a green ball in liquid where it quickly disintegrates.

Binders

In the development of the iron ore pelletizing processes, literally hundreds of materials have been investigated for use as binders. Bentonite of the free-swelling sodium type has generally been the most satisfactory because of its usefulness in all phases of the process. That is, it provides green strength during formation and transport of the green ball, contributes to dry strength when the binding liquid has been removed, and may enter into the final indurated strength to some degree. A given balling problem must be evaluated according to the performance required of the binder. In the case of a need for green strength only, many binders may perform as satisfactorily as bentonite and at lower cost.

Type of Binders. These vary widely and are dependent upon the performance required, availability, and cost. Among the more commonly used binders are bentonite, other clays, ferrous sulfate, lignin sulfite liquor, asphalt compounds, starches, calcium compounds, and sodium compounds. They can be grouped into four general types:

1. soluable salts,
2. bentonite,
3. inorganic chemicals,
4. organic materials.

Benefits of the Various Binders. These are dependent upon the process requirements. Balling systems in which water is the major binding liquid require a binder miscible with water. Other systems, for example, using asphaltic compounds, may have only a trace of water in the final green ball. In most cases, binders are used to form green balls of sufficient strength that can be transported and placed in a packed bed for further processing. Beds wherein the green balls are subjected to the weight of a deep column of material or the pressure of flowing process gases must not collapse as the binding liquids are removed. Such conditions require that the binders provide dry strength in the green ball. Calcium hydroxide used in some instances in iron ore pelletizing provides a flux which at high temperature results in the formation of slag bonds with the fired product

Influence of Economics. A choice of binder often must be determined experimentally. For example the cost of bentonite varies greatly from place to place. Bentonite has largely replaced lower cost ferrous sulfate and calcium oxide in iron ore pelletizing operations because better product at higher production rates can be obtained with bentonite and it is overall a more economical binder. High value minerals such as chrome concentrates may justify the use of more costly sodium silicate binders which can produce green balls of a coarser size structure than water.

Particle Size

The particle size and size distribution are key factors in determining the ability to produce green balls of suitable strength and production rate. It is often found that additional grinding beyond that required for beneficiation is necessary to accomplish a satisfactory balling operation. An economic balance between additional grinding capacity and the use of greater amounts of binder or more costly binders is frequently a necessary determination.

Surface Area. The binding forces within a green ball are enhanced by increasing fineness of material which results in a greater number of contact point and particle surfaces. Surface area and size distribution influence the growth mechanisms which occur in two distinct stages: 1) nuclei or seed formation and 2) pellet growth. In general, extremely fine powders of large surface area tend to form nuclei of small size often at the expense of final growth to the desired size. It may be found that such materials produce strong green balls so densely packed that subsequent processing, such as drying, may be impaired. In this case, the resistance to diffusion of the liquid vapour becomes so great that the green ball bursts. Excessively coarse materials, on the other hand, do not develop sufficient green ball strength to withstand the usual handling and may generate fines.

Size Distribution. A proper size distribution within the green ball is necessary for green strength as well as for final indurated strength. It was found that the ease of agglomeration is proportional to the total surface area or to the number of contact points. The need for particles of different sizes to fill the interstices among larger particles leads to the concept of binary grinding. In this case, a small portion of the particles is ground to very fine size and admixed with the coarser material for balling. The concept may offer considerable grinding power savings. Conversely, it is desirable in some cases to increase the porosity of the green ball. For example, iron ores of high alumina content which result in green balls of such density that drying rates are impaired, may be improved by the addition of coarser particle sizes. The net effect of size and distribution of particles on porosity and green ball strength depends on the ratio of the particle diameters and proportions of each size fraction in the system. Porosity will be markedly reduced in a two-constituent system wherein the ratio of the diameters exceeds 4:1 and approximately 25% of the small constituent is used. The practical significance of size distribution is often experimentally determined because achievement of the ideal distribution is either too costly or complicated for most commercial operations.

Ore Types

The balling process has been used extensively in recent years in a wide variety of mineral processing plants. These minerals differ widely in physical characteristics which are also a factor in determining ballability of the materials.

Particle Shape. The type of particles from which green balls may be made range from distinctly crystalline to amorphous. The particle shape influences the packing arrangement which can be achieved and the strength of the binding forces developed. Specular hematites, for example, exhibit tabular grains of generally large

crystal size which are more difficult to ball to suitable strengths than magnetite which has a cubical grain structure. Earthy hematites are mixtures of iron oxides and may contain crystalline hematite, magnetite, and products of weathering such as goethite which may be finely crystalline or amorphous. Such minerals are easy to grind and produce a size distribution and surface area favourable for balling. As discussed earlier, these minerals may produce green balls of excessive density. Unfavourable particle shapes may be improved by additional grinding, but power consumption may become excessive when the size is reduced beyond the natural grain size. Alternative methods include blending of easily ground minerals or binary grinding.

Reagent Influence. Balling is normally one unit operation in an overall processing complex wherein the minerals are previously treated, for example, by flotation. Such processes may result in contamination of the particle surfaces by hydrophobic films or residual reagents which influence the surface tension of the binding liquids. A cleaning step may be used to remove the surface contaminates; however, the costs are often prohibitive and regrinding is a frequently used means of correcting the problem. It is thought that regrinding produces fresh uncontaminated surface as well as producing additional surface area to compensate for the reduced strength of the binding medium. Completely dry particle surfaces likewise impair balling and a prewetting mixer is often required to add a part of the balling liquid before the material enters the balling device.

Growth Mechanism. Two distinct phases in ball growth occur: 1) nucleation or seed formation, and 2) growth or snow balling. The first phase can be described as a coalescence of the mineral particles by a liquid film into a small seed of 3 to 6 mm diameter. The second phase consists of addition of particles to the surface of the seed again by coalescence and by the mechanical packing force exerted by the balling device. The moisture content of the green ball is among the most important variables controlling the growth rate. Optimum moisture content at which the greatest strength can be achieved is related to the particle size and distribution, but is in the range of 9 to 10% for typical iron ore concentrates.

Balling drums and disks are the most commonly used machines for producing green balls. Although the principles of operation vary somewhat, the objective in each is to mix the mineral particles and binding liquid so as to allow the particles to coalesce into a nuclei or seed ball. Further rolling supplies the mechanical force to arrange the particles in the closest possible packing arrangement for the given size distribution and particle shape. Details of construction and operation are given below.

Feed preparation

Balling. The first requirement in making a good fired pellet is make a good green ball. It is essential to base the proper size consist of the feed material. A rough rule-of-thumb is that to be ballable the feed should have at least 65%, by weight, finer than 80 μm. A much better guide is to measure the amount of surface in the starting material. This is usually done with a Blaine indicator which measures the total area in cm^2 per gram. The operable balling range is from 1100 to about 2500 cm^2/g. At the coarser end of the range the material is somewhat granular and is difficult ball, and the balls formed have little strength. At the fine end of the range the balls become plastic and deform readily. Fine material with a Blame number of 2100 cm^2/g or more also becomes difficult to filter

After the feed has been ground to the proper fineness and filtered, is important that if water and additives are needed they be thoroughly mixed with the feed before introduction into the balling device. The moisture content is extremely important in making a good ball. The optimum moisture will vary with the material and the grind. With an iron ore concentrate having a Blaine surface of 1300 to 1400 cm^2/g, the optimum moisture may be 8.5%. With a very fine material (>2000 cm^2/g) the moisture may be 11.0 to 12.0%. Fortunately, the usual rotary vacuum filter, if operated properly, will give a moisture just under that required to make a good ball. The moisture of the filter cake should be held to 0.5% to 1.5% less than that required for balling. If the moisture content is too high to make good balls, there is little that can be done other than to discard the material or to soak up the excess moisture by increasing bentonite. This latter is a costly solution and also adds silica to the finished product. Additives such as bentonite are almost always added to the feed prior to balling, to improve the physical characteristics of the green ball and to prevent breakage during firing. The best practice is to thoroughly mix most of the additional water required and the additive prior to charging the material to the balling device. This is usually done with a conveyor belt mixer or by a separate mixer-muller.

The conveyor belt mixers consist of mixing wheels and sometimes a muller wheel positioned over the flat load-carrying portion of the belt, in an enclosure to contain flying material. A sketch of a typical Pekay belt-type mixer is shown in Fig. 9. Such a mixer takes no additional floor space and results in substantially better bentonite utilization. This type of mixer is used in over 90% of the world's plants. The adding of most of the water ahead of the mixer rather than in the balling device is an advantage, since large additions of water to the balling drum results in the production of some large, soft, and incompletely packed balls.

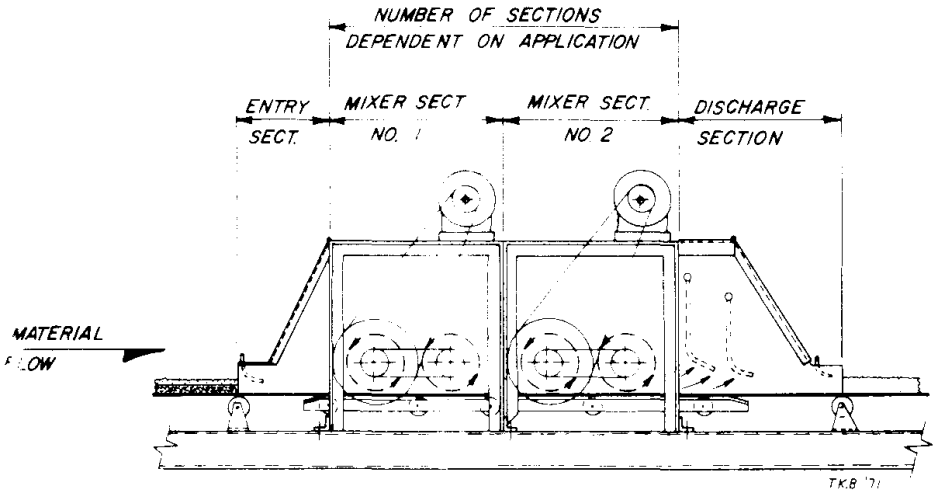

Fig. 9. Typical Pekay belt-type mixer [Pekay Machine & Engineering Co., Chicago. Ill., USA]

Some pelletizing plants secure a saving in bentonite and a uniformity of moisture by mechanically mixing the needed bentonite with the fiber cake and then storing the mixture in large table-discharge-type circular bins prior to feeding the balling device. In the usual practice of adding dry bentonite to the filtered concentrate directly ahead of the balling device, the total elapsed time from the adding of the bentonite to the feeding of the green balls into the furnace may be as little as 3 min. It is highly unlikely that the bentonite can take up its ultimate moisture content (approximately six times its weight) in this short time. At the Hilton mine at Shawville, Que, where large bins are provided for storing the blended magnetite filtered concentrate and bentonite for a period of hours, the amount of bentonite used is only 5 kg per ton, which is 40 to 60% of the amount used in the Lake Superior taconite industry.

Years of experience have shown that green balls, to be satisfactory, must have a certain minimum green strength and plasticity to withstand the mechanical transfer and handling from the balling device into the pelletizing furnace. They must also possess a minimum dry strength to prevent their failure during the initial drying stages.

Additives. At the high production rates demanded in present pelletizing practice, it is essential in most cases that additives be used to improve the quality of the green balls and to prevent serious dusting and exfoliation of the ball concentrate during the furnacing stage before it becomes heat hardened. The use of additives is not so essential with natural iron ores, since the size consist is different and where the drying rates must be kept necessarily low.

A summary of the test methods used in the laboratories to measure the required properties is:

1. *Wet drop strength*. Moist balls are dropped from a 45 cm height onto a steel plate until the first sign of failure occurs. The number of drops required to produce failure is recorded.
2. *Wet compressive strength*. Moist balls are compressed to failure at a constant loading rate of 450 N/min. The gross force required to produce failure is reported.
3. *Plastic deformation*. During the compression test, the deformation as a function of load is continuously measured and recorded. The deformation expressed as a percentage of the initial load diameter is reported, both at fracture and at the 4.5 N loading point.
4. *Dry compressive strength*. Wet balls are dried overnight at 120°C and then compressed to failure at a constant loading rate of 450 N/min. The gross force required to produce failure is reported.

The major problems in producing good balls for the pellet furnaces are to secure:

1. uniform size of feed,
2. uniform balling feed mixture,
3. uniform addition of additives,
4. good mixing of additives,
5. maintaining clean screening surfaces (screens or trommels to give fines-free balls).

The importance of all of these qualities cannot be overemphasized. The presence of even a small amount of fines (<6 mm) in the feed to the furnace will cause a high pressure drop across the pelletizing bed, uneven firing with resultant production of some poor pellets, and an increase in fuel consumption. Good screening at the balling device and even a rescreening with a roll-type feeder ahead of grate- type furnaces, with the rejection and recirculation of all < 6 mm material fed to the furnace, will usually pay big dividends.

Balling practice

Balling for production plants may be done in balling drums, balling pans or disks, or cones. Balling drums for large plants are usually 3 to 4 m in diameter and from 7 to 10 m long (Fig. 10b). They are rotated to give a peripheral speed of from 1.4 to 1.5 m/s. Some drums are provided with a variable speed control, but most drums, after experimental work is finished and the proper speed determined, are operated at a constant speed. The usual practice in pelletizing iron ores is to produce a finished ball that is in the size range of 10 mm to 16 mm. Most producers aim at producing an even more closely sized ball, namely 12 mm to 16 mm. Balling drums are so operated that the balls are formed slowly and the discharge from the drum will contain material ranging from a size 16 mm down to 3 mm size. It is therefore necessary to size the discharge either by a trommel integral with the drum or by a separate vibrating or roller screen. These openings, in common practice, are such as to give a separation at about 10 mm. The oversize is the feed to the pelletizing furnace and the undersize is returned to the head of the balling circuit where it is mixed with new feed and returned to the balling drum. The amount of undersize return is usually about twice the amount of finished balls. Balling drums are usually built with an expanded metal lining spot-welded to the shell. This is done so that a layer of compacted concentrate is built up on the shell, on which the balls form, are rolled, and compacted. On a smooth steel shell the material would simply slide and not roll. The metal mesh lining keeps the built-up lining from falling out. The thickness of this layer is kept relatively uniform by a reciprocating cutter bar or a rotating shaft. Each of these devices is equipped with narrow (approx. 6 mm) tungsten carbide cutting teeth. These cutting teeth are spaced about 10 cm apart on a reciprocating cutter bar or a corresponding distance apart on a rotating shaft to give the like effect. The desired surface is one of controlled roughness, where balls will roll. A smooth, slick surface, such as would be produced by a continuous blade, is definitely undesirable, since here again the balls would slide and not roll. Pertinent data relative to balling drums are given in Table 3.

Table 3. Data on balling drums.

Size: diam. x length (m)	*Rotation speed (rpm)*	*Output (t/h magnetite)*
2.7 x 9.3	12.0	60
3.0 x 9.6	11.2	80
3.6 x 9.9	9.3	120

Fig. 10a. Balling pan (Allis).

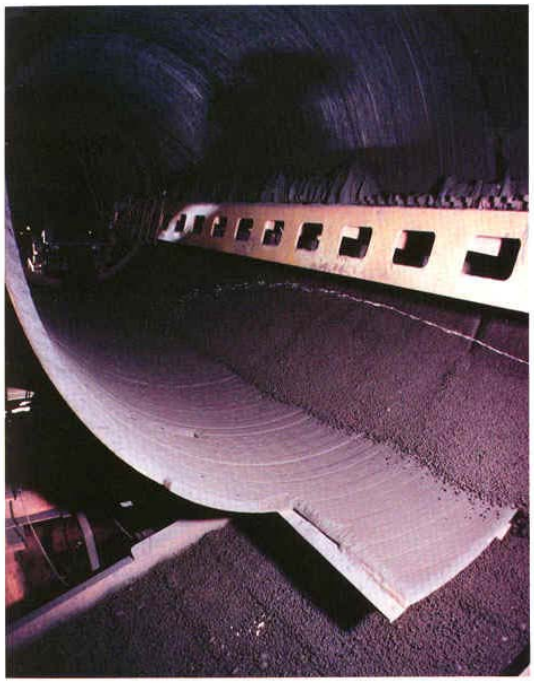

Fig. 10b. Balling drum with cutter bar.

Balling Pans or Disks. These devices may have a simple flat-bottomed shallow pan shape or may have two or more stepped zones (Fig. 10a, 11). They are usually of larger diameter than balling drums and are steeply inclined (45° to 55°). The material to ball is held in the drum until balls of a desired size are reached, when they overflow the lip of the drum. The discharge is usually not screened. The size of the balls formed is determined largely by the moisture additions and to a lesser degree by the slope and speed of the balling pan. Pertinent operating data on a common type of balling pan disk are given in Table 4. The balling pan requires more headroom but less floor space than a balling drum. Balling drums, because of their auxiliary positive sizing devices, usually are easier to control, and tend to give a more uniform and more closely sized product than balling pans or disks. Balling pans find their greatest use in balling natural sticky iron ores rather than the more difficult ballable, fine, iron ore concentrates. The balling surface of the pans or disks is kept free from buildup by means of a rotary cutting mechanism mounted on an oscillating arm (Fig. 10a).

Table 4. Data on balling pans.

Size: inner diam. (m)	*Rotation speed (rpm)*	*Output (t/h magnetite)*
4.5	9.0	60
6.3	7.5	80
7.59	6.2	120

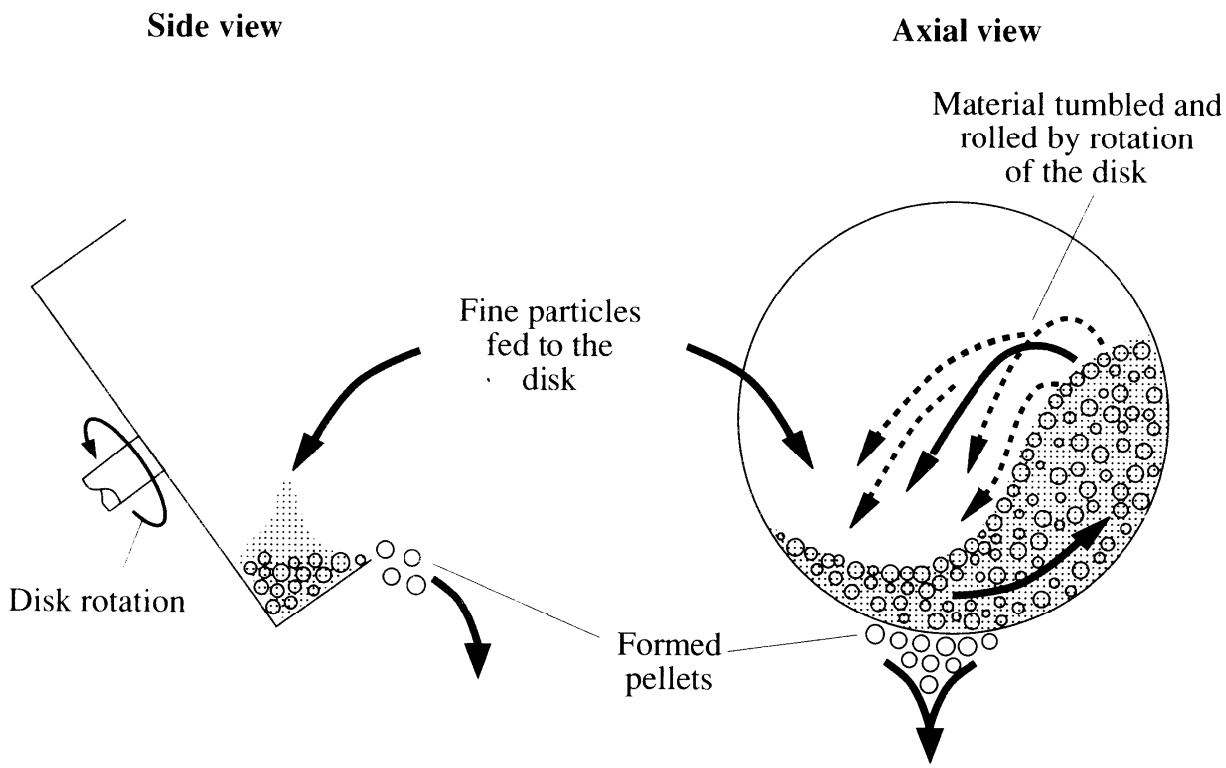

Fig. 11. Principle of balling pan [Woollacott and Eric].

5. THERMAL DRYING

5.1. Introduction

In drying the moisture level is reduced by transferring heat. The water is removed by direct evaporation or by the transfer into a heated gas into which the material is fed, such as incineration off-gas. Thermal drying is more expensive than mechanical dewatering (dewatering screen, centrifuge, filters), and therefore only applied to reduce the moisture content below the maximum dewatering rates that can be obtained by mechanical means. Heat can be transferred to the material by means of:

- Convection (transfer from surrounding hot gasses to the particles)
- Contact (with a heated surface or tube)
- Radiation (transfer by IR radiation from heat emitting surface)

Within solids heat transfer by contact is the only possible way. The higher kinetic energy from neighbouring molecules is exchanged in this process. The determining mechanism is heat transfer by convection wherever there is a flowing medium.

Coal drying plant [KHD Humbold-Wedag]

In a stationary and one dimensional case (temperature T is constant with time and depends only on the co-ordinates of the system), Fourier's law gives the heat flow $\dot{Q}$ crossing a perpendicular surface A:

$$\dot{Q} = -\lambda A \frac{dT}{dx}$$

λ is the heat transfer coefficient (W/mK) and x the coordinate in the direction of the temperature gradient.

In the 3D case, T depends on spatial co-ordinates (T=f(x,y,z)) and Fourier's law is defined by the partial differential equations $\frac{\partial T}{\partial x}, \frac{\partial T}{\partial y}, \frac{\partial T}{\partial Z}$.

If T depends on time (instationary case), Fourier's law for the one-dimensional case becomes:

$$\frac{\partial T}{\partial t} = a \frac{\partial^2 T}{dx^2} \quad \text{with} \quad a = \frac{\lambda}{\rho c}$$

where *a* is the temperature conductivity, ρ the density and c the specific heat capacity. The ranges of λ in W/mK for various materials at 20°C is given by:

Material	*Minimum*	*Maximum*
Metal	8	400
Rock	1	5
Plastics	0.2	0.8
Fluids	0.1	0.6
Gas, air	0.01	0.15
Dry construction materials	0.15	2.5
Heat insulating materials	0.025	0.15

The feed to be dryed is usually a porous and loose material. After mechanical dewatering the pores are partially filled with water and partially with air. The material can be modelled as an array of parallel plates with variable spacings filled with either air or water (Fig. 1). Successively λ of the boundary cases can be calculated and plotted as function of ε. Empirically determined values for λ of various porous materials can be placed inside the boundary case limits, also as function of the porosity ε (Fig. 2).

Figure 1 – Simplified models of porous material defining limiting values for λ as function of ε in air (left) and in water (right) [Schubert, Vol. II].

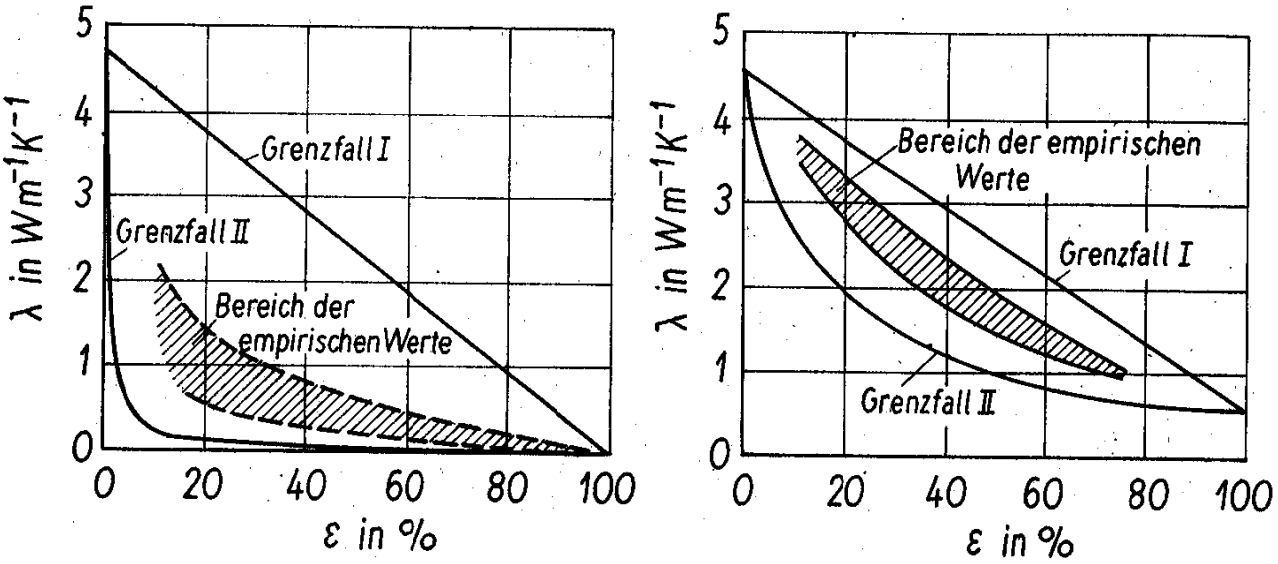

Figure 2 – Empirical values for λ of dry and wet porous material as function of ε, limited by the simplified models from Fig. 1 [Schubert, Vol. 2].

Other methods than convection, contact and radiation such as vacuum drying, diëlectrical, zeolites, freeze drying etc. are not relevant in mineral processing. The direct heat rotary dryer is the usual work horse in mineral processing and therefore a closer look to convection drying is especially relevant.

5.2. Heat and mass balance

The energy requirement of a dryer varies greatly depending on the material, mode of operation and dryer design. For convection dryers we look at the total heat requirement q_G per kg of water removed from the

material ($q_G = \frac{Q_G}{m_w}$, m_w is the mass of water removed (kg) and Q_G the required heat (J) for that). Absorbed water that may be bound on the particle surface is neglected. q_G is an addition of all heat required for drying and the compensation of heat losses in the process:

$$q_G = q_W + q_T + q_L + q_F + q_A$$

The various components are:

q_W	Heat required for heating and evaporation of the water from the material and overheating of steam until reaching the off-gas temperature
q_T	Heat for heating up the feed material
q_L	Heat loss due to radiation and contact from the dryer
q_F	Heat loss due to false air
q_A	Heat loss to off-gas

The major part is q_W. With h_v=2500 kJ/kg required for evaporation and a heat capacity c_p=1.84 kJ/kg for steam we get:

$$Q_w = 2500 + 1.84(T_A - T_F) \quad kJ/kg$$

with T_A the off-gas temperature of the dryer (usually between 80 and 120°C) and T_F the temperature of moist feed material (usually somewhere between 10°C and 20°C). This relationship is graphically shown in Fig. 4.

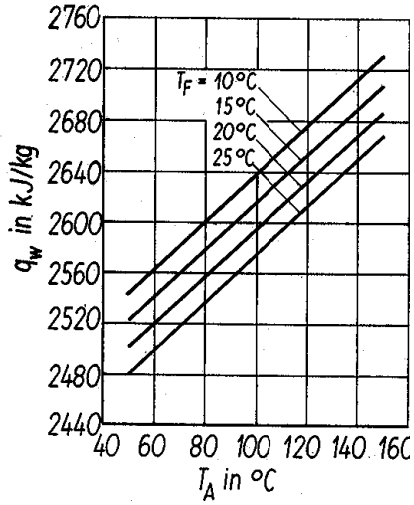

Figure 4 – Heat requirement for a convection dryer: q_w [Schubert Vol. 2]

For heating up the feed q_T is needed. It is given by:

$$q_T = \frac{1 - w_1}{w_1 - w_2} c_s (T_T - T_F) = \frac{1}{Y_1 - Y_2 \frac{1 + Y_1}{1 + Y_2}} c_s (T_T - T_F)$$

w_1, w_2	Start and final moisture content in kg water / kg feed
Y_1, Y_2	Start and final moisture content in kg water /kg dry product
c_s	Specific heat capacity of feed
T_T	Final temperature of product (usually between 65°C and 90°C)

For c_s=1.35 kJ/kg this relationship is given in Fig. 5.

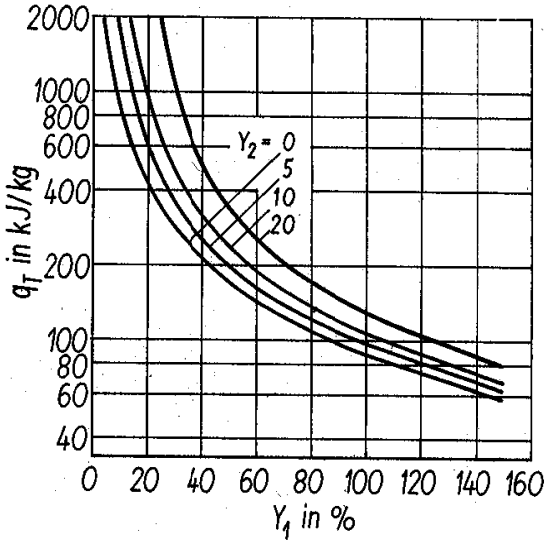

Figure 5 - Heat requirement for a convection dryer: q_T [Schubert Vol. 2]

Relative to q_w it can be seen that q_T becomes irrelevant for total drying of very wet feed. When the feed is 5 – 20% wet, q_T cannot be neglected anymore and can in some cases even reach the same order of magnitude as q_w.

The heat losses q_L are usually small and typically amount 1.5 to 4% of $q_W + q_T$.

The heat spend on heating "false air", q_F, is determined by:

$$q_F = \overline{c}_{pL} V_F (T_A - T_u) \quad \text{kg/kJ}$$

c_{pL}	Average specific heat capacity of ingoing air (kJ/kgK)
V_F	Ingoing air (false air) in m^3_N per kg of evaporated water (typically 0.3<VF<2.5)
T_U	Outside air temperature

For c_{pL} =1.3 kJ/kgK q_F is given by Fig. 6.

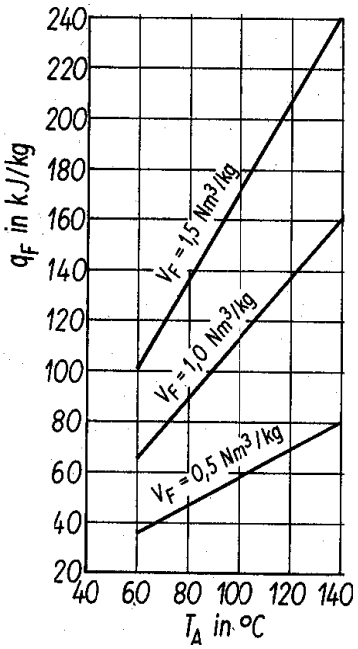

Figure 6 - Heat requirement for a convection dryer: q_F [Schubert Vol. 2]

Off gas temperature is considerably higher that the outside air temperature. q_A gives the required heat:

$$q_A = \frac{(q_W + q_T + q_L + q_F) c_p (T_A - T_U)}{h_1 - h_2}$$

c_p Specific heat capacity of the gases
h_1, h_2 Specific enthalpy of gases at the entrance / exit of the dryer

The relationship is shown in Fig. 7 as function of $q_W+q_T+q_L+q_F$ and input gas temperature T_1, assuming $T_A=90^oC$ and $T_U=10^oC$. It is obvious that a higher T_1 is very favourable.

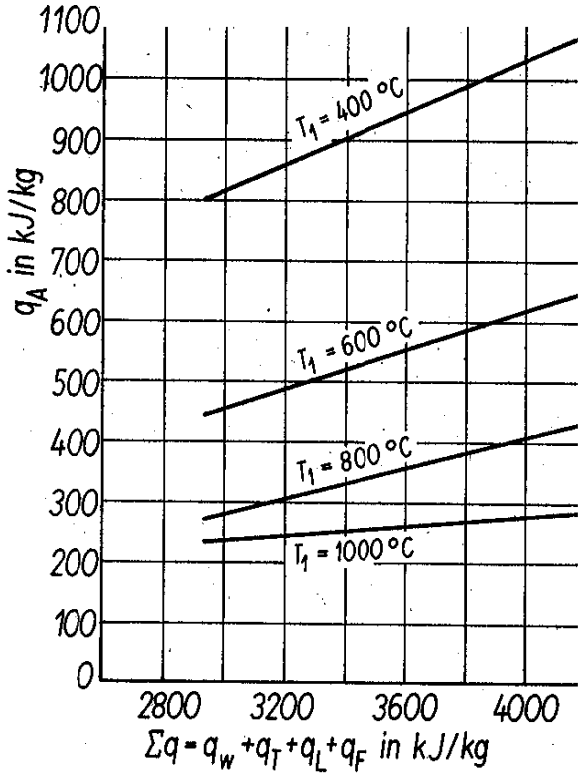

Figure 6 - Heat requirement for a convection dryer: q_A [Schubert Vol. 2]

The total calorific value from the required fuel is obtained by dividing the total heat requirement q_G by the efficiency of the burner. Per kg of water removed it is typically between 3300 and 6000 kJ/kg, and most usual between 3800 and 4200 kJ/kg. Avoidable losses are only the conductive and radiation losses (q_L), the false air losses (q_F), and, to a certain extend, heat loss to off gas (q_A).

5.3. Drying process and drying speed

Fig. 7 shows the drying process for hydrophylic (solid line) and hydrophobic (dashed line) feed materials. In zone AB the material surface is sufficiently wet to allow a constant drying speed. In zone BC the surface is already dry and the moisture has to diffuse through the pores outward. Only in case the feed is hydrophylic the third zone (CD) exists. In this zone absorped water is removed until a level that equilibrium is obtained. Drying speed then becomes zero. Drying curves like Fig. 7 are established by means of laboratory trials. By comparison with curves from known applications the design of a drying application can be optimised.

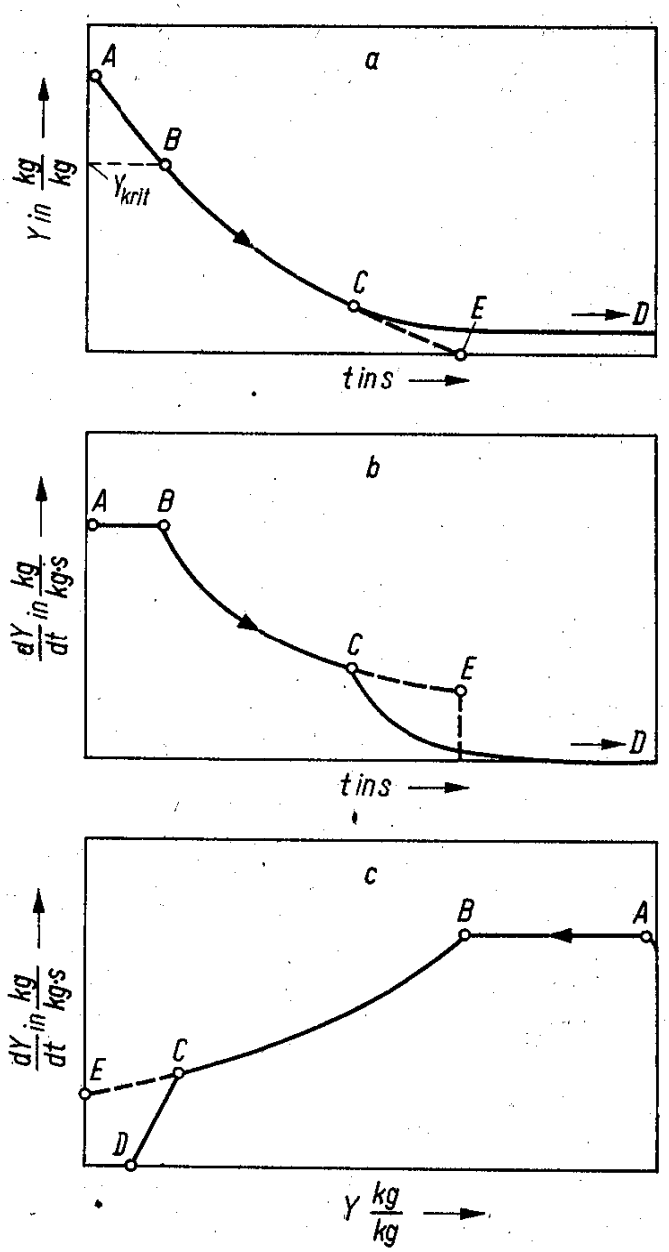

Figure 7 – Drying process, solid =hydrophylic, dashed = hydrophobic [Schubert Vol. 2]
a: moisture content as function of time
b: drying speed as function of time
c: drying speed as function of residual moisture content

5.4. Dryers

For only drying when no chemical of phase transition is required (calcining, lime burning, pelletizing etc) the feed is usually heated between 100 and 200 °C. The following dryers can be applied:

- Direct heat rotary dryers
- Indirect heat rotary dryers
- Steam tube dryers
- Indirect heat screw dryers (Holo-Flite)
- Fluid bed dryers

Besides specific drying equipment, in applications such as pulverised coal combustion combination of drying with grinding, classification and pneumatic transport is common. Besides the dryer itself a system comprises

feed and product handling, combustion system, offgas handling, dust collection system (wet or dry) and occasionally cooling systems.

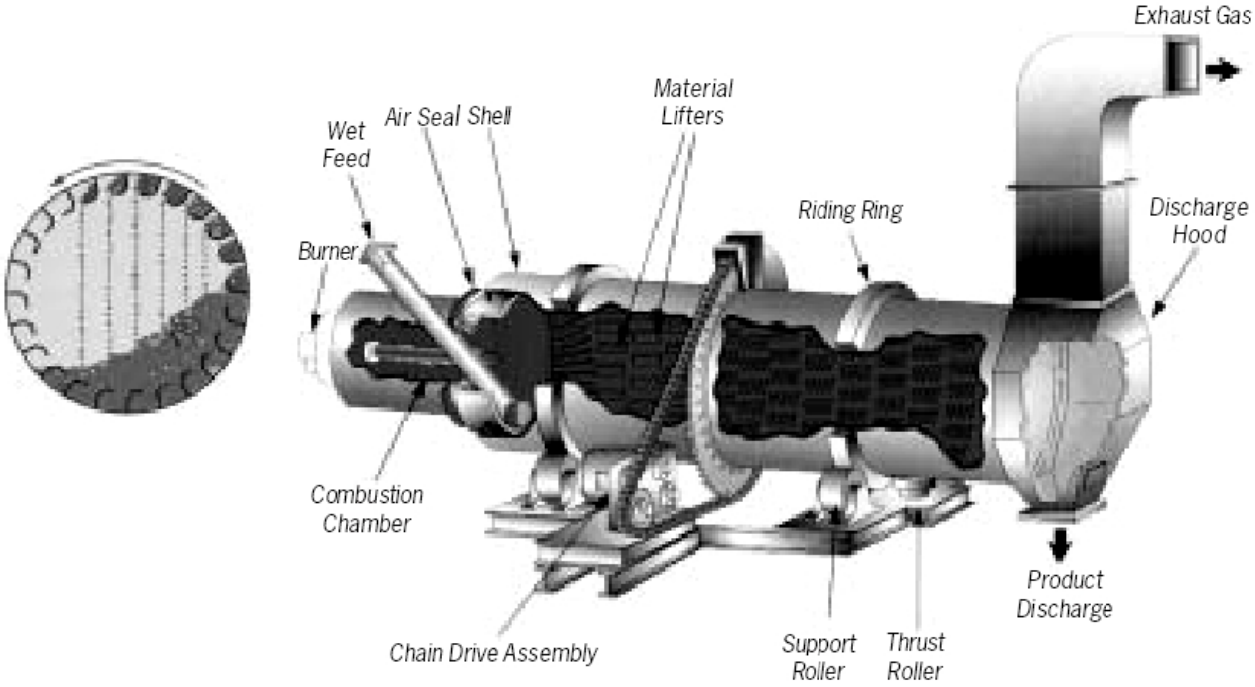

Figure 8 – Direct heat rotary dryer (cascade type) [METSO Handbook]

The **direct heat rotary dryer** is the work horse of the mineral industry (Fig. 8). This is mainly because of its reliability, robustness and high capacity. The design of the interior can be adapted to optimise the operation (Fig. 9). Diameters in use vary between 0.6 and 5 meters, length between 5 and 30 meters (diameter is 7 to 25% of the length). Circumferal speed is between 0.1 and 1 m/s. Co-current as well as counter current dryers are operated. Feed rates vary between 1 and 500 t/h. Industrial performance ranges between 50 and 120 kg of water removed per m^3 material and per h. Residual moisture contents typically range from 0.3% to as much as 6%. They are applied for minerals, clay, sand, aggregates, heavy chemicals and fertilisers. They are not suitable for very fine material, since it is carried away by the gas flow. Disadvantages are their large dimensions.

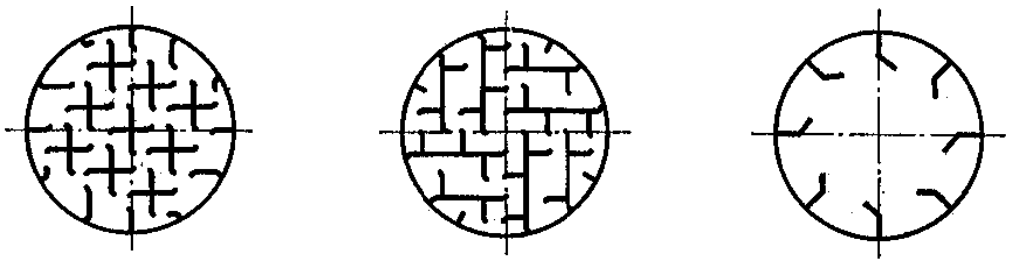

Figure 9 – Crosses, quadratic and lifters in rotary dryers.

When there should be no contact between combustion gases and the feed, **indirect heat rotary dryers** can be applied (Fig. 11). They rely on heat transfer by conduction and radiation only. The product gases or vapours can be collected seperately. This is for instance required in regeneration of active carbon or pyrolysis applications. Typical dimensions are similar as direct heat rotary dryers.

Figure 10 - Coal rotary dryer [KHD Humbold Wedag]

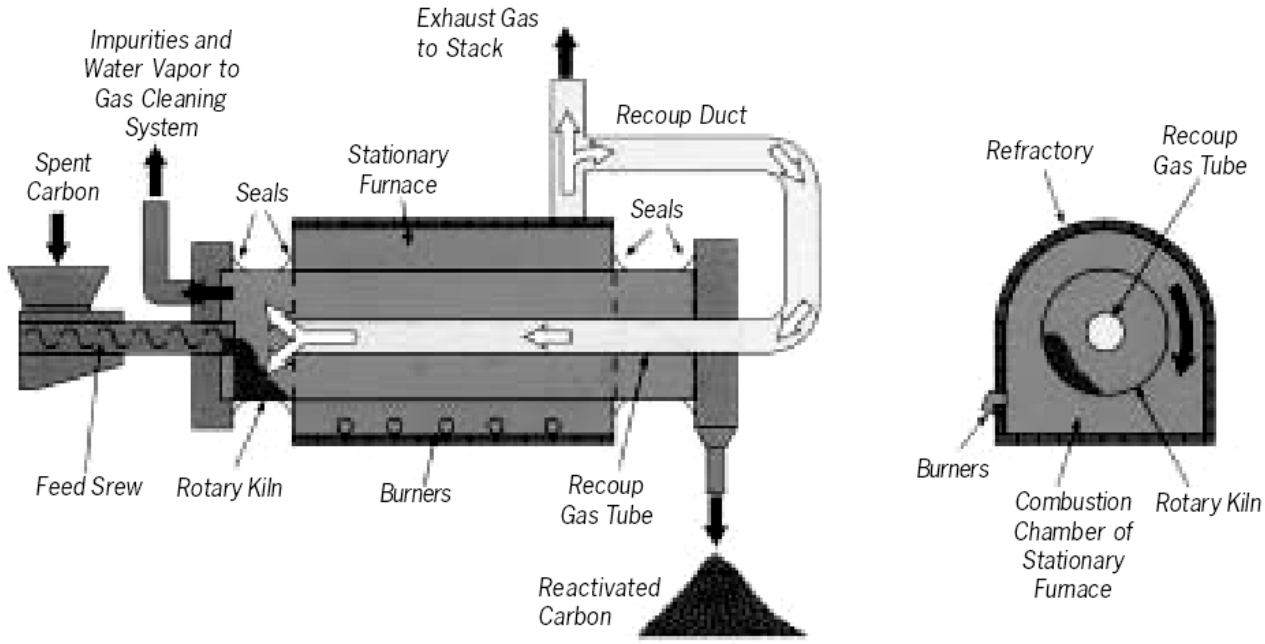

Figure 11 – indirect heat rotary dryer (kiln) [METSO]

The **steam tube dryer** is another indirect heat dryer that can utilise (waste) steam (Fig. 12). Pressures can range from 1.5 to 20 bar. Feed capacities are 3 to 50 t/h. heating surface can be as large as 2250 m^2. Applications are the drying of heat sensitive materials (see above).

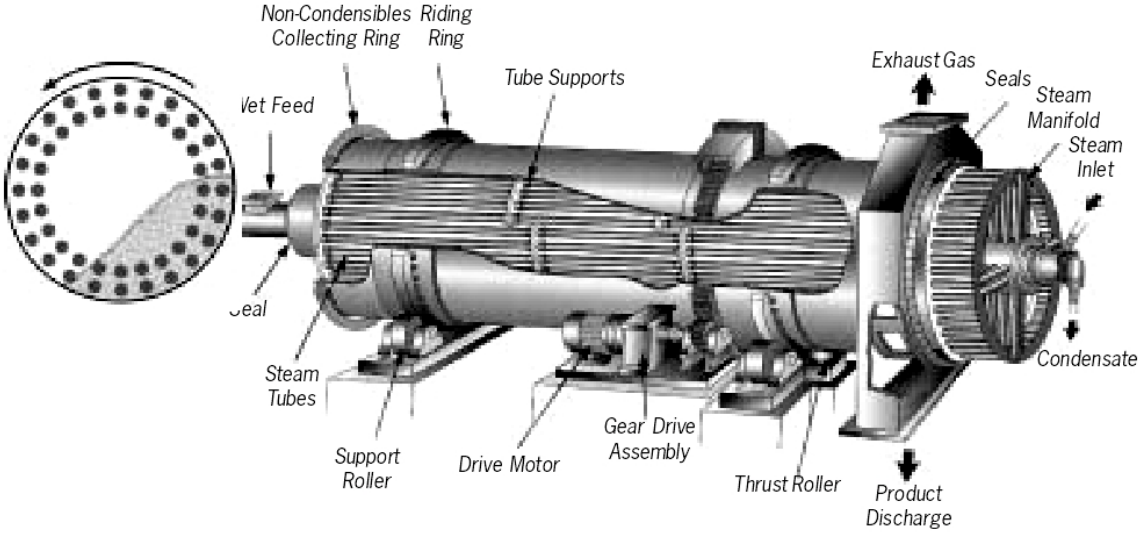

Figure 12 – Steam tube dryer [METSO]

Granular and powdery material (< 6 mm) can be dryed in a **fluid bed dryer** (Fig. 13). A 0.25*1.0 mm feed is optimal. Air flows evenly trough a particle bed, that becomes fluid at sufficient flow rate. Intense mixing and air/particle contact promotes a consistent product and rapid dry rates. Typically drying temperature is around 100°C. Capacity is up to 300 t/h. Fluid bed applications in calcining, combustion, roasting etc. can have operating temperatures up to 1200°C.

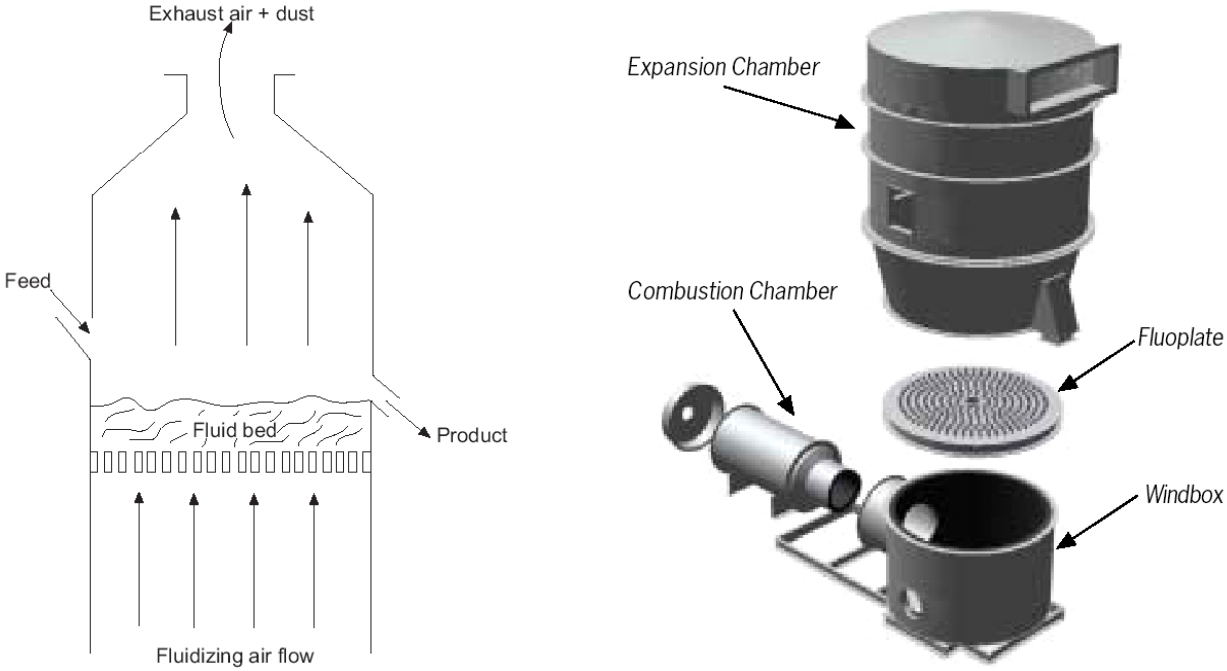

Figure 13 – Fluid bed dryer [METSO]

Other drying principles are **belt dryers, tunnel dryers, stream dryers** (combination of pneumatic transport and drying) and **drying combined with grinding and classification**.

5.5. References

- Metso Handbook, Metso Minerals, 2002.
- H. Schubert: Aufbereitung fester mineralischer Rohstoffe (Verlag für Grundstoffenindustrie, Leipzig, 1983. Volume 2, Chapter 2.
- Coulson, Richardson: Chemical Engineering, Vol. 2. Pergamon, 1991.

6. DUST CONTROL

Dry processing may lead to significant dust emission when no appropriate technical measures are taken. Problems may occur when the moisture content of a given feed material shows strong fluctuation. In these cases proper control, adequate maintenance and a fundamental understanding of the dedusting circuit is the key for effective dust control.

Fig. 6.1 - Dust generation at a conveyor transfer point.

In the first place dust control systems are needed for health, safety and environmental reasons:

- To reduce dust related health hazard and discomfort for plant personnel
- To prevent air pollution and dust settling at nearby sites
- To prevent premature failure and excessive maintenance of sensitive equipment
- To prevent explosion hazard

Dedusting systems make up a considerable part of the investment costs of a dry process. Proper integrated engineering in an early stage prevents problems and dust hazard afterwards. In this way “emergency” fixing of dust problems by improvised equipment, water spraying, and extensive manual cleaning and wearing of dust masks can be prevented.

The design of an in-plant dedusting system contains the following elements:

- Hoods and enclosures for effective dust removal at all relevant sources requiring minimum air flow and power consumption
- Ductwork for transporting dust-laden air with no internal settling and minimum pressure loss.
- Dust collection system that conforms air pollution ordinances.
- Fan and motor providing necessary air volume for the total system resistance. For cold climates motor power must be based on minimum operating temperatures.

6.1. Dust extraction

Deliberate dust extraction, in order to prevent dust problems further on, may be carried out by passing air upwards through a flow of material. Usually this airflow is adjusted to remove the majority of free < 1 mm material. Dust removal can be carried out in advance in a specifically designed chamber or chute with air-locks. Instead of this deliberate dust removal stage as a separate unit, dedusting by suction of air from enclosures or hoods that encapsulate crushers, screens, conveyors and separators is more common (Fig. 6.2). Within the enclosures under-pressure is maintained by a central fan installed downstream after the dust extraction system, often a sequence of cyclone and filter bag. For multiple systems such as crushers, screen,

etc., a separate dust collector for each system is usually preferred. For parallel processing lines it is preferable to use independent dust collectors for each line.

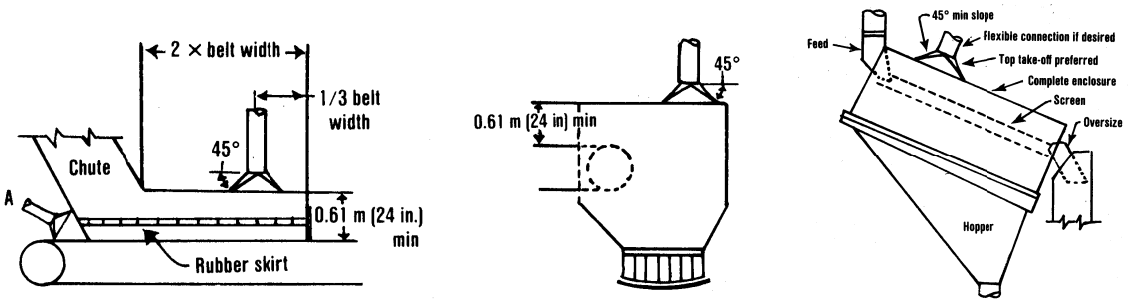

Fig. 6.2 - Enclosure design for conveyor belt transfer points (left and middle) and flat screen (right) [Leonard et al.].

Dust pickup hoods must be carefully designed to utilize the direction of the air currents produced by the flow of material and movements of machinery. Where buildings are tightly enclosed, proper "makeup" air must be provided to prevent "starving" of the dust control system and building of high negative pressure. An average air velocity over the entire opening of at least 90 m/min suffices to prevent the escape of dust. Air use must be minimised since too much air use gives excessive dedusting costs due to energy consumption and the large volumes of air that must be led through the dust removal system. To minimise air use, hoods of minimum opening and ductwork of minimum resistance should be designed. Hoods, cover plates and ductwork must be designed for easy removal for maintenance of the machines.

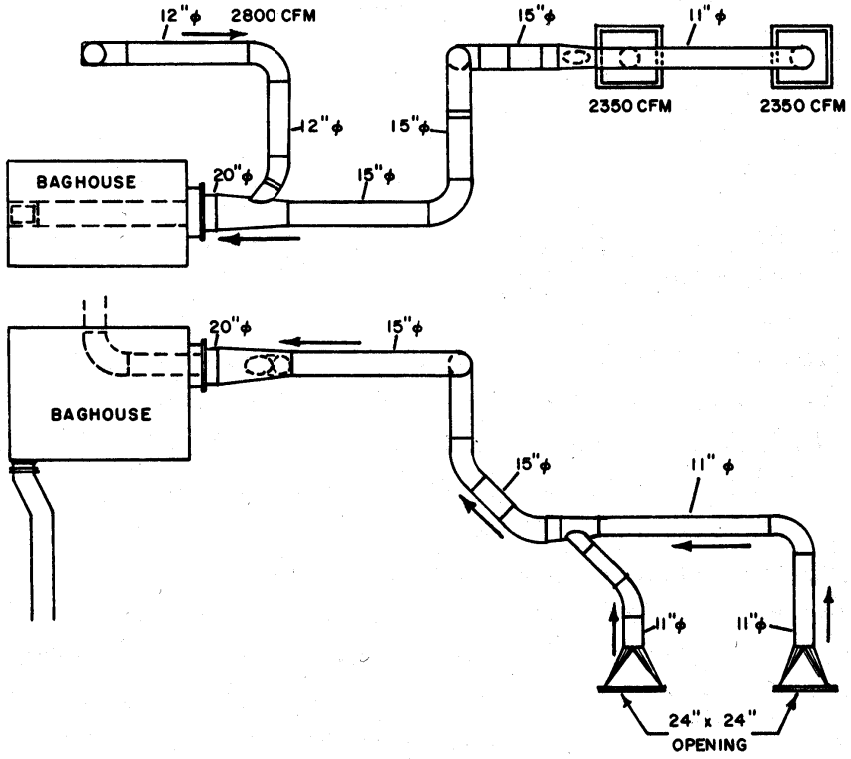

Fig. 6.3 - Example of ductwork arrangement [Leonard et al.].

In the ductwork itself a minimum velocity of approximately 1200 m/min should be maintained to prevent settling of the coarser dust. The air ducts should be kept as straight and short as possible (Fig. 6.3). A total length exceeding 25 meters is often considered impractical: use of several dedusting systems in parallel is considered more favourable for extended sites. Branches should enter the main duct at an angle of about 30^{o} and certainly not exceeding 45^{o}. It should preferably be constructed of steel and be sufficiently strong to carry the load when accidentally plugged. The use of highly corrosion resistant steels may be required. Bends and elbows should be of a radius not less than twice the duct diameter in order to prevent excessive wear and resistance.

6.2. Dust collection

Airborne dust is usually removed by consecutive stages that often contain expansion chamber, cyclone and filter bags.

Expansion chamber

Dedusting expansion chambers are in essence the same as those used for larger sized solids removal. The high-speed air carrying the dust is delivered into a large expansion chamber (also known as gravity separator), which reduces the air velocity considerably (Fig. 6.4). This allows the 1 mm to 0.2 mm particles to settle to the bottom of the chamber. The settled dust is usually removed from the chamber by periodically opening an air lock at the bottom. When Q is the supply capacity of the dust bearing air in m^3/s, w the width of the chamber, and l its length in m, settling occurs when:

$$v_s < \frac{Q}{wl} \qquad \text{Eq. 6.1}$$

v_s is the settling velocity of the particles in air, which are calculated using a force balance.

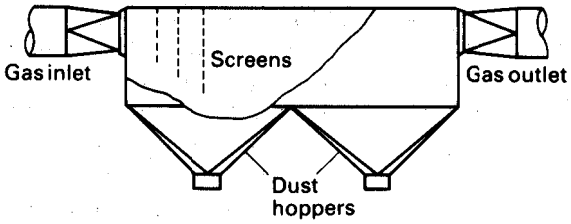

Fig. 6.4 - Expansion chamber [Leonard et al.].

Expansion chambers are used when the concentration of dust is high, because they are easy to clean and have a low pressure drop. Disadvantage is their bulky volume and low efficiency for finer dust (below 0.2 mm). Therefore they are usually applied as first dedusting stage and in older installations only.

Momentum separator

Momentum separators remove the dust by relying on the increased momentum of the dust relative to the air, so that the dust does not follow the same path if the direction of flow is suddenly changed (Fig. 6.5). The dust drops to the bottom where it is removed via hoppers. The velocity of the gas must be arranged so that it is sufficient for effective separation without the danger of re-entraining the particles from the bottom. Because of their low efficiency for fine particles they are rarely used anymore in modern plants.

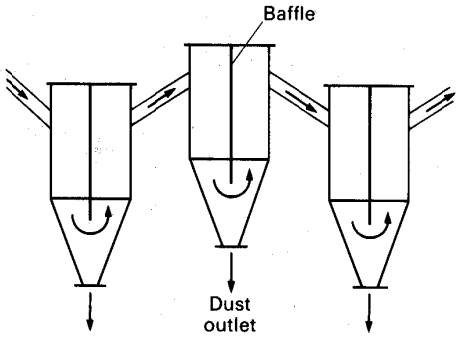

Fig. 6.5 - Momentum or inertia separator [Coulson & Richardson].

Air cyclone

A cyclone uses centrifugal force to precipitate the fine material on the cyclone walls that is suspended in the air. In a reverse flow cyclone all air exits the air outlet and it is optimised to retain as much of the solid material in the base hopper (apex) as possible. The dust-laden air enters the body of the cyclone tangentially

and spirals downwards in a vortex motion. The motion is caused by admitting the air to the static cyclone body tangentially. The air leaves the unit axially upwards in a spinning vortex. Particles that have moved to the wall continue to move downwards to the collection hopper where they are removed. The cyclone can be used effectively to remove the sizes from 200 μm (0.2 mm) down to 10 μm. Cyclone efficiency drops off rapidly below 10 μm but can be extended to smaller size collection if multiple diameter cyclones are used and higher air velocities are employed.

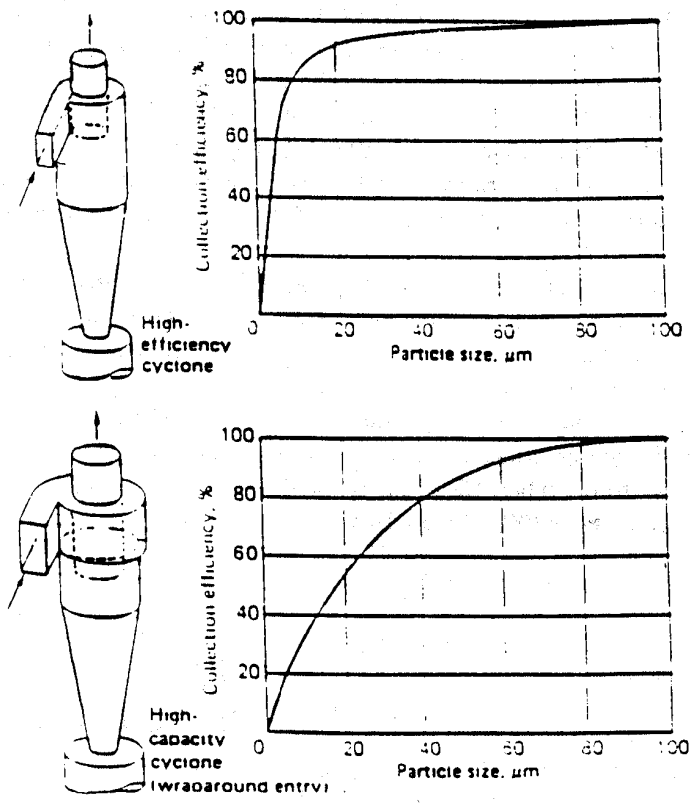

Fig. 6.6 - High efficiency and high capacity cyclone design with their respective size efficiency curve [Scarlett].

The cyclone diameter is usually about half that of the gas outlet. Cyclone capacity is controlled by cyclone diameter, inlet size and inlet air velocity that is usually in the range of 15 to 25 m/s). For a given pressure a large capacity corresponds to a large diameter cyclone. Two extremes in cyclone design can be distinguished (Fig. 6.6):

1. "High efficiency" types in which the gas outlet tube and hence vortex have a small diameter and which have a relatively large length to diameter ratio.
2. "High gas throughput" types in which the outlet is relatively large and the ratio of height to cyclone diameter is small. These units often have a scroll inlet.

Cyclones of intermediate design are now most widely applied. Typically the diameter is in the range 0.2 – 2 m.

Secondary circulation, which is detrimental to efficient operation, may be induced at the roof of the cyclone. With bad design the inner vortex may protrude into the discharge hopper causing further secondary circulation with possible re-entrainment. Re-entrainment may also result from excessive turbulence, particle bounce from the internal surfaces and at the base of the cyclone where the dust enters the discharge hopper.

The inside surface should be as smooth as possible to minimise turbulence and hence reduce back mixing. The vortex finder stabilises the inner vortex and prevents particle bypassing between the inlet and gas outlet. It should extend a little below the inlet. The outlet pipe should be straight for a few diameters otherwise

vortex instability may again result. It is important that the outlet into the hopper at the base of the unit be greater than the diameter of the inner vortex which is about half that of the outlet. Otherwise excessive wear at the bottom neck, dust carry over and vortex instability will result. The hopper depth should be at least one cyclone diameter for the same reasons.

Usually the cyclone is operated at a pressure lower than atmospheric. Therefore a good seal at the exit of the hopper is essential to prevent dust carryover. A common hopper serving a number of cyclone units may be employed. In this case, division plates may be located in the hopper to prevent air circulation between cyclones with consequent dust carryover. A large length to diameter ratio (usually 2.5 to 4.0) ensures an adequate residence time for particles to be centrifuged outwards and again minimises dust pickup from the base. In the interest of airflow stability a small cone angle, of the order of 15 degrees, is advisable. With easily flowing dusts, cyclones can be used with extremely high loads. The collection efficiency tends to increase with loading and the pressure drop is reduced.

Bag filter [Cited from Coulson & Richardson]

"Bag filters are designed to remove the finest dust that is normally below 10 μm and not removed by the cyclone (Fig. 6.7). The application of bag filters is especially relevant for the prevention of health risks, since the finest dusts (10 μm – 1 μm) are the most hazardous. The outlet air discharged from the cyclone is passed to a bag filter. It consists of cylindrical tubes of woven fabric and the air stream is passed at low velocity through the fine fabric. The fine dust is trapped by the fine weave fabric and forms its own filter medium on the high-pressure side of the fabric. Large filter areas are required so the bag filter is usually a large installation and the fine dust is periodically shaken from the fabric either mechanically, by reverse jet blow rings or by reversal of the fan.

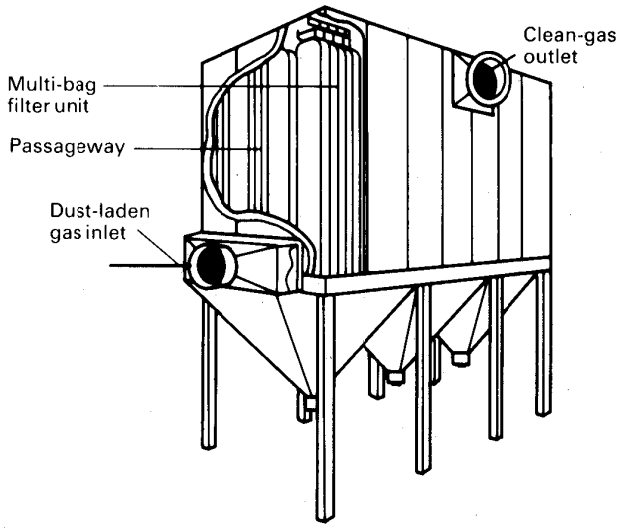

Fig. 6.7 - Bag house filter unit [Coulson & Richardson].

In fabric filters the particles are trapped by impingement on the fine hairs, which span the apertures. Typically the main strands of the material have a diameter of 500 μm with 100- 200 μm spacing. The individual textile fibres with a diameter of 5 – 10 μm crisscross the aperture and form effective impingement targets capable of removing particles down to 1 μm. Only after a loose "floc" has been built the efficiency starts to build up, since in fact these flocs form the effective filter for the ultra-fine dust particles. The air velocity passing the filter must be low, typically 0.005 – 0.003 m/s, in order to avoid compaction of flocs and high pressure drops."

Wet scrubbers

Instead of bag filters wet scrubbers can be applied for fine dust removal (Fig. 6.8). Wet scrubbers create conditions enabling the fine dust to adhere to finely dispersed larger droplets of water. Removal from the air is then easier accomplished by impingement, inertial or centrifugal separation. When the dust-laden air encounters a droplet of water, the air will flow around it, while the dust particles, because of their greater inertia, will impinge on the droplet. Wet scrubbers have a similar efficiency in fine particle removal as filter

cloth. Disadvantage is the capture of dust as wet slurry. This disadvantage is less restrictive when wet processing is practiced on the same site: the fine dust fractions usually comprise a relatively small fraction of the total production an can be added to existing wet treatment routes. When there are space limitations their more compact design relative to bag filters may be advantageous.

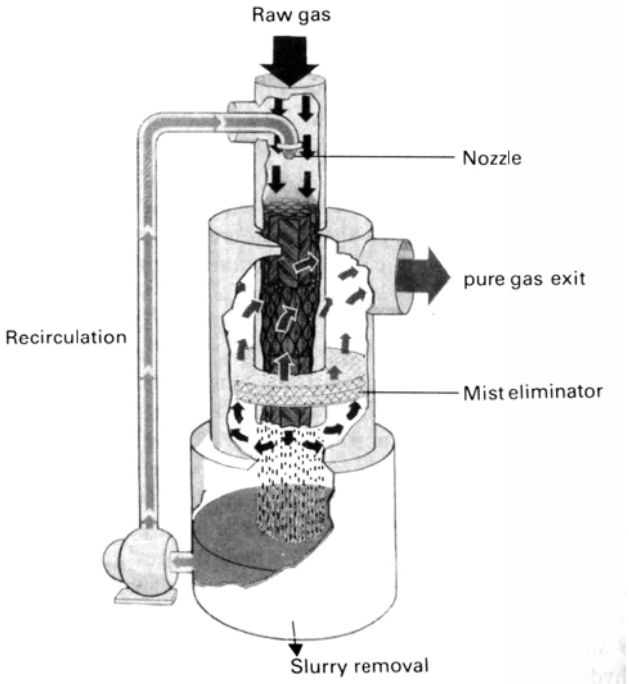

Fig. 6.8 - Wet scrubber for fine particle removal with water recirculation [Coulson & Richardson].

Despite the availability of advanced scrubber designs, in an entirely dry operation the use of bag filters is usually more favourable because of the dry dust product and the absence of the possibility to feed the fine sludge to a larger water circuit. Where freezing can occur, dry collection is preferred above scrubbers.

6.3. Dedusting circuit

Fig. 6.9 shows a typical dust collection circuit in three stages for coarse, fine and superfine dust removal. The dust-laden air that is collected from several spots in the process via ductwork is fed on the left side of expansion chamber C. Fan A causes underpressure throughout the circuit and effects a strong airflow. The coarse dust is extracted in expansion chamber C through a weighted seal gate or air lock. Fine dust is successively precipitated in cyclone D and also removed through a seal gate at the cyclone underflow nozzle. Bag filter E removes superfine dust, again via an air lock. The clean air is discharged through fan A to atmosphere.

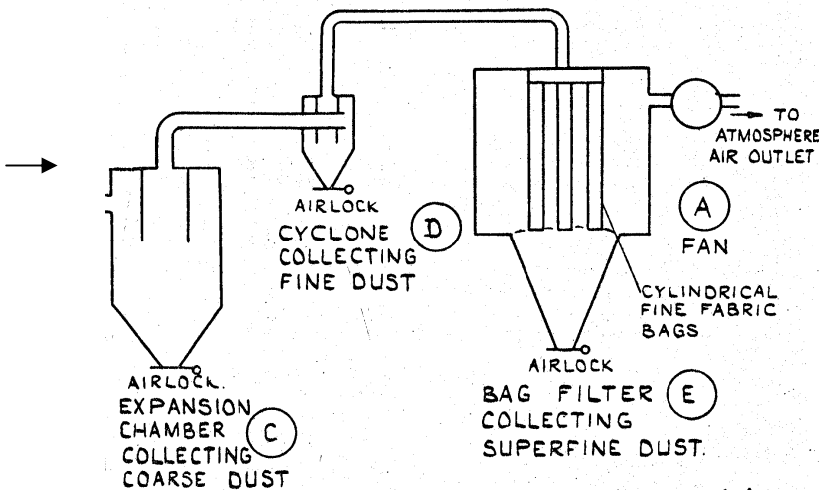

Fig. 6.9 - Typical dedusting circuit [SACPC, 1977].

It is important to mention that moisture may reduce the efficiency of a dedusting circuit. The fine particles agglomerate and may form layers of cake on surfaces and inside air-tubes. However, if the material is sufficiently moist so that during processing dust generation remains below acceptable limits it may not be necessary to employ a dedusting circuit at all. In practice poor control of the moisture content of the processed material, resulting in strong moisture fluctuations may cause problems. In this situation the dedusting circuit may become inefficient after dedusting moist material, after which it is unable to effectively dedust dry material in a later stage due to excessive pressure losses due to blinding, cake formation and clogging at the air locks within the dedusting system. In such cases better moisture control of the feed will be more effective than considerable modification of the dedusting system. This and modern dedusting circuits consisting of cyclones combined with filter bags or wet scrubbers usually suffices to meet applicable clean-air standards.

6.4. Conclusions

Proper dedusting is indispensable for dry classification and separation processes. Well-designed systems keep dust hazard to an acceptable minimum. Maintaining these conditions is more a matter of proper engineering and management than a technical problem. Difficulties may arise when older and/or modified installations are operated, where there is insufficient space or dedusting capacity and especially when moisture levels are fluctuating. When dust generation is unacceptably high the "worst" generating spots should be located and dedusting hoods installed, when needed personnel should be adequately protected with dust masks, and dust emission kept to a minimum by regular cleaning and local spraying with finely dispersed water.

References

Coulson, J.M., Richardson, J.F.: Chemical Engineering, Vol. 2. 4th edition. Pergamon press, Oxford,1991.

Leonard, J.W. (ed.) et al.: Coal preparation. 4th ed. Chapter 14. The American Inst. of Mining, Metall. and Petr. Engrs, Inc., New York, 1979.

SACPC Coal preparation course, Vol. I, Section 7. South African Coal Processing Society, March 1977

Scarlett, B., van Drunen, M.A., Mollinger, A.M. Deeltjestechnologie. July 1991, Delft University of Technology, Delft.Johannesburg.

Wills, B. A. Mineral processing technology. Pergamon Press, 4th edition, 1988

7. DEWATERING

[This is an electronic reproduction of part B of Chapter 4 from Woollacott and Eric, 1994 / 2001]

7.1. Introduction

Solid—liquid separations perform two functions in minerals engineering. In the first place, they are employed to control the liquid content of a solid—liquid system. This is done by the removal of liquid from a system, the removed liquid being essentially free of solids. The process is referred to as dewatering and is applied for any of the following reasons:

- to control the solids concentration of a slurry
- to dewater a slurry so as to produce a moist solid
- to reduce the moisture level of a damp solid.

Such requirements often arise in wet mineral-beneficiation circuits, as well as in hydrometallurgical processing.

A second area where solid—liquid separations are required is that in which the solid phase needs to he processed differently from the liquid phase. The most important application of this is in hydrometallurgical circuits, where solid—liquid separations are frequently utilized as a means of separating valuable from non-valuable components. The metallurgist achieves this by arranging matters so that the values are present predominantly in one phase and not in the other. Separation of the two phases will then achieve the desired result. Unfortunately, it is not possible in practice to achieve a complete separation of the phases. To produce a liquid that is free of solids is relatively straight-forward, but the reverse—the production of solids free of liquid—is not. This problem will be discussed in more detail shortly.

The dewatering of solid—liquid phases and their separation are achieved by the same procedures. These vary depending on whether the solids are coarse or fine. In addition, different techniques are employed for solid—liquid systems of high, intermediate, and low liquid content.

7.2. Types of Solid—Liquid Separation

Coarse Solids

Liquid can be separated easily from a coarse solid by a process of drainage. The solid—liquid mixture is passed over a perforated surface that allows only the liquid to pass through and leaves a dewatered solid behind on the surface. However, some of the liquid will remain in the interstices of the solid phase and as surface moisture on the particles. This type of separation is achieved using screens or centrifuges.

Fine Solids

When the solid phase consists of fine particles, the removal of liquid from the solids becomes more difficult and more expensive. In this case, the relative proportion of liquid present strongly influences the type of separation process that must be applied. Three different types are available.

1. *Thickening*. This is used when the liquid-to-solids ratio is high, i.e. when the system to be dewatered is a dilute slurry. The object of thickening is to remove liquid from the slurry so that the latter has a higher solids concentration. The mechanism employed is one of sedimentation, where the solids are allowed to settle through the liquid phase. This results in the formation of two regions: a liquid that is essentially solid-free, and a slurry with a higher concentration of solids (i.e. a thickened slurry).

2. *Filtration*. This technique is used to dewater a slurry in which the liquid- to-solids ratio is about as low as can be achieved by thickening operations. The object of filtration is to produce a solid phase with as low a moisture content as can be achieved by purely mechanical means. The principle in filtration is the same as that in dewatering with a screen or centrifuge, except that the apertures of the

surface are much smaller. The slurry is held on a porous surface (the filter cloth) and the liquid is drawn through the surface, leaving the solids behind as a damp solid known as a filter cake.

3. *Drying*. This technique is used when the solid—liquid system is essentially a damp solid and it is necessary to reduce its moisture content. The mechanism involved is that of thermally enhanced evaporation, and the process is termed drying.

Very often the dewatering of a dilute slurry of fine solids is achieved incrementally by the use of the above techniques in the sequence given. The cost of the dewatering process increases in the same sequence. Thickening is often used independently merely to increase the solids concentration of a slurry, no further dewatering being necessary. Filtration is virtually never conducted on dilute slurries, and the feed to a filtration operation has usually been thickened first.

7.3. Constraints in Solid—Liquid Separation

Complete separation difficult. While it is possible to dewater a solid material to a bone-dry condition by prolonged thermal drying, it is not usually economical or practically necessary to do so. Complete separation is certainly not possible by non-thermal means alone because the surface tension forces are sufficiently great to ensure that no amount of shaking or filtering will remove all the liquid from a solid.

Effect of particle size. The finer the size of the particles being dewatered, the greater is the surface area of the solid phase and the larger is the quantity of water that is bound by surface tension. The consequence of this is that there is a positive correlation between the average particle size of a solid phase and the minimum water content that can be attained in a mechanical (non-thermal) dewatering process. The smaller the particle size, the higher will this minimum be.

Residual liquid. In many hydrometallurgical situations, the fact that the solid cannot be completely separated from the liquid phase causes problems in that the liquid contains values or contaminants. In such cases, the entrainment of some liquid with the solid phase constitutes either a loss of values (if the liquid is value-bearing) or a contamination of the solids (if the liquid carries some undesirable species). To overcome this problem, the liquid that remains entrained with the solids after a dewatering operation must be replaced by a second liquid that is free of either values or contaminant. In filtration, this is done simply by washing of the filter cake with a second liquid. In thickening operations, it can be done by a process known as countercurrent decantation. The washing of filter cake is discussed later in this chapter.

Dewatering agents. A reduction in the magnitude of the surface tension in a solid—liquid system can enhance the performance of a solid—liquid separation process. Such a reduction can be achieved by the addition of appropriate reagents to the system. This approach is sometimes used to achieve lower moisture levels in screening, centrifuging, and filtering operations.

7.4. Separation of Liquids from Coarse Solids

It the average particle size of the solids in a solid—water system is relatively large (above about 0.5 mm), water can be removed mechanically from that system by the use of screens. The operation is obvious: most of the liquid phase simply drains through the screen, leaving behind a damp solid phase.

Centrifuges can also be used for the dewatering of coarse solids. The separating mechanism is the same as on a screen, except that the drainage through the screen surface is enhanced centrifugally. A solid product of lower moisture content can therefore be obtained.

A typical centrifuge designed for coarse material is shown in Figure 1. The solid—liquid mixture (usually solids with a high moisture level) is fed onto the inside of a rotating conical basket that is perforated. The rotation of the basket forces water through the perforations. The solids remain on the basket and migrate down its inner slope as indicated. Vigorous vibration of the basket facilitates this movement of solids.

The screens generally used for the dewatering of solids larger than about 10 mm are of the same type as those used for the sizing of solids. A special dewatering screen has been designed for solids in the size range

0.5 to about 10 mm. Because of the large interstitial volume and surface area of material in this size range, the moisture level of the dewatered product can be rather high. In an effort to reduce this level, the dewatering screen operates at a high frequency to increase the drainage forces. In addition, the screen is so designed that a deep bed of solids forms on it. The thickness of the bed creates a pressure within the bed that reduces the interstitial volume and so assists in the removal of liquid.

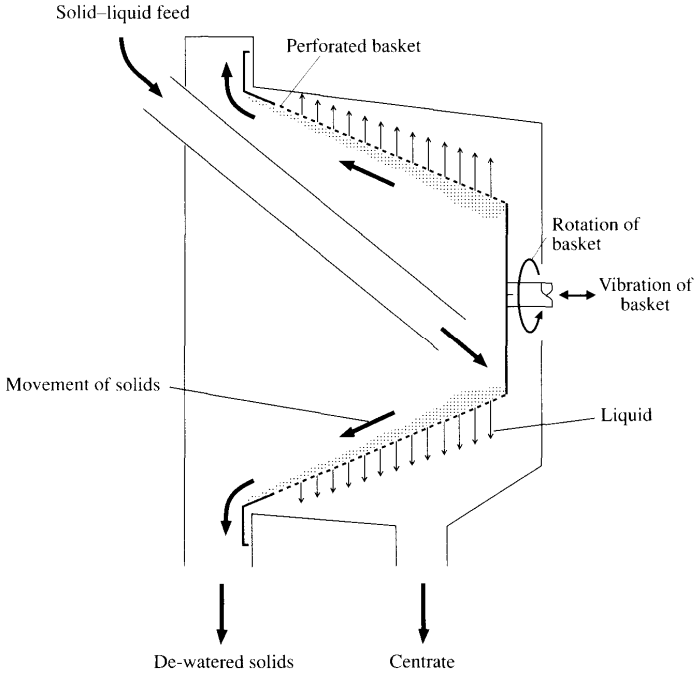

Figure 1. Vibrating-basket centrifuge

7.5. Thickening

The object of thickening is to remove liquid from a slurry in order to increase the concentration of the solids. This is achieved under quiescent conditions by the process of sedimentation. The principle is very simple, and can be illustrated by reference to the standard settling test depicted in (a) of Figure 2. A sample of the slurry to be thickened is placed in a measuring cylinder on which there is a vertical graduated scale. The slurry is mixed thoroughly and is then allowed to stand. Under the force of gravity, the solid particles start to settle through the liquid. A clear 'mud line' usually marks the interface between clear liquid (the supernatant liquid) and the region of settling solids. As settling progresses, this mud-line moves downwards. The progress of sedimentation can be studied from plots showing the height of the mud-line as a function of time. Such a plot, termed a settling curve, is given in (b) of Figure 2.

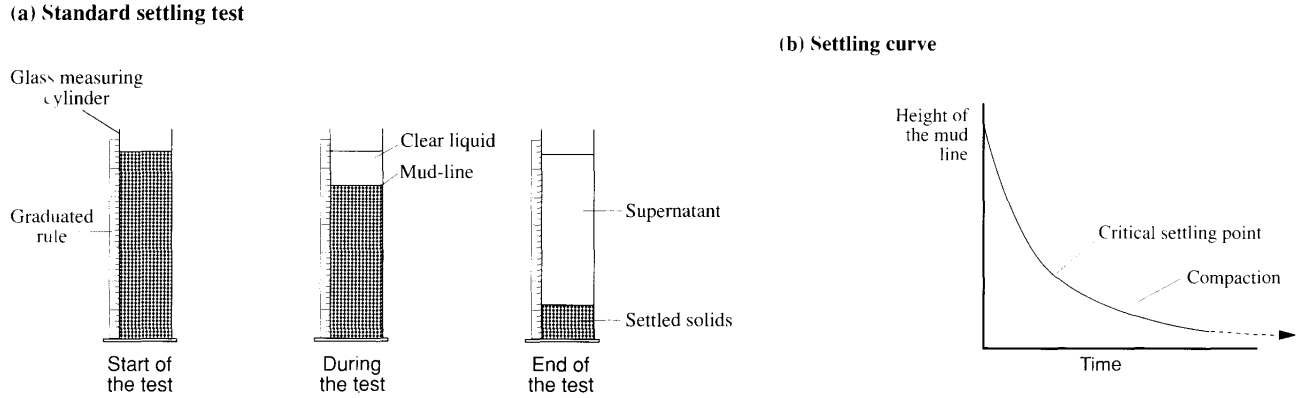

Figure 2. Sedimentation test.

It can be seen from this settling curve that the settling rate, as implied by the rate of descent of the mud-line, is relatively rapid initially and then begins to slow down. This is because, in the region where the solids are settling, the interaction between the particles increases as the concentration of solids increases. This interaction hinders settlement, and the settling rate decreases as a result.

At the bottom of the vessel, the interaction between particles becomes more intense as settling continues. Bridging between particles starts with those particles which reach the bottom of the vessel first. A bed of loose sludge is formed that begins to become more compacted as more solids settle into it. Settling, although considerably retarded, does not stop at this point: liquid is squeezed out of the bed as compaction progresses. This process of compaction can be aided if some sort of stirring arm is slowly rotated in the sludge bed. What this does is to create vertical channels in the bed through which the liquid squeezed out by compaction can rise.

It is relatively straight-forward to exploit the sedimentation process as described here for the thickening of a slurry on a continuous basis. Once two well-defined regions of supernatant liquid and settling solids have been established, it is a simple matter to separate the one from the other and so produce a clear liquid and a thickened slurry. The ways in which this can be done in practice are described shortly. First, however, it is necessary to consider the ways in which the settling rate of solids, particularly of very fine solids, can be increased.

Flocculation and Coagulation

The factors that influence the rate at which a particle will settle through a fluid were dealt with in the chapter on classification. Of greatest importance to the present discussion is the influence of size: the finer the particle, the slower the settling rate. Very small particles tend to remain in suspension and not to settle at all. In that case, no clear mud-line is formed, the supernatant liquid is hazy, and thickening operations are generally rather difficult.

It is not uncommon in practice to find a situation in which the settling rates of particles are too slow and the capacity of a given thickening device is insufficient. Under these circumstances, some fine solids remain suspended in the supernatant liquid and a solid-free liquid is not obtained. In such situations, it is necessary either to reduce the load on the thickener or to increase the settling rates of the solids.

To achieve the latter, the particles in the slurry must be agglomerated in some way so that their effective size is increased. This is achieved either by coagulation or by flocculation. Coagulation occurs when two or more fine particles collide and remain in contact, being bound together by weak electrostatic attraction. Flocculation involves the attachment of particles to long-chain polymers to form large aggregates of particles called ‘flocs’.

Both coagulation and flocculation are controlled by surface chemical effects. In essence, these are the same kind of effects that are important in froth flotation. As indicated in that discussion, the chemistry of the solution can be altered in ways that strongly affect the surface properties of the solids.

One way of promoting coagulation is by the addition of ionic reagents (coagulants), such as slaked lime, $Ca(OH)_2$, or alum, e.g. $NaAl(SO_4)_2.12H_2O$, that have cations of high valency (e.g. Ca^{2+}, Al^{3+}). These affect the electric double-layer around particles so as to reduce the repulsive forces that keep them apart and thus hinder coagulation.

Flocculants are widely used in thickening operations to solve thickening problems. They are water-soluble, long-chain compounds that have a multitude of chemically active sites along the polymer chains. If the right polymer is used, particles are attracted to the active sites and become attached to the polymer chain. Because of the length of these chains, many particles are bound together in any one floc and will settle together at a rate determined by the size of that floc. Even the very fine particles that would normally remain in suspension can be flocculated. Not only does this increase the overall settling rate of a particulate material, but it also improves the clarity of the supernatant liquid.

As with coagulants, the solution chemistry in a liquid has a strong influence on the efficiency of a particular flocculant. Consequently, a large variety of flocculants is available. These vary according to both their chemistry and their molecular weight, larger molecular weights giving rise to longer polymer chains. Both natural and synthetic compounds are used. The most important are polyacrylamides and guar gum, but tannins (Quebracho), lignosulphonates, and carboxymethylcellulose are also used. Polyacrylamides are

particularly useful because conditions in their manufacture can be manipulated so that polymers of various molecular weights can be made.

To achieve optimum results in flocculation, the optimum dosage must be used, the flocculant must be well mixed in the slurry, and the conditions must be quiescent. The flocs are rather fragile and tend to break down if conditions become excessively turbulent.

Thickening Equipment

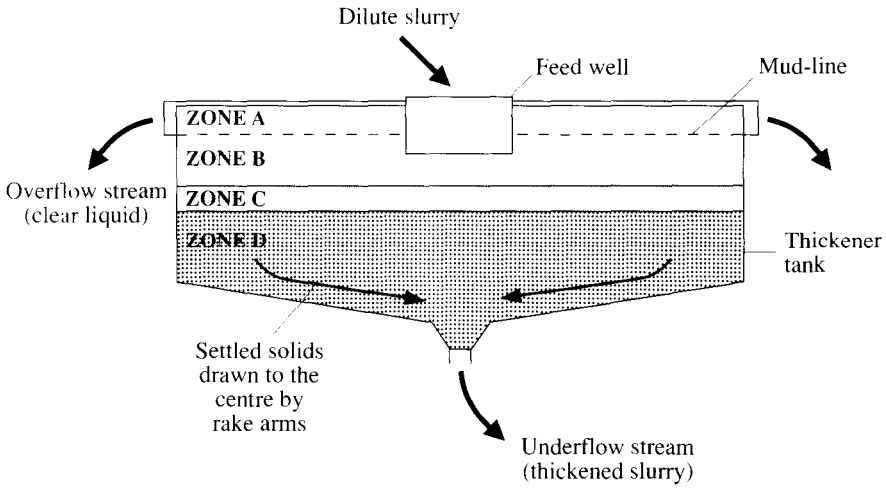

Figure 3. Zones in a conventional thickener

The thickening operation requires fine particles to settle through a liquid under quiescent conditions. When gravity is used, the settling rate is slow and the thickening equipment must be large to give an appreciable throughput. The devices are generically termed thickeners. Increased settling rates are possible if centrifugal forces are used to drive the sedimentation process. Two devices that operate in this fashion are the hydrocyclone and the sedimentation centrifuge. These are discussed briefly in the following section.

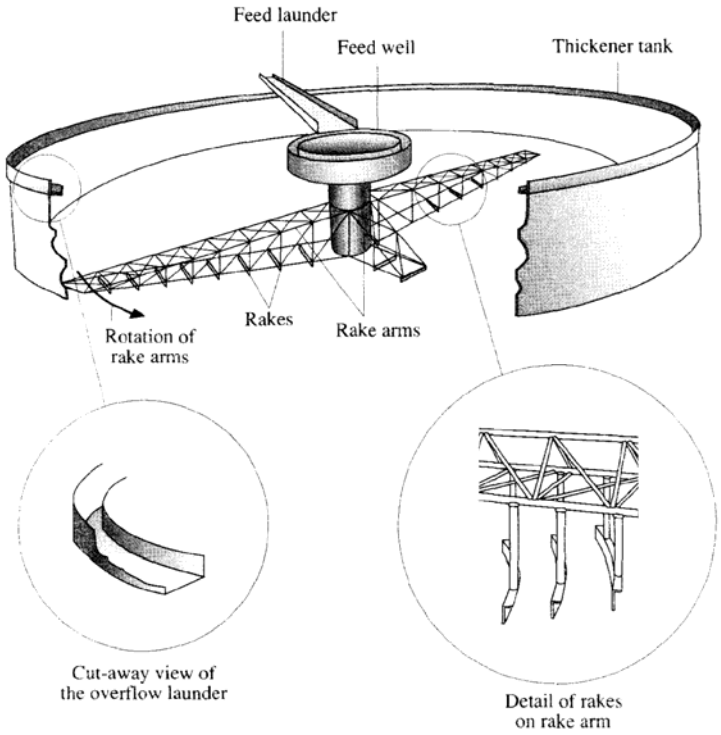

Figure 4. Cut-away view of a conventional thickener

The conventional thickener. The conventional thickener consists of a large, shallow cylindrical tank with a conical bottom sloping towards the centre (Figures 3 and 4). The feed slurry enters the thickener continuously through a central feed well. If flocculant is used, this is normally added to the feed slurry in the

launder before it is discharged into the feed well. In the bottom of the tank, mechanical sludge-raking arms, known as rakes, rotate slowly so as to draw the settled solids into the centre and assist in the compression of the sludge bed. The thickened slurry is drawn off continuously from the bottom of the conical section, and is referred to as the thickener underflow. The supernatant liquid, which is now virtually free of solids, flows continually over the perimeter lip of the tank into a collecting launder, and is removed as the thickener overflow stream.

Settlement occurs within the tank in the same way as was described for the settling test. The only difference is that the process is continuous. As a result, different zones are maintained within the thickener that correspond roughly to the different stages of settlement. These zones can roughly be described as follows.

There is a zone spreading out from the feed well, where the slurry has approximately the same pulp density as the feed, zone B in Figure 3. The top of this zone is marked by a mud-line, above which is the region of supernatant liquid, zone A. At the bottom of the tank, zone D. the settled solids have formed a sludge bed that is continually under compression assisted by the motion of the rakes. Between the sludge bed and zone B is a region where the concentration of solids varies from that of the feed to that of the sludge bed. This is zone C in the diagram.

As slurry enters the thickener, the solids settle through zones B to D until they are removed in the underflow stream. Most of the liquid in the feed slurry enters the supernatant zone, rising from the different zones below, until it flows over the perimeter of the tank.

By virtue of its large volume (some thickeners have diameters as large as 100 m), a conventional thickener can provide significant surge capacity in a circuit. Fluctuations in the feed rate of slurry or in the rate of withdrawal of the underflow cause the volumes of the different zones in the thickener to change. If the thickness of the sludge bed increases, the torque on the rake arms also increases, and this is a signal to the operator that the thickener load has increased. To protect the raking system from damage due to excessive torque, it is usually fitted with a mechanism that is able to lift the rakes out of the sludge bed to a greater or lesser degree.

If the rotation of the rakes is stopped during operation, the performance of the thickener is severely impaired. The rakes can very quickly become buried in the sludge bed, and they cannot be restarted without taking the thickener out of operation and physically washing out the sludge; a tedious and time-consuming process.

Other types of thickener. Thickeners of various design are available. These include differences in geometry and in the way in which the feed slurry is introduced to the thickener.

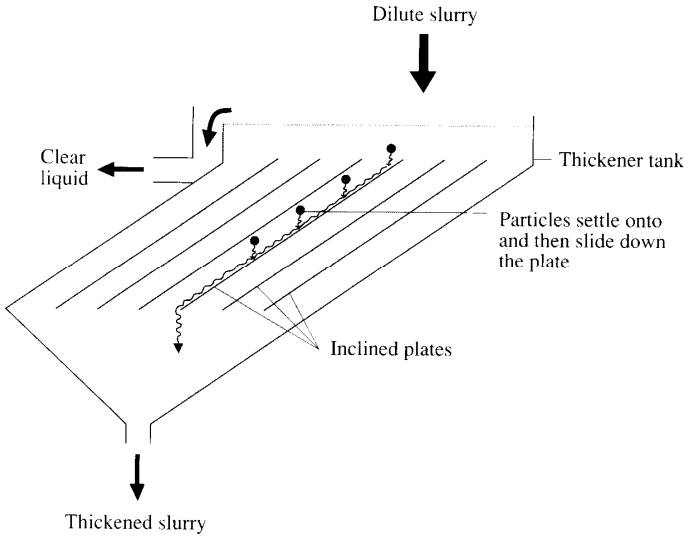

Figure 5. The lamella thickener.

A somewhat different concept is employed in the lamella thickener (Figure 5). It is fitted with inclined plates within the body of the thickener. What this does is to reduce the distance through which the solids have to settle. Once the solids encounter the plates, they slide down into the sludge bed, rather than having to settle

further through the liquid phase. The net effect of this arrangement is to considerable increase the thickening capacity of a tank of given volume.

Equipment for Centrifugal Sedimentation

Two types of devices use centrifugal forces to accelerate settling rates: the hydrocyclone and the sedimentation centrifuge. As discussed in the chapter on classification, a hydrocyclone operates to some extent as a sedimentation device. As such, it can be used for thickening purposes. Two sedimentation centrifuges are in common use—the solid-bowl and the screen-bowl centrifuge.

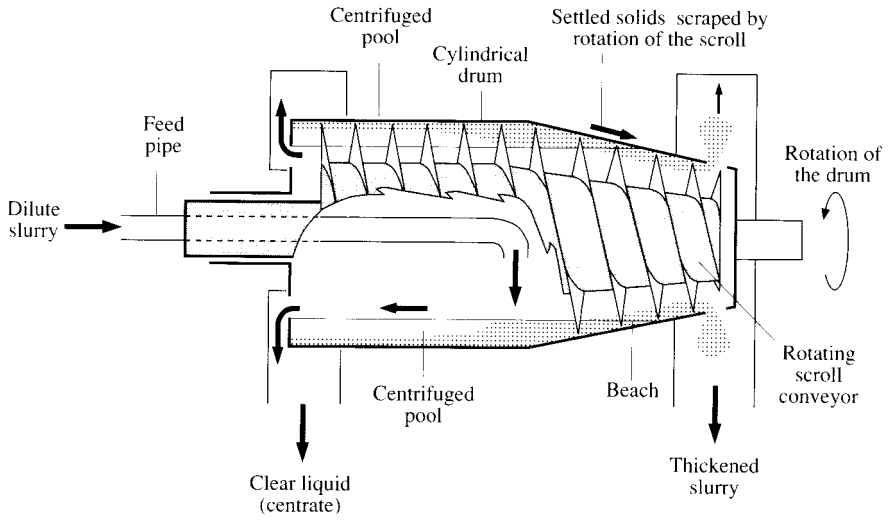

Figure 6. Cut-away side view of a solid-bowl centrifuge

As shown in Figure 6, a solid-howl centrifuge consists of a cylindrical drum that rotates at high speed, up to 6000 r/min. The slurry is introduced to the inside of this drum and is centrifuged to form a pool as shown. Solids settle to the surface of the drum. A scroll, known as the conveyor, rotates at a slightly slower speed than the bowl and so scrapes the settled solids to one end of the drum. The drum at his end tapers inwards so that the scraped solids are drawn above the level of the liquid, as shown, and discharge through the end of the drum. The tapered section of the drum is referred to as the 'beach'. The clear supernatant liquid overflows from the lip at the other end of the drum and is discharged from the machine as the centrate.

The screen-bowl centrifuge is very similar to the solid-bowl centrifuge. The major difference is that the beach area is perforated. Liquid with some fine solids is removed through the perforations and is combined with the centrate. The result of this arrangement is that greater dewatering rates are achieved at the expense of a higher solids content in the centrate.

7.6. Filtration

The Principles of Filtration

In filtration, liquid is removed from a slurry by being drawn through a porous filter medium, the filter cloth, which prevents the passage of the solid particles. The solids build up on the medium and form a cake. As the cake builds up, it acts as a filtration medium in itself, allowing passage only to the liquid phase (Figure 7). The liquid that passes through the cake and the cloth is termed the filtrate.

The size of the pores in the filter cloth is selected according to the size and proportion of the finest particles in the material to be filtered and the degree of clarity required in the filtrate. Both the cake and the filter cloth offer very significant resistance to the passage of liquid, and hence to the rate of filtration and cake formation. The resistance is determined by the viscosity of the liquid, the pore size of the cloth, and the size of the interstices in the cake. In order to overcome this resistance and so obtain a reasonable rate of liquid removal, pressure must be applied to the system.

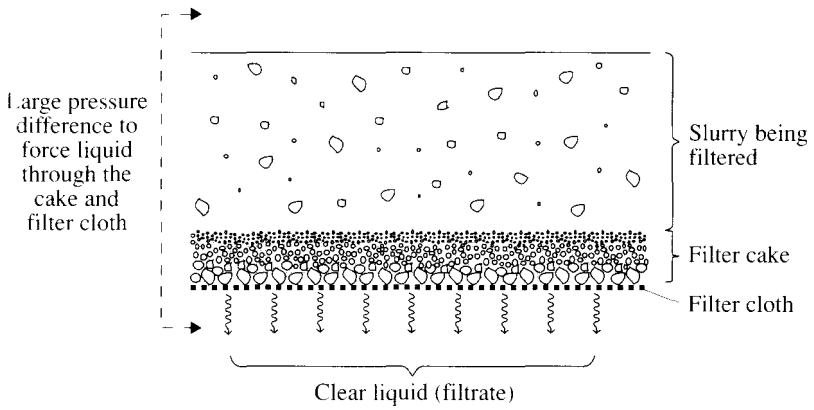

Figure 7. The formation of a filter cake

Once a cake has been built up, a significant quantity of liquid remains associated with the solids, being retained in the interstices of the cake. This residual moisture can be reduced considerably if air under pressure is drawn through the cake. The resistance offered by the cake and filter cloth to the passage of air is very much less than that offered to the passage of liquid. As a result, relatively high air velocities through the cake are possible. This forces much of the interstitial liquid through the cake and filter cloth, thus producing a drier cake. The rate at which a cake can be dried is influenced by the surface tension of the liquid, as well as by the same factors that affect the rate of liquid removal and cake formation.

When a cake has been formed and dried, it must be removed from the filtration machine. The way in which this is done varies for different machines, as will be discussed shortly.

From the descriptions given so far, it will be evident that filtration is not a single-stage process. Three different operations must be performed in order to achieve as low a moisture level as possible in the filter cake. These are:

- formation of the cake
- drying of the cake
- removal of the cake.

It is this multi-stage aspect of the process that complicates the engineering of a robust and reliable filtration device for large-scale continuous operation.

Factors Affecting Filtration

A variety of options are available in order to maximize the capacity of a given filtration device. The more important are as follows.

Increased filtration pressure. Pressure must be applied in order to force liquid through the cake and the filter cloth. This can be done in one of two ways. The method most widely used is the application of a vacuum on the filtrate side of the filter cloth. This results in a differential pressure of something less than one atmosphere across the cake and filter cloth. Significantly higher pressures can be applied if the system is pressurized on the slurry side of the cloth. It is considerably more difficult, and costly, to engineer a continuous filtration system using this approach, but in certain situations the cost is justified.

Increased pore size. Larger pores in the filter cloth reduce the resistance to the flow of liquid through the cloth at the expense of allowing a higher proportion of the very fine solids to enter the filtrate.

Manipulation of the cake formation. It is common practice to attempt to control the way the cake is formed so that the coarsest particles form a layer closest to the filter cloth, as shown in Figure 7. The interstices in this layer will be relatively large so that the rate of filtration is not reduced significantly. As filtration progresses, finer particles penetrate these interstices to some extent and form further layers as the cake builds

up. This approach produces a thicker cake than would be obtained if particles of all sizes were allowed to be incorporated in the first layers of the cake.

Use of flocculants or filter aids. Filtration rates can be increased by the use of various reagents that facilitate a reduction in the resistance of the cake to the passage of the liquid phase. Flocculants can be useful in this regard by agglomerating fine particles with coarse ones in the way that was described earlier. This makes the cake more porous because of the presence of the large aggregates of particles that are formed, and because of a reduction in the proportion of fine particles that are free to fill up the interstices. Filter aids have a different action. They reduce the viscosity or surface tension of the liquid phase. This results in a greater flow rate of liquid through the cake under a given filtration pressure. The speed of cake formation and of drying is thereby increased.

Washing of the filter cloth. Just as fine particles may fill up the interstices of the cake, so they are able to block the pores in the filter medium and 'blind' the cloth. Obviously, if this happens extensively and persists, the filtration performance deteriorates. In applications where this is a problem, the filter cloth is washed at some stage in the filtration cycle. Water sprays are directed appropriately so that any particles in the pores of the cloth are dislodged and washed out.

7.7. Vacuum Filtration

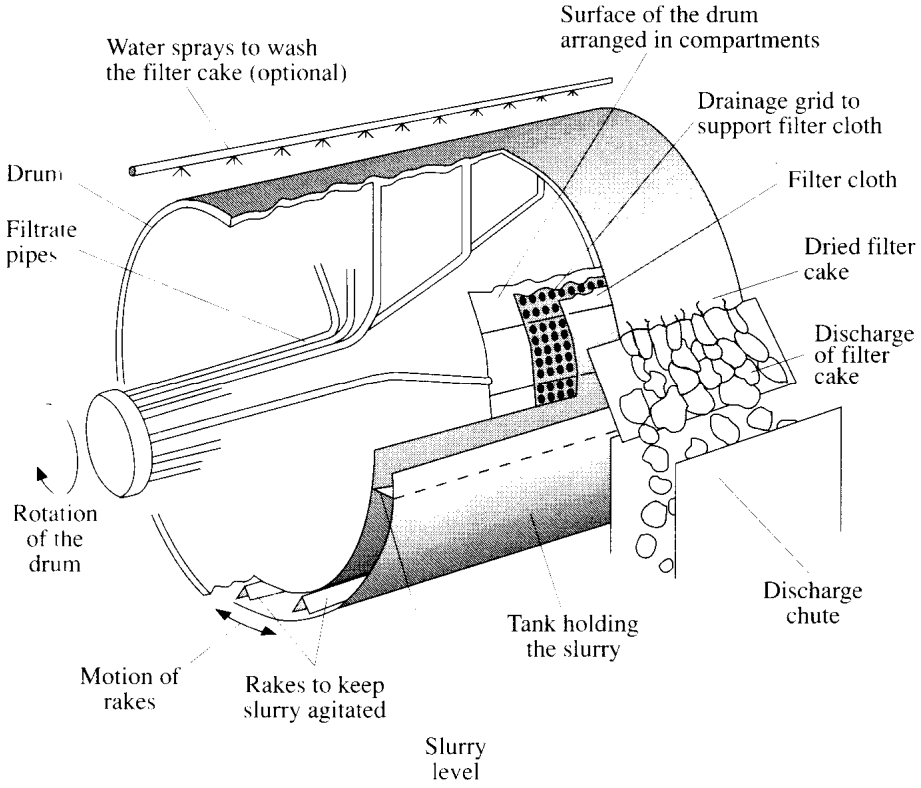

Figure 8. Cut-away view of a drum filter.

The most widely used type of filtration in minerals engineering is vacuum filtration. The principle in this type of filter is to create an effective differential pressure across the filter cloth and cake by the application of a vacuum on the filtrate side of the cloth.

Three different types of equipment are commonly used: drum, disk, and horizontal-belt filters. As mentioned before, there are three stages in filtration that must he engineered in each filtration device. The filtration surface must be moved into a region where a vacuum is applied so that a cake can be formed. From there, the cake must be moved to a region where air can be drawn through it to dry it. This is the region in which the cake is washed if washing is required. Following this, the filtration surface must carry the dried cake to a region where the cake can be discharged. The way in which these three stages are engineered distinguishes the three major types of vacuum filters.

Drum Filters

The drum filter consists of a large cylindrical shell. As indicated in Figure 8, the outside of the drum is covered with shallow compartments about 25 mm deep, each of which is covered with a drainage grid. These compartments are arranged in rows as indicated. Around the outside of these compartments, the filter cloth is wrapped and held tightly in position by a wire that is wound round the drum across its width. On the inside of the drum, pipes are connected to each of the compartments. Through these, either a vacuum or compressed air can be applied, depending on the stage reached by the compartment in the filtration cycle.

The drum is partially immersed in the slurry that is to be filtered and rotates slowly about its axis. The slurry is held in an agitated tank, as indicated in Figure 8. If the agitation of the slurry is not too vigorous, the slurry at the bottom of the filter tank will have a higher proportion of coarser particles than the slurry at the top of the tank.

As the drum is rotated, each row of compartments is moved progressively through the three stages of filtration. When the row of compartments is immersed in the slurry, vacuum is applied to each compartment in the row, and liquid is drawn through the filter cloth, via the pipes attached to each compartment, and into the filtrate-receiving system. In the process, the cake forms on the outside of the filter cloth. This part of the cycle is usually started when the compartments are in the lowest part of the tank so that the cake is formed initially with the coarser particles.

When the cake emerges from the slurry, the vacuum is maintained, but now air is drawn through the cake and the drying stage starts. As can be seen from Figure 8, this drying period is fairly extensive, occupying about two-thirds of the rotational cycle of the drum. If the cake is to be washed, this is done during the drying cycle and is accomplished by rows of sprays installed above the drum at one or more locations. Just before the row of compartments is again submerged in the slurry to begin a further filtration cycle, the vacuum to the compartments is turned off and compressed air is applied to blow the cake off the cloth. The cake falls into a chute and is transported away.

Disk Filters

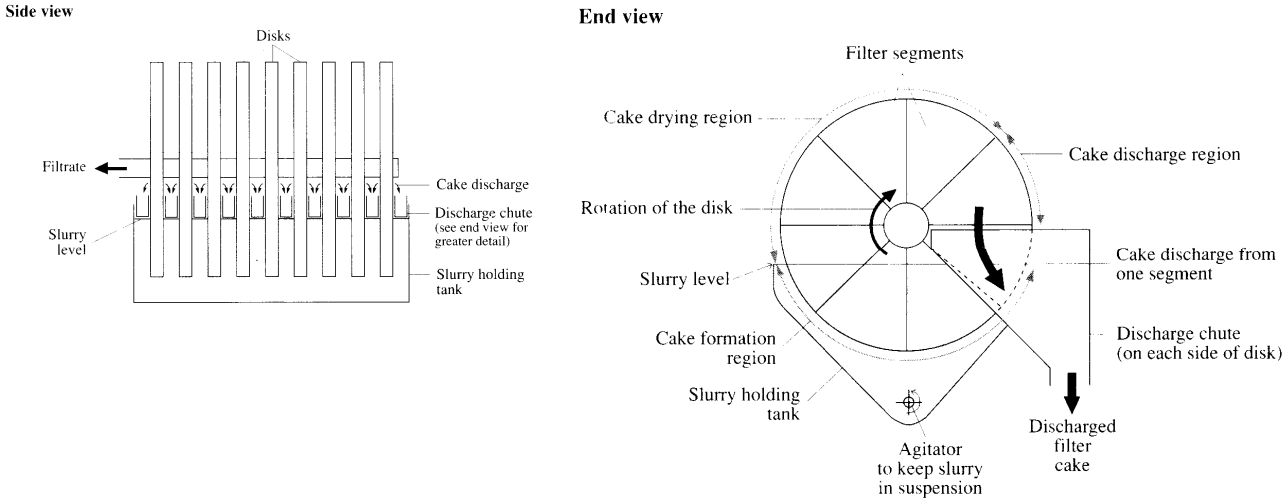

Figure 9. The disk filter.

The disk filter is similar in concept to the drum filter but, in order to increase the surface area for filtration, disks are used instead of a drum. The result is a much increased capacity for a given size of unit.
A disk filter consists of a number of disks that are mounted co-axially, as shown in Figure 9. Each disk consists of a number of segments, which are equivalent to the compartments on a drum filter. The major differences from the situation in a drum filter are, firstly, that each compartment is double-sided so that cake is formed on both sides and, secondly, each compartment is shaped as a segment of a circle. It is very evident from the diagram that this arrangement leads to a filtration-surface area that is considerably greater than is possible with a drum filter of similar diameter and width.

The filtration process follows the same sequence as described for a drum filter, but slight modifications have to be made to accommodate the difference in geometry. The most significant is that the discharge system must be placed so as to receive cake from both sides of each disk. In addition, it is difficult to install an effective cake-washing system, and it is not as easy to control the way in which the cake is formed. Because of the geometry of the filter, each segment on a disk is exposed to a complete cross-section of the slurry pool during the cake- formation cycle. This is different from the situation with a drum filter, where it is possible to expose each compartment to coarser particles first and so build up a thicker cake. For this reason, both the cake formation and the cake discharge are inferior to those in a drum filter. However, despite its disadvantages, the disk filter has a very important role as the cheapest filtration option for slurries that are easy to filter.

Horizontal-belt Filters

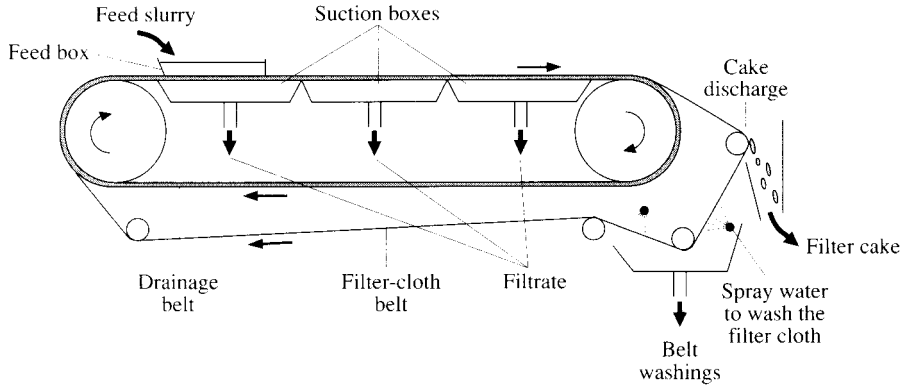

Figure 10. The horizontal-belt filter.

In this device, the filter cloth is formed into a continuous belt that is passed over an arrangement of pulleys, as shown in Figure 10. The belt is supported on a drainage belt made of perforated rubber and moves with it. Below this drainage belt, a series of suction boxes is installed along the length of the filter. The slurry to be filtered flows into a feed box at one end of the belt. Cake formation begins immediately. As the belt moves towards the discharge end, it draws the formed cake with it. In this way, the cake is carried over the other suction boxes, where the cake is dried. Cake washing can be applied at these points if necessary.
To discharge the cake, the belt is passed over a small-diameter roll. The curvature imparted to the cloth is sufficiently great for the cake to peel off and be discharged into the chute. Several sprays are arranged as shown to wash the belt and remove any fine particles that may be trapped in the pores of the filter cloth. In addition, any undischarged cake is removed.

A horizontal-belt filter is generally used where other types of filters are unable to achieve the required filtration duty. Better performance is possible for the following reasons:

1. The system of cake discharge is superior to a blow-off system, especially when the cake is sticky.
2. The cyclic removal of fines from the pores of the filter cloth improves the filtration rates.
3. The slurry does not have to be agitated. Indeed, in the other types of filters agitation is needed to prevent settling out of the solids in the filter tank. With the belt filter, settlement is encouraged because it aids filtration.
4. Because particle settlement is encouraged, the coarser particles tend to reach the cloth before the finer particles. The first layers of the cake are therefore coarser, which, as mentioned before, promotes the formation of thicker cakes.
5. On a belt filter, the control of cake formation, drying, and (if needed) cake washing is superior to that in any other vacuum filter. The reason for this is that the length, and even the intensity, of any particular part of the filtration cycle can be manipulated very easily. In addition, it is possible to classify the feed slurry and to deposit the coarser fraction at the feed end and the finer fraction in a second feed box placed further along the belt.

However, the belt filter has several disadvantages. In the first place, it is a more complex, and therefore more expensive, device than other filters of similar capacities. Secondly, it has rather high operating costs owing mainly to the high rates of wear on the drainage belt. This results from the fact that the drainage belt has to

be dragged (under suction) over the stationary suction boxes. Not only does wear of the belt affect the operating costs, it also results in a gradual deterioration in filtration performance.

Filtrate-receiving System

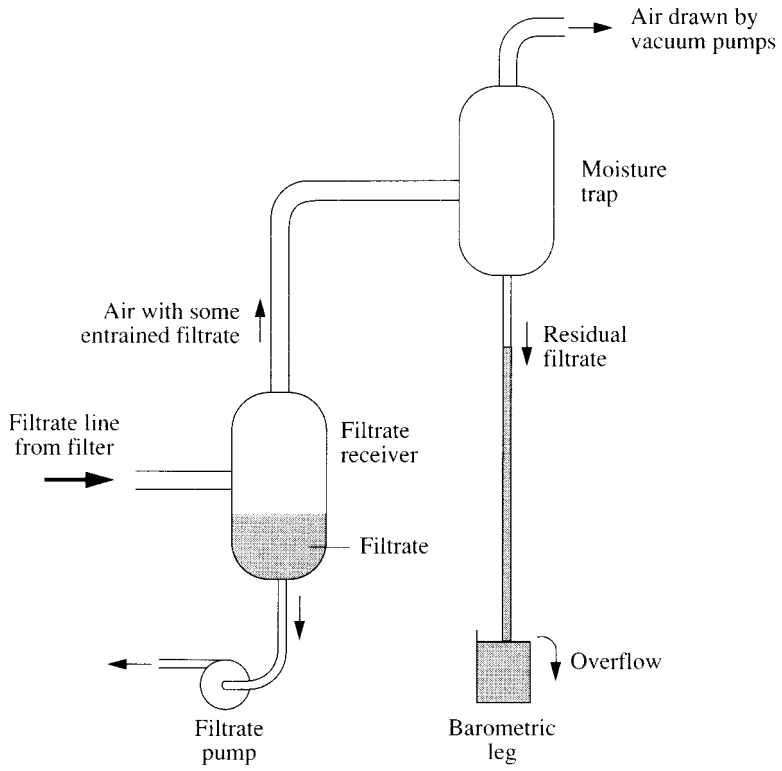

Figure 11. Filtrate-receiving system.

The filtrate that is drawn from a vacuum filter during the cake-formation, drying and washing stages is handled in a filtrate-receiving system. A typical design is shown in Figure 11. The engineering problem here is that, in order to apply a vacuum, air must be pumped continually from the system. Mixed with the air, however, is a large volume of filtrate that is continually being drawn from the filter. The vacuum pumps are precision pumps and can be damaged if both the filtrate (which is never entirely free of solids) and the air pass through the pump continually. Accordingly, the filtrate and air are separated in a specially designed receiver. The liquid is pumped from the bottom of this, while the air, containing some entrained liquid, flows through the top. The remaining entrained liquid is removed in a moisture trap, from which it drains by gravity through a barometric leg.

7.8. Pressure Filtration

A mentioned before, the performance of a filtration device can be improved by an increase in the differential pressure across the cake and filter cloth. Vacuum filters are restricted to differential pressures that are always less than one atmosphere. In that case, the differential pressure is created by the application of suction on the filtrate side of the cloth. In pressure filters, a positive pressure is applied on the slurry side of the cloth. The important implication of this difference is that much higher differential pressures can be used with pressure fibres, pressures of about 4 bars being common. Consequently, drier cakes and, in principle at least, higher filtration rates are possible.

The major difficulty with pressure filters lies in the engineering of a viable high-capacity continuous machine. From an engineering point of view, the advantage of vacuum filtration is that the slurry-handling system and the control of the filtration cycle can be performed under atmospheric conditions. With pressure filtration, this must all be done in a pressurized environment. As an illustration of the difficulties that this imposes, a batch device that is used in the industry is described. This is the plate-and-frame press (Figure 12).

It consists of a series of plates and frames that are stacked alternately as shown. The plates correspond to the compartments in a drum filter and are covered with a filter cloth. The interior of the plate is grooved, or is designed in some way so that the filtrate that is forced through the filter cloth can drain away. The frames create a hollow cavity between one plate and the next into which the slurry can be pumped under pressure. The series of plates and frames are screwed together so that the system is water-tight. When slurry is pumped into the frames, the pressure of the slurry forces the liquid through the cloth and into the plates, from where it drains into the filtrate-receiving system. The concentration of solids in the frames increases steadily, and the flow rate of slurry decreases accordingly. When the flow of slurry has stopped (i.e. the frames are full of cake), the cake can be washed by pumping fresh liquid or water through the press. The cake is then dried by the application of compressed air. When this part of the filtration cycle has been completed, the plates and frames are separated and the filter cake is discharged.

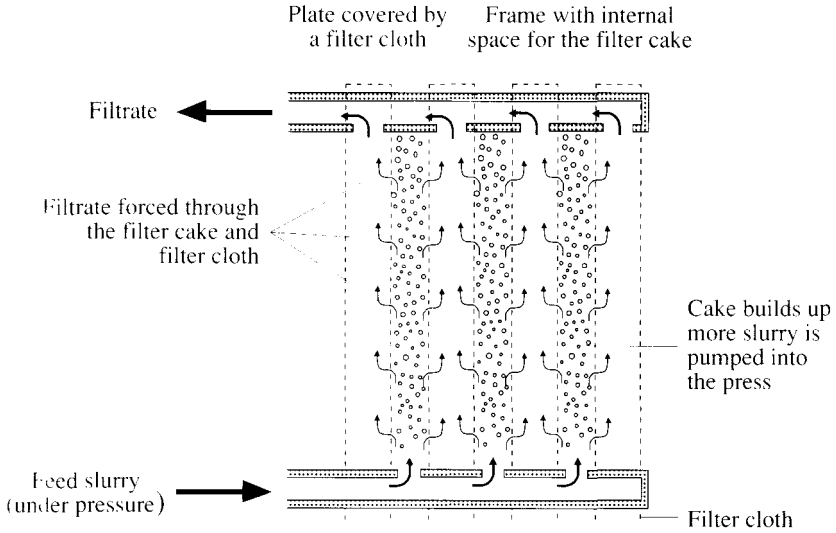

Figure 12. Plate-and-frame filter press.

All pressure filters operate on a basis similar to that described for the plate-and-frame press. It can be appreciated that the need to progress through a sequence of at least three different stages of filtration under pressure makes the engineering of continuous filtration very difficult. To date, the best that has been done is to devise a multiple-hatch arrangement so that feed can be pumped continuously, but not always into the same frames. Even so, there are mechanical difficulties in the designing of a robust and reliable system for taking each frame-and-plate compartment through the different stages of the operation.